Frontiers in Science and Engineering
International Journal

Edited by The Hassan II Academy of Science and Technology of Morocco

Mathematics, Applied Mathematics, Computer Sciences

Contents

ACADEMY Press MA

Volume 6 - Number 1 - 2016

Editorial board

Frontiers in Science and Engineering
International Journal

Edited by The Hassan II Academy of Science and Technology of Morocco

Mathematics, Applied Mathematics, Computer Sciences

Contents

Dépôt légal : 2012 PE 0007
ISSN : 2028 - 7615

ACADEMY Press MA

Email : fse@academiesciences.ma
www.academiesciences.ma/fse/

Layout by : AGRI-BYS S.A.R.L (A.U)
Printed by : Imprimerie LAWNE
11, rue Dakar, 10040 - Rabat

WELCOME TO FSE

Frontiers in Science and Engineering, an International Journal edited by The Hassan II Academy of Science and Technology uses author-supplied PDFs for all online and print publication.

The objective of this electronic journal is to provide a platform of exchange of high quality research papers in science and engineering. Though it is rather of wide and broad spectrum, it is organized in a transparent and simple interactive manner so that readers can focus on their direct interest.

All papers are submitted to the normal peer-review process. Publication criteria are based on :
i) Novelty of the problem or methodology and problem solving, **ii**) Salience of the approach and solution technique, **iii**) Technical correctness and outputs, **iv**) Clarity and organization.

Papers are first reviewed by the Executive Board Director who receives the paper and, if relevant in terms of the overall requirements, it is then proposed to one of the most appropriate associate editor on the field who will select 2 to 3 expert reviewers. Electronic printing will allow considerable time savings for submission delays which will be reduced drastically to less than three to six months. Prospective authors are therefore invited to submit their contribution for assessment while subjected to similar quality criteria review used in paper journals.

Authors are notified of acceptance, need for revision or rejection of the paper. It may be noted that papers once rejected cannot be resubmitted. All the details concerning the submission process are described in another section. This electronic journal is intended to provide :

- the announcement of significant new results,
- the state of the art or review articles for the development of science and technology,
- the publication of proceedings of the Academy or scientific events sponsored by the Academy,
- the publication of special thematic issues.

So that the scientific community can :
- promptly report their work to the scientific community,
- contribute to knowledge sharing and dissemination of new results.

The journal covers the established disciplines, interdisciplinary and emerging ones. Articles should be a contribution to fundamental and applied aspects, or original notes indicating a significant discovery or a significant result.

The topics of this multidisciplinary journal covers amongst others :
Materials Science, Mathematics, Physics, Chemistry, Computer sciences, Energy, Earth Science, Biology, Biotechnology, Life Sciences, Medical Science, Agriculture, Geosciences, Environment, Water, Engineering and Complex Systems, Science education, Strategic and economic studies, and all related modeling, simulation and optimization issues, etc. ...

Once, a certain number of papers in a specific thematic, is reached, the Academy might edit a special paper issue in parallel to the electronic version.

FOREWORD

The present volume of "Frontiers in Sciences and Engineering" is a special issue dedicated to the memory of our friend and colleague Abdelghani BELLOUQUID, born on February 2, 1966 and who passed away on August 31, 2015.

Upon his sudden death, late Abdelghani BELLOUQUID was a Professor of Mathematics at Cadi Ayyad University, and corresponding member (since February 2013) of the Hassan II Academy of Sciences and Technology. He was very active in research and has made several important contributions in kinetic theory for active particles and modeling complex systems. The authors of the articles in this volume are colleagues and friends of Abdelghani BELLOUQUID. Through their contributions, they wish to pay tribute to him. All the papers have been evaluated positively by peer referees.

The paper of N. Bellomo (Torino) and N. Chouhad (Essaouira) deals with the derivation of macroscopic tissue models, for binary mixtures of multi-cellular systems, from the underlying description delivered, by methods of the kinetic theory. The paper of F. Golse (Paris) establishes the mean-valued convergence of a system of charged particles to a regularized relativistic Vlasov-Maxwell system. The paper by M. Delitala (Torino), M. Ferraro (Torino) and E. Piretto (Torino) presents a mathematical model for cancer development. The contribution of A. Noussair (Bordeaux) deals with models of active cell-to-cell biological interactions. The paper of E.M. Ouhabaz (Bordeaux) is about boundedness of the Littlewood-Paley-Stein functionals associated with Schrödinger operators. The contribution of A. Azizi (Oujda), M. Taous (Errachidia) and A. Zekhnini (Nador) is in number theory and deals with 2-class groups, Hilbert class and 2-metacyclic groups. A review of different approaches in machine intelligence is given in the paper by M. Ghallab (Toulouse) and F. Ingrand (Toulouse). Finally, the paper submitted by L.M Rebaiaia (Quebec) and D. Ait-Kadi (Quebec) is on reliability evaluation of networks and algorithms.

We wish to express our gratitude to the Editors of "Frontiers in Sciences and Engineering" and more particularly Professors Omar Fassi-Fehri and Driss Ouazar for their precious help and for agreeing to publish this special issue of FSE.

Guest Editors :

Pr. El Maati OUHABAZ
Université de Bordeaux, Talence. France
Corresponding member of the Hassan II Academy of Sciences and Technology

Pr. Youssef OUKNINE
Université Cadi Ayyad, Marrakech. Maroc
Resident member of the Hassan II Academy of Sciences and Technology

In Memorium

Abdelghani BELLOUQUID *(2/2/1966–8/31/2015)*

On Monday, August 31, 2015, we learnt with deep sorrow and sadness the passing away of our colleague Professor Abdelghani BELLOUQUID, appointed corresponding member of the Hassan II Academy of Science and Technology in February 2013 by His Majesty the King -May God protect Him-. In this painful circumstance, we present on behalf of all members of the Academy our sincere condolences to his entire family, to his relatives and friends, assuring them of our compassion and our sympathy in this cruel ordeal and imploring God the Almighty to surround his sole with His holy mercy and clemency and to receive him in His vast paradise among the venerable elects and to provide patience and consolation to his family members.

Born in 1966, the late Professor Abdelghni BELLOUQUID happened to be the youngest member of our Academy. Having obtained his Bachelor's Degree in Mathematics in 1987 from the Semlalia Faculty of Sciences in Marrakech, he went to France to prepare his Diploma of Advanced Studies at the Paris 7 University, where he earned it in 1989. He was then enrolled in the same University to pursue his doctoral studies, which he defended in 1995 in the discipline of applied mathematics. In 1996 he began his professional career as a faculty member at the Ecole Normale Supérieure in Cachan, France. Between 1997 and 1999, he became a temporary teaching and research associate at the University of Evry. Between 2000 and 2001, he was recruited as teacher at the University of Evry and at the University of Marne la Vallée in France. From 2001 to 2005, he was recruited as a researcher at the Ecole Polytechnique de Turin in Italy. In 2005, he returned to Morocco and was recruited as an Assistant Professor at Cadi Ayad University in Marrakech and assigned to ENSA in Safi.

Professor Abdelghani BELLOUQUID's teaching and research activities focused on modeling, mathematical analysis and numerical simulation of complex systems. His research work was accompanied during his professional track by the publication of several scientific papers in international journals. He is known for the publication of 2 books, 4 book chapters more than fifty (52) scientific articles in peer-reviewed journals. He has also been editor and member of editorial boards of several international scientific journals, as he was the recipient of the 2009 Grand Prize for Invention and Research in Science and Technology. Two of his publications have been identified as the most cited ones in the field of applied mathematics in May 2006 and January 2007. He also took on several responsibilities at Cadi Ayad University as : member of the University Council, member of the Scientific Committee, member of thesis committee and board member of the institution.

Since his appointment by His Majesty the King as a corresponding member of our Academy, the important personal contribution of Professor BELLOUQUID, his valuable help and his availability, particularly in the framework of the activities of the Academy's College of Modeling and Information Sciences made the Academy forever grateful.

The death of Prof. Abdelghani BELLOUQUID is certainly a big loss for our Company but also a great loss for the research community of our country. Throughout his professional career, the missing colleague has never ceased to conduct his research activities. He has participated in a multitude of national and international conferences. He made numerous scientific visits to several countries. He has also been able to carry out many partnerships and scientific collaboration.

Prof. BELLOUQUID had perfect knowledge of his scientific discipline. Gifted with talent, he was recognized for his competence as well as for his abnegation and his devotion in carrying his duties and assuming his responsibilities. He was a well admired teacher, talented researcher and a great scientist in the field of Applied Mathematics in Morocco.

His remembrance will remain alive among all those who have known him and worked with him. During the short period he spent in our Academy as a corresponding member, his contribution was highly appreciated. He will be missed very much.

We implore God Almighty to welcome our late colleague in his vast paradise among the Prophets, Saints, Martyrs and Virtuous and grant him ample reward for the praiseworthy endeavors and good work he has accomplished at the service of his country.

In these painful circumstances, we once again wish to express our deepest condolences and sympathy to the family of the Prof. BELLOUQUID and all of his beloved ones; imploring the Almighty to have him in His Holy Mercy.

"We are to God and to Him we shall return."

Biography
of late Prof. Abdelghani BELLOUQUID

1. Scientific achievements

The scientific research of late Prof. Abdelghani BELLOUQUID has been mainly devoted to the theory and applications, in various fields of life sciences, of methods of the mathematical kinetic theory and derived from the well known Boltzmann equation. More in detail, it has been focused on the following main topics:

1- Mathematical modeling, qualitative analysis, and simulations of multicellular systems in biology with special focus on the modeling of the competition between cancer and immune cells;

2- Mathematical modeling, qualitative analysis, and simulations of complex systems devoted to the study of the dynamics of vehicular traffc and pedestrian crowds;

3- Analytic aspects of the mathematical theory of the classical and relativistic Boltz-mann equation;

4- Derivation of macroscopic models from the underlying description at the micro-scopic scale of biological system and of self-propelled particles.

Several features witness the excellence of the scientific activity of Prof. A. BELLOUQUID, mainly :

- Almost all papers are published, for each of the four aforementioned topics, in highly ranked journals. For Example “SIAM Journal of Applied Mathematics”, ” SIAM Multiscale Modeling and Simulations”, “Mathematical Models and Methods in Applied Sciences”, “J. Differential Equations”, ”Nonlinear Analysis TMA”.
- 6-7 Papers are “highly cited”, namely they are above the top 1% threshold of citations for papers published on journals of mathematics;
- Prof. A. BELLOUQUID has written, with M. Delitala (PhD), a book on the immune com-petition published by Birkhauser (Boston); this book is currently the guideline of various PhD dissertations at international level;
- Some outstanding results have been achieved, for example the derivation of the celebrated Keller-Segel model and the modeling of Darwinian type dynamics at the cellular level;
- Prof. A. BELLOUQUID contributed to the development of the so-called kinetic theory for active particles, which in a mathematical theory nowadays used by several mathematicians to model living, hence complex systems.

2. Resereach activity of Prof. A. BELLOUQUID

2.1. The modeling and simulation of complex (living) systems

This research is mainly based on the following motivation:

The modeling and simulation of complex (living) systems can be regarded as a challenging, however diffcult, new frontier of applied mathematics. Moreover, their study always needs a multiscale approach, where the

first step is the selection of the observation scale and of the related representation by mathematical variables and equations, while the second step is the search of the mathematical links between the scales used for the modeling approach. More precisely the link between macroscopic equations and to the underlying scale of individuals. The literature in the field is still looking for consistent approach, as the mathematical tools valid for the inert matter cannot be straightforwardly transferred to the living matter.

According to the above motivation, the scientific research of Prof. A. BELLOUQUID focuses on some multiscale issues related to the study of large living (hence complex) systems constituted by many living entities undergoing nonlinearly additive interactions. This topic has recently received a great deal of interest, first from physicists and subsequently from researchers in various other fields such as biology, economy and social sciences. Indeed, complexity characteristics are present not only in biology, but also in all sciences, where the human behaviors can modify, sometimes in a large amount, the dynamics of the class of systems under consideration. More recently a growing interest is witnessed among applied mathematicians, who look at this new research field by arguing that it offers a challenge to develop new mathematical theories or, at least, new mathematical methods. In fact, one of the many diffculties that are encountered along this ambitious path is the lack of first principles that characterize living systems.

2.1.1. Biological expression and interactions

Let us consider a large system of interacting entities, where each of them express specific biological functions, which depend on their phenotype structure as well as on that of the other entities. More precisely, this expression is modified by interactions, which are nonlinearly additive. Therefore, this ability has to be inserted into the said structure. Some papers have already taken into account this aspect. The first example arguably is the paper by Jager and Segel [JK] concerning the social behavior in large populations of interacting entities, namely the action of some insects to impose their behavioral rules to the others. The highly cited papers [15-16] of Prof. A. BELLOUQUID are focused more precisely on developmental biology, where the micro-state is the progression of epithelial cells, which have lost their differentiation and move toward the state of cancer cells featured by different sequential abilities such as proliferation, escape from the immune system up to metastatic competence. Several papers [10, 11, 22, 27, 30, 36, 45, 49, 57, 58] of Prof. A. BELLOUQUID were developed following [15]. The most important ideas are proposed in the book [56] privileging the cellular scale and the statistical mechanics approach, where a detailed presentation of the overall approach is given covering the whole path from modelling to simulation through a detailed study of analytic problems, namely existence of solutions and asymptotic analysis to derive macroscopic tissue models from the underlying description at the micro-scale. However, it has to be observed that this approach needs now some developments to include nonlinear features of interactions and Darwinian type mutations and selections. Additional needed developments will be discussed in the next referring specifically to the mathematical approach. The problem of identification of the parameters in a model of immune competition was treated in [48], where an approach of inverse problems toward the identification from measurements of densities of cells population was used.

2.1.2. Mutations, selection, and evolution

As it is known [WE], the onset and development of genetic diseases has an origin related to the dynamics at a cellular level as it can contribute to a dynamics at a cellular level when, during replication, the daughter cell exhibits a phenotype different from that of the mother cell, despite both belong to the same genotype [BR]. This dynamics can be viewed within the general theory of evolution [ER]. The highly cited paper [40]

indicates some features of the dynamics which should be retained by mathematical models, quoting [40]: *Interactions include proliferative events, which normally generate individuals with the same phenotype, but also, although with a small probability, new individuals, with a different phenotype: either more or less suited to a changing environment. As a consequence, the number of populations can evolve in time. If a number of populations constitutes the inner system that interacts with the external environment that evolves in time due to the aforementioned interaction. The distribution of the phenotypes is heterogeneous and can evolve in time. The net proliferation rate of the new born population depends on its fitness with respect to the environment*.

According to the above motivation, the pioneer paper [40] provides a general mathematical structure suitable to include a variety of specific biological dynamics such as the immune competition in the presence of mutations and selection. Moreover, it contributes to the challenging objective of reaching a deeper understanding of the laws of Darwinian evolutionary theory [AO].

2.1.3. From cells to tissues

The introduction of a space structure, followed by asymptotic methods can lead to the derivation of tissue models at the macro-scale. Asymptotic methods technically amount to expanding the distribution function in terms of a small dimensionless parameter related to the intermolecular distances (the space-scale dimensionless parameter) that is

equivalent to the connections between the biological constants. The limit that we obtain is singular and the convergence properties can be proved under suitable technical assumptions. In [12], biological systems are considered where interactions do not follow classical mechanical rules, and biological activity (biological progression, proliferative and destructive events for cancer cells in competition with the immune system) may play a relevant role in determining the dynamics. The main idea consists in perturbing the transport equation by a velocity jump process, which appears appropriate to model the velocity dynamics of cells modelled as living particles. Various works, among others [18-21, 23, 25-27, 30-31, 37, 50, 60], have contributed to this research line reviewed in the highly cited survey paper [34]. It is worth mentioning that this method leads to the derivation (see the highly cited paper [28], and [41-42,47, 51]), of classical models of the continuum mechanics of biology such as the celebrated models by Keller-Segel and Patlak to model chemotaxis phenomena, and the flux limited pattern formation in biological tissues where theoretical and experimental studies motivated the derivation of macro-scale models consistent with biological reality. The strong paper [53] focused on chemotaxis models in biology, namely the classical Keller-Segel model and subsequent modifications, in several cases, are developed to obtain models that prevent non physical bow up of solutions as flux limited models. Moreover this paper is devoted to the qualitative analysis of analytic problems such as existence of solutions, blow up, traveling waves, and the derivation of macroscopic models from the underlying description delivered by kinetic theory methods. This approach leads to the derivation of classical models as well as of new models, which might deserve attention toward related analytic problems. More recently, Prof. A. BELLOUQUID developed a computational approach to a class of pattern formation models derived from the celebrated Keller-Segel model obtained by the underlying description delivered by generalized kinetic theory methods. The derivation is based on a decomposition with two scales, namely the microscopic and the macroscopic one technically related by suitable small parameters accounting for the time and space dynamics (see [55]). The novelty of [55] is that the computational scheme follows precisely the derivation hallmarks by using the same decomposition and parameters. This idea improves the stability properties of the solutions with respect to classical approaches known in the literature.

2.1.4. Mathematical Challenges Toward Multiscale Modeling of Behavioral Crowd Dynamics

The mathematical literature on the modeling pedestrian crowd has rapidly developed in the last decade due to the interest in the contribution that the study of these systems can bring to the society, as well as to the challenging analytic and computational problems, generated by the derivation of models and by their application to real world dynamics. The existing literature is reported in some survey papers, which offer to applied mathematicians different view points and modelling strategies in a field where a unified, commonly shared, approach does not exists yet. The papers [32, 44, 59] introduce the concept of the crowds as a living, hence complex system and subsequently the search of mathematical tools suitable to take into account, as far as it is possible, the complexity features of the system. The hints proposed in [32, 44, 59] have been developed for a dynamics in unbounded domains. These papers introduce the concept of behavioral crowd, namely of a dynamics which depends on the strategy and behaviors that walkers develop based also to interactions, mechanical and social, with the surrounding walkers. In principle, one may look at this type of dynamics as at a new branch of dynamics, where the aforementioned complex interactions require new ideas and mathematical tools, which are object of an increasing interest by researchers active in the field. Interesting results concerning the derivation of macroscopic equations by suitable asymptotic methods in crowds dynamic is already available [54], which is arguably the first one where this interesting topic was addressed.

2.1.5. On the modeling of traffc

From a mathematical point of view, traffc flow phenomena can be modeled at three different scales: microscopic, kinetic and macroscopic. The microscopic description refers to vehicles individually identified and leads to systems of ordinary differential equations, while continuum mechanics assumptions lead to macroscopic models stated in terms of partial differential equations corresponding to fluid dynamic equations. The approach offered by the kinetic theory, developed after the pioneer contribution by Prigogine and Herman, uses Boltzmann and/or Vlasov-type equations to model the complex system under consideration. The highly cited paper [35] focuses on the use of kinetic theory methods which are, in the author's opinion, a useful approach that can be properly developed to capture the complexity of the physical reality of the dynamics of vehicular traffc. The basic idea is to consider each vehicular-driver system as a, so-called, active particle of a large complex system, to model the heterogeneous behavior of the micro-systems that compose the overall system. The evolution of the system is ruled by interactions between the active particles described by stochastic games. The modelling approach consider the heterogeneous behavior (well remarked by the engineer Daganzo) of the driver-vehicle micro-system, as real flow include different driving experience, quality of the vehicles to be also related to the quality of the environment. The derivation of hydrodynamic-type models should be obtained by suitable asymptotic limit from the kinetic description, namely by letting the distance between vehicles tend to zero. Therefore, the mathematical structure of macroscopic models should not be heuristically postulated a priori. The said program identifies precisely the aims and contents of the papers [33, 46], which are based on the modelling of nonlinearly additive and delocalized interactions. Subsequently, models of the kinetic theory for active particles are derived and, finally, by asymptotic methods, equations at the macroscopic scale are derived.

2.2. Mathematical methods in nonlinear kinetic theory

2.2.1. The hydrodynamical limit of the nonlinear models of kinetic theory

In his sixth problem, Hilbert asked for a full mathematical justification of fluid mechanics equation starting from particles systems. If we take a Boltzmann equation as a starting point, this problem can be stated as an asymptotic problem. Namely, starting from Boltzmann equation, can we derive fluid mechanics equations

and in which regime? From a physical point of view, we expect that a gas can be described by a fluid equation when the mean free path (Knudsen number) goes to zero. During the last two decades this problem got a lot of interest. A program in this direction was initiated by Bardos et al who, using the renormalized solutions to the Boltzmann equation constructed by Diperna and Lions, set an asymptotic regime where one can derive different fluid equations (and in particular incompressible models) depending on the chosen scaling. This is a theme on which Prof. A. BELLOUQUID has been working since the beginning of his PhD, and precisely he has developed a robust program [1-8, 13-14,17, 29] concerning these (rigorous) derivation from general kinetic models, and has obtained interesting results in the case of regular solutions for the most three classical equations of fluid mechanics in the incompressible or compressible regime, namely the incompressible Navier-Stokes equa¬tions, the Stokes equations, the diffusive equations, the compressible Euler equation by considering general models of kinetic theory and in particular the classical Boltzmann equation, discrete velocity models of Boltzmann equation, BGK equation, Kac equation,etc. More recently [43], Prof. A. BELLOUQUID was interested in the hyperbolic limits in kinetic theory, and proposed a nonstandard scaling to be understood as a sort of intermediate hyperbolic limit, which connects the (macroscopic) hyperbolic limiting behavior of the physical system with the microscopic properties usually obtained under parabolic scalings. He presented the strong result by means of a general kinetic frame for the intermediate hyperbolic limit which covers some well-known examples in kinetic theory (Vlasov-Poisson, Fokker-Planck systems and linear relaxation for Boltzmann-type equations in semiconductor theory, among others).

2.2.2. Analytic aspects of the mathematical theory of the classical and relativistic Boltzmann equation

A. Existence of some classical and relativistic kinetic models

Prof. A. BELLOUQUID studied the global existence for a certain spatially inhomogenous classical kinetic equations, such as Boltzmann, BGK models [1, 9, 39], Vlasov-Kac equation [24]. For such equations, the solution exists globally in time. The global existence for discrete models of vehicular traffic has been developed in [38].

B. Convergence to equilibrium of some classical and relativistic kinetic models

From physical point of view, the density of particle is assumed to converge to an equi-librium represented by a Maxwellien of the velocity v when time becomes large. The goal of work introduced in [1, 9] was to give some mathematical results in these topics. Prof. A. BELLOUQUID developed a new constructive approach to this problem for a large class of classical kinetic equations. The idea of the approach is to prove a weak coercive estimate, which implies polynomial convergence rate. The method works very well for the classical Boltzmann and BGK equations. In the case of relativistic kinetic theory, Prof. A. BELLOUQUID got recently a mathematical description of a relativistic gas in certain relaxation regimes. This was done in terms of the relativistic BGK equation. In that framework, such gases are regarded as consisting of many microscopic structures less particles. Concerning the mathematical study of the relativistic BGK equation, several issues related to this model which seem to have been overlooked in the previous physical literature were considered in [39], including the unique determination of associated physical parameters, the construction of the relativistic BGK system, classical, ultra-relativistic and hydrodynamical limits, maximum entropy principles, the analysis of the linearized operator, and the near-global-Maxwellian existence of the linearized BGK relativistic model. The global existence of the nonlinear relativistic BGK model and rapid time convergence to equilibrium was an open problem, and it was treated this year in [52], where Prof. A. BELLOUQUID studied the well-posedness and the rapid polynomial time decay at infinity of solutions.

REFERENCES

[AO] AOP, Laws in Darwinian evolutionary theory. Phys Life Rev, 2, 2005, 117-156. [BR] Burger. R, Willensdorfer. M, Nowa. KMA, Why are phenotypic mutation rates much higher than genotypic mutation rates? Genetics, 172, 2006, 197-206. [ER] Erwin. DH, Extinction: how life on earth nearly ended 250 million years ago. Princeton University Press; 2006. [JK] Jager. E, Segel. LA. On the distribution of dominance in populations of social organisms. SIAM J Appl Math, 52 1992, 1442-1468 [WE] Weissing. FJ. Genetic versus phenotypic models of selection: can genetics be neglected in a long-term perspective? J Math Biol, 34, 1996, 533-555.

3. Researcher

The education and scientific activity of Prof. A. BELLOUQUID developed at an international level. An additional feature is the interdisciplinary research activity. These statements are documented in the following.

3.1. Education

- 2001: Doctorat d' Etat at University of Semlalia Marrakech Morrocco and Ecole Normale Sup´erieure de Cachan (France). Advisor: Claude Bardos (Professor, University of Paris 7).
- 1995: Ph.D. in Applied Mathematics at University of Paris 7, France. Advisors: Claude Bardos (Professor, University Paris 7) and Francois Golse (Professor, Ecole Polytechnique).
- 1990: M. Sc. in Mathematics, University of Paris 7, France.
- 1989: B. Sc. in Mathematics, University Cadi Ayyad, Marrakech, Morocco.

3.2. Editorial Boards

Journals: Communications In Applied and Industrial Mathematics (Journal of the Italian Society of Applied and Industrial Mathematics), Abstract And Applied Analysis, International journal of mathematical models and methods in applied sciences, International journal of cancer and diagnosis, The Scientific World Journal, Mthematical Analysis, International journal of theoretical and mathematical physics, ISRN Applied Mathematics, American Journal of Applied Mathematics and Statistics, Applied Science Segment, Ilirias Journal of Mathematics, Journal of Scientific Research and Reports.

3.3. Research Interests

Mathematical methods in nonlinear kinetic theory; Asymptotic and hydrodynamic regimes; Mathematical models of complex systems in immunology and biology; Multi-scale cancer modeling; Mathematical models of vehicular traffic and crowds; General Relativity; Numerical analysis.

3.4. Professional experience

Associate Professor at University Cadi Ayyad, ENSA, Marrakech, Morocco 2005-present. Associate Researcher at Politecnico of Torino, Italy (2001-2005).

Recruited in the European Research Project with Title: Using Mathematical Modeling and Computer

Simulation to Improve Cancer Therapy (HPRN-CT-2000-00105) (see the WEB page: http://calvino.polito.it/biomat).

Teaching and Research Position(Attaché temporaire à l'enseignement et à la recherche, University Evry, France (1999-2001). Teaching-Assistant at University of Evry, France (1996-1999).

3.5. Participation in Research Projects

- Research Training Network (RTN) Project: Using Mathematical Modelling and Computer Simulation to Improve Cancer Therapy, 2001-2005.
- Research Project funded by The Hassan Il Academy of Sciences and Technology, (Morocco)-University Cadi Ayyad: Mathematical methods for modelling and simulation for cancer, 2011-2016 (Coordinator).

4. Scientific Publications

Refereed Articles

1. BELLOUQUID A., Existence Globale et Comportement Asymptotique du Probl`eme de Cauchy pour le Modèle de BGK, C.R. Acad. Sci. Paris, t. 321, Série I, 1637-1640, (1995).

2. BELLOUQUID A., The Hydrodynamical Limit of the Carlemann Equation, C.R. Acad. Sci. Paris, t.321, Série I, 655-658, (1995).

3. BELLOUQUID A., Limite Asymptotique pour le Mod`ele de BGK, C. R. Acad. Sci. Paris, t. 324, S´erie I, 951-956, (1997).

4. BELLOUQUID A., Limite Hydrodynamique de Quelques Mod`eles de la Théorie Cinétique Discrète, C.R. Acad. Sci. Paris, t. 330, Srie I, 951-956, (2000).

5. BELLOUQUID A., The Hydrodynamical Limit of the Non Linear Boltzmann Equation. Transp. Theory Statist. Phys., 28 (1), 25-57, (1999).

6. BELLOUQUID A., The Incompressible Navier-Stokes Limit for the Nonlinear Discrete Velocity Kinetic Equations. J. Nonlinear Math. Phys., 9, 426-445 (2002).

7. BELLOUQUID A., From Microscopic to Macroscopic: Asymptotic Analysis of The Broadwell Model Towards The Wave equation. Math. Comp. Modeling, 36, 1169-1181, (2002).

8. BELLOUQUID A., Diffusive Limit for the Nonlinear Discrete Velocity Models, Math. Models Meth. Appl. Sci., 13, 33-58, (2003).

9. BELLOUQUID A., Global Existence of BGK Model for a Gas With Non Constant Cross Section, Transp. Theory Statist. Phys., 32 (2), 157-184, (2003).

10. BELLOMO N., BELLOUQUID A, DE ANGELIS E., Lectures Notes, On the Modeling of the Immune Competition by Generalized Kinetic Boltzmann Models -A Review and Research Perspectives, Math. Comp. Modeling, 37, 65-86, (2003).

11. BELLOUQUID A., DELITALA M., Kinetic (Cellular) Models of Cell Progression and Competition with Immune System. Z. Agn. Math. Phys (ZAMP), 55, 295-317, (2004).

12. BELLOMO N., BELLOUQUID A., From a Class of Knetics Models to The Macroscopic Equations for Multicellular Systems in Biology, Discrete and Continuous Dynamical Systems., 4(1), 59-80, (2004).

13. BELLOUQUID A., The Compressible Euler and Acoustic Limit for Kinetic Models. Math. Models Meth. Appl. Sci., 6 (14), 853-882, (2004).

14. BELLOUQUID A., The Linearized Compressible Euler for The Discrete Boltzmann Equation, Electronic Journal Differential Equation, 104, 1-18, (2004).

15* . BELLOMO N., BELLOUQUID A., DELITALA M., Mathematical Topics on the modelling of Multicellular Systems in the competition between Tumor and Immune cells, Math. Models Meth. Appl. Sci. 8 (15), 1-51, (2004).
*(Highly cited paper in the field of Mathematics, May 2006).
http://www.esi-topics.com/nhp/2006/may-06-NicolaBellomo.html

16* BELLOUQUID A., DELITALA M., On a Mathematical Kinetic Theory toward Modeling Complex Systems in Biology. Math. Models Meth. Appl. Sci., 15, 1-28, (2005).
*(Highly cited paper in the field of Mathematics, December 2006).
http://www.esi-topics.com/fbp/2006/december06-Delitala-Bellouq

17. BELLOUQUID A., On the Asymptotic Analysis of Boltzmann Equation Towards the Stokes Equations, Applied Mathematics Letters, 18(12), 1400-1407, (2005).

18. BELLOMO N., BELLOUQUID A., On the onset of nonlinearity for diffusion models of binary mixtures of biological materials by asymptotic analysis, Int. J. Nonlinear Mechanics, 41, 281–293, (2006).

19. BELLOMO N., BELLOUQUID A., On the Derivation of Macroscopic Equations In the Mathematical Kinetic Theory of Active Particles with Discrete States, Mathematical and Computer Modelling, 44, 397-404, (2006).

20. BELLOMO N., BELLOUQUID A., HERRERO M., From the microscopic to macro-scopic description for multicellular systems and biological growing tissues, Computers and Mathematics with Applications 53, 647-663, (2007).

21. BELLOMO N., BELLOUQUID A., NIETO J., SOLER J., Multicellular biological growing systems: Hyperbolic limits towards macroscopic description, Math. Models Meth. Appl. Sci., 17, 1-18, (2007).

22. BELLOMO N., BELLOUQUID A., DELITALA M., From the mathematical kinetic theory of actives particles to multiscale modelling of Complex Biological Systems, Mathematical Comp. Modeling, 47, 687-698, (2008).

23. BELLOMO N., BELLOUQUID A., SOLER J., On the derivation of hyperbolic macroscopic tissues models from the mathematical kinetic theory for active particles, Mathematical and Comp. Modeling, 49, 2083-2093, (2009).

24. BELLOUQUID A., On the global existence for the Kac Model with some external force, Mathematical Comp. Modeling, 49, 1531-1538, (2009).

25. BELLOMO N., BELLOUQUID A., On the Derivation of Macroscopic Hyperbolic Equations for Binary Multicellular Growing Mixtures, Computer and Mathematics with Applications, 57,744-756, (2009).

26. BELLOMO N., BELLOUQUID A., On the derivation of macroscopic tissue equations from hybrid models of the kinetic theory of multicellular growing systems- The effect of the global equilibrium, Nonlinear Analysis: Hybrid Systems, 3, 215-224, (2009).

27. BELLOMO N., BELLOUQUID A., NIETO J., SOLER J., Complexity and Mathematical Tools Towards the modelling Multicellular Growing System In Biology, Mathe-matical and Comp. Modelling, 51, 441-451, (2010).

28* . BELLOMO N., BELLOUQUID A., NIETO J., SOLER J., Multiscale Derivation of biological Tissues Models For Mixtures of Multicellular Growing Systems : Application to Flux-Limited Chemotaxis, Math. Models Meth. Appl. Sci., Appl. Sci. Vol. 20, No. 7, 1-29, (2010).

29. BELLOUQUID A., On the asymptotic analysis of the BGK model toward the incompressible linear Navier-Stokes equation, Math. Models Meth. Appl. Sci., Vol. 20, No. 8, 1299 -1318, (2010).

30. BELLOUQUID A., BIANCA C., Modeling aggregation-fragmentation phenomena by kinetic theory for actives particles Models, Mathematical and Comp. Modeling, 52, 802-813, (2010).

31. BELLOUQUID A., ANGELIS DE., From Kinetic Models of Multicellular Growing Systems to Macroscopic Biological Tissue Models, Nonlinear Analysis: Real World. Applications, 12, 1111–1122, (2011).

32. BELLOMO N., BELLOUQUID A., On the modeling of crowd dynamics looking at the beautiful shapes of swarms, Networks and Heterogeneous Media, (6), 383-399, (2011).

33. BELLOUQUID A., DELITALA M., Asymptotic limits of a discrete kinetic theory model of vehicular traffic, Applied Mathematics Letters., 24(5), 672-678, (2011).

34* . BELLOMO N., BELLOUQUID A., NIETO J., SOLER J., On the asymptotic theory from microscopic to macroscopic growing tissus models: An overview with perspectives, Models Meth. Appl. Sci. and Methods in Applied Sciences, (12), 1-37, (2012).

35* . BELLOUQUID A., ANGELIS DE., FERMO L., Towards the modeling of vehicular traffic as a complex system: a kinetic theory approach, Math. Models Methods Appl.Sci (22), 1-35, (2012).

36. AFRAITES L, ATLAS A, BELLOUQUID A, CH-CHAOUI M, Modelling the complex immune system response to cancer cells, Mathematics in Engineering, Science and Aerospace, (3), 269-283, (2012).

37. BELLOUQUID A, An asymptotic Analysis From Kinetic to Macroscopic Scale For Multicellular Growing Systems, Mathematics in Engineering, Science and Aerospace, (3), 259-268, (2012).

38. BELLOMO N., BELLOUQUID A., Global solution to the Cauchy problem for discrete velocity models of vehicular traffic, J. Differential Equations, 252, 1350-1368, (2012).

39. BELLOUQUID A, CALVO J, NIETO J, SOLER J, On the Relativistic BGK-Boltzmann Model: Asymptotics and Hydrodynamics, J. Stat Phys, 284-316, (2012).

40* . BELLOUQUID. A, E. De ANGELIS, KNOPPOF. D, From The Modeling of The Immune Hallamrks of Cancer To A Black Swan In Biology, Models Meth. Appl. Sci.and Methods in Applied Sciences, DOI: 10.1142/S0218202512500650, (2013).

41. BELLOMO. N, BELLOUQUID. A, NIETO. J, SOLER. J, Modeling chemotaxis from L2–closure moments in kinetic theory of active particles, Discrete and Continuous Dynamical Systems -Series B, Vol 18, N 4, (2013).

42. BELLOUQUID. A, A Micro-Macro Scaling for Flux Limited Models: Commentary to the paper "Morphogenetic action through flux-limited, Phys Life Rev, 10(4), 477-478 (2013).

43. BELLOUQUID A, CALVO J, NIETO J, SOLER J, Hyperbolic versus Parabolic Asymptotics in Kinetic Theory toward Fluid Dynamic Models, SIAM J. Appl. Math., 73(4), 1327-1346, (2013).

44. BELLOMO. N, BELLOUQUID. A, KNOPPOF. D, On the multiscale models of pedestrian crowds-From mesocopic to macroscopic, SIAM, Multiscale Modelling, 11(3), 943-963, (2013).

45. BELLOUQUID. A, Mathematical tools towars the modeling of biological system, International journal of cancer research and disgnosis, 1(1), 1-4, (2013).

46. BELLOMO. N, BELLOUQUID. A, NIETO. J, SOLER. J, On the multiscale modelling of vehicular traffic, from kinetic to hydrodynamics, Discrete and Continuous Dynamical Systems -Series B, 19 (7), 1869-1888, (2014).

47. BELLOMO. N, BELLOUQUID. A, On the derivation of Angiogenesis models: from the micro- to macro-scale, Mathematics and Mechanics of Solids, 19 (8), 1-13, (2014).

48. AFRAITES. L, BELLOUQUID. A, Global optimization approaches to parameters identification in an immune competition model, Communications in Applied and Industrial Mathematics, 468-486, (2014).

49. BELLOUQUID. A, CH-CHAOUI. M, Asymptotic analysis of a nonlinear integro-differential system modeling the immune response, Computers and Mathematics with Applications, 68, 905-914, (2014).

50. BELLOMO. N, BELLOUQUID. A, Derivation of new chemotaxis models by asymptotic analysis of kinetic models for large binary cell mixtures, Frontiers in Science and Engineering (An International Journal Edited by Hassan II, Academy of Science and Technology), 4(2), 1-26, (2014).

51. BELLOUQUID. A, From systems biology to analytic problems, Phys Life Rev, 12, 68-69, (2015).

52. BELLOUQUID. A, NIETO. J, URRITIA. L, Global existence and asymptotic stability near equilibrium for the relativistic BGK Model, Nonlinear Analysis Serie A: Theory, Methods and Applications, 114, 87-104, (2015).
Meth. Appl. Sci.and Methods in Applied Sciences, DOI: 10.1142/S021820251550044X, (2015).

53. BELLOMO. N, BELLOUQUID. A, TAO. Y, WINKLER. M Towards a Mathematical Theory of Keller-Segel Models of Pattern Formation in Biological Tissues, Models
Meth. Appl. Sci.and Methods in Applied Sciences, DOI: 10.1142/S021820251550044X, (2015).

54. BELLOMO. N, BELLOUQUID. A On multiscale models of pedestrians crowds: from mesocopic to macroscopic, Journal of mathematical sciences. 13(39), (2015).

55. BELLOUQUID. A, TAGOUDJEU. J, An asymptotic preserving scheme for kinetic models for chemotaxis phenomena, Accepted in Applied Numerical Mathematics, (2015).

Books

56. BELLOUQUID A., DELITALA M., Mathematical Modelling of Complex Biological Systems. A Kinetic Theory Approach, Birkh¨auser-Springer, Boston (2006).
(http://www.springer.com/sgw/cda/frontpage/0,,5-40296-72-52117598-0,00.html)

Refereed research articles in Books

57. BELLOMO N., BELLOUQUID A., DELITALA M., Methods and tools of math-ematical kinetic theory towards modelling complex biological systems. Transport phenomena and kinetic theory, 175-193, Model. Simul. Sci. Eng. Technol., Birkhäuser, Springer, Boston, 2007.

58. BELLOUQUID A., DELITALA M., From kinetic theory for active particles to modelling immune competition. Selected topics in cancer modeling, 31-47, Model. Simul. Sci. Eng. Technol., Birkh¨auser-Springer, Boston, 2008.

59. BELLOMO N., BELLOUQUID A., On the modelling of vehicular traffic and crowds by kinetic theory of active particles. Mathematical modeling of collective behavior in socio-economic and life sciences, 273-296, Model. Simul. Sci. Eng. Technol., Birkhäuser-Springer, Boston, 2010.

60. BELLOMO N., BELLOUQUID A., DE ANGELIS E., On the derivation of Biological Tissue Models From Kinetics Models of Multicellular Growing models. B. Albers, Ed., Continuous Media with Microstructure, 131-145, Springer Berlin Heidelberg, 2010.

5. A list of the most significant publications

1. BELLOMO. N, BELLOUQUID. A, TAO. Y, WINKLER. M Towards a Mathematical Theory of Keller-Segel Models of Pattern Formation in Biological Tissues, Models Meth. Appl. Sci.and Methods in Applied Sciences, DOI: 10.1142/S021820251550044X, (2015).

2. BELLOUQUID. A, NIETO. J, URRITIA. L, Global existence and asymptotic stability near equilibrium for the relativistic BGK Model, Nonlinear Analysis Serie A: Theory, Methods and Applications, 114, 87-104, (2015).

3. BELLOMO. N, BELLOUQUID. A, NIETO. J, SOLER. J, On the multiscale mod-elling of vehicular traffic, from kinetic to hydrodynamics, Discrete and Continuous Dy-namical Systems -Series B, 19 (7), 1869-1888, (2014).

4* . BELLOUQUID. A, E. De ANGELIS, KNOPPOF. D, From The Modeling of The Immune Hallamrks of Cancer To A Black Swan In Biology, Models Meth. Appl. Sci.and Methods in Applied Sciences, DOI: 10.1142/S0218202512500650, (2013).

5. BELLOUQUID A, CALVO J, NIETO J, SOLER J, Hyperbolic versus Parabolic Asymptotics in Kinetic Theory toward Fluid Dynamic Models, SIAM J. Appl. Math., 73(4), 1327-1346, (2013).

6. BELLOMO. N, BELLOUQUID. A, NIETO. J, SOLER. J, Modeling chemotaxis from L2–closure moments in kinetic theory of active particles, Discrete and Continuous Dynamical Systems -Series B, Vol 18, N 4, (2013).

7. BELLOMO. N, BELLOUQUID. A, KNOPPOF. D, On the multiscale models of pedestrian crowds-From mesocopic to macroscopic, SIAM, Multiscale Modelling, 11(3), 943-963, (2013).

8* . BELLOMO N., BELLOUQUID A., NIETO J., SOLER J., On the asymptotic theory from microscopic to macroscopic growing tissus models: An overview with perspectives, Models Meth. Appl. Sci. and Methods in Applied Sciences, (12), 1-37, (2012).

9. BELLOUQUID A, CALVO J, NIETO J, SOLER J, On the Relativistic BGK-
Boltzmann Model: Asymptotics and Hydrodynamics, J. Stat Phys, 284-316, (2012).

10* . BELLOUQUID A., ANGELIS DE., FERMO L., Towards the modeling of vehicular trafic as a complex system: a kinetic theory approach, Math. Models Methods Appl.Sci (22), 1-35, (2012).

11. BELLOMO N., BELLOUQUID A., Global solution to the Cauchy problem for discrete velocity models of vehicular traffic, J. Differential Equations, 252, 1350-1368, (2012).

12. BELLOUQUID A., ANGELIS DE., From Kinetic Models of Multicellular Growing Systems to Macroscopic Biological Tissue Models, Nonlinear Analysis: Real World. Applications, 12, 1111–1122, (2011).

13*. BELLOMO N., BELLOUQUID A., NIETO J., SOLER J., Multiscale Derivation of biological Tissues Models For Mixtures of Multicellular Growing Systems : Application to Flux-Limited Chemotaxis, Math. Models Meth. Appl. Sci., Appl. Sci. Vol. 20, No. 7, 1-29, (2010).

14. BELLOMO N., BELLOUQUID A., NIETO J., SOLER J., Multicellular biological growing systems: Hyperbolic limits towards macroscopic description, Math. Models Meth. Appl. Sci., 17, 1-18, (2007).

15. BELLOMO N., BELLOUQUID A., On the onset of nonlinearity for diffusion models of binary mixtures of biological materials by asymptotic analysis, Int. J. Nonlinear Mechanics, 41, 281–293, (2006).

16*. BELLOUQUID A., DELITALA M., On a Mathematical Kinetic Theory toward Modeling Complex Systems in Biology. Math. Models Meth. Appl. Sci., 15, 1-28, (2005).

17*. BELLOMO N., BELLOUQUID A., DELITALA M., Mathematical Topics on the modelling of Multicellular Systems in the competition between Tumor and Immune cells, Math. Models Meth. Appl. Sci. 8 (15), 1-51, (2004).

18. BELLOUQUID A., The Compressible Euler and Acoustic Limit for Kinetic Models. Math. Models Meth. Appl. Sci., 6 (14), 853-882, (2004).

19. BELLOUQUID A., Global Existence of BGK Model for a Gas With Non Constant Cross Section, Transp. Theory Statist. Phys., 32 (2), 157-184, (2003).

20. BELLOUQUID A., The Hydrodynamical Limit of the Non Linear Boltzmann Equation. Transp. Theory Statist. Phys., 28 (1), 25-57, (1999).

6. Information on previous awards, honours, recognition received by Prof. A. BELLOUQUID

- Member of the Hassan II Academy of Science and Technology, Morocco.
- Grand Prize for Invention and Research in Science and Technology, Morocco, 2009-Edition.
- Thomson ESI December 2006 and January 2007 -Special Topics: Hot Paper on Mathematics for the article: Mathematical Methods and Tools of Kinetic Theory towards Modelling Complex Biological Systems. Interview available at www.esi-topics.com/fbp/december06-delitala-Bellouq.html.
- Thomson ESI May 2006-Special Topics: Hot Paper on Mathematics for the article: Mathematical Topics on the modeling of Multicellular Systems in the competition between Tumor and Immune cells. Interview available at: www.esi-topics.com/nhp/2006/ may-06-NicolaBellomo.html.
- Papers [15, 16, 28, 34, 35, 40] are “highly cited”, namely they are above the top 1% threshold of citations for papers published on journals of mathematics.

Developments of the Hilbert Methods in the Kinetic Theory for Active Particles: Derivation of Cross Diffusion Models

N. Bellomo[1] and N. Chouhad[2]

1- Department of Mathematics, Faculty of Sciences,
King Abdulaziz University, Jeddah, Saudi Arabia
Politecnico di Torino, 10129 Torino, Italy
nicola.bellomo@polito.it

2- Cadi Ayyad University, EST, Essaouira, Morocco
chouhadn@gmail.com

Abstract

This paper deals with the derivation of macroscopic tissue models, for binary mixtures of multi-cellular systems, from the underlying description delivered, by methods of the kinetic theory. The derivation refers to the parabolic scaling by asymptotic methods within the framework of the Hilbert perturbation method in classical kinetic theory, developed to the case of active particles.

1 Introduction

Parabolic diffusion models can be obtained by a phenomenological approach, where the local growth of a physical substance, in the elementary space volume is equated to net flux, due to the gradients of a certain substance or physical quantity. Different models can be obtained according to suitable phenomenological assumptions on the relation between fluxes and gradients. Linear models are obtained when the link is a direct proportionality, while nonlinear models correspond to relationships depending on the density and gradients of the aforementioned quantity.

The term cross diffusion for a binary mixture is used when both substances contribute to the diffusion of each of them, while the term transport-diffusion is used when gradients contribute also to the transport of the two substances. As it is known, the approach of continuum mechanics leads to the derivation of models at the macroscopic scale starting from conservation, or equilibrium

[2010]**Mathematics Subject Classification** 35Q20, 82C22, 92B05
Keywords: kinetic theory, multicellular systems, micro-macro asymptotic, cross diffusion models

equations, involving locally averaged quantities suitable to describe the state of the system.

A general structure of cross diffusion models is as follows:

$$\begin{cases} \partial_t w_1(t,x) = \nabla_x \cdot J_1(t,x,w_1,w_2) + H_1(t,x,w_1,w_2), \\ \\ \partial_t w_2(t,x) = \nabla_x \cdot J_2(t,x,w_1,w_2) + H_2(t,x,w_1,w_2), \end{cases} \tag{1}$$

where $w_1 = w_1(t,x)$ and $w_2 = w_2(t,x)$ denote the density, at position $x \in \Omega \subseteq \mathbb{R}^3$, and time $t \in \mathbb{R}_+$, of the two substances, J_1 and J_2 representing the fluxes of w_1 and w_2, and H_1 and H_2 are two source terms, which can model different phenomena such as production and/or degradation rates, reaction terms, and many others.

Models derived within this framework have been obtained, e. g. diffusion in multicellular systems, population dynamics, heat transfer phenomena. On the other hand, a criticism is that conservation equations need phenomenological models on the material behavior of the system. These models are generally valid at equilibrium, while diffusion models should operate far from equilibrium. It is worth mentioning, that this approach has not been limited only to applications in biology, as the derivation has been also focusing on different classes of self-propelled particles such car-drivers in vehicular traffic [7] and pedestrians in human crowds [2].

Therefore an alternative approach consists in the micro-macro derivation, where the derivation at the large scale is obtained from the underlying description at the microscopic scale of particles or, in the case of biological tissues, of cells. This approach has been developed in a sequel of papers [4, 5, 6], where the dynamics at the low scale is modeled by the kinetic theory of active particles [9]. This equation is expanded in terms of a small parameter corresponding to the mean distance between pair of particles, which is closed by neglecting terms of higher order.

A typical example is the Keller and Segel [12, 13] that, despite its successful ability to describe interesting biological phenomena, it shows non physical blow up phenomena. Therefore a number of heuristic modifications have been proposed to revise contradiction. The survey paper [8] is devoted to the mathematical theory of the aforementioned model, where interested readers can find several results on the micro-macro derivation. Indeed, new models have been suggested that are now object of an intense research activity focused on enlightening their properties and predictive ability.

The micro-macro derivation is developed by modeling the dynamics at the microscopic scale by the kinetic theory of active particles. Then, while the distance between particles is made to tend to zero, the time-space scaling generates a small parameter corresponding to such distance. The solution is obtained by an expansion in powers of the said parameter. A the approach developed in [3] has allowed to derive a variety of cross diffusion model. Additional bibliography can be found in the book [1] as well in the papers that initiated to deal with this class of mathematical problems [14, 15, 16].

Our paper develops the method for a binary mixture toward cross diffusion models. More in detail, we first consider a binary mixture, whose dynamics are modeled by the aforementioned kinetic theory approach, then we show how a large variety of nonlinear cross diffusion models can be derived, where each model corresponds to different assumptions on interactions at the microscopic scale. In more detail, Section 2 defines the kinetic framework modeling the mixture and presents the Hilbert method corresponding to the parabolic scaling; Section 3 shows how a general approach leads to the derivation of a specific model of cross diffusion chosen as a case study; Section 4 is devoted to a critical analysis and some research perspectives to understand how the methodological approach can be further developed.

2 A parabolic Hilbert method for binary mixture

Let us consider a binary mixture of cells, or biological substances, which can be modeled by suitable generalizations of the kinetic theory for active particles [9]. This section first defines a quite general framework to model the system, subsequently defines the parabolic scaling and some technical assumptions, and finally develops a Hilbert type method in order to derive macroscopic tissue models from the said underling kinetic description. These topics are treated in the next two subsections.

2.1 Kinetic framework

Let us consider binary biological mixture such that the overall state is described by the probability distributions $f_i = f_i(t, x, v)$, $i = 1, 2$ denoting, respectively, the density of cell, and chemical concentration, depending on time t, position $x \in \Omega \subset \mathbb{R}^d$ and velocity $v \in V \subset \mathbb{R}^d$, with $d = 1, 2, 3$. Macroscopic variables, such as the densities n, S are given by moments of the probability distributions. In particular, the number densities are defined, under suitable integrability conditions, as follows:

$$n(t,x) = \int_V f_1(t,x,v)\,dv, \quad S(t,x) = \int_V f_2(t,x,v)\,dv. \tag{2}$$

Let us now consider a system such that the overall dynamics is modeled by the following structure:

$$\begin{cases} \big(\partial_t + v \cdot \nabla_x\big) f_1 = \nu_1\, \mathcal{T}_1[f_2](f_1) + \mu_1 G_1(f_1, f_2, v), \\ \big(\partial_t + v \cdot \nabla_x\big) f_2 = \nu_2 \mathcal{T}_2(f_2) + \mu_2 G_2(f_1, f_2, v), \end{cases} \tag{3}$$

where G_1, G_2 model the interaction between particles and are assumed to depend on f_1, f_2 and v, while the operators $\mathcal{T}_i(f_i)$ model the space dynamics by a

velocity-jump process:

$$\mathcal{T}_i(f) = \int_V \Big[T_i(v, v^*) f(t, x, v^*) - T_i(v^*, v) f(t, x, v) \Big] \, dv^*, \quad i = 1, 2, \tag{4}$$

where $T_i(v, v^*)$ is the kernel probability for the new velocity $v \in V$ assuming that the previous velocity was v^*; The operators $\mathcal{T}_i$ may depend on f_1 and f_2; in fact, we will assume that T_1 depends on the population f_2. The set of possible velocities denoted by $V \subset \mathbb{R}^d$ is assumed to be bounded, radial symmetric; ν_1 and ν_2 denote the interaction rates.

2.2 Parabolic scaling

System (3) can be set in a dimensionless form with the introduction of a small parameter ε such that

$$t \longrightarrow \varepsilon t, \qquad \nu_1 = \nu_2 = \frac{1}{\varepsilon}, \qquad \mu_1 = \mu_2 = \varepsilon.$$

Then, (3) is written as follows:

$$\begin{cases} \big(\varepsilon \partial_t + v \cdot \nabla_x\big) f_1^\varepsilon = \frac{1}{\varepsilon} \mathcal{T}_1[f_2^\varepsilon](f_1^\varepsilon) + \varepsilon G_1(f_1^\varepsilon, f_2^\varepsilon, v), \\ \big(\varepsilon \partial_t + v \cdot \nabla_x\big) f_2^\varepsilon = \frac{1}{\varepsilon} \mathcal{T}_2(f_2^\varepsilon) + \varepsilon G_2(f_1^\varepsilon, f_2^\varepsilon, v). \end{cases} \tag{5}$$

These macroscopic equations can be obtained in the regime $\nu_1, \nu_2 \to +\infty$ corresponding to the asymptotic $\varepsilon \to 0$. Some technical assumptions are needed to achieve this objective.

Assumption 2.1. *The turning operator $\mathcal{T}_1[f_2]$ is supposed to be decomposed as follows:*

$$\mathcal{T}_1[f_2](g) = \mathcal{T}_1^0(g) + \varepsilon \mathcal{T}_1^1[f_2](g), \tag{6}$$

where $\mathcal{T}_1^i$ for $i = 0, 1$ is given by

$$\mathcal{T}_1^i(g) = \int_V \Big[T_1^i g(t, x, v^*) - T_1^{i^*} g(t, x, v) \Big] \, dv^*, \tag{7}$$

with $T_1^{i^*} = T_1^i(v^*, v)$. Therefore, the dependence on f_2 of the operator $\mathcal{T}_1^1[f_2]$ stems from T_1^1, while we suppose that $\mathcal{T}_1^0$ is independent on f_2.

Assumption 2.2. *We assume that the turning operators $\mathcal{T}_1$ and $\mathcal{T}_2$ satisfy the following equalities*

$$\int_V \mathcal{T}_1(g) dv = \int_V \mathcal{T}_1^0(g) dv = \int_V \mathcal{T}_1^1[f_2](g) dv = \int_V \mathcal{T}_2(g) dv = 0. \tag{8}$$

Assumption 2.3. *There exists a bounded velocity distribution $M_i(v) > 0$, $i = 1, 2$ independent of t, x, such that the detailed balance*

$$T_1^0(v, v^*) M_1(v^*) = T_1^0(v^*, v) M_1(v), \tag{9}$$

and

$$T_2(v, v^*)M_2(v^*) = T_2(v^*, v)M_2(v) \tag{10}$$

holds. Moreover, the flow produced by these equilibrium distributions vanishes, and M_i are normalized, i.e.

$$\int_V v\, M_i(v)dv = 0, \quad \int_V M_i(v)dv = 1, \quad i = 1, 2. \tag{11}$$

In addition, the kernels $T_1^0(v, v^*)$ and $T_2(v, v^*)$ are supposed to be bounded, and there exists a constant $\sigma_i > 0$, $i = 1, 2$, such that

$$T_1^0(v, v^*) \geq \sigma_1 M_1(v), \quad T_2(v, v^*) \geq \sigma_2 M_2(v), \tag{12}$$

for all $(v, v^*) \in V \times V$, $x \in \Omega$ and $t > 0$.

The above assumptions yield the following Lemma

Lemma 1. *Let now $L_1 = \mathcal{T}_1^0$, $L_2 = \mathcal{T}_2$ and suppose that Assumptions 2.2 holds. Then, the following properties of the operators L_1 and L_2 hold true:*

i) The operator L_i is self-adjoint in the space $L^2\left(V, \dfrac{dv}{M_i}\right)$.

ii) For $f \in L^2$, the equation $L_i(g) = f$, $i = 1, 2$, has a unique solution $g \in L^2\left(V, \dfrac{dv}{M_i}\right)$, which satisfies

$$\int_V g(v)\, dv = 0 \quad \text{if and only if} \quad \int_V f(v)\, dv = 0.$$

iii) The equation $L_i(g) = v\, M_i(v)$, $i = 1, 2$, has a unique solution that we call $\theta_i(v)$.

iv) The kernel of L_i is $N(L_i) = vect(M_i(v))$, i=1,2.

2.2.1 A Hilbert method toward hydrodynamical limits

Let us consider a general form of the scaled transport equation (5), that by using (6), can be written as follows:

$$\begin{cases} \left(\varepsilon^2\partial_t + \varepsilon v \cdot \nabla_x\right) f_1 = \mathcal{T}_1^0(f_1) + \varepsilon\mathcal{T}_1^1[f_2](f_1) + \varepsilon^2 G_1(f_1, f_2, v), \\ \left(\varepsilon^2\partial_t + \varepsilon v \cdot \nabla_x\right) f_2 = \mathcal{T}_2(f_2) + \varepsilon^2 G_2(f_1, f_2, v). \end{cases} \tag{13}$$

In order to develop asymptotic analysis of Eq.(13), additional assumptions on the operator $\mathcal{T}_1^1$, and G_i are needed.

Assumption 2.4. *We assume that the turning operators $\mathcal{T}_1^1$ and the interaction terms G_1 and G_2 satisfy the following asymptotic behavior:*

$$\mathcal{T}_1^1[g + \varepsilon h + \varepsilon^2 f] = \mathcal{T}_1^1[g] + \varepsilon R_1^1[g, h, f] + O(\varepsilon^2), \quad \forall g, h, f, \tag{14}$$

and

$$G_i(f+\varepsilon g, h+\varepsilon q, v) = G_i(f,h,v) + O(\varepsilon), \quad \forall f,g,h,q, \quad i=1,2. \tag{15}$$

Then, (8) rapidly yields:

$$\int_V R_1^1[g,h,f](k)dv = 0, \quad \forall k. \tag{16}$$

Since we are only interested in the solution of Eq.(13) on the diffusion time scale, we a regular perturbation expansion

$$f_1(x,v,t) = \sum_{j=0}^{2} \varepsilon^j g_j(x,v,t) + O(\varepsilon^2),$$

and

$$f_2(x,v,t) = \sum_{j=0}^{2} \varepsilon^j h_j(x,v,t) + O(\varepsilon^2).$$

Then the following sequence of systems follow by comparing terms of equal order in ε^j for $j=0,1,2$:

$$\varepsilon^0: \quad \begin{cases} \mathcal{T}_1^0(g_0) = 0, \\ \\ \mathcal{T}_2(h_0) = 0, \end{cases} \tag{17}$$

$$\varepsilon^1: \quad \begin{cases} \mathcal{T}_1^0(g_1) = v\cdot\nabla g_0 - \mathcal{T}_1^1[h_0](g_0), \\ \\ \mathcal{T}_2(h_1) = v\cdot\nabla h_0, \end{cases} \tag{18}$$

$$\varepsilon^2: \quad \begin{cases} \mathcal{T}_1^0(g_2) &= \partial_t g_0 + v\cdot\nabla g_1 - \mathcal{T}_1^1[h_0](g_1) - G_1(g_0,h_0,v) \\ &- R_1^1[h_0,h_1,h_2](g_0), \\ \\ \mathcal{T}_2(h_2) &= \partial_t h_0 + v\cdot\nabla h_1 - G_2(g_0,h_0,v). \end{cases} \tag{19}$$

The first equation (17) implies that $g_0 \in vect(M_1(v))$ and $h_0 \in vect(M_2(v))$, therefore $\exists n(t,x)$, and $\exists S(t,x)$ such that

$$g_0 = M_1 n, \quad \text{and} \quad h_0 = M_2 S. \tag{20}$$

From (18), we conclude that solvability conditions are satisfied, therefore g_1 and h_1 are given by

$$\begin{cases} g_1 = (\mathcal{T}_1^0)^{-1}(v.\nabla g_0) - (\mathcal{T}_1^0)^{-1}(\mathcal{T}_1^1[h_0](g_0)), \\ \\ h_1 = (\mathcal{T}_2)^{-1}(v.\nabla h_0). \end{cases} \tag{21}$$

The calculation of g_2 and h_2 are obtained from the solvability conditions at $O(\varepsilon^2)$, which are given by the following:

$$\begin{cases} \displaystyle\int_V \Big(\partial_t g_0 + v\cdot\nabla g_1 - \mathcal{T}_1^1[h_0](g_1) - G_1(g_0,h_0,v) - R_1^1[h_0,h_1,h_2](g_0)\Big)dv = 0, \\ \displaystyle\int_V \Big(\partial_t h_0 + v.\nabla h_1 - G_2(g_0,h_0,v)\Big)dv = 0. \end{cases} \tag{22}$$

Using (8), (16) and (20), Eqs.(22), can be rewritten as follows:

$$\begin{cases} \partial_t n + \big\langle v\cdot\nabla(\mathcal{T}_1^0)^{-1}(v\,M_1\cdot\nabla n)\big\rangle - \big\langle v\cdot\nabla(\mathcal{T}_1^0)^{-1}(\mathcal{T}_1^1[M_2\,S](M_1\,n))\big\rangle \\ -\langle G_1(M_1\,n, M_2\,S, v)\rangle = 0, \\ \partial_t S + \big\langle v\cdot\nabla(\mathcal{T}_2)^{-1}(v\,M_2\cdot\nabla S)\big\rangle - \langle G_2(M_1\,n, M_2\,S, v)\rangle = 0. \end{cases} \tag{23}$$

As $\mathcal{T}_1^0$ and $\mathcal{T}_2$ are self-adjoint operators in $L^2(V, \frac{dv}{M_1(v)})$ and $L^2(V, \frac{dv}{M_2(v)})$, one has the following computations:

$$\big\langle v\cdot\nabla_x(\mathcal{T}_1^0)^{-1}(vM_1\cdot\nabla_x n)\big\rangle = div_x\Big(\langle v\otimes\theta_1(v)\rangle\cdot\nabla_x n\Big),$$

$$\big\langle v\cdot\nabla_x(\mathcal{T}_2)^{-1}(vM_2\cdot\nabla_x S)\big\rangle = div_x\Big(\langle v\otimes\theta_2(v)\rangle\cdot\nabla_x S\Big),$$

$$\big\langle v\cdot\nabla_x(\mathcal{T}_1^0)^{-1}(\mathcal{T}_1^1[M_2(v)S](M_1(v)n))\big\rangle = div_x\left\langle\frac{\theta_1(v)}{M_1(v)}n\mathcal{T}_1^1[M_2(v)S](M_1(v))\right\rangle,$$

where θ_1 and θ_2 are given in Lemma 1.

Therefore, the macroscopic model (23) can be written as follows:

$$\begin{cases} \partial_t n + div_x\,(n\alpha(S) - D_1\cdot\nabla_x n) = H_1(n,S), \\ \partial_t S - div_x(D_2\cdot\nabla_x S) = H_2(n,S), \end{cases} \tag{24}$$

where D_1, D_2, and $\alpha(S)$ are, respectively, given by

$$D_1 = -\int_V v\otimes\theta_1(v)dv, \qquad D_2 = -\int_V v\otimes\theta_2(v)dv, \tag{25}$$

and

$$\alpha(S) = -\int_V \frac{\theta_1(v)}{M_1(v)}\mathcal{T}_1^1[M_2(v)S](M_1(v))dv, \tag{26}$$

while $H_1(n,S)$ and $H_2(n,S)$ are given by the following:

$$H_1(n,S) = \int_V G_1(M_1 n, M_2 S, v)dv, \tag{27}$$

and

$$H_2(n,S) = \int_V G_2(M_1 n, M_2 S, v)dv. \tag{28}$$

3 Derivation of Cross Diffusion Models

This section shows how the theoretical approach proposed in Section 2, specifically the mathematical structure (14), can lead to the derivation of a cross diffusion model selected as a possible example.

Let us consider the case where the set for velocity is the sphere of radius $r > 0$, $V = rS^{d-1}$, and let (f_1, f_2) be a solution of (13), where we assume that

$$T_1^0(v, v') = \frac{\sigma_1}{\mid V \mid}, \qquad T_2(v, v') = \frac{\sigma_2}{\mid V \mid}, \quad \text{with} \quad \sigma_1, \sigma_2 > 0,$$

and

$$M_i(v) = \frac{1}{\mid V \mid}, \quad i = 1, 2.$$

Then one has:

$$\mathcal{T}_1^0(g) = -\sigma_1\Big(g - \frac{\langle g \rangle}{\mid V \mid}\Big), \qquad \mathcal{T}_2(g) = -\sigma_2\Big(g - \frac{\langle g \rangle}{\mid V \mid}\Big). \tag{29}$$

Hence, Assumptions 2.2 and 2.3 are satisfied.

Let now

$$T_1^1[f_2] = K(S, v, v^*) \cdot \nabla_x f_2, \tag{30}$$

where $K(S, v, v^*)$ is a vector valued function, and

$$G_1 = f_1\bigg(a_0 + \frac{a_1}{\int_V M_1^2 dv} f_1 + \frac{a_2}{|\Omega|}\int_\Omega n dx\bigg), \quad G_2 = f_1 - f_2. \tag{31}$$

Then $\mathcal{T}_1^1[f_2]$ satisfies (8), (14), G_1 and G_2 satisfies (15).

The terms g_1, h_1 given by (21) can be computed as follows:

$$\mathcal{T}_1^1[h_0](g_0) = \frac{n}{\mid V \mid^2}\Phi(S, v) \cdot \nabla_x S,$$

with

$$\Phi(S, v) = \int_V (K(S, v, v^\star) - K(S, v^\star, v))dv^\star, \quad \text{with} \quad \int_V \Phi(S, v)dv = 0.$$

Hence

$$(\mathcal{T}_1^0)^{-1}(\mathcal{T}_1^1[h_0](g_0)) = -\frac{1}{\sigma_1}\,\mathcal{T}_1^1[h_0](g_0),$$

while g_1, h_1 are given by

$$g_1 = -\frac{1}{\sigma_1 \mid V \mid} v \cdot \nabla_x n + \frac{n}{\sigma_1 \mid V \mid^2 \Phi(S, v) \cdot \nabla_x S}, \tag{32}$$

and

$$h_1 = -\frac{1}{\sigma_2 \mid V \mid} v \cdot \nabla_x S. \tag{33}$$

In the same way, $R_1^1[h_1](g_0)$ is computed as follows:

$$R_1^1[h_1](g_0) = \frac{n}{\mid V \mid} \int_V \Big(K(S, v, v^\star) \cdot \nabla_x h_1(v) - K(S, v^\star, v) \cdot \nabla_x h_1(v^\star) \Big) dv^\star$$
$$= \frac{n}{\mid V \mid^2 \sigma_2} div_x \Big(\Big(\langle v^\star \otimes K(S, v^\star, v) \rangle_{v^\star} - \langle v \otimes K(S, v, v^\star) \rangle_{v^\star} \Big) \cdot \nabla_x S \Big).$$

The solutions $\theta_1(v)$, $\theta_2(v)$ of $\mathcal{T}_1^0(\theta_1(v)) = vM_1(v)$, and $\mathcal{T}_2(\theta_2(v)) = vM_2(v)$ are given by

$$\theta_1(v) = -\frac{1}{\mid V \mid \sigma_1} v, \qquad \theta_2(v) = -\frac{1}{\mid V \mid \sigma_2} v.$$

Therefore the diffusion tensors D_1 and D_2 are isotropic and are given by:

$$D_1 = \frac{1}{\mid V \mid \sigma_1} \int_V v \otimes v dv = \frac{r^2}{\sigma_1 d} I, \quad D_2 = \frac{1}{\mid V \mid \sigma_2} \int_V v \otimes v dv = \frac{r^2}{\sigma_2 d} I. \quad (34)$$

Equation (30) yields:

$$\mathcal{T}_1^1[M_2 S](M_1) = \psi(S, v) \cdot \nabla_x S,$$

where

$$\psi(S, v) = \frac{1}{\mid V \mid^2} \int_V \Big(K(S, v, v^*) - K(S, v^*, v) \Big) dv^*.$$

Finally, $\alpha(S)$ in (26) is given by

$$\alpha(S) = \chi(S) \cdot \nabla_x S, \quad (35)$$

where the chemotactic sensitivity $\chi(S)$ is given by the matrix

$$\chi(S) = \frac{1}{\sigma_1} \int_V v \otimes \psi(S, v) dv. \quad (36)$$

Moreover, from (31), one gets:

$$H_1(n, S) = n(a_0 + a_1 n + \frac{a_2}{|\Omega|} \int_\Omega n dx), \quad H_2(n, S) = n - S. \quad (37)$$

Finally, using (24), (34)-(35) and (37):

$$\begin{cases} \partial_t n + \ div_x(n\chi(S) \cdot \nabla_x S) = \delta \Delta n + n(a_0 + a_1 n + \frac{a_2}{|\Omega|} \int_\Omega n dx), \\ \\ \partial_t S = \mu \Delta S + n - S, \end{cases} \quad (38)$$

where the corresponding diffusion coefficients for the cells and chemical concentrations are given by:

$$\delta = \frac{r^2}{\sigma_1 d}, \qquad \mu = \frac{r^2}{\sigma_2 d},$$

and the chemotaxis sensitivity χ is given by (36).

4 Closure

The Hilbert method, which is well known in the classical kinetic theory, has been developed to obtain hydrodynamic equations from the underlying description delivered by the Boltzmann equation. Our paper has shown how this method can be developed, in the case of parabolic limit, to derive macroscopic cross diffusion models. The approach is quite general and can be further developed to deal with the deviation of different types of models at the large scale such as population dynamics, multicellular dynamics including proliferative and destructive dynamics. An interesting field of applications consists in deriving macro scale models in models that include mutations and selection, hence systems with variable number of equations. Therefore, our paper appears to provide the conceptual framework for a perspective research plan focused on the derivation of tissue equations from the underlying description at the microscopic scale.

References

[1] J. Banasiak and M. Lachowicz, **Methods of Small Parameter in Mathematical Biology**, Series: Modeling and Simulation in Science, Engineering and Technology, Birkhäuser, Boston, (2014).

[2] N. Bellomo and A. Bellouquid, On multiscale models of pedestrian crowds from mesoscopic to macroscopic *Comm. Math. Sci.*, **19** (2015), 1649-1664.

[3] N. Bellomo, A. Bellouquid, and N. Chouhad, From a multiscale derivation of nonlinear cross diffusion models to Keller-Segel models in a Navier-Stokes fluid, submitted.

[4] N. Bellomo, A. Bellouquid, J. Nieto, and J. Soler, Multicellular growing systems: Hyperbolic limits towards macroscopic description, *Math. Mod. Meth. Appl. Sci.*, **17**, (2007), 1675-1693.

[5] N. Bellomo, A. Bellouquid, J. Nieto, and J. Soler, Multiscale derivation of biological tissues models for mixtures of multicellular growing systems: application to flux–limited chemotaxis, *Math. Mod. Meth. Appl. Sci.*, **20**, (2010), 1179-1207.

[6] N. Bellomo, A. Bellouquid, J. Nieto, and J. Soler, On the asymptotic theory from microscopic to macroscopic growing tissue models: an overview with perspectives, *Math. Mod. Meth. Appl. Sci.*, **22**, (2012), paper n. 1130001.

[7] N. Bellomo, A. Bellouquid, J. Nieto, and J. Soler, On the multi scale modeling of vehicular traffic: from kinetic to hydrodynamics, *Discr. Cont. Dyn. Syst. Series B*, **19** (2014), 1869-1888.

[8] N. Bellomo, A. Bellouquid, Y. Tao, and M. Winkler, Toward a mathematical theory of Keller-Segel models of pattern formation in biological tissues, *Math. Mod. Meth. Appl. Sci.*, **25** (2015), 1663-1763.

[9] N. Bellomo, D. Knopoff, and J. Soler, On the difficult interplay between life, complexity, and mathematical sciences, *Math. Mod. Meth. Appl. Sci.*, **23** (2013), 1861-1913.

[10] A. Bellouquid and N. Chouhad, Kinetic models of chemotaxis towards the diffusive limit: asymptotic analysis, Math. Models Meth. Appl. Sci. (2015), DOI: 10.1002/mma.3758.

[11] A. Bellouquid and E. De Angelis, From kinetic models of multicellular growing systems to macroscopic biological tissue models, *Nonlinear Analysis: Real World. Appl.*, **12**, (2011), 1111–1122.

[12] E.F. Keller and L.A. Segel, Initiation od slide mold aggregation viewed as an instability, *J. Theor. Biol.*, **26**, (1970), 399–415.

[13] E.F. Keller and L.A. Segel, Model for chemotaxis, *J. Theor. Biol.*, **30**, (1971), 225–234.

[14] T. Hillen and H.G. Othmer, The diffusion limit of transport equations derived from velocity jump processes, *SIAM J. Appl. Math.*, **61(3)**, (2000), 751–775.

[15] H.G. Othmer, S.R. Dunbar, and W. Alt, Models of dispersal in biological systems, *J. Math. Biol.*, **26**, (1988), 263–298.

[16] H.G. Othmer and T. Hillen, The diffusion limit of transport equations II: chemotaxis equations, *SIAM J. Appl. Math.*, **62**, (2002), 1222–1250.

FROM THE DYNAMICS OF CHARGED PARTICLES TO A REGULARIZED VLASOV-MAXWELL SYSTEM

François GOLSE

(F.G.) CMLS, Ecole polytechnique, CNRS, Universite Paris-Saclay,
91128 - Palaiseau, Cedex, France
E-mail address: francois.golse@polytechnique.edu

Abstract. The present paper establishes the mean-field limit of the Abraham system for a system of identical charged particles subject to the electromagnetic interaction. This mean-field limit leads to a regularized variant of the relativistic Vlasov-Maxwell system. The result obtained here is similar to the one obtained in [F. Golse, Commun. Math. Phys. 310 (2012), 789–816], but is obtained by a purely Eulerian description of the particle dynamics.

1. Introduction

In 1977, K. Braun and W. Hepp [3] established the mean-field limit for a N-particle system leading to a regularized variant of the Vlasov-Poisson model where the Coulomb potential is replaced with a smooth (at least C^2) function. Their analysis was based on earlier contribution [15] by H. Neunzert and J. Wick, who studied particle methods for the Vlasov-Poisson system.

The result obtained by Braun and Hepp can be summarized as follows: assuming that the particle interaction force is Lipschitz continuous, the weak convergence of the initial phase-space distribution of particles is propagated by the dynamics of the regularized Vlasov equation. However, Braun and Hepp do not provide a convergence rate for the mean-field limit. This was done by R. Dobrushin [4] in 1979, who estimated the rate of convergence in that limit in terms of the Monge-Kantorovich distance by a very clever argument. Without diminishing the merits of Dobrushin's lucid analysis of the mean-field limit, it should be mentioned that the bounded Lipschitz distance, which is equal to the Monge-Kantorovich distance of exponent 1 by the Kantorovich duality theorem [19], already appears in the work of Braun-Hepp (see formulas (2.8)-(2.9) in [3]).

While either the Braun-Hepp and the Dobrushin results apply only to Lipschitz continuous interaction force field, the most interesting case is that of the Coulomb interaction, or of the Newton gravitation force. The former case corresponds to the Vlasov-Poisson system for electrically charged particles, one of the most fundamental equations of plasma physics. The latter case leads to the gravitational Vlasov-Poisson system for massive particles and is used in cosmology. Unfortunately, proving the mean-field limit for the dynamics of point particles subject to the Coulomb or the gravitational interaction remains an open problem at the time of this writing. There has been some recent progress however in the mathematical analysis of the mean-field limit with singular interaction forces. For instance, M. Hauray and P.-E. Jabin [9] have treated the case of interaction forces of order

$O(r^{-\alpha})$ with $0 < \alpha < 1$ as the inter-particle distance $r \to 0$ — notice that this falls short of the Coulomb singularity in space dimension 2, which is $O(1/r)$ as $r \to 0$.

Another approach to the mean-field limit leading to the Vlasov-Poisson system, with either the Coulomb repulsive interaction between charged particles (with charges of the same sign), or the Newton, attractive gravitational force between massive particles, is to start from a cutoff interaction, and to remove the cutoff as the particle number N tends to infinity. Perhaps the most striking result in this direction is [14, 12] — see also [9] — which can be understood as the mean-field limit for particles of vanishing radius in the large N limit.

In view of this progress on such a fundamental issue in plasma physics, it is natural to study the following problem.

Problem: can one derive in this way mean-field models for magnetized plasmas? for instance, can one derive the Vlasov-Maxwell system from some appropriate particle system?

This problem has been discussed in [7], which established the mean-field limit for a regularized variant of the Vlasov-Maxwell system. More recently, D. Lazarovici [13] was able to go further in the direction outlined in [7] by removing the regularization in the electromagnetic interaction as the particle number N tends to infinity.

In the present paper, we return to the problem discussed in [7], and propose a new and possibly simpler approach, which might be helpful to simplify, and perhaps improve the result in [13].

2. A short review of the Braun-Hepp-Dobrushin argument

Before going further in the discussion of the problem outlined above, we recall the main features in the Dobrushin approach [4].

Let $G \equiv G(x) = G(-x) \in C_b^2(\mathbf{R}^d)$. (Typically, one should think of G as a regularization of the Coulomb potential.) Consider the system of Newton's equations for a system of N identical point particles located at the positions $x_1(t), \dots, x_N(t) \in \mathbf{R}^d$:

$$\ddot{x}_i(t) + \tfrac{1}{N} \sum_{j=1}^{N} \nabla_x G(x_i(t) - x_j(t)) = 0\,, \qquad i = 1, \dots, N\,. \tag{1}$$

Each solution $t \mapsto (x_1(t), \dots, x_N(t)) \in \mathbf{R}^{dN}$ of the system (1) defines empirical measures

$$\mu_N(t, dxdv) := \tfrac{1}{N} \sum_{i=1}^{N} \delta_{x_i(t)} \otimes \delta_{\dot{x}_i(t)}\,, \qquad \rho_N(t, dx) := \tfrac{1}{N} \sum_{i=1}^{N} \delta_{x_i(t)} = \int_{\mathbf{R}^d} \mu_N dv\,. \tag{2}$$

A striking feature of the mean-field limit of the N-body problem in classical mechanics is that $t \mapsto (x_1(t), \dots, x_N(t))$ is a solution of (1) if and only if the empirical measure f is a (weak) solution of the Vlasov equation

$$\partial_t \mu_N + v \cdot \nabla_x \mu_N - (\rho_N \star_x \nabla G) \cdot \nabla_v \mu_N = 0$$

Because of this crucial observation, the "convergence" of the solution of the N-body problem to a solution of the Vlasov-Poisson type equation

$$\partial_t f + v \cdot \nabla_x f - \left(\int_{\mathbf{R}^d} f dv \star_x \nabla G \right) \cdot \nabla_v f = 0 \tag{3}$$

is equivalent to continuous dependence of the solution of the Vlasov equation (3) on the initial data in the weak topology of measures. This is precisely the approach chosen in [3] — without any attempt to obtain a modulus of continuity for this dependence.

At variance with the result obtained in [3], Dobrushin [4] obtains an estimate of the Monge-Kantorovich distance

$$W_1\left(f(t,\cdot,\cdot), \frac{1}{N}\sum_{i=1}^{N} \delta_{x_i(t)} \otimes \delta_{\dot{x}_i(t)}\right)$$

in terms of its initial value at $t = 0$ by the Gronwall inequality involving the Lipschitz constant of ∇G. Since the Monge-Kantorovich distance metrizes the topology of weak convergence of probability measures (see Theorem 1 in Chapter 1 of [19]), this estimate provides a convergence rate for the mean-field limit established in [3].

There are some conceptual difficulties in adapting Dobrushin's program to the Vlasov-Maxwell system:

(a) the source term in Maxwell's systems of equations is the charge+current density, i.e. a 4-vector, and not a probability measure,

(b) the solution of Maxwell's system of equations involves a retarded potential, and this may destroy the structure involving transportation of measure which is at the core of Dobrushin's argument.

In addition to these difficulties, there is another, perhaps more elementary question: can one preserve the Hamiltonian structure of the Vlasov-Maxwell system by regularization, or at least the energy conservation?

The issue (b) was partially addressed by Y. Elskens, M.K.H. Kiessling and V. Ricci in [5]: they treated a simplified variant of the RVM system without magnetic field, and where the electric potential is a solution to the wave equation with source term the charge density. However, their approach circumvents the issue (a).

3. A scalar formulation of Vlasov-Maxwell

For simplicity, we consider the relativistic Vlasov-Maxwell (RVM) system for a single species of charged particles. (Realistic models would involves several species of charged particles, so that the complete particle system is electrically neutral.)

The unknown of the RVM system is (f, E, B), where $f \equiv f(t,x,\xi)$ is the distribution function of the charged particles, $E \equiv E(t,x)$ is the electric field and $B \equiv B(t,x)$ is the magnetic field. The position variable is $x \in \mathbf{R}^3$, while $\xi \in \mathbf{R}^3$ is the momentum variable. The RVM system is

$$\text{(4)} \qquad \begin{cases} \partial_t f + v(\xi)\cdot\nabla_x f + (E + v(\xi)\times B)\cdot\nabla_\xi f = 0\,, \\ \\ \operatorname{div}_x B = 0\,, \quad \partial_t B + \operatorname{curl}_x E = 0\,, \\ \\ \operatorname{div}_x E = \rho_f\,, \quad \partial_t E - \operatorname{curl}_x B = -j_f\,. \end{cases}$$

In the Vlasov equation, we have used the notation

$$v(\xi) := \nabla e(\xi) = \frac{\xi}{\sqrt{1+|\xi|^2}}\,,$$

where

$$e(\xi) := \sqrt{1+|\xi|^2}$$

is the energy density for a particle with momentum ξ. Moreover

$$\rho_f(t,x) := \int_{\mathbf{R}^3} f(t,x,\xi)d\xi$$

is the charge density, while

$$j_f(t,x) := \int_{\mathbf{R}^3} v(\xi)f(t,x,\xi)d\xi$$

is the current density. In this formulation of the RVM system, several physical constants (such as the speed of light, the charge and the mass of the particles and so on) are set to 1, without loss of generality.

In this formulation of the RVM system, the source term in the field equations (i.e. in Maxwell's system of equations) is the 4-vector $(\rho_f, j_f)(t,x) \in \mathbf{R}^4$, instead of the charge density, as in the case of the Vlasov-Poisson system, where the electric potential is a solution to the Poisson equation

$$-\Delta_x \phi(t,x) = \rho_f(t,x)\,.$$

In the latter case, the right hand side of the field equation is a probability density, and this is a important feature in the Dobrushin approach [4].

3.1. **Density of Liénard-Wiechert potential.** In this section, we explain how to address the issue (a) above. The key idea is taken from [2], and is based on a "kinetic representation" of the solution to the Maxwell system in terms of the density of Linard-Wiechert potential attached to each charged particle. We recall that the electromagnetic potential created in the vacuum by a moving charged particle can be computed at each instant of time t in a Galilean frame centered at the position $x(t)$ of the particle at time t, such that the velocity of that particle at time t in that Galilean frame is 0. (The particle velocity at other instants of time $t' \neq t$ is in general nonzero in that Galilean frame.) The electromagnetic potential created at time t by that particle reduces to the electrostatic (Coulomb) potential in that frame, since the particle speed is 0 at time t. The corresponding electromagnetic potential in an arbitrary Galilean frame is then obtained by some appropriate Lorentz transform (see [11], §63).

The idea used in [2] involves a statistical superposition of Linard-Wiechert potentials distributed under f, and can be formulated as follows.

Define $u_f :\equiv u_f(t,x,\xi) \in \mathbf{R}$ to be the solution of

$$\Box_{t,x} u_f(t,x,\xi) = f(t,x,\xi)\,, \qquad u_f\big|_{t=0} = \partial_t u_f\big|_{t=0} = 0\,.$$

Assume the initial data of the RVM system is of the form

$$B\big|_{t=0} = 0\,, \quad E\big|_{t=0} = -\nabla\phi^{in}\,, \quad \phi^{in} = (-\Delta)^{-1}\int_{\mathbf{R}^3} f^{in}d\xi\,,$$

and define ϕ_0 to be the solution of

$$\Box_{t,x}\phi_0 = 0\,, \qquad \phi_0\big|_{t=0} = \phi^{in}\,, \quad \partial_t\phi_0\big|_{t=0} = 0\,.$$

Observe that ϕ_0 and u_f are obtained by solving linear wave equations, which is a relatively simple matter.

Knowing ϕ_0 and u_f, one reconstructs the electromagnetic potential by the formulas

$$\phi_f := \phi_0 + \int_{\mathbf{R}^3} u_f d\xi\,, \qquad A_f := \int_{\mathbf{R}^3} v(\xi) u_f d\xi\,.$$

The electromagnetic field is given in terms of the electromagnetic potential by the usual formulas:

$$E_f := -\partial_t A_f - \nabla_x \phi_f\,, \quad B_f := \mathrm{curl}_x\, A_f\,.$$

Moreover, because of the continuity equation

$$\partial_t \int_{\mathbf{R}^3} f d\xi + \mathrm{div}_x \int_{\mathbf{R}^3} v(\xi) f d\xi = 0$$

one easily sees that the electromagnetic potential (ϕ_f, A_f) satisfies the Lorentz gauge

$$\partial_t \phi_f + \mathrm{div}_x\, A_f = 0\,.$$

3.2. **Scalar formulation of RVM.** In view of the representation of the electromagnetic field obtained in the previous section, we can recast the RVM system as follows:

$$\text{(5)} \qquad \begin{cases} \partial_t f + v(\xi)\cdot\nabla_x f + F[f]\cdot\nabla_\xi f = 0\,, \quad f\big|_{t=0} = f^{in}\,, \\ \Box_{t,x} u_f = f\,, \qquad u_f\big|_{t=0} = 0\,, \qquad \partial_t u_f\big|_{t=0} = 0\,, \\ \Box_{t,x}\phi_0 = 0\,, \qquad \phi_0\big|_{t=0} = \phi^{in}\,, \quad \partial_t\phi_0\big|_{t=0} = 0\,, \\ F[f] = -\nabla_x\phi_0 - \displaystyle\int_{\mathbf{R}^3} (\nabla_x + v(\eta)\partial_t) u_f(t,x,\eta) d\eta\,, \\ \qquad\qquad + \displaystyle\int_{\mathbf{R}^3} v(\xi)\times \mathrm{curl}_x(u_f(t,x,\eta)v(\eta)) d\eta\,. \end{cases}$$

The idea of splitting the electromagnetic potential into the contribution of u_f and that of ϕ_0, which may have appeared as somewhat arbitrary in the previous section, can be justified as follows: only the contribution of u_f in the RVM system appears in the nonlinear part of the interaction term $F[f]\cdot\nabla_\xi f$. It is obviously the most critical part of the electromagnetic field to be controlled in the mean-field limit.

Let us recall that the forward fundamental solution of the wave equation in $\mathbf{R}_t \times \mathbf{R}^3_x$ is given by

$$\text{(6)} \qquad Y := \frac{\mathbf{1}_{t>0}}{4\pi t}\delta(|x| - t)\,.$$

By Kirchhoff's formula giving the solution of the Cauchy problem for the wave equation in $\mathbf{R}_t \times \mathbf{R}^3_x$, one has

$$F[f] = \int K(\xi,\eta) \star_{t,x} f(d\eta) + S \star_x \int f^{in}(d\eta)\,,$$

where

$$K(\xi,\eta) := -(\nabla_x + v(\eta)\partial_t) Y - v(\xi)\times(v(\eta)\times\nabla_x) Y$$

$$S(t) := -\nabla_x \partial_t Y(t,\cdot) \star_x \Gamma$$

and where

$$\Gamma(x) := \frac{1}{4\pi|x|}$$

is the fundamental solution of $-\Delta$ vanishing as $|x| \to \infty$. Therefore the system (5) can be recast as

$$\text{(7)} \qquad \begin{cases} \partial_t f + v(\xi)\cdot\nabla_x f + F[f]\cdot\nabla_\xi f = 0\,, \quad f\big|_{t=0} = f^{in} \\ F[f] = \displaystyle\int K(\xi,\eta)\star_{t,x} f(d\eta) + S\star_x \int f^{in}(d\eta) \end{cases}$$

3.3. **The regularized RVM system.** At this point, we seek to replace the fundamental solution Y by a regularized variant — much in the same way that Braun and Hepp considered the mean-field limit for the Vlasov-Poisson system, with the Coulomb potential replaced by a C_b^2 function.

Let $\chi \in C_c^\infty(\mathbf{R}^3)$ satisfy

$$\chi(x) = \chi(-x) \geq 0\,, \quad \operatorname{supp}\chi \subset B(0,1)\,, \quad \int_{\mathbf{R}^3} \chi(x)dx = 1$$

and define the regularizing sequence $\chi_\epsilon(x) := \epsilon^{-3}\chi(x/\epsilon)$.

Set

$$Y_\epsilon := \chi_\epsilon \star_x \chi_\epsilon \star_x Y$$

for each $\epsilon > 0$.

The regularized RVM system is

$$\text{(8)} \qquad \begin{cases} \partial_t f_\epsilon + v(\xi)\cdot\nabla_x f_\epsilon + F_\epsilon[f_\epsilon]\cdot\nabla_\xi f_\epsilon = 0\,, \quad f_\epsilon\big|_{t=0} = f^{in}\,, \\ F_\epsilon[f_\epsilon] = \displaystyle\int K_\epsilon(\xi,\eta)\star_{t,x} f_\epsilon(d\eta) + S_\epsilon\star_x \int f^{in}(d\eta)\,, \\ K_\epsilon(\xi,\eta) = -(\nabla_x + v(\eta)\partial_t)Y_\epsilon - v(\xi)\times(v(\eta)\times\nabla_x)Y_\epsilon\,, \\ S_\epsilon(t,\eta) = -\nabla_x\partial_t Y_\epsilon(t,\cdot)\star_x \Gamma\,. \end{cases}$$

One might question the need for the double convolution by χ_ϵ in the regularization of the RVM system above. Obviously, replacing Y by $Y\star_x\chi_\epsilon$ in (7) would have been enough, since $Y\star_x\chi_\epsilon$ is as much a C^∞ function as Y_ϵ.

However, the seemingly unnecessary complication in considering Y_ϵ instead of $Y_\star\chi_\epsilon$ will pay its dividends when discussing the energy conservation. Observe that the regularized force is

$$F_\epsilon[f_\epsilon] = \chi_\epsilon\star_x E_\epsilon + v(\xi)\times(\chi_\epsilon\star_x B_\epsilon)$$

with

$$\begin{cases} \operatorname{div}_x B_\epsilon = 0 & \partial_t B_\epsilon + \operatorname{curl}_x E_\epsilon = 0\,, \\ \operatorname{div}_x E_\epsilon = \chi_\epsilon\star_x \rho_{f_\epsilon} & \partial_t E_\epsilon - \operatorname{curl}_x B_\epsilon = -\chi_\epsilon\star_x j_{f_\epsilon}\,. \end{cases}$$

(In other words, one convolution by χ_ϵ is used in the source terms of the Maxwell system for the electromagnetic field, while another convolution by χ_ϵ is used in the formula for the Lorentz force.)

The variation of kinetic energy is the work of the regularized force; it can be expressed as the integral of the inner product of the electric field by the current density.:

$$\begin{aligned}\frac{d}{dt}\iint_{\mathbf{R}^3\times\mathbf{R}^3} e(\xi) f_\epsilon dx d\xi &= \int_{\mathbf{R}^3} j_{f_\epsilon}\cdot(\chi_\epsilon \star_x E_\epsilon)dx \\ &= \int_{\mathbf{R}^3} (\chi_\epsilon \star_x j_{f_\epsilon})\cdot E_\epsilon dx \\ &= -\frac{d}{dt}\int_{\mathbf{R}^3} \tfrac{1}{2}(|E_\epsilon|^2+|B_\epsilon|^2)dx\,.\end{aligned} \tag{9}$$

In this chain of equalities, the first one is obtained by multiplying both sides of the Vlasov equation with $e(\xi)$ and integrating in x,ξ. Notice that the term involving the magnetic field

$$\begin{aligned}v(\xi)\times(\chi_\epsilon\star_x B_\epsilon)\cdot\nabla_\xi f_\epsilon &= \mathrm{div}_\xi(f_\epsilon v(\xi)\times(\chi_\epsilon\star_x B_\epsilon)) - f_\epsilon(\mathrm{curl}_\xi\, v)\cdot B_\epsilon \\ &= \mathrm{div}_\xi(f_\epsilon v(\xi)\times(\chi_\epsilon\star_x B_\epsilon))\end{aligned}$$

since $v=\nabla e$. By the same token, integrating by parts shows that

$$\int_{\mathbf{R}^3} e(\xi)\,(v(\xi)\times(\chi_\epsilon\star_x B_\epsilon)\cdot\nabla_\xi f_\epsilon)\,d\xi = -\int_{\mathbf{R}^3}\nabla e(\xi)\cdot(v(\xi)\times(\chi_\epsilon\star_x B_\epsilon))\,f_\epsilon d\xi = 0$$

which explains why the contribution of the magnetic field to the work of the Lorentz force is identically 0.

The key obseration in (9) is of course the second equality, which is a consequence of the fact that χ_ϵ is even. In other words, the operator $\phi\mapsto\phi\star\chi_\epsilon$ is self-adjoint on $L^2(\mathbf{R}^3)$ because χ_ϵ is even, as one can check by a straightforward application of the Fubini theorem.

The following result is an almost immediate consequence of the Cauchy-Lipschitz theorem, and of the method of characteristics for the transport equation.

Theorem 3.1. *For any $f^{in}\in\mathcal{P}(\mathbf{R}^3_x\times\mathbf{R}^3_\xi)$ satisfying*

$$\iint_{\mathbf{R}^3\times\mathbf{R}^3} e(\xi) f^{in}(dxd\xi) < \infty\,,$$

there exists a unique solution $f_\epsilon\in C(\mathbf{R}_+; w-\mathcal{P}(\mathbf{R}^3_x\times\mathbf{R}^3_\xi))$ of the regularized RVM system (8) satisfying

$$\iint_{\mathbf{R}^3\times\mathbf{R}^3} e(\xi) f_\epsilon(t,dxd\xi) + \int_{\mathbf{R}^3}\tfrac{1}{2}(|E_\epsilon|^2+|B_\epsilon|^2)(t,x)dx = \textit{Const.}$$

The regularization by $\chi_\epsilon\star\chi_\epsilon$, i.e. the idea of replacing Y by Y_ϵ (instead of $Y\star_x\chi_\epsilon$, which would have been a simpler choice) has been proposed[1] in [17].

4. The particle system and the mean-field limit

4.1. **The particle system.** We consider a system of N particles with positions $x_1(t),\dots,x_N(t)$ and momenta $\xi_1(t),\dots,\xi_N(t)\in\mathbf{R}^3$ at time t, whose evolution is

[1] G. Rein kindly informed me that he learned this idea from E. Horst's Habilitationsschrift.

governed by the system of differential equations

$$(10)\qquad \begin{cases} \dot{x}_i = \xi_i \\ \dot{\xi}_i = \dfrac{1}{N}\displaystyle\sum_{j=1}^{N} S_\epsilon(t, x_j(0)) + \frac{1}{N}\sum_{j=1}^{N}\int_0^t K(t-s, x_j(s), \xi_i(t), \eta_j(s))ds \end{cases}$$

Because of the finite speed of propagation for solutions of the wave equation, this is a nonlocal *delay* differential equation, at variance with the particle system for the Vlasov-Poisson case, which is an ordinary differential equation — and more precisely a Hamiltonian system.

Lemme 4.1. *The $2N$-tuple $t \mapsto (x_1, \xi_1, \dots, x_N, \xi_N)(t)$ is a solution of the particle system if and only if the phase-space empirical measure*

$$f_{\epsilon,N} = \frac{1}{N}\sum_{i=1}^{N} \delta_{x_i(t)} \otimes \delta_{\xi_i(t)}$$

satisfies

$$\begin{cases} (\partial_t + v(\xi)\cdot\nabla_x) f_{\epsilon,N} + F_\epsilon[f_{\epsilon,N}]\cdot\nabla_\xi f_{\epsilon,N} = 0\,, \quad f_{\epsilon,N}\big|_{t=0} = f_N^{in} \\ F_\epsilon[f_{\epsilon,N}] = \displaystyle\int K_\epsilon(\xi,\eta) \star_{t,x} f_{\epsilon,N}(d\eta) + S_\epsilon \star_x \int f_N^{in}(d\eta) \end{cases}$$

In other words, the $2N$-tuple $t \mapsto (x_1, \xi_1, \dots, x_N, \xi_N)(t)$ is a solution of the particle system (10) if and only if the associated phase-space empirical measure is a solution of the regularized RVM system (8). This property is obviously essential, since it reduces the proof of the mean-field limit of the particle system (10) to the continuous dependence of the solution of (8) in terms of the initial data for the weak topology of probability measures.

4.2. **The Monge-Kantorovich distance.** We first recall the notion of Monge-Kantorovich distance, which we shall be using in the convergence rate for the mean-field limit. The notation $\mathcal{P}(\mathbf{R}^d)$ denotes the set of Borelt probability measures on $\mathbf{R}^d$.

Definition 4.2 (Monge-Kantorovich distance W_1)**.** *For $\mu, \nu \in \mathcal{P}(\mathbf{R}^6)$ s.t.*

$$\int_{\mathbf{R}^6} (|x| + |\xi|)(\mu(dxd\xi) + \nu(dxd\xi)) < \infty\,,$$

let $\Pi(\mu,\nu)$ be the set of $\pi \in \mathcal{P}(\mathbf{R}^6 \times \mathbf{R}^6)$ satisfying

$$\iint_{\mathbf{R}^6\times\mathbf{R}^6} (\phi(x,\xi) + \psi(y,\eta))\pi(dxd\xi dyd\eta) = \int_{\mathbf{R}^6} \phi(x,\xi)\mu(dxd\xi) + \int_{\mathbf{R}^6} \psi(y,\eta)\nu(dyd\eta)$$

for each $\phi, \psi \in C_b(\mathbf{R}^6)$, and

$$W_1(\mu,\nu) = \inf_{\pi\in\Pi(\mu,\nu)} \iint (|x-y| + |\xi-\eta|)\pi(dxd\xi dyd\eta)\,.$$

An important result (obtained by convex duality) is the following identity, due to Kantorovich (see [19], Theorem ???).

$$W_1(\mu,\nu) = \sup_{\mathrm{Lip}(\phi)\leq 1} \left| \int \phi(x,\xi)(\mu-\nu)(dxd\xi) \right| .$$

4.3. **Propagation of the convergence rate.** The main result in [7] is the following quantitative mean-field limit for the regularized RVM system (8).

Theorem 4.3. *Let $x_1^{in},\dots,x_N^{in},\xi_1^{in},\dots,\xi_N^{in} \in B(0,R)$ and let $f^{in} \in \mathcal{P}(\mathbf{R}^6)$ satisfy $\mathrm{supp}(f^{in}) \subset B(0,R)$. Let $x_1,\dots,x_N,\xi_1,\dots,\xi_N$ be the solution of the particle system with initial data $x_1^{in}\dots,x_N^{in},\xi_1^{in},\dots,\xi_N^{in}$, and let f be the solution of RVM with initial data f^{in}.*

Then

$$W_1\left(f(t),\frac{1}{N}\sum_{i=1}^N \delta_{(x_i(t),\xi_i(t))}\right) \leq W_1\left(f^{in},\frac{1}{N}\sum_{i=1}^N \delta_{(x_i^{in},\xi_i^{in})}\right)$$
$$\times(1+A[\epsilon,R,m])(1+t)^4\exp(\tfrac{1}{5}(1+A[\epsilon,R,m])(1+t)^5)$$

for all $t \geq 0$.

The initial positions and $x_1^{in},\dots,x_N^{in},\xi_1^{in},\dots,\xi_N^{in}$ can be chosen by applying some variant of the strong law of large numbers: we shall return to this later.

4.4. **An Eulerian proof of Theorem 4.3.** The main novelty in this paper is the strategy used in the proof of Theorem 4.3, which avoids the slightly unpleasant construction of the mean-field delay flow in section 4 of [7] — see in particular Proposition 4.1 there.

The key idea is to replace the formulation of the problem in terms of characteristics as in [7] by a purely Eulerian (PDE) approach, as in [8].

It should be mentioned[2] that the idea of writing a PDE governing the dynamics of couplings of two solutions of a porous media equation appeared earlier in a paper by Otto and Westdickenberg [16]. Perhaps the idea of using the Eulerian formulation on a transport equation such as the Vlasov equation was less immediate, since the Lagrangian formulation is more natural in the context of kinetic models.

4.4.1. *Propagation of couplings.* First, we write a PDE governing the propagation of couplings of two solutions of the regularized RVM system (8).

Lemme 4.4. *Let $f^{in},g^{in} \in \mathcal{P}(\mathbf{R}^6)$ be compactly supported, and let f and g the solutions of RVM with initial data f^{in} and g^{in} respectively. Let $\pi^{in} \in \Pi(f^{in},g^{in})$, and let π be the (weak) solution of the transport equation*

$$\text{(11)} \qquad \begin{cases} \partial_t\pi = -\operatorname{div}_x(\pi v(\xi)) - \operatorname{div}_y(\pi v(\eta)) \\ \qquad\qquad - \operatorname{div}_\xi(\pi F_\epsilon[f](t,x,\xi)) - \operatorname{div}_\eta(\pi F_\epsilon[g](t,y,\eta)) , \\ \pi\big|_{t=0} = \pi^{in} . \end{cases}$$

Then $\pi(t) \in \Pi(f(t),g(t))$ for all $t \geq 0$.

[2] I am indebted to L. Ambrosio for this reference.

Proof. By finite speed of propagation, $\operatorname{supp}\pi(t)$ is compact for all $t \geq 0$. Averaging both sides of the π-equation in y, η (resp. in x, ξ) leads to the equations

$$\partial_t \pi_1 = -\operatorname{div}_x(\pi_1 v(\xi)) - \operatorname{div}_\xi(\pi_1 F_\epsilon[f](t,x,\xi))\,, \quad \pi_1\big|_{t=0} = f^{in}\,,$$
$$\partial_t \pi_2 = -\operatorname{div}_y(\pi_2 v(\eta)) - \operatorname{div}_\eta(\pi_2 F_\epsilon[g](t,y,\eta))\,, \quad \pi_2\big|_{t=0} = g^{in}\,,$$

for the first and second marginals of $\pi(t)$ (corresponding to the product $\mathbf{R}^6_{x,\xi}\times\mathbf{R}^6_{y,\eta}$).

Hence the marginals of π satisfy

$$\pi_1 = f\,, \qquad \text{and} \qquad \pi_2 = g$$

by uniqueness of the solution of the Cauchy problem for the transport equation in phase-space. □

4.4.2. *An integral inequality for $W_1(f(t), g(t))$.* Given $t \mapsto \pi(t) \in \mathcal{P}(\mathbf{R}^6 \times \mathbf{R}^6)$, we define the quantity

$$D[\pi](t) := \iint\!\!\iint (|x-y| + |\xi-\eta|)\pi(t, dxd\xi dyd\eta)\,.$$

Multipling each side of (11) by $|x-y| + |\xi-\eta|$, and integrating by parts in x, ξ, y, η, we see that $D[\pi](t)$ satisfies the differential equality

$$\frac{dD[\pi]}{dt} = \iint\!\!\iint (v(\xi) - v(\eta)) \cdot \frac{x-y}{|x-y|}\pi(t, dxd\xi dyd\eta)$$
$$\iint\!\!\iint (F_\epsilon[f](t,x,\xi) - F_\epsilon[g](t,y,\eta)) \cdot \frac{\xi-\eta}{|\xi-\eta|}\pi(t, dxd\xi dyd\eta)$$
$$=: I + J\,.$$

(There is not difficulty with the behavior of the integrand as $|x|+|\xi|+|y|+|\eta| \to \infty$ since $\pi(t)$ is compactly supported for all $t \geq 0$, as noticed above.)

Next we estimate I and J separately. Observe that

$$\nabla v(\xi) = \frac{(1+|\xi|^2)I - \xi\otimes\xi}{(1+|\xi|^2)^{3/2}} \quad \text{ so that } |\nabla v(\xi)| \leq 2\,.$$

Hence

$$|I| \leq 2\iiiint |\xi-\eta|\pi(t, dxd\xi dyd\eta) \leq 2D[\pi](t)\,.$$

Now for J: split J as

$$J = \iint\!\!\iint (F_\epsilon[f](t,x,\xi) - F_\epsilon[f](t,y,\eta)) \cdot \frac{\xi-\eta}{|\xi-\eta|}\pi(t, dxd\xi dyd\eta)$$
$$+ \iint\!\!\iint (F_\epsilon[f](t,y,\eta) - F_\epsilon[g](t,y,\eta)) \cdot \frac{\xi-\eta}{|\xi-\eta|}\pi(t, dxd\xi dyd\eta)$$
$$=: J_1 + J_2\,.$$

The term J_1 is controlled by

$$|J_1| \leq \operatorname{Lip}(F_\epsilon[f])(t) \iiiint (|x-y| + |\xi-\eta|)\pi(t, dxd\xi dyd\eta)$$
$$= \|F_\epsilon[f]\|_{W^{1,\infty}_x}(t) D[\pi](t)\,.$$

The term J_2 is controlled by

$$|J_2| \le \iiiint |F_\epsilon[f] - F_\epsilon[g]|(t,y,\eta)\pi(t,dxd\xi dyd\eta)$$
$$= \iint |F_\epsilon[f] - F_\epsilon[g]|(t,y,\eta)g(t,dyd\eta)$$
$$\le \|F_\epsilon[f-g]\|_{L^\infty}(t)\,.$$

At this point, we use the Sobolev embedding theorem. Choosing $m > \frac{3}{2}$, there exists a positive constant C_m such that

$$\|\nabla_{x,\xi} F_\epsilon[f]\|_{W^{1,\infty}_x}(t) \le 3C_m(\|\nabla_x E_\epsilon[f]\|_{H^m_x} + \|\nabla_x B_\epsilon[f]\|_{H^m_x})(t)\,,$$

while

$$\|F_\epsilon[f-g]\|_{L^\infty}(t) \le C_m(\|E_\epsilon[f-g]\|_{H^m_x} + \|B_\epsilon[f-g]\|_{H^m_x})(t)\,.$$

The electromagnetic field $(E_\epsilon[f], B_\epsilon[f])$ is defined in terms of f by solving the linear hyperbolic system

$$\partial_t E_\epsilon[f] - \mathrm{curl}_x\, B_\epsilon[f] = -\chi_\epsilon \star \chi_\epsilon \star_x \int v(\xi) f(d\xi)\,,$$
$$\partial_t B_\epsilon[f] + \mathrm{curl}_x\, E_\epsilon[f] = 0\,,$$

with initial data

$$E_\epsilon[f]\big|_{t=0} = -\nabla_x(-\Delta_x)^{-1}\chi_\epsilon \star_x \chi_\epsilon \star_x \int f^{in}(d\xi)\,, \quad B_\epsilon[f]\big|_{t=0} = 0\,.$$

This system is equivalent to Maxwell's system of equations provided that f satisfies the continuity equation (i.e. the local conservation law of charge):

$$\partial_t \rho[f] + \mathrm{div}_x\, j[f] = 0\,,$$

where we denote

$$(\rho, j)[f] := \int (1, v(\xi)) f(d\xi)\,, \quad (\rho_\epsilon, j_\epsilon)[f] := \chi_\epsilon \star_x \chi_\epsilon \star_x (\rho, j)[f]\,.$$

Indeed, the two missing equations, i.e. the Gauss equation and the absence of magnetic monopoles

$$\mathrm{div}_x\, E_\epsilon[f] = \rho_\epsilon[f]\,, \qquad \mathrm{div}_x\, B_\epsilon[f] = 0$$

are consequences of the identities

$$\partial_t\, \mathrm{div}_x\, E_\epsilon[f] = -\,\mathrm{div}_x\, j_\epsilon[f]\,, \quad \partial_t\, \mathrm{div}_x\, B_\epsilon[f] = 0\,,$$

of the continuity equation and of the initial data.

The energy balance for the above system takes the form

$$\frac{d}{dt}(\|E_\epsilon[f]\|^2_{L^2_x} + \|B_\epsilon[f]\|^2_{L^2_x})(t) = -2\int E_\epsilon[f](t,x)\cdot j_\epsilon[f](t,dx)$$
$$\le 2(\|E_\epsilon[f]\|^2_{L^2_x} + \|B_\epsilon[f]\|^2_{L^2_x})^{1/2}(t)\|j_\epsilon[f]\|_{L^2_x}(t)\,.$$

Applying this to $(I-\Delta_x)^m(E_\epsilon[f], B_\epsilon[f])$, we see that

$$(\|E_\epsilon[f]\|^2_{H^m_x}(t) + \|B_\epsilon[f]\|^2_{H^m_x})^{1/2}(t)$$
$$\le \|E_\epsilon[f]\|_{H^m_x}(0) + \int_0^t \|j_\epsilon[f]\|_{H^m_x}(s)ds\,.$$

With this inequality, we immediately estimate J_1 as follows: for each $t \geq 0$,

$$|J_1| \leq 3C_m(1+t)\|\chi_\epsilon \star_x \chi_\epsilon\|_{H^{m+1}} D[\pi](t)\,.$$

We estimate J_2 in the same way:

$$|J_2| \leq \sqrt{2}C_m\|\nabla(-\Delta)^{-1}\chi_\epsilon\|_{H^m}\|\chi_\epsilon \star_x \rho[f^{in}-g^{in}]\|_{L^1} + \sqrt{2}C_m\|\chi_\epsilon\|_{H^m}\int_0^t \|\chi_\epsilon \star_x j[f-g]\|_{L^1}(s)ds\,.$$

By Kantorovich duality, one has

$$\left|\chi_\epsilon \star_x \rho[f^{in}-g^{in}]\right| \leq \|\nabla\chi_\epsilon\|_{L^\infty} W_1(f^{in},g^{in})\,,$$
$$|\chi_\epsilon \star_x j[f-g]| \leq 3\|\chi_\epsilon\|_{W^{1,\infty}} W_1(f,g)$$

for all $t \geq 0$. Moreover, by finite speed of propagation, one has also

$$\mathrm{supp}(f^{in},g^{in}) \subset \bar{B}(0,R)\times\mathbf{R}^3 \Rightarrow \mathrm{supp}(f(t),g(t)) \subset \bar{B}(0,R+t)\times\mathbf{R}^3$$

for all $t \geq 0$. Hence

$$|J_2| \leq \tfrac{4\sqrt{2}}{3}\pi R^3 C_m\|\nabla(-\Delta)^{-1}\chi_\epsilon\|_{H^m}\|\nabla\chi_\epsilon\|_{L^\infty} W_1(f^{in},g^{in}) + 4\sqrt{2}\pi(R+t)^3 C_m\|\chi_\epsilon\|_{H^m}\|\chi_\epsilon\|_{W^{1,\infty}}\int_0^t W_1(f(s),g(s))ds$$

Eventually, we arrive at the following differential inequality for $D[\pi](t)$:

$$\frac{dD[\pi]}{dt} \leq (2+3C_m a_\epsilon(1+t))D[\pi](t) + \tfrac{4\sqrt{3}}{3}\pi R^3 C_m^2 a_\epsilon^2 W_1(f^{in},g^{in}) + 4\pi(R+t)^3 C_m^2 a_\epsilon^2\int_0^t D[\pi](s)ds\,,$$

where

$$a_\epsilon := \|\chi_\epsilon\|_{H^{m+1}} + \|\nabla(-\Delta)^{-1}\chi_\epsilon\|_{H^{m+1}}\,.$$

Integrating on $[0,t]$ both sides of the inequality

$$\frac{dD[\pi]}{dt}(t) \leq A[\epsilon,R,m](1+t)^3\left(D[\pi](t)+\int_0^t D[\pi](s)ds + D[\pi](0)\right)$$

leads to the integral inequality

$$D[\pi](t) \leq (1+A[\epsilon,R,m])(1+t)^4\left(D[\pi](0)+\int_0^t D[\pi](s)ds\right)$$

for all $t \geq 0$.

By Gronwall's lemma, we conclude that

$$W_1(f(t),g(t)) \leq D[\pi](t) \leq D[\pi](0)(1+A[\epsilon,R,m])(1+t)^4\exp(\tfrac{1}{5}(1+A[\epsilon,R,m])(1+t)^5)$$

Notice that the first inequality above follows from the definition of W_1 as an inf.

We conclude by minimizing the right hand side of the second inequality above over all initial couplings $\pi(0) \in \Pi(f^{in},g^{in})$. This concludes the proof of Theorem 4.3.

5. Conclusions

We have extended the Dobrushin quantitative estimate for the mean-field limit in the case of Lipschitz forces with infinite speed of propagation to an analogue of the Vlasov-Maxwell system with "blob"-type charged particles.

At variance with the Vlasov-Poisson case, the analogous problem with point charges does not seem to be physically relevant because of the difficulties with the self-interaction in classical electrodynamics. Self-interaction is a well-identified difficulty in electrodynamics, and has been studied in depth. The interested reader is referred in particular to chapter 2 in [18] for a mathematical description of the difficulty related to the self-interaction in classical (i.e. non quantum) electrodynamics. A more physical description of this difficulty can be found in chapter 28-4 of [6] — see also chapter 3 in [18] for a very interesting and detailed historical discussion on this problem. The idea of smearing the charge as done in the present paper is due to Abraham [1], and the particle dynamics described in (10) is referred to as "Abraham's system": see chapters 11 and 2.4 in [18].

Otherwise, the ultimate goal of this line of research is obviously to produce a rigorous justification for the RVM system on the basis of a first principle, microscopic description of the dynamics of charged particles. (Whether the Abraham system can be regarded as such a first principle equation for the dynamics of charged particles is of course highly debatable.) The most natural idea is of course to let the cutoff parameter ϵ vanish as $N \to \infty$. As indicated in Proposition 6.2 in [7], weak solutions of the RVM system are limits of subsequences of the family of empirical measures built on solutions of the Abraham system (10). While Proposition 6.2 in [7] does not specify the rate of convergence in this limit, it can be readily estimated from Theorem 5.1 (the main result in [7]). The best (smallest) "particle radius" (i.e. cutoff parameter ϵ) obtained by using the method in [7] is found to be of order $1/\sqrt{\ln N}$ — which is of course too large to be of much physical relevance. At the time of this writing, the best result on the derivation of the RVM system from Abraham's dynamics is Theorem 5.3 in [13]. Lazarovici uses several ideas from [7], together with additional, more elaborate estimates on the electromagnetic field, by which he can handle particles with a radius of order $N^{-1/2}$. The method of proof used in [13] involves particle paths, and is rather technical. Perhaps the Eulerian approach proposed here could help simplifying the analysis in [13].

References

[1] Abraham, M.: *Prinzipien der Dynamik des Elektrons*. Ann. Physik **10**, 105–179, (1903)

[2] Bouchut, F., Golse, F., Pallard, C.: *Classical solutions and the Glassey-Strauss theorem for the 3D Vlasov-Maxwell system*. Arch. Rat. Mech. Anal. **170**, 1–15, (2003)

[3] Braun, W., Hepp, K.: *The Vlasov dynamics and its fluctuations in the 1/n limit of interacting classical particles*. Commun. Math. Phys. **56**, 101–113, (1977)

[4] Dobrushin, R.L.: *Vlasov equations*. Func. Anal. Appl. **13**, 115–123; (1979)

[5] Elskens, Y., Kiessling, M.K.-H., Ricci, V.: *The Vlasov limit for a system of particles which interact with a wave field*. Commun. Math. Phys. **285**, 673–712, (2009)

[6] Feynman, R.:

[7] Golse, F.: *The mean-field limit for a regularized Vlasov-Maxwell dynamics*. Commun. Math. Phys. **310**, 789–816, (2012)

[8] Golse, F., Mouhot, C., Paul, T.: *On the Mean Field and Classical Limits of Quantum Mechanics*. Commun. Math. Phys. **343**, 165–205, (2016)

[9] Hauray, M., Jabin, P.-E.: *Particle approximation of Vlasov equations with singular forces*. Ann. Sci. Ecol. Norm. Sup. **48**, 891–940, (2015)

[10] Fournier, N., Guillin, A.: *On the rate of convergence in Wasserstein distance of the empirical measure*. Probab. Theory Rel. Fields **162**, 707–738, (2015)

[11] Landau, L.D., Lifshitz, E: "The Classical Theory of Fields", Course in Theoretical Physics Vol. 2, 4th Revised English Ed. Butterworth-Heinemann, 1994.

[12] Lazarovici, D.: *The VlasovPoisson dynamics as the mean-field limit of rigid charges*. `arXiv:1502.07047` (preprint)

[13] Lazarovici, D.: *A particle approximation for the relativistic Vlasov-Maxwell dynamics*. `arXiv:1602.07251` (preprint)

[14] Lazarovici, D., Pickl, P.: *A mean-field limit for the VlasovPoisson system*. `arXiv:1502.04608` (preprint)

[15] Neunzert, H., Wick, J.: *Die Approximation der Lösung von Integro-Differentialgleichungen durch endliche Punktmengen*. Lecture Notes in Math. Vol. 395, Springer, Berlin, 1974, pp. 275–290

[16] Otto, F., Westdickenberg M.: *Eulerian calculus for the contraction in the Wasserstein distance*. SIAM J. Math. Anal. **37**, 1227–1255, (2005)

[17] Rein, G.: *Global weak solutions of the relativistic Vlasov-Maxwell system revisited*. Commun. Math. Sci. **2**, 145–158, (2004)

[18] Spohn, H.: "Dynamics of Charged Particles and their Radiation Fields". Cambridge University Press, 2004

[19] Villani, C.: "Topics in Optimal Transportation". Amer. Math. Soc., Providence RI, 2003

Cancer development: a population theoretical perspective

M. Delitala[1*], M. Ferraro[2] and E. Piretto[1]

1- Politecnico di Torino, Dipartimento di. Scienze Matematiche,
corso Duca degli Abruzzi 24, 10129 Torino, Italy

2- Università di Torino, Dipartimento di Fisica,
via P. Giuria 1, 10125 Torino, Italy

* Politecnico of Turin, dip. Scienze Matematiche,
corso Duca degli Abruzzi 24, 10129 Torino, Italy
e-mail: marcello.delitala@polito.it; Tel: 0110907537

In the history of life, immune system and cancer have been engaged in an evolutionary arms race driven by the twin forces of mutation and selection. Ideally therapies should be a resolutive weapon, but, despite great progresses during the last 50 years or so, the race still goes on. The aim of this paper is to present a mathematical model, which can be used as in silico laboratory, to provide some indication on the effectiveness of therapies. Here we focus on two cancer populations competing for resources and subjected to the action of two types of immune system cells: thus the model results in a system of 4 differential equation that is analytically and computationally studied to elucidate its properties and emerging behaviors. At the beginning, some specific subsystems are analyzed and the effects of different therapies simulated; in particular first the system comprising a single cancer and immune cells type is considered and next the case of two cancer clones in absence of the immune cells. The complete model is then presented, which yields a rich variety of behaviors; in particular it is shown that for strong intertumoral competition, and high recognition levels by the immune system, stable stationary states are replaced by sustained oscillations. Finally some conclusion about therapy effectiveness are drawn, based on the results of simulations.

Keywords: Cancer Modeling and Therapies, Population Dynamics, In Silico Laboratory, Tumor Immune Interaction.

1 Introduction

Cancer is an evolutionary disease, an idea originated from the seminal work by Nowell [1] which has become nowadays commonplace and has exerted a profound influence not just on our understanding of cancer emergence but also on the development of antitumoral therapies [2, 3, 4, 5].

Indeed it has become clear that the blind processes, through which we and other species have emerged, carry with them inevitable limitations, and trade-offs which, for accidental or adaptive reasons, make us susceptible to cancer or other diseases.

Tumorigenesis is intrinsically multiscale, in that emerging phenomena at the macroscopic level express a self-organizing ability, resulting from the interactions between entities at the microscopic level. For instance selection of successful subclones emerges from the dynamics at the cellular and sub cellular level and shapes macroscopic features of the cellular populations and their environment. Emerging characteristics are then the outcome of bottom-up process, from lower to higher level representations. On the other hand, top-down mechanisms may also operates (the so-called ”immergence”), thus closing a feedback loop: the emerging patterns may affect and perturb the lower levels. For instance, the environment (macroscopic level) acts on the cellular (microscopic) level.

At the molecular level cancer arises during the replication and recombination of genes, processes that may result in the occurrence of occasional deleterious mutations, including those that can initiate cancer: DNA damages continuously arise and, even though they are are balanced by DNA-repair functions, the net result is still a vulnerability to cancer [6].

Evolutionary pressures work also at the macroscopic level: interactions between organisms and cancer have existed from the early stages of multicellular

life and have shaped the evolution of complex organisms. The need to suppress cancer has played an important part in how multicellular organisms have evolved: powerful protecting mechanisms have been necessary to allow the development of animals with large bodies and long lives. On the other hand tumor types have emerged which have developed resistance to the immune system and, nowadays, therapy [7]. Thus, in the history of life, immune system and cancer have been engaged in an evolutionary arms race driven by the twin forces of mutation and selection.

Mutations do not just produce cancer cells but they are clearly at the hearth of cancer heterogeneity, which has has been invoked to explain one of major aspects of cancer development, namely acquired drug resistance, by which phases of remission are often followed by a rapid growth of tumor cells. Mutations ensure that, even though therapies exist that can decimate a cancer cell population, one or more variants are present in the tumor population which are resistant, leading to the resurgence of treatment-refractory disease [8] . In turn, natural selection promotes cell clones that have acquired advantageous heritable characteristics [8].

The emerging picture, then, is that of coexisting cancer populations, embedded in an environment comprising normal and immunes system cells [9]. Interactions with environmental factors clearly shape the growth, or otherwise, of the different tumor types, so in this sense it is possible to talk of an ecology of cancer [10],[11].

Environment operates a selection of cancer cells in two ways: they compete for resources and are selectively attacked by immune cells. The fitness of tumor species, i.e. the ability to adapt and grow, depends on how effectively it outcompetes the others and how successfully develops mechanism to escape detection and elimination by the immune system.

This suggest that a basic way to investigate the effects of evolutionary factors in tumor development is provided by the theory of populations which takes naturally into account different environmental factors such as finiteness of resources, competition between species and predation. A population theoretical approach is used in the present paper: two competing types of cancer are considered together with a pair of immune system clones, each specific for one cancer species. Thus the model takes into account cancer heterogeneity and the interaction among clones.

The model presented here is, admittedly, a drastic simplification of the processes underlying cancer evolution, and, in some sense, can be considered a minimal model that takes into account some of the important factors involved in cancer development, i.e. the activity of immune system, the competition between cancer species and effects of medical treatments.

Given the relevance of the problem it is not surprising that multifaceted aspects of cancer have been the focus of much theoretical and experimental work: more relevantly for the work presented here is the fact that a variety of mathematical tools has been used to model cancer dynamics and the effects of therapies, among them differential equations [12, 13, 14, 15, 15, 16, 17, 18, 19], stochastic models [20, 21, 22], theory of games [23, 24, 25]. For a review see for instance and references therein [26, 27, 28].

In the literature there exist models considering the effects of specific aspect of cancer in greater detail than is done here; for instance, as concerns the interaction of cancer with the immune system, see and the review in [26].

However, at best of our knowledge the present work is the first to bring to-

However, at best of our knowledge the present work is the first to bring together the aspects of immune action with the competition between different clones, both of cancer and immune cells.

In the next section the model will be presented, and in the next two sections specific subsystems will be presented: subsection 3.1 will consider just one cancer type together with the corresponding immune system cells to study in detail the effect of the "predation" term, while in 3.2 the effect of the competition between cancer clones will be considered.

In subsection 3.3 all elements of the models, i.e. competition and predation are brought together and the resulting emergent properties of cancer populations are discussed.

Finally section 4 provides some conclusions and research perspectives.

2 Material and Methods

This section provides the mathematical formalization of the model: two competing types of cancer are considered together with two types of immune system cells, each detecting and attacking a specific cancer species.

In the following $x_1 = x_1(t)$, $x_2 = x_2(t)$ will denote, when ambiguity does not arise, both the tumor types and their numerousness and the variables $z_1 = z_1(t)$ and $z_2 = z_2(t)$ will represent the types and numerousness of the immune system cells.

A natural way to model the evolution of interacting populations is via a system of differential equations [29]; we have adopted this approach here, and, in conclusion, the system comprises four equations, two describing the evolution of the

cancer clones, whereas the others model the dynamics of corresponding clones of the immune system.

As argued before equation of model must contain competition and predation terms, and the equations are follows:

$$\begin{aligned}
\frac{dx_1}{dt} &= \underbrace{r_1 x_1}_{proliferation} \underbrace{- \frac{b_{11}}{K_1} x_1^2 - \frac{b_{12}}{K_1} x_1 x_2}_{competition} \underbrace{- \frac{c_1}{K_1} x_1 z_1}_{predation}, \\
\frac{dx_2}{dt} &= r_2 x_2 - \frac{b_{22}}{K_2} x_2^2 - \frac{b_{21}}{K_2} x_1 x_2 - \frac{c_2}{K_2} x_2 z_2, \\
\frac{dz_1}{dt} &= \underbrace{\beta_1 z_1}_{proliferation} + \underbrace{\frac{\alpha_1}{H} x_1 z_1}_{recognition} \underbrace{- \gamma z_1 \left(\frac{z_1 + z_2}{H} \right)}_{competition} \\
\frac{dz_2}{dt} &= \beta_2 z_2 + \frac{\alpha_2}{H} x_2 z_2 - \gamma z_2 \left(\frac{z_1 + z_2}{H} \right),
\end{aligned} \tag{1}$$

where all parameters are supposed to be positive.

Consider tumor species x_1, with net reproduction rate $r_1 = b_1 - d_1$, b_1 and d_1 being the birth and death rate, respectively. In absence of other cancer species and of the immune system, x_1 growth is limited solely by intra-specific competition, represented by term $b_{11}x_1^2/K_1$. Setting $b_{11} = r_1$, the maximum value x_1 can attain is K_1, which then plays the role of carrying capacity [29]. In the full system the growth of x_1 is further limited by inter-specific competition for resources (measured by the term $b_{12}x_1x_2/K_1$), and by the interaction with the immune system (the term $c_1x_1z_1/K_1$).

We turn now our attention to the immune system. Growth of z_1 is due to two factors: it is produced by the organism with a net rate β_1 and it is further enhanced

by the interaction with the tumor x_1, weighted by the parameter α_1, which can be thought of as measure of how well immune cells detect and recognize cancer cell. Finally intra and inter-specific competitions between cells of immune system limit the growth of z_1. As before, in isolation, H is the carrying capacity of z_1. The case for species x_2 and z_2 is similar.

This system of equations can be modified in a simple way to take into account the response of cancer cells to medical treatments. For instance the effect of drugs reducing rates of growth r_i, $i = 1, 2$, such as many types of chemotherapies, [30] can be modelled by adding to equations describing cancer evolution a term of the form $-g_i(t)x_i$, (see [12]) where $g_i(t)$ account for the drugs kinetics in the organism. This is equivalent to define a new growth rate $r_i' = r_i - g_i(t) = b_i - d_i - g_i(t)$: if $r_i' < 0$ the number of tumor cells x_i decreases, to grow again when the concentration of the drug becomes lower than some threshold g_{th}. Time course of g can be modeled, for instance, with methods of the compartment theory, but to keep the treatment simple here g will be assumed to be constant, corresponding to a situation in which drugs are administered continuously so that g does not vary much. The other end of the spectrum is represented by therapies where drugs are dispensed in sequences of relatively short bursts [13]; this kind of treatment will be also considered. Therapies reducing the rate of growth will be denoted, in the following, as r-terapies.

A different way to treat cancer is "starving" it by making more difficult for tumor cells to access resources: this is the idea, for instance, behind anti-angiogenesis therapies [31].

Here the effects of this kind of treatment will be simulated by decreasing the carrying capacities K_1, K_2 to lower values K_1', K_2': cures of this type will be called s-therapies.

Alternatively immune therapies, in the sequel denoted as $i-$therapies, can be adopted, which enhance the recogniton performance of immune system cells for instance [32, 33]. In the framework of the present model this corresponds to increase α_1 to new values α_1'.

Before presenting results of the complete system, in subsections 3.1 and 3.2 specific subsystems will be studied in the framework of different "experimental conditions": in other words the system will considered an *in silico* laboratory.

In all numerical explorations the time unit is one day (approximately the cell cycle). Simulations have been implemented using Mathematica®.

3 Results and Discussion

This section presents the results and discussion of theoretical and computational analysis of the model.

First some specific cases are studied (see subsections 3.1 and 3.2) and next properties of the general model are investigated (subsection 3.3).

3.1 One cancer type with immune system

In this section the focus is on the interaction between a single cancer species and the corresponding immune system cells: condition will be derived for the eradication or control of cancer by the action of the immune system.

To this aim we consider a subsystem of (1) comprising just a cancer type and the corresponding immune cells:

$$\begin{aligned} \frac{dx_1}{dt} &= r_1 x_1 - \frac{b_{11}}{K_1} x_1^2 - \frac{c_1}{K_1} x_1 z_1, \\ \frac{dz_1}{dt} &= \beta_1 z_1 + \frac{\alpha_1}{H} x_1 z_1 - \gamma z_1 \left(\frac{z_1}{H}\right), \end{aligned} \tag{2}$$

and to simplify the analysis we set $r_1 = b_{11}$, $\gamma_1 = \beta_1$: this way K_1 and H are the carrying capacity of x_1, z_1, when considered isolated systems.

This system of equations somehow simplifies more complete models, present in literature, see, for instance [26].

It is straightforward to show that in the phase space (x_1, z_1) there exist 4 stationary points of (2), which will be denoted by P_i, $i = 1, \ldots 4$ whose components are the stationary values x_1^*, z_1^*, of x_1, z_1 respectively

The stationary points are

$$\begin{aligned} P_1 : x_1^* &= 0, z_1^* = 0, \quad P_2 : x_1^* = K_1, z_1^* = 0, \quad P_3 : x_1^* = 0, \quad z_1^* = H, \\ P_4 : x_1^* &= \frac{\beta_1(K_1 r_1 - c_1 H)}{\alpha_1 c_1 + \beta_1 r_1}, z_1^* = \frac{r_1(\beta_1 H + \alpha_1 K_1)}{\alpha_1 c_1 + \beta_1 r_1}; \end{aligned} \tag{3}$$

of course, to have a biological meaning, P_4 components must be both positive and that occurs if and only if

$$r_1 > \frac{c_1 H}{K_1}. \tag{4}$$

Points P_1 and P_2 are unstable, as it can be easily shown by standards methods of stability analysis: P_1 is an unstable node and P_2 a saddle. More interesting are

the points P_3 and P_4 as they correspond, respectively, to tumor free and coexistence states.

The Jacobian matrix of the system at P_3 is

$$J(0,H) = \begin{bmatrix} r_1 - c_1 H/K_1 & 0 \\ \alpha_1 & -2\beta_1 \end{bmatrix}$$

thus the tumor free state is stable if and only if

$$-2\beta_1 \left(r_1 - \frac{c_1 H}{K_1} \right) > 0, \qquad -2\beta_1 + \left(r_1 - \frac{c_1 H}{K_1} \right) < 0$$

and both conditions are satisfied if

$$r_1 \leq \frac{c_1 H}{K_1}. \tag{5}$$

Condition (5) contrasts the growth rate r_1 to an "immunity coefficient" $c_1 H/K_1$ which in turn depends on how efficiently the immune system fights the tumor and on the ratio between the carrying capacity of z_1 and x_1 respectively. A similar coefficient, called "resistance coefficient" has been derived in [12].

Note that the condition making P_3 unstable also shifts the coexistence point P_4 in the positive quadrant of the phase space and analysis of the Jacobian matrix, calculated at P_4, shows that if $r_1 > c_1 H/K_1$ then P_4 is stable: in other words the same condition ensuring the existence of P_4 in the positive quadrant guarantees its stability, thus ruling out the existence of limit cycles.

The existence, or otherwise, of P_4 does not depend on the parameters α_1, β_1, which, however, affect the values of x_1^*, z_1^*, as shown by Eq. (3). The model then shows that even though parameters values do not satisfy condition (5) and

complete eradication does not occur, containment to relatively low, harmless level is still possible, if α_1 or β_1 are large enough.

In Fig 1 some examples of cancer and immune cells dynamics are presented. Parameters of the curves in panel (A) satisfy condition (5) and thus the cancer is eliminated; the initial increase is due to the delay in the response of the immune system.

Curves in panels B e C show two different coexistence configurations, characterized by different values of α_1, representing the effect of different recognition levels.

Finally, consider, in analogy to what has been done in [13] a case of r-therapy and $i-$therapy: as explained before this amounts to introduce new parameters $r_1' = r_1 - g(t)$ and $\alpha_1' > \alpha_1$.

Simulations have been carried out assuming an short duration / high dose protocol and results are presented are presented in panels A and B of Fig. 2, for r- and immunotherapy, respectively. The figure show a good qualitative agreement with computations reported in [13], using a more detailed model of interactions between cancer and immune system.

In the case of a continuous therapy, where r' is constant if $r_1' < c_1 H/K_1$ the immune system will be able to eradicate cancer.

On the other end immunotherapies, which enhance the recognition performance of immune cells, do not *per se* eliminate cancer, but they can contain it to low, acceptable levels.

3.2 Two cancer types "*in vitro*"

Consider now the case in which the immune system is absent, and the two tumor clones compete for resources; this allows to investigate the interplay between competition and effect of therapy, as in experiments carried out *in vitro* [3].

Now the model is as follows:

$$\begin{aligned} \frac{dx_1}{dt} &= r_1 x_1 - \frac{b_{11}}{K_1} x_1^2 - \frac{b_{12}}{K_1} x_1 x_2, \\ \frac{dx_2}{dt} &= r_2 x_2 - \frac{b_{22}}{K_2} x_2^2 - \frac{b_{21}}{K_2} x_1 x_2. \end{aligned} \tag{6}$$

For simplicity set $r_1 = b_{11} > 0$ and $r_2 = b_{22} > 0$, thus the system is the usual model for competing populations [29]. Even though this is a rather simple system, still it is of interest as it allows to investigate the effect of heterogeneity and more specifically of competition when therapy is administered, and this can lead to interesting results.

Equilibrium points are

$$\begin{aligned} P_1 : x_1^* &= x_2^* = 0, \quad P_2 : x_1^* = K_1, x_2^* = 0, \quad P_2 : x_1^* = 0, x_2^* = K_2, \\ P_4 : x_1^* &= \frac{b_{12}K_2 r_2 - K_1 r_1 r_2}{b_{12}b_{21} - r_1 r_2}, x_2^* = \frac{b_{21}K_1 r_1 - K_2 r_1 r_2}{b_{12}b_{21} - r_1 r_2}, \end{aligned} \tag{7}$$

and P_4 exists only if

$$b_{12}b_{21} \neq r_1 r_2.$$

Define

$$a_{12} = \frac{b_{12}K_2}{r_1 K_1}, \quad a_{21} = \frac{b_{21}K_1}{r_2 K_2}, \tag{8}$$

competitions parameters a_{12}, a_{21} can be considered relative measure of fitness of x_1, x_2, as they determine which species will eventually survive [29].

The coordinates of point P_4 can be written as

$$x_1^* = K_1 \frac{1 - a_{12}}{1 - a_{12}a_{21}}, \quad x_2^* = K_2 \frac{1 - a_{21}}{1 - a_{12}a_{21}},$$

and for P_4 to exist in the positive quadrant it must be either $a_{12}, a_{12} > 1$ or $a_{12}, a_{12} < 1$.

Stability condition of stationary points can be determined by standard methods of analysis. The point P_1 is always unstable; considering the other stationary points, there exist 4 possible configurations.

In two of these configurations P_4 does not belong to the positive quadrant: if $a_{12} > 1$, $a_{12} < 1$ the point P_2 is globally stable, and, symmetrically, if $a_{12} < 1$, $a_{12} > 1$ P_3 is globally stable. These configurations will be denoted in the following as S_1 and S_2 respectively. From an evolutionary point of view S_1 and S_2 are examples of survival of the fittest.

Suppose now or $a_{12}, a_{12} > 1$: this condition makes both P_2 and P_3 locally stable, P_4 is a saddle point and the phase space is partitioned in two basins of attraction (configuration Ic). In other words the fate of the system depends on the initial conditions, a situation that in evolution studies is referred as survival of the first.

In all cases considered so far the principle of competitive exclusion applies, in that of the two tumor types just one survives.

On the contrary if $a_{12}, a_{12} < 1$, the point of coexistence P_4 is globally stable (configuration Co).

Figure 3 shows the stream-plots of these configurations.

3.2.1 r-therapy: decreasing rate of growth

Consider a r-therapy, e.g. administration of a drug aiming to decrease the rates of growth of the tumors: let new rates of growth be $r_i' = r_i - g(t)$, $i = 1, 2$. Ideally the therapy would make r_1' and r_2' negative, so that both x_1 and x_2 will decrease exponentially, but, unfortunately this very rarely happens in real life situations, as demonstrated by the finding of many studies showing a small number of cells resistant to any agent are always present, see for instance [8, 30].

Next assume $0 < r_i' < r_i$, $i = 1, 2$, and let a_{12}', a_{21}' be the fitness values obtained from Eq. (8) by replacing r_1, r_2 with r_1' and r_2' respectively. Since decreasing r_1', r_2' amounts to increase a_{12}' and a_{21}', respectively, the effect of the therapy is to move the system toward states of stronger competitive interaction between cancer clones. Therefore, discounting the case of the drug being ineffective, the possible transitions are

$$Co \to S_i, \quad Co \to Ic, \quad S_i \to Ic, \quad i = 1, 2,$$

which can also be combined to give

$$Co \to S_i \to Ic, \quad i = 1, 2,$$

and the only invariant configuration is Ic, as in this case, a_{12} and a_{21} are greater than 1.

A general result is the disappearance of heterogeneity, a beneficial effect since coexistence of different cancer types clearly increase the probability, via mutations, that new cancer lines appear, which can be resistant to existing therapies. Furthermore, obviously, heterogeneity makes targeting cancer more difficult.

The question remains whether cancer cell numbers are reduced, that is if the asymptotic total cancer load $x^* = x_1^* + x_2^*$, which would result in absence of the therapy, is larger than the carrying capacity of the clone surviving the transition from coexistence to competitive exclusion, in whatever final configuration. A straightforward calculation shows that inequalities $a_{21} < K_1/K_2$ and $a_{12} < K_2/K_1$ provide a sufficient condition for the relation

$$x^* = x_1^* + x_2^* > \max(K_1, K_2) \tag{9}$$

to hold. More specifically if $K_1 > K_2$ (resp. $K_2 > K_1$) then just $a_{12} < K_2/K_1$ (resp. $a_{21} < K_1/K_2$) suffices.

Suppose $K_1 > K_2$ and let Co be the initial configuration: if condition (9) is satisfied, the best therapy is to induce a $Co \to S_2$, that is to target selectively the species x_1.

Let x_1 be the fitter clone and S_1 as initial configuration: a decrease of r_2 just enhances the effect of selection, leading to the disappearance of x_2. On the contrary if x_1 is affected by the therapy, a transition to Ic may occur: suppose now $K_2 > K_1$ then x_2 can out-compete x_1 leading to the counterintuitive result that the asymptotic number of cancer cells is larger than in absence of treatment.

Turning now to the actual dynamics of x_1, x_2 it should be noted that the model predicts the emergence of the well known rebound effect: the total cancer load x initially decreases to grow again at a later time. This effect can be explained as the result of a transition from coexistence configuration to any competitive exclusion configuration, where the the lack of competition allow a cancer type to expand limited solely by its the carrying capacity. Then, after and initial transient, the total load x will tend to equal x_i, where i denotes the surviving cancer family. This type of behavior is confirmed by numerical calculations and it is clearly visible in panel (A) of Fig. 4, and more markedly in panel (B), where the insert provides a more detailed representation. These results are agreement with the finding reported obtained in [20, 3], using a probabilistic model to fit experimental data.

Summing up, in case of weak interaction between the two cancer types, e.g. if clones access different resources, r-theraphies must be strong enough to eliminate heterogeneity, since that implies, usually, also a decrease of the total cancer load: ideally the treatment should target the clone with the largest carrying capacity. Note that this is a somewhat surprising result, as it shows that the fitter clone is not necessarily the most harmful.

Once a situation is reached where the competition is strong, r-therapies do not produce positive effects, and occasionally may be disadvantageous, with the temporary resurgence of heterogeneity in the Ic configuration, and uncertainty on which cancer type will survive.

3.2.2 $s-$ therapy: starving cancer cells

Besides the traditional chemotherapies in more recent years new therapies have appeared based on the notion of starving cancer cells of food, for instance by inhibiting angiogenesis.

In the framework of the present model these therapies reduce cancer carrying capacities, from that K_i to K_i' $i = 1, 2$: defining $\kappa' = K_1'/K_2'$; Eq. (8) now becomes

$$a_{12}' = \frac{b_{12}}{r_1 \kappa'}, \quad a_{21}' = \frac{b_{21}\kappa'}{r_2}. \tag{10}$$

Fitness measures a_{12}', a_{21}' have opposite trends as κ' varies, in that if a_{12}' decreases a_{21}' increases, and vice-versa; the invariant configurations are S_1, (resp. S_2) if κ' increases (resp. decreases), and only transitions between the heterogeneous configurations Co and Ic are forbidden. In particular, reducing carrying capacities of the fitter clone allows occurrence of transitions $S_i \to Co$, $i = 1, 2$, where i denotes the fitter clone; the system can move from competitive exclusion to coexistence, a somehow counterintuitive result, whose implications will be discussed in the sequel.

Let the initial configuration be Co, $a_{12}, a_{21} < 1$; if x_1 is more affected by the therapy with respect to x_2, κ' decreases and, consequently, when a_{21} becomes larger than 1 then a transition $Co \to S_2$ occurs. If the starting configuration is S_1 three transitions may occur, namely

$$S_1 \to Co, \quad S_1 \to Ic, \quad S_1 \to S_2, \quad S_1 \to Co,$$

since there are three possible pairs inequalities that, from $a_{12} < 1, a_{21} > 1$, can be

reached by increasing a_{12} while decreasing a_{21}. Finally, transitions from I_c to S_1 or S_2 may take place the final state depending on the particular clone is targeted.

Consider first $S_1 \to Co$, occurring when the therapy is aimed to the fitter cancer clone. In evaluating this result it should be remembered that before treatment, x_1 dominates x_2 and, therefore the asymptotic total cancer load x^* is $x^* = K_1$, whereas, after treatment, the condition on the asymptotic total cancer load is, after treatment,

$$x^* = x_1^* + x_2^* > \max\left(K_1', K_2'\right), \tag{11}$$

which, in principle, can be less than K_1: thus heterogeneity does not necessarily results in an increase of the total cancer load x.

If a transition may lead to S_1 or S_2, clearly the best results are obtained targeting the clone with the largest carrying capacity, otherwise an increase of x may occur.

Some example of different effects of medical treatment are illustrated in Fig. **5.**

Panel (A) represents the case of a relatively under-performing therapy, which, in an initial configuration Co, do not eliminate any of the tumor types but which induces a switch in their the relative fitness, and the initially fitter type is decreased and so the total load; treatment, by decreasing x_1, can also result in the survival of the less fit type, which, otherwise, would eventually disappear (compare panel (B)). Enhanced effectiveness of treatment leads to the disappearance of x_1, starting from two heterogeneous configuration namely Co and Ic, respectively as depicted in panels (C) and (D); as a consequence, if $K_2 > K_1$, large rebound can occur,

here more evident in panel (D). Note also that, in the last two cases the asymptotic total load is $x^* = K_2$.

From these examples it is apparent that a the safest therapy is to target clones with the large carrying capacity, since at the worst the therapy is useless, but not harmful.

As a final caveat it is worth remembering that therapies tried in experiments *in vitro* yield outcomes that do not necessarily remain valid *in vivo* , in presence of the immune system, however, situations occurring *in vitro* can provide an useful approximation in the limit of weak immune system or weak competition.

3.3 Bringing all pieces together

In the previous subsections we have taken separately factors such as immune system and competition, to study how they influence cancer growth, and furthermore, how they affect results of different therapies. In other words, we have simulated *in vitro* experiments in which the complex situation are simplified to allow specific factors to be analyzed. Obviously a complete picture of cancer evolution, in the framework of the present model, needs all these factors to be considered together. The result is a rich variety of new dynamical behaviors: some of them are presented in the sequel.

Plots of Fig. 6 highlight the effect of an increased action of immune cells on a system of competing cancer types. These examples clearly show that, differently from what happens *in vitro*, competition parameters a_{ij} are now not enough to uniquely determine the fate of the cancer population, and that recognition and

predation by the immune system play an important role.

Note that situation of competitive exclusion can mutate into coexistence, via damped oscillations, or oscillatory behavior, as the effect of the immune system increase; oscillations have been clinically observed during cancer development, an effect known as the Jeff phenomenon [12].

It should be noted that results from subsections 3.1 and 3.2 clearly indicate that "predation" of the immune system or competition between cancer types alone are not enough to generate limit cycles; both these factors need to be present. In this case an Hopf bifurcation can occur and Fig. 7 presents an example of transition from a stable focus to a limit cycle, obtained by changing the carrying capacity K_2.

In general numerical explorations have shown that, in the parameter space a_{12}, a_{21}, oscillatory behavior takes place below a curve along which a_{21} decreases as a_{12} increases. Therefore it seems that oscillations can occur if competition between cancer types is not too strong. The location of the parameter region containing limit cycles is also determined by the recognition levels α_i, in the sense that increasing α_i makes the occurrence of oscillation more likely to happen, since, in this case, the immune system adapts more slowly to the cancer levels.

The immune system, obviously, affect also the results of therapies. As shown in the sequel, both r- and s-therapies can, in some instances, be counterproductive. Consider first r-therapies: In some case they suppress oscillations, see Fig. 8, panel (A), where from the initial oscillating state, the system relaxes to competitive exclusion configuration S_2. Initially x_1, x_2 have similar a_{ij} parameters.

The therapy has made x_1 less competitive, and therefore it is eliminated by natural selection. Note that the total cancer load decreases because here the type with the largest carrying capacity has been targeted.

The case of panel (B) shows clearly the effect of the recognition parameters α_i: initially clone x_1 out-competes x_2 though $\alpha_1 > \alpha_2$; a small increase of a_{12} it is enough to curtail x_1, and to push upward x_2. In other word the therapy, by making the competition more even, allows for a greater impact of the recognition by the immune system. In conclusion, it is more difficult for x_1 to survive and, consequently, the clone x_2 increases, because of the reduced competition. Note that now the total cancer load increases, due to the heterogeneity of the system.

S-therapies appear to work well with the immune system in eliminating, or at least controlling cancer, as it happens in panel (C) of Fig. 8 where initially clones coexist (configuration Co) with $K_1 > K_2$: if x_1 is targeted so that $K_1' = K_2'$ clone x_2 will become dominant, but, since it is more easily recognized by the immune system, will be, in turn, eradicated. This is an almost prototypical example of how, selection, predation ans therapy can contribute to cancer eradication: the therapy, by weakening the clone less likely to be recognized, makes it possible its elimination by the second one, which in turn is eliminated by the immune system. Finally in panel (D) it is shown that, targeting the strongest clone, and hence evening selective pressure, can generate sustained oscillations, and hence heterogeneity.

It is then possible to draw some conclusions for the above cases, namely that to be effective a therapy must make more asymmetric the contest between the

two cancer species, to avoid heterogeneity and, consequently, to make easier the eradication, or control, by the immune system, of the surviving cancer. Ideally one should try to target the type with the largest carrying capacity, or the type less likely to be recognized by the immune system.

4 Conclusions

The starting point of this paper is that cancer development is ruled by the same selective forces shaping the evolution of species. In a population-theoretical perspective here a model of competing cancer species subjected to the action of immune system cells has been proposed. At best of our knowledge the present work is the first to bring together the competition between different cancer clones and the action of the immune system.

Analysis and numerical simulations confirm that this model is able to reproduce some of the experimental finding about cancer development, and, also, the effects of therapy and, therefore, it can provide an *in silico* laboratory by which different experimental conditions can be tested. Here we have mostly considered two classes of therapies: r-therapies aim to reduce the rate of growth of cancer cells, as do conventional chemo or radiotherapies and s-therapies by which the cancer is starved, like in antiangiogenetic treatments.

In absence of the immune system, the *in vitro* case of subsection 3.2, analysis suggests that, when the competition is weak, medical treatments, in the form of r- or $s-$therapies, can eliminate or, at least control cancer. However it has been also shown that if the cancer type with smaller carrying capacity is targeted total

cancer load may actually increase after therapies are applied. In case of strong competition medical treatment may not produce positive effects, and occasionally be disadvantageous, with the temporary resurgence of heterogeneity and uncertainty on which cancer type will survive.

The description of cancer development is, obviously, more complex when, besides competition, also to recognition and predation by the immune cells are considered. However, the results presented in 3.3 allow to formulate, albeit tentatively, this conclusion: in general it is beneficial to "break the symmetry" in the contest between cancer clones, targeting the type with the larger carrying capacity. Alternatively one should select for treatment the type less recognizable by the immune system.

Therapies must be adapted, not just to the different cancer types, but also to their interactions, and this requires also the knowledge of the environmental constraints under which tumor develops. In this respect important variables are competitions parameters a_{ij}, the carrying capacities K_i and recognition parameters α_i.

In perspective, preliminary results suggest that immunotherapies have more predictable effect, compared to r- and s-therapies, and it is clear that a more thorough investigation of their properties is necessary to asses their impact on the arm race between cancer and immune system.

Acknowledgment

Prin Project: Problemi matematici in teoria cinetica ed applicazioni - 2012AZS52J

References

[1] Nowell P C. The clonal evolution of tumor cell populations. *Science*, 194(4260):23–28, 1976.

[2] Anderson A R Basanta D, Gatenby R A. Exploiting evolution to treat drug resistance: combination therapy and the double bind. *Molecular pharmaceutics*, 9(4):914–921, 2012.

[3] Tong J Peraza-Penton A Lallo A Baldi F Lin KH Truini M Trusolino L Bertotti A Di Nicolantonio F Nowak MA Zhang L Wood KC Bardelli A Misale S, Bozic I. Vertical suppression of the egfr pathway prevents onset of resistance in colorectal cancers. *Nature communications*, 6, 2015.

[4] Reid B J Maley C C Merlo L M F, Pepper J W. Cancer as an evolutionary and ecological process. *Nature Reviews Cancer*, 6(12):924–935, 2006.

[5] Maley C C Greaves M. Clonal evolution in cancer. *Nature*, 481(7381):306–313, 2012.

[6] Greaves M. Darwinian medicine: a case for cancer. *Nature Reviews Cancer*, 7(3):213–221, 2007.

[7] DeGregori J Casás-Selves M. How cancer shapes evolution and how evolution shapes cancer. *Evolution: Education and outreach*, 4(4):624–634, 2011.

[8] Swanton C Gerlinger M. How darwinian models inform therapeutic failure initiated by clonal heterogeneity in cancer medicine. *British journal of cancer*, 103(8):1139–1143, 2010.

[9] Polyak K Marusyk A, Almendro V. Intra-tumour heterogeneity: a looking glass for cancer? *Nature Reviews Cancer*, 12(5):323–334, 2012.

[10] Dingli D Pacheco J M, Santos F C. The ecology of cancer from an evolutionary game theory perspective. *Interface focus*, 4(4):20140019, 2014.

[11] Lewis M A Hillen T. Mathematical ecology of cancer. In *Managing Complexity, Reducing Perplexity*, pages 1–13. Springer, 2014.

[12] A De Pillis L G, Radunskaya. A mathematical tumor model with immune resistance and drug therapy: an optimal control approach. *Computational and Mathematical Methods in Medicine*, 3(2):79–100, 2001.

[13] Radunskaya A E de Pillis L G, Gu W. Mixed immunotherapy and chemotherapy of tumors: modeling, applications and biological interpretations. *Journal of theoretical biology*, 238(4):841–862, 2006.

[14] Hochberg M E Clairambault J Perthame B Lorz A, Lorenzi T. Populational adaptive evolution, chemotherapeutic resistance and multiple anticancer therapies. *ESAIM: Mathematical Modelling and Numerical Analysis*, 47(2):377–399, 2013.

[15] Knopoff D Bellouquid A, De Angelis E. From the modeling of the immune hallmarks of cancer to a black swan in biology. *Mathematical Models and Methods in Applied Sciences*, 23(05):949–978, 2013.

[16] Delitala M Bellouquid A. *Mathematical modeling of complex biological systems*. Springer, 2006.

[17] Schattler H d'Onofrio A, Ledzewicz U. On the dynamics of tumor-immune system interactions and combined chemo-and immunotherapy. In *New Challenges for Cancer Systems Biomedicine*, pages 249–266. Springer, 2012.

[18] Levy D Wilson S. A mathematical model of the enhancement of tumor vaccine efficacy by immunotherapy. *Bulletin of mathematical biology*, 74(7):1485–1500, 2012.

[19] Hughes B D Landman K A Frascoli F, Kim P S. A dynamical model of tumour immunotherapy. *Mathematical biosciences*, 253:50–62, 2014.

[20] Allen B Antal T Chatterjee K Shah P Moon Y S Yaqubie A Kelly N Le D T Bozic I, Reiter J G et al. Evolutionary dynamics of cancer in response to targeted combination therapy. *Elife*, 2:e00747, 2013.

[21] Agliari E Barra A. A statistical mechanics approach to autopoietic immune networks. *Journal of Statistical Mechanics: Theory and Experiment*, 2010(07):P07004, 2010.

[22] De Ninno A Schiavoni G Gabriele L Gerardino A Mattei F Barra A Businaro L Agliari E, Biselli E. Cancer-driven dynamics of immune cells in a microfluidic environment. *arXiv preprint arXiv:1402.0451*, 2014.

[23] Gillies R J Frieden B R Gatenby R A, Silva A S. Adaptive therapy. *Cancer research*, 69(11):4894–4903, 2009.

[24] Vincent T Gatenby R A, Brown J. Lessons from applied ecology: cancer control using an evolutionary double bind. *Cancer research*, 69(19):7499–7502, 2009.

[25] Gatenby R A Gillies R J, Verduzco D. Evolutionary dynamics of carcinogenesis and why targeted therapy does not work. *Nature Reviews Cancer*, 12(7):487–493, 2012.

[26] Jonathan L Earn J D Eftimie R, Bramson J L. Interactions between the immune system and cancer: a brief review of non-spatial mathematical models. *Bulletin of mathematical biology*, 73(1):2–32, 2011.

[27] Gerstung M Markowetz F Beerenwinkel N, Schwarz R F. Cancer evolution: mathematical models and computational inference. *Systematic biology*, page syu081, 2014.

[28] Delitala M Bellomo N. From the mathematical kinetic, and stochastic game theory to modelling mutations, onset, progression and immune competition of cancer cells. *Physics of Life Reviews*, 5(4):183–206, 2008.

[29] Murray J D. Mathematical biology i: An introduction, vol. 17 of interdisciplinary applied mathematics, 2002.

[30] Chu E DeVita V T. A history of cancer chemotherapy. *Cancer research*, 68(21):8643–8653, 2008.

[31] Reynolds A R Vasudev N S. Anti-angiogenic therapy for cancer: current progress, unresolved questions and future directions. *Angiogenesis*, 17(3):471–494, 2014.

[32] Couzin-Frankel J. Cancer immunotherapy. *Science*, 342(6165):1432–1433, 2013.

[33] Wild C P Stewart B et al. World cancer report 2014. *World*, 2016.

Figures

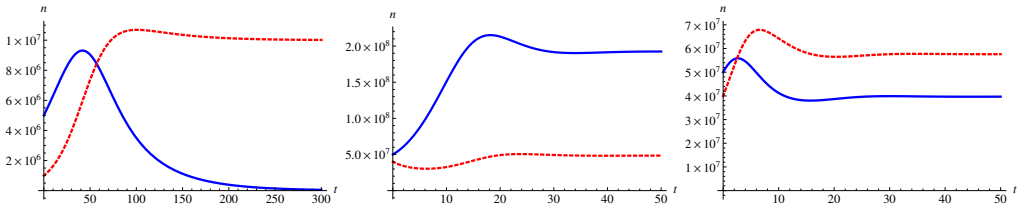

(A) (B) (C)

Figure 1: **Dynamics of cancer and immune cells**. Panels A, B, C: The continuous and dashed curves represent, respectively, the number of cancer and immune cells. Parameters values are $c_1 = 5$, $h = 10^7$, $K_1 = 10^9$, $\gamma_1 = \beta_1 = 0.05$, $r_1 = b_{11}$, in all panels; in (A) $r_1 = 0.03$, $\alpha_1 = 0.01$, in (B) $r_1 = 0.3$, $\alpha_1 = 0.01$ and in (C) $r_1 = 0.3$, $\alpha_1 = 0.06$.

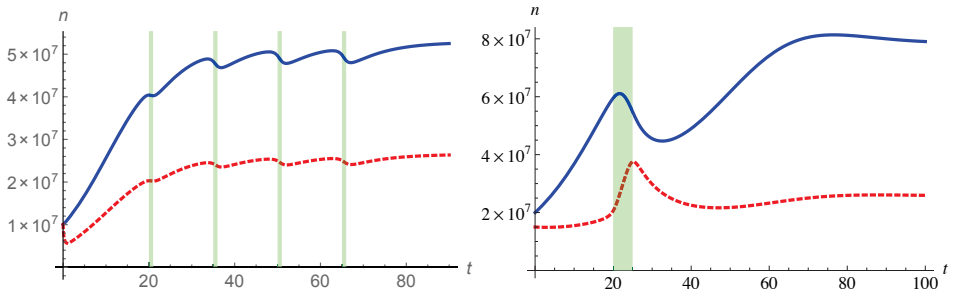

(A) *Chemotherapy.* (B) *Immunotherapy.*

Figure 2: **Comparison of effect of $r-$ and $i-$ therapy** . Parameters are $K_1 = 10^9$, $\gamma_1 = \beta_1 = 0.05$, $r_1 = b_{11} = 0.14$, $c_1 = 5$, for both panels. In (A) $h = 10^5$, $\alpha_1 = 0.025$, $r_1' = 0.01$. In (B) $h = 10^7$, $\alpha_1 = 0.01$, $\alpha_1' = 0.05$.

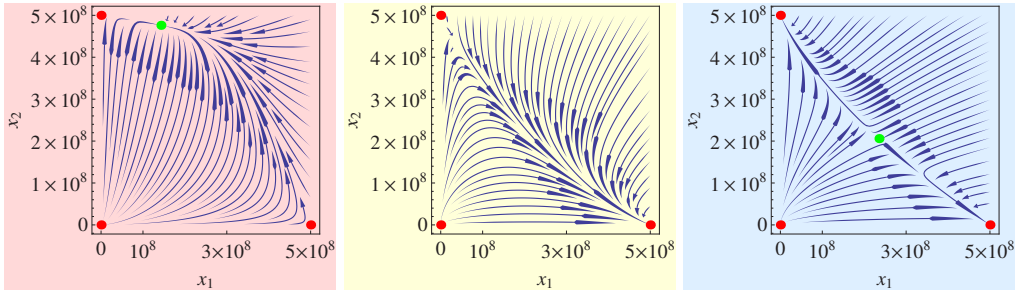

(A) *Coexistence.* (B) *Competitive exclusion, S_2.* (C) *Competitive exclusion with dependence on initial conditions.*

Figure 3: **Vector fields of different configurations**. Panels A, B, C, show, respectively, representations of vector field for coexistence of the two clones, competitive exclusion (here dominance of clone x_1), and competitive exclusion with dependence from initial conditions.

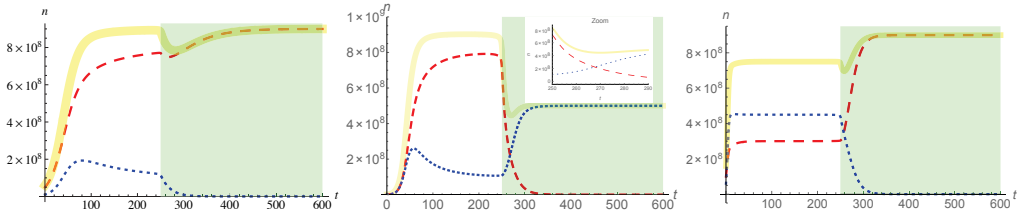

Figure 4: **Effects of $r-$therapy** *in vitro*.
In all panels dashes (red in color) and points (blue) represent the trajectories of the first and second clonal family, respectively, and the continuous line (yellow) depicts the total number of cancer cells. The green area indicates the time frame of the continuous therapy. Values of parameters are $K_1 = 9 \cdot 10^8$, $K_2 = 5 \cdot 10^8$, $b_{11} = r_1$, $b_{22} = r_2$ in all panels and x_1 is the fitter clone. The starting condition is Co Panel (A): non selective therapy. Parameters values are $a_{12} = 0.56$, $a'_{12} = 1.67$, $a_{21} = 0.9$ and $a'_{21} = 7.2$. Panel (B):targeting clone x_2. Parameters:$a_{12} = 0.52$, $a'_{12} = 3.22$ and $a_{21} = 0.9$ Panel (C):targeting clone x_1. Parameters: $a_{12} = 0.74$, $a_{21} = 0.3$, $a'_{21} = 1.8$ The rebound is presented in greater detail in the insert of panel (B).

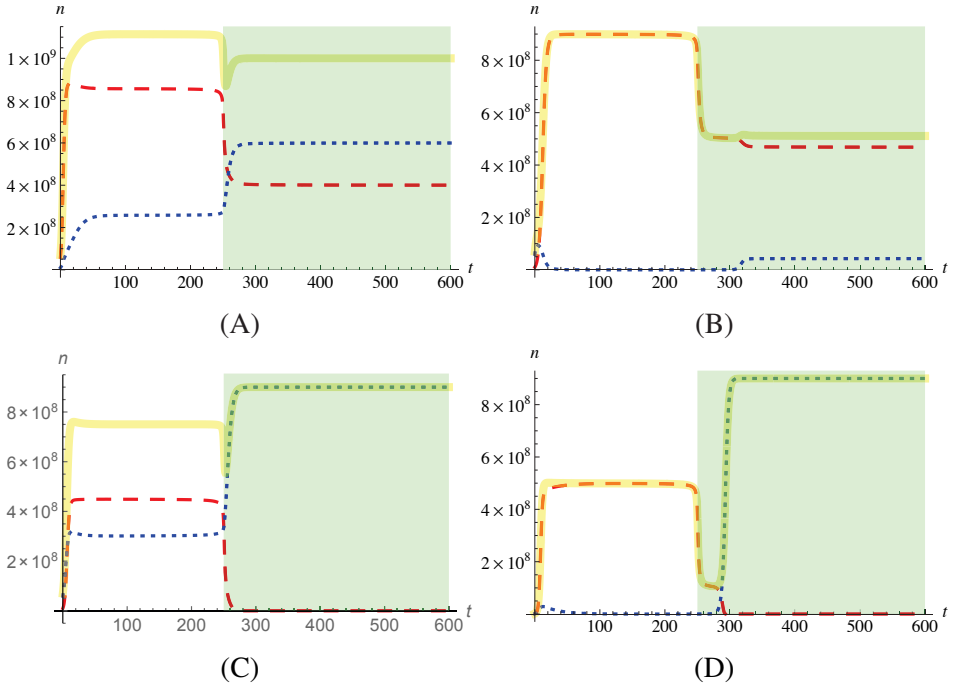

Figure 5: **Effects of $s-$ therapy** *in vitro*. Code for curves representation is as in Fig. 4. The cancer type x_1 is supposed to be less resistant to the therapy, compared to x_2, furthermore $K_2 > K_1$. Values of parameters and transitions are as follows. Panel (A): $a_{12} = 0.17$, $a'_{12} = 0.3$, $a_{21} = 0.75$, $a'_{21} = 0.42$, $Co \to Co$ Panel (B) $a_{12} = 0.08$, $a'_{12} = 0.15$, $a_{21} = 1.1$, $a'_{21} = 0.61$, $S_1 \to Co$. Panel (C) $a_{12} = 0.3$, $a'_{12} = 1.5$, $a_{21} = 0.74$, $a'_{21} = 0.15$, $Co \to S_2$, Panel (D) $a_{12} = 1.54$, $a'_{12} = 7.71$, $a_{21} = 1.11$, $a'_{21} = 0.22$, $Ic \to S_2$, Note, in this panel, the large rebound

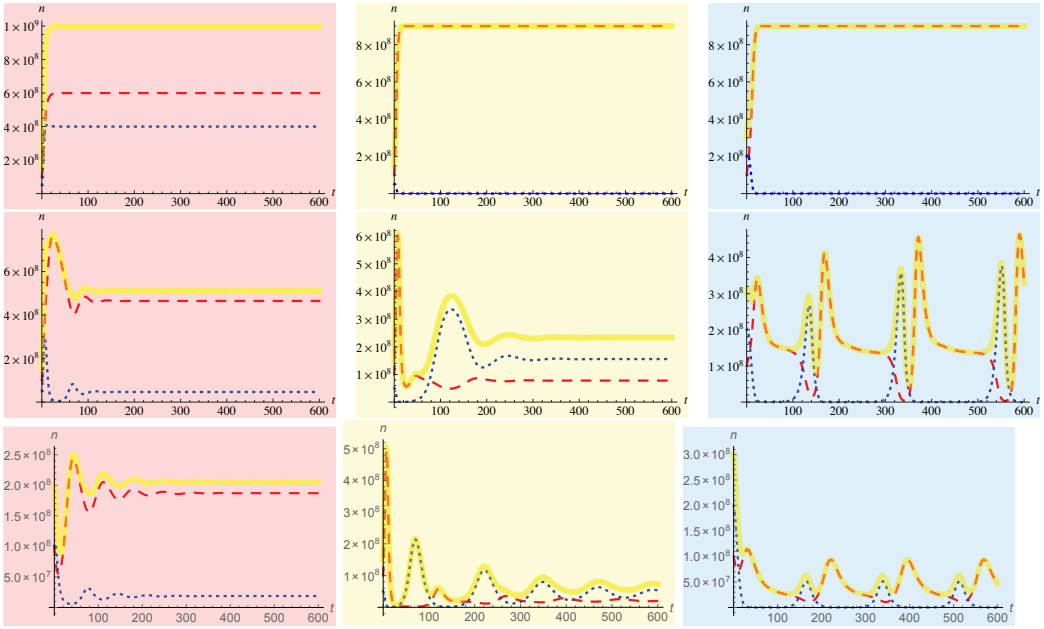

(A) (B) (C)

Figure 6: **Effects of the immune system**. Code for curves representation is as in Fig. 4. In the first row $c_1 = c_2 = 0$, i.e. the immune system is absent as in subsection 3.2, and in the second and third rows $c_1 = c_2 = 20$, $c_1 = c_2 = 40$, respectively. Values of parameters for all panels are: $h = 10^7$, $\beta_1 = \beta_2 = \gamma_1 = \gamma_2 = 0.05$, $K_1 = 9 \cdot 10^8$, $K_2 = 5 \cdot 10^8$. Panel (A): $a_{12} = 0.42$, $a_{21} = 0.3$, $\alpha_1 = 0.001$, $\alpha_2 = 0.01$ (Co configuration). Panel (B): $a_{12} = 0.33$, $a_{21} = 5.4$, $\alpha_1 = 0.006$, $\alpha_2 = 0.003$ (S_1). Panel (C): $a_{12} = 1.11$, $a_{21} = 3.6$, $\alpha_1 = 0.002$, $\alpha_2 = 0.008$ (Ic).

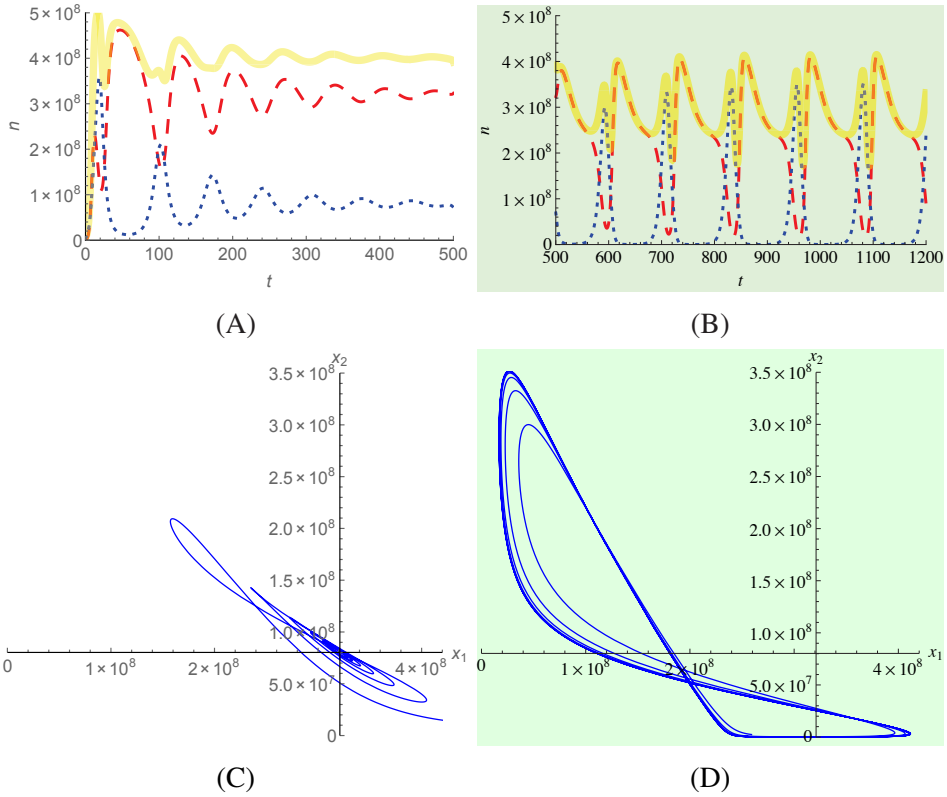

Figure 7: **Hopf bifurcation**. Trajectories of x_1, x_2 for bifurcation parameter K_2 below and above the bifurcation point. In panels (A) and (B) code for curves representation is as in Fig. 4, panel (C) and (D) trajectories of x_1, x_2 are represented in the phase space. Values of parameters are $h = 10^7$, $\beta_1 = \beta_2 = \gamma_1 = \gamma_2 = 0.05$, $c_1 = c_2 = 10$, , $\alpha_1 = 0.002$, $\alpha_2 = 0.008$, $K_1 = 5 \cdot 10^8$ for all panels, and carrying capacity K_2 varies from $K_2 = 9 \cdot 10^8$, $K_2' = 5 \cdot 10^8$, $K_1 = 5 \cdot 10^8$,

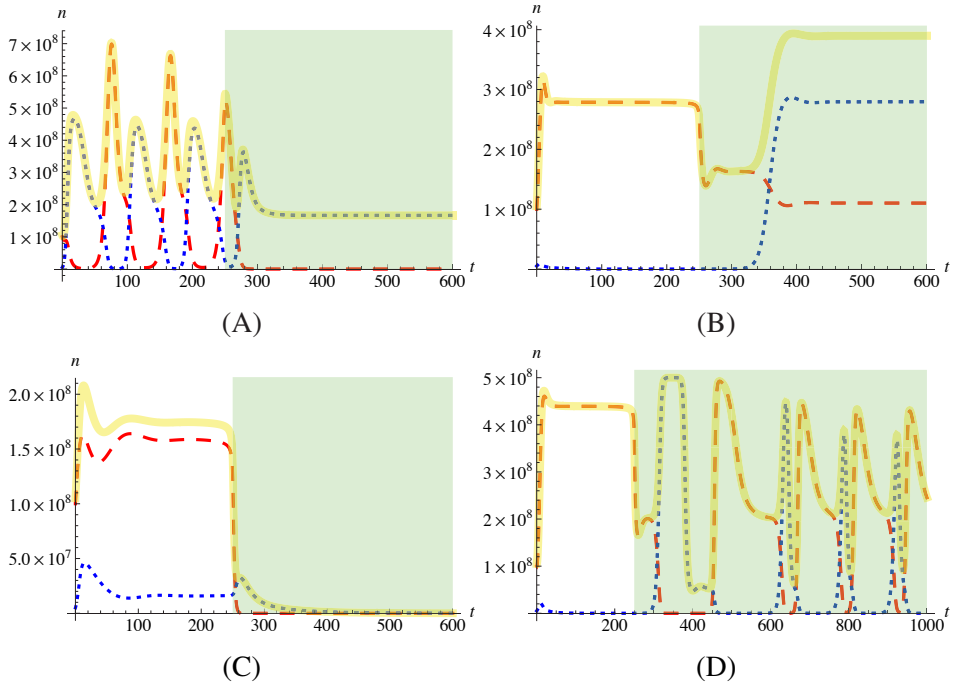

Figure 8: **Effects of the r- and s-therapy.** Curve codes are as in Fig. 4 and the green area indicates the time frame of the continuous therapy. Values of parameters are, for all panels: $h = 10^7$, $\beta_1 = \beta_2 = \gamma_1 = \gamma_2 = 0.05$, $c_1 = c_2 = 10$. Panel (A): $a_{12} = 1.11$, $a'_{12} = 4.44$,$a_{21} = 1.54$, $\alpha_1 = \alpha_2 = 0.004$. Panel (B): $a_{12} = 0.24$ $a'_{12} = 0.42$, $a_{21} = 3.6$, $\alpha_1 = 0.006$, $\alpha_2 = 0.003$. Panel (C): $a_{12} = 0.2$ $a'_{12} = 1$, $a_{21} = 0.83$, $a'_{21} = 0.17$, $\alpha_1 = 0.001$, $\alpha_2 = 0.01$. Panel (D): $a_{12} = 0.83$, $a'_{12} = 1.5$, $a_{21} = 2.25$, $a'_{21} = 1.25$, $\alpha_1 = 0.002$, $\alpha_2 = 0.008$.

On some models of active cell-to-cell biological interactions

Ahmed NOUSSAIR

UMR CNRS 5251 IMB, Université de Bordeaux
France

Abstract

We consider two models of biological interactions and transfer processes between cells interacting and exchanging some transferable materials. Starting from detailed description of microscopic interactions we derive discrete and continuous integrodifferential models. The first problem is related to the transfer of proteins motivated by advantages of cell transfer therapies for the treatment of cancers. The second case concerns the activity transfer between immune and tumour cells. We give here a qualitative analysis including asymptotic behaviour of the solutions, we provide some numerical tests and we prove the convergence of the solutions from the discrete model to the continuous model.

Keywords: Cell-to-cell interaction, transfers rules, discrete models, kinetic theory of active particles, asymptotic stability, numerical analysis.

1. Introduction

The subject of this paper is the modelling of transfer processes occurring between population of cells in a living system constituted by a large number of entities which interact with different strategies and exchange some quantities of transferable materials. To construct the models we will start by considering a detailed description of microscopic interactions which include not only modifications of the microscopic state, but also proliferation and destruction of cells. We will present in this paper two different case of study. The first problem is related to the transfer of proteins or a transferable matter between interacting cells. The work is motivated by advantages of cell transfer therapies for the treatment of cancers [7, 8]. While the second problem concerns transfer of activity between immune and tumour cells. The motivation is that the stage of the early growth of a tumor belongs to the so-called free cell regime, in which the tumour cells are not yet condensed in

a macroscopically observable spatial structure, and the interaction between tumour and immune system occur at the cellular level. This make the kinetic approach particularly appropriate. The goal is to provide some new models for transfers which can be used in practice to fit real experimental data.

For both models, the mathematical framework is defined by a system of integrodifferential equations which describe the evolution in time of the distribution function over the microscopic state of cells, this makes the kinetic approach particularly appropriate. The methods can be regarded as particular cases of Methods of mathematical kinetic theory for active particles which have been recently introduced in the . general mathematical framework of the ," Theory of Active Particles ", introduced by N Bellomo,and can be regarded as new mathematical approach which develops method of kinetic theory to deal with active particles (cells) rather than classical particles. The microscopic state includes biological functions. The modelling of microscopic interactions also refers to the ability and the behaviour of cells to interact and communicate with other cells, including proliferation and destruction.[2, 3, 4]. An interesting prospect is that biological transfer processes will be supported by rigorous investigation methods and tools, similar to what happened in the case of mechanical and physical sciences. It is not an easy task, considering that new mathematical methods may be needed to deal with the inner complexity of biological systems which exhibit features and behaviours very different from those of inert matter. Indeed, cells organize their dynamics according to the above functions, while classical particles follow deterministic laws of Newtonian mechanics.

For more informations on biological transfers processes, recent studies have shown that cells can communicate by the transfer of membrane proteins [6]. Inter cellular transfer of proteins is a mode of communication between cells that is crucial for certain physio- logical processes. For instance, the direct transfer of protein P-glycoprotein (P-gp) between cells was studied in [1, 10]. Because P-gp may act as a drug-efflux pump, its transfer may confer resistance against cytotoxic drugs to cancer cells. Another example is the transfer of human immunodeficiency virus (HIV) from an infected cell to an uninfected cell [5]. It has been shown in recent studies that the α-synuclein can transfer from one cell to another and could be a key element in the spread of Parkinson disease pathology [9].

The paper is organized as follows, the section 2 is devoted to the first problem which involves transfers with mass conservation. We describe the transfer rules,we derive a fully discrete model and we give its associated continuous model. In section 3, we consider two population of cells, immune

cells and tumour cells,exchanging their level of activities, we give a generalized framework and study the qualitative analysis and the main aim here is to prove the asymptotic behaviour of the solutions. The next section we present some numerical results. At the end of the paper in an appendix we show the convergence of the discrete model to the continuous model.

2. Transfers with mass conservation: An individual based model

2.1. Transfer rules

Consider a population of cells in a co-culture, where each cell possesses a amount of protein to be partially transferred due to some specific rules. Assuming that cells continually encounter other cells. Each pairwise of encounter during the transfer time results a winner "Recipient cell" and a loser "Donor cell" or a loser "Recipient cell" and a winner "Donor cell". Then in order to fully determine the transfer rules we will use two types of (deterministic type) transfers. The first type of transfer will ocurs with an efficiency rate f_1 and the second with efficiency f_2 depending on which type of cells win or lose. The basic assumptions used to describe the transfers are the following.

Assumption 2.1. *(A1) The probability that a pair of two individuals are involved in a transfer event is independent of their x values and the pairing is chosen randomly from all individuals.*

(A2) Let $f_1, f_2 \in L^\infty(\mathbb{R})$ be two even functions with $0 \leq f_1 \leq 1/2$ and $0 \leq f_2 \leq 1/2$ (two transfer efficiency). If two individuals whose difference in quantity is x are involved in a transfer, then the one with higher value loses $f_1(x)$ (respectively $f_2(x)$) times the difference of their x values and the one with lower x value gains exactly this amount with the probability $\pi_1(x)$ (respectively with the probability $\pi_2(x)$).

More precisely we will make that following assumption

Assumption 2.2. *We assume that $0 \leq (f_1 + f_2)(x) < 1$ for almost every $p \in \mathbb{R}$.*

Then we will defined the probabilities $\pi_1(x)$ and $\pi_2(x)$ defined by

$$\pi_1(x) := \frac{[\frac{1}{2} - f_2(x)]}{[1 - (f_1 + f_2)(x)]} \text{ and } \pi_2(x) := \frac{[\frac{1}{2} - f_1(x)]}{[1 - (f_1 + f_2)(x)]}. \tag{2.1}$$

One may observe that

$$\pi_1(x) + \pi_2(x) \equiv 1.$$

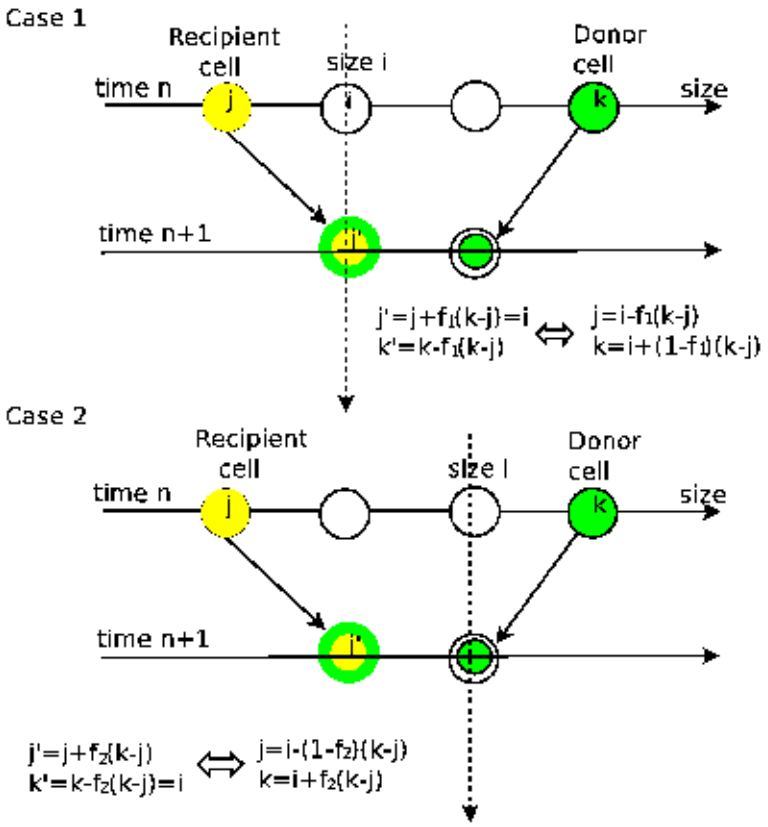

Figure 1: Transfert rules

The transfer rules read as follow:

Let y^{old} , z^{old} are the pre-transfer content sizes before transfer of the the interacting cells,and whose difference in quantity is $l = z^{old} - y^{old}$, and let y^{new}, z^{new} are the post-transfer content sizes, that are related to y^{old} and z^{old} by the relations

1. *First transfer with transfer efficiency f_1 "Recipient cells win"*

$$y^{new} = y^{old} + f_1(l)l \quad z^{new} = z^{old} - f_1(l)l$$

In this situation, the size of the content increases from y^{old} to a value x then $y^{new} = x$ and $y^{old} = x - f_1(l)l$

2. *Second transfer with transfer efficiency f_2 " Donor cells win"*

$$y^{new} = y^{old} + f_2(l)l \quad z^{new} = z^{old} - f_2(l)l$$

In this situation, the size of the content is decremented from z^{old} to a value x then $z^{new} = x$ and $z^{old} = x + f_2(l)l$.
The probability $\pi_1(l)$ that the "Recipient cells win" and the probability $\pi_2(l)$ that the "Donor cells win". Because of the two events "Recipient wins, Donor loses" and "Recipient loses, Donor wins " are complementary we have

$$\pi_1(l) + \pi_2(l) = 1$$

2.2. The discrete Model

Given the maximal value of the transferable quantity x_{max} and its minimal value x_{min}, we consider a partition

$$0 = x_1 < x_2 < ... < x_i = x_1 + i\Delta x < ... < x_{I_L} = L$$

with $x_{i+1} - x_i = \Delta x, \forall i = 1, I_L - 1$.

Starting from an initial distribution $u_0(x)$ for all sizes x in $\Omega_L := [x_{min}, x_{max}]$, we introduce an initial sequence u_i^0, $i = 1, ...I_L$, by

$$u_i^0 = \frac{1}{\Delta x}\int_{x_i}^{x_{i+1}} u_0(x)dx \simeq u_0(\frac{x_{i+1} + x_i}{2}).$$

We suppose that all the values u_i^n for $i = 1, ..., I_L$ are known, and we propose to build the (u_i^{n+1} for $i = 1, ...I_L$ by the following scheme:

$$\begin{aligned} u_i^{n+1} = u_i^n \quad & +\Delta t \sum_j \pi_1(l_j) \underbrace{\overline{u}^n_{i-f_1(l)l_j}\Delta x}_{\text{Recipient cells}} \underbrace{\overline{u}^n_{i+(1-f_1(l))l_j}\Delta x}_{\text{Doner cells}} \\ & +\Delta t \sum_j \pi_2(l_j) \underbrace{\overline{u}^n_{i-(1-f_2(l_j))l_j}\Delta x}_{\text{Recipient cells}} \underbrace{\overline{u}^n_{i+f_2(l_j)l_j}\Delta x}_{\text{Doner cells}} \\ & -\Delta t \underbrace{u_i^n \sum_{j=1}^{I_L} u_j^n \ \Delta x}_{\text{To other sizes}} \end{aligned} \tag{2.2}$$

where $l_j = j\Delta x$ is the difference of the transferable quantities between two partner cells, the quantities $i - f_1(l_j)l_j$, $i + (1 - f_1(l_j)l_j$, $i - f_2(l_j)l_j$ and $i + (1 - f_2(l_j)l_j$ are understood respectively as their integer part in the system (2.2), and

$$\overline{u}_i := \begin{cases} u_i \text{ if } i = 1, ..., I_L, \\ 0 \text{ otherwise.} \end{cases}$$

Let us rewrite the above scheme under the compact form

$$u_i^{n+1} = u_i^n + \Delta t Q_i^n \tag{2.3}$$

with

$$Q_i^n := \sum_j \sum_k K_{ijk} u_j^n u_k^n - u_i^n \sum_{j=1} u_j^n \tag{2.4}$$

where K_{ijk} will be defined precisely in section 5.

Similarly to the continuous case, for any sequence $(\phi_i)_{i=1,...,I_L}$ we have the following inequality

$$\sum_{i=1}^{I_L} \phi_i Q_i^n \quad = \sum_{j=1}^{I_L} \sum_{k=1}^{I_L} \left(\sum_{i=1}^{I_L} K_{i,j,k} \phi_i - \frac{\phi_j + \phi_k}{2} \right) u_j^n u_k^n \tag{2.5}$$

Therefore

$$\sum_{i=1}^{I_L} \phi_i Q_i^n = 0$$

if

$$\sum_{i=1}^{I_L} \phi_i K_{i,j,k} = \frac{\phi_j + \phi_k}{2}.$$

Theorem 2.3. *The total number of cell $\sum_{i=1}^{I_L} u_i^n$ is constant in time for the solution of the discrete model (2.3) if and only if*

$$\sum_{i=1}^{I_L} K_{i,j,k} = 1, \forall j, k = 1, ..., I_L. \tag{2.6}$$

The total mass of transferable quantities is preserved in time for the solution of the discrete model (2.3) if and only if

$$\sum_{i=1}^{I_L} x_i K_{i,j,k} = \frac{x_j + x_k}{2}. \tag{2.7}$$

2.2.1. Transfer kernel

According to Assumption 2.2, If a cell C_j and a cell C_k have, respectively, a quantity x_j and x_k of P-gp activity before transfer with $x_j \geq x_k$, then, after transfer, C_j (respectively, C_k) will have an activity $x_j - (x_j - x_k) f_1(x_j - x_k)$ with the probability $\pi_1(x_j - x_k)$ (respectively, $x_k + (x_j - x_k) f_2(x_j - x_k)$ with

the probability $\pi_2(x_j - x_k)$). So the fraction transferred is $f_1(x_j - x_k)$, with a probability $\pi_1(x_j - x_k)$ (resp. $\pi_2(x_j - x_k)$) for C_j (respectively, C_k) which depends on the difference between x_j and x_k (the distance between the P-gp activities of C_j and C_k).

Together with these considerations, one can define the transfer kernel K satisfying the properties of Theorem 2.3 as follows:

$$K_{i,j,k} := \begin{cases} \pi_1(x_j - x_k) \text{ if } \ x_i = x_j - (x_j - x_k) f_1(x_j - x_k), \\ \\ \pi_2(x_j - x_k) \text{ if } \ x_i = x_k + (x_j - x_k) f_2(x_j - x_k), \\ \\ 0 \ \text{ otherwise.} \end{cases} \tag{2.8}$$

3. From discrete to continuous model

In this section we show the convergence of the scheme (2.2). It means that the difference $|u - u^\Delta|_1$ between the approximate solution u^Δ of the discrete model (2.2) and the solution u of the continuous model (3.1) tends to zero as the meshsizes $\Delta t, \Delta x$ goes to zero (for simplicity we set $\Delta t = r\Delta x$). Here the approximate solution u^Δ is defined as the piecewise constant function defined on $]0, T[\times\Omega_L$

$$u^\Delta(t,x) = u_i^n \text{ For all } (t,x) \in,]t_n, t_{n+1}[\times]x_i, x_{i+1}[$$

where the values u_i^n are computed by (2.2) and u is the solution of the following continuous Cauchy problem

$$\begin{cases} \dfrac{\partial u(t,x)}{\partial t} = Q(u(t,.))(x), \ \text{for } x \in \mathbb{R}, \\ u(0,.) = u_0 \in L^1_+(\mathbb{R}). \end{cases} \tag{3.1}$$

The operator describing the rule for one transfer is defined by

$$\begin{aligned} Q(u)(x) \ &:= \ \int_{\mathbb{R}} \pi_1(x) u(x + f_1(x)p) u(x - (1 - f_1(x))p) dx \\ &+ \ \int_{\mathbb{R}} \pi_2(x) u(x + f_2(x)p) u(x - (1 - f_2(x))p) dx \\ &- \ u(t,x) \int_{\mathbb{R}} u(t,x) dx \end{aligned}$$

We will prove that the following theorem holds:

Theorem 3.1. *Let $u_0 \in (L^1 \cap L^\infty)(\Omega_L)$ with total variation bounded locally in Ω_L, $u_0 \geq 0$, then as the mesh size Δx tends to zero, there is a subsequence of $(u^\Delta)_{\Delta x>0}$, the family of approximate solution of the discrete model, converging in $L^1_{loc}([0,T]\times\Omega_L)$ to a function $u \in L^1_{loc}([0,T]\times\Omega_L)$ and the limiting function u is solution of the solution of the continuous problem.*

Proof. See Appendix. ■

The preservation of the total number of cells, and the preservation of the total mass of transferable quantity follows from the following equalities.

Lemma 3.2. *Let Assumptions 2.1 and 2.2 be satisfied. We have the following properties*

(i) ***(Preservation of the total number of cells)*** *For each $u \in L^1_+(\mathbb{R})$ we have $Q(u) \in L^1_+(\mathbb{R})$ and*

$$\int_{\mathbb{R}} Q(u)(x)dx = \int_{\mathbb{R}} u(x)dx$$

(ii) ***(Preservation of the total mass of transferable quantities)*** *For each $u \in L^1_+(\mathbb{R})$ such that $\int_{\mathbb{R}} xu(x)dx < +\infty$ we have*

$$\int_{\mathbb{R}} xQ(u)(x)dx = \int_{\mathbb{R}} xu(x)dx$$

Proof. We have

$$\begin{aligned}\int_{\mathbb{R}} \phi(x)[Q(u)(x)dx &= \int_{\mathbb{R}}\int_{\mathbb{R}} [\pi_1(l)\phi(y+f_1(l)l) + \pi_2(l)\phi(y+l-f_2(l)l) \\ &\quad - \frac{\phi(y)+\phi(y+l)}{2}]u(y)u(y+l)dldy.\end{aligned}$$

Therefore $V = 0$ whenever

$$\pi_1(l)\phi(y+f_1(l)l) + \pi_2(l)\phi(y+l-f_2(l)l) \equiv \frac{\phi(y)+\phi(y+l)}{2}. \qquad (3.2)$$

To conclude it is sufficient to verify the above equality respectively when $\phi(x) \equiv 1$ and $\phi(x) = x$ and we obtain (i) and (ii). ■ We have the following result.

Theorem 3.3. *Let be $\tau > 0$. Let Assumptions 2.1 and 2.2 be satisfied. For each initial distribution $u_0 \in L^1_+(\mathbb{R})$ (3.1) has a unique global positive solution $u(t,.)$. Moreover the first and second moment of the distribution*

u_0 *are preserved in time. Namely we have the following properties for each* $t \geq 0$

$$\int_{\mathbb{R}} u(t,x)dx = \int_{\mathbb{R}} u_0(x)dx \text{ and } \int_{\mathbb{R}} xu(t,x)dx = \int_{\mathbb{R}} xu_0(x)dx.$$

4. Activity transfert in tumour-immune system

4.1. A general model

Assumption 4.1. *The physical system is constituted by n interacting cells populations. Each population individual may be found in a state described by a variable* $x \in [0,1]$.

Assumption 4.2. *The probability density functions is defined, for each population, by*

$$u^k = u^k(t,x) : [0,\infty) \times [0,1] \longrightarrow \mathbf{R}^+.$$

Therefore, the probability of finding, at the time t an individual of the i-population in the state interval $[0,1]$ *is given by*

$$P_i(t) = \int_0^1 u^k(t,x)dx.$$

Assumption 4.3. *Interactions can be subdivided into conservative encounters which modify the state of the cells but not their number. The evolution due to conservative encounters modifies the progression of tumor cells and the activation of immune cells; Cell interactions in the case of mass conservative encounters will be defined by means of the two quantities : the encounter rate* η^{kl} *and the transition probability density* ψ^{kl}*, where* $\eta^{kl}(y,z)$ *denotes the number of encounters per unit volume and unit time between cell pairs of the* $(i,j)^{th}$ *populations with states y and z, respectively, we have*

$$\eta^{kl}(x,y) = \eta^{kl}(y,x)$$

and $\psi^{kl}(y,z,x)$ *denotes the probability of transition of the* i^{th} *cell to the state x, given its initial state y and the state z of the encountering cells belonging to the* j^{th} *population.*

Assumption 4.4. *Proliferating cells will be described by the vital birth rate* $\beta^k(.,x)$ *where* β^k *denotes the number of cells produced per unit volume and unit time of the* $(i)^{th}$ *species with state x.*
Destructive cells will be described by the vital death rate $\mu^k(.,x)$ *which is the*

number of i^{th} species with state x destroyed.
In this case, these functions depend also on the population quantity

$$P(t) = (P_1(t), ..., P_n(t))^T .$$

The evolution equation obtained using the above assumption consists of the following system of n coupled integro differential equations:

$$\begin{cases} \dfrac{\partial u^k(t,x)}{\partial t} + \underbrace{\dfrac{\partial\big(v^k(P(t),x)u^k(t,x)\big)}{\partial x}}_{Self\ activity-growth} + \underbrace{\mu^k(P(t),x)u^k(t,x)}_{Aptosis} = \\ \underbrace{\sum_{j=1}^{n} Q^{kl}(u^k,u^l)(t,x)}_{Transfer} + \underbrace{\sum_{j=1}^{n}\int_0^1 \beta^k(P(t),x)u^k(t,x)dx}_{Distributed\,Proliferation}, \\ v^k(P(t),0)u^k(t,0) = \underbrace{\int_0^1 \beta^k(P(t),x)u^k(t,x)dx}_{Punctual\,proliferation} \\ u^k(t,0) = f_{i0}(x), \end{cases} \tag{4.1}$$

where

$$Q^{kl}(u^k,u^l) = Q^{kl+}(u^k,u^l) - Q^{kl-}(u^k,u^l) \tag{4.2}$$

with

$$Q^{kl+}(u^k,u^l)(t,x) = \int_0^1\int_0^1 \eta^{kl}(y,z)\psi^{kl}(y,z,x)u^k(t,y)u^l(t,z)dydz \tag{4.3}$$

$$Q^{kl-}(u^k,u^l)(t,x) = u^k(t,x)\int_0^1 \eta^{kl}(x,y)u^l(t,y)dy. \tag{4.4}$$

Q^{kl+} and Q^{kl-} correspond, respectively, to the gain and loss of cells in the state x due to conservative encounters.

4.2. Qualitative Analysis

This Section deals with the asymptotic behaviour of a two population model of the type classified as (4.1) as $t \to \infty$.

More precisely, the general framework proposed in Section 4.1 can be specialized to model the immune competition at the cellular level between immune cells and abnormal cells. The following specific assumptions will be needed:

Assumption 4.5. *The system is constituted by two interacting cell populations: environmental and immune cells, labelled, respectively, by the indexes* $i = 1$ *and* $i = 2$. *homogeneously distributed in space.*

Assumption 4.6. *The functional state of each cell is described by a real variable* $x \in [0, 1]$. *For the environmental cells, the above variable refers to the natural state (normal cells) for* $x = 0$ *and to the abnormal state (abnormal cells) for* $x \in]0, 1]$. *For the immune cells,* $x = 0$ *correspond to non activity or inhibition;* $x \in]0, 1]$ *correspond to activation.*

Assumption 4.7. *The encounter rate is assumed to be constant and equal to unity for all interacting pairs, hence* $\eta^{kl} = \eta = 1,\ \forall i,\ j = 1,\ 2.$

Assumption 4.8. *The transition probability density related to conservative interactions is assumed to be delta functions :*

$$\psi^{kl}(y, z, x) = \delta(x - m^{kl}(y, z))$$

where m^{kl} *corresponds to the output which may depend on the microscopic state of the interacting pair. The basic restrictions on* m^{kl} *are their non negativity, and also* $0 \leq m^{kl}(y, z) \leq 1,\ 0 \leq y,\ z \leq 1,$ *to ensure that dominance values range between zero and unity.*

- ***Conservative encounters of abnormal cells:*** *Cells of the first population show a tendency to degenerate with most probable output given as follows:*

$$m_{11}(y, z) = (1 - \alpha_{11})y + \alpha_{11},$$

where $0 \leq \alpha_{11} < 1$ *is a parameter related to the inner tendency of both a normal and an abnormal cell to degenerate. Here, we consider that the cells do not show a natural tendency to degenerate, i.e.* $\alpha_{11} = 0.$

If a abnormal cell encounters an active immune cell, its state decreases with most probable output given as follows:

$$m_{12}(y, z) = (1 - \alpha_{12})y,$$

where $0 \leq \alpha_{12} < 1$ *is a parameter which indicates the ability of the immune system to reduce the state of cells of the first population.*

- ***Conservative encounters of active immune cells:*** *The only encounters with non-trivial output are those between active immune cells and abnormal cells:*

$$m_{21}(y,z) = (1-\alpha_{21})y, \;\; m_{22}(y,z) = y$$

where $0 \leq \alpha_{21} < 1$ *is a parameter which indicates the ability of the abnormal cells to inhibit immune cells. For more detail see [4].*

The last assumption concerns the growth rate and the proliferation rate

Assumption 4.9. *We assume that a fraction of the energy is channelled to growth of the activity, and a fraction to the punctual proliferation. For more simplicity we assume that there is no distributed proliferation. We also assume that for an individual of activity* x *in the* k^{th} *subpopulation,* $g(P)x$ *is the rate at which maintenance needs energy and* $g(P)(1-x)$ *is what remains for growth.*
Mathematically, we assume, according to the framework of the present paper, no dynamics for the Energy resource and, therefore, the Energy resource uptake rate g *will depend on the total population* P*, i.e.,*$g = g(P)$*. In particular,* $g(P)$ *will be a smooth decreasing positive function satisfying* $g(0) = 1$ *and tending to* 0 *when* P *goes to* ∞*.*

Thus we have the following sub-models for the growth and reproduction rates for each sub-population

$$v^k(P,x) = v^k g(P)(1-x), \text{ and } \beta^k(P,x) = \beta^k g(P)x, \tag{4.5}$$

where v^k and β^k are positive constants. In addition, we will assume the mortality rate m^k, for an individual in the i^{th} subpopulation, a function of P only and positive. Based on the above modelling of cell interactions, the evolution system becomes as follows, for all $i \neq j = 1, 2$,

$$\begin{aligned}
\frac{\partial u^k(t,x)}{\partial t} &+ v^k g(P(t)) \frac{\partial\Big((1-x)u^k(t,x)\Big)}{\partial x} + \mu^k(P(t))u^k(t,x) \\
&= \frac{1}{1-\alpha^{kl}} u^k(t, \frac{x}{1-\alpha^{kl}})\chi(\frac{x}{1-\alpha^{kl}})P^l(t) - u^k(t,x)P^l(t), \qquad (4.6)\\
v^k u^k(t,0) &= \beta^k \int_0^1 x u^k(t,x)dx, \qquad (4.7)\\
u^k(t,0) &= f_{i0}(x), \qquad (4.8)
\end{aligned}$$

Where χ is the characteristic function for $[0,1]$, shown below:

$$\chi(x) = 1, \text{for } 0 \leq x \leq 1;\ \chi(x) = 0 \text{ for } x < 0,\ x > 1.$$

The factors $\chi(\frac{x}{1-\alpha^{kl}})$ must appear in $(4.6) - (4.8)$ to ensure that we are integrating well-defined quantities on $[0,1]$.

We are now in a position to investigate the asymptotic behaviour of $(4.6) - (4.8)$ as $t \to \infty$. To be precise, we are interested in the evolution of the zeroth order moment $\{P^k(t)\}_{i=1}^2$ and the first order moments, related to the activity of each population:

$$A^k(t) = \int_0^1 xu^k(t)(x)dx,\ \ i = 1,2$$

Integrating (4.6) and multiplying (4.6) by x and integrating also, and using (4.7) in both integrals, we obtain, after an integration by parts in the second one, the following ordinary differential equations system, for all $(i \neq j = 1,2)$

$$\dot{P^k}(t) = \beta^k g(x) A^k(t) - \mu^k(x) P^k(t) \tag{4.9}$$

$$\dot{A^k}(t) = v^k g(x) P^k(t) - \left(v^k g(x) + \mu^k(x) + \alpha^{kl} P^l\right) A^k(t), \tag{4.10}$$

This system is supplemented by initial conditions

$$P^k(0) = \int_0^1 u^k(0,x)dx,\ A^k(0) = \int_0^1 xu^k(0,x)dx \leq P^k(0). \tag{4.11}$$

To this end, we impose additional the following Assumption on the parameter μ^k, for $(i = 1,2)$.

- (H_μ^4) μ^k is strictly quasi-increasing in $\mathbf{R}^+ \times \mathbf{R}^+$ [i.e. The function $h^k(y_1, y_2)$ is said to be strictly quasi-increasing (resp. -decreasing) in a subset $\mathcal{C}$ of $\mathbf{R}^2$ if h^k is strictly increasing (resp. decreasing) in y^l for $j \neq i$ and there exists a constant $M^k \geq 0$ such that $h^k(y_1, y_2) + M^k y^k$ is strictly increasing (resp. decreasing) for $(y_1, y_2) \in \mathcal{C}$.]

Notice that there exists only positive , $P^{k,0} > 0,\ (i = 1,2)$, such that $\delta_1(P_1^0, 0) = \beta_1$ and $\delta_2(0, P_2^0) = \beta_2$, if and only if

$$\delta^k(0,0) < \beta^k,\ (i = 1,2). \tag{4.12}$$

Moreover, For all $P^k > Pk, 0,\ (i = 1, 2),\ \beta_1 < \delta_1(P_1, 0),\ \beta_2 < \delta_2(0, P_2)$.

Any region of the form

$$\Omega = \{h = (P_1, A_1, P_2, A_2) \in \mathbf{R}^4 :\ 0 \leq A^k \leq P^k \leq P^{1,k},\ (i = 1, 2)\}$$

with $P^{k,1} > Pk, 0$, is positively invariant. This assumption will be confirmed by the following theorem.
The ODEs $(4.9) - (4.11)$ can be written in the compact form as :

$$\begin{cases} \dot{h}(t) = & G(h), \\ h(0) = & h_0 \in \Omega \end{cases} \tag{4.13}$$

The non-linear operator G is defined on Ω by $G = \big(G_1, G_2, G_3, G_4\big)$,
$G^k(h) = \beta^k g(x) A^k(t) - \mu^k(x) P^k(t)$, for $(i = 1, 3)$ and
$G^k(h) = v^k g(x) P^k(t) - \big(v^k g(x) + \mu^k(x) + \alpha^{kl} P^l\big) A^k(t)$, for $(i = 2, 4)$.

Theorem 4.10. *If conditions $(H^3_\mu) - (H^4_\mu)$ and (4.12) are satisfied, then there exists a unique mild solution $h(t) \in \Omega$ of the initial value problem (4.13), for all $h(0) \in \Omega$ and for all $t \geq 0$.*

Proof. In order to apply the result given in Theorem 5.1 [11, p. 238], we need the following lemmas concerning the nonlinear operator G, involved in the dynamics $(4.9) - (4.10)$. Easy manipulations show that: for $h_1,\ h_2 \in \Omega$,

$$\|G(h_1) - G(h_2)\| \leq l \|h_1 - h_2\|.$$

Consequently, G is an l-dissipative operator on Ω [11, p. 245]. Finally, the following subtangential condition holds: For each $h \in \Omega$,

$$\lim_{\tau \to 0^+} \frac{1}{\tau} d(h + \tau G(h); \Omega) = 0. \tag{4.14}$$

Since G is a continuous function from Ω into $\mathbf{R}^4$ that maps bounded sets into bounded sets and due to the above previous lemmas, for each $h_0 \in \Omega$ there is a unique mild solution $h \in \Omega$ to (4.13) on $[0, \infty)$. ∎

4.3. Equilibrium Profiles

We now investigate the existence of steady states of $(4.9) - (4.11)$. Let

$$f^{ss} = \big(P_1, A_1, P_2, A_2\big)^T$$

be a steady state of $(4.9) - (4.11)$. It satisfies, for all $(i \neq j = 1, 2)$

$$\beta^k A^k \ = \ \delta^k(x) P^k \tag{4.15}$$

$$v^k g(x) P^k \quad = \quad \big(v^k g(x) + \mu^k(x) + \alpha^{kl} P^l\big) A^k \tag{4.16}$$

From (4.15), we find

$$P^k = 0 \quad \text{or} \quad \beta^k v^k g(x) = \big(v^k g(x) + \mu^k(x) + \alpha^{kl} P^l\big)\delta^k(x)$$

Case 4.11. *A first steady state,* $\big(0,0,0,0\big)^T$.

Let, for $(i = 1, 2)$

$$\gamma^k \quad = \quad v^k \frac{\sqrt{1 + 4\dfrac{\beta^k}{v^k}} - 1}{2} > 0,$$

$$\overline{\gamma^k} \quad = \quad v^k \frac{\sqrt{1 + 4\dfrac{\beta^k}{v^k}} + 1}{2}.$$

A non-trivial steady states,

$$f_2^{ss} = \big(0, 0, \underline{P_2}, \underline{A_2}\big)^T,\ f_1^{ss} = \big(\underline{P_1}, \underline{A_1}, 0, 0\big)^T,\ \overline{f^{ss}} = \big(\overline{P_1}, \overline{A_1}, \overline{P_2}, \overline{A_2}\big)^T$$

would satisfy the following cases respectively, from (4.15) − (4.16).

Case 4.12. $\beta_2 \underline{A_2} = \delta_2(0, \underline{P_2})\underline{P_2}$ *with* $\underline{P_2}$ *solution of*

$$\gamma_2 = \delta_2(0, P_2)$$

In this case, there is only non-trivial equilibrium positive f_2^{ss} *if and only if*

$$\delta_2(0,0) \quad < \gamma_2 \quad , \tag{4.17}$$

When, (4.17), holds $\underline{P_2}$ *is the unique value of* P_2 *such that the unbounded strictly increasing function* $\delta_2(0, P_2)$ *takes the value* γ_2, *and* $\underline{A_2} = \dfrac{\delta_2(0, \underline{P_2})}{\beta_2}\underline{P_2}$.

Case 4.13. $\beta_1 \underline{A_1} = \delta_1(\underline{P_1}, 0)\underline{P_1}$ *with* $\underline{P_1}$ *solution of*

$$\gamma_1 = \delta_1(P_1, 0).$$

Analogously, there is only non-trivial equilibrium positive f_1^{ss} *if and only if*

$$\delta_1(0,0) \quad < \quad \gamma_1, \tag{4.18}$$

In this case, $\underline{A_1} = \dfrac{\delta_1(\underline{P_1}, 0)}{\beta_1}\underline{P_1}$.

Since, $\gamma^k < \beta^k$, then, notice that $\delta^k(0,0) < \gamma^k$ imply inequality (4.12).

Case 4.14. $\beta^k\overline{A^k} = \delta^k(\overline{P_1},\overline{P_2})\overline{P^k}$
with $\overline{P}$ *solution of*

$$P_1 = \frac{g(P_1,P_2)\Big(\gamma_2 - \delta_2(P_1,P_2)\Big)\Big(\delta_2(P_1,P_2) + \overline{\gamma_2}\Big)}{\alpha_{21}\delta_2(P_1,P_2)}, \tag{4.19}$$

$$P_2 = \frac{g(P_1,P_2)\Big(\gamma_1 - \delta_1(P_1,P_2)\Big)\Big(\delta_1(P_1,P_2) + \overline{\gamma_1}\Big)}{\alpha_{12}\delta_1(P_1,P_2)} \tag{4.20}$$

Although at this stage we cannot carry out existence and stability analysis for Case 4.14. It is interesting to observe that, when (4.19) − (4.20) *are independent of* P_2 *and* P_1 *respectively, the existence and the instability of this positive equilibrium are guaranteed (see the following section).*

Throughout this paper, we consider that

- (H_μ^5) μ^k will be a smooth function in $\mathbf{R}^+ \times \mathbf{R}^+$.

For simplicity, let

$$g^k = \frac{\partial g}{\partial P^k},\ \delta^{kl} = \frac{\partial \delta^k}{\partial P^l}\ \mu^{kl} = \frac{\partial \mu^k}{\partial P^l} \text{ and } b^{kl} = \delta^{kl}P^k g,\ \ (i,j = 1,2).$$

4.4. Application

Consider the case when (4.19) − (4.20) are independent of P_2 and P_1 respectively:

$$P_1 = \frac{g(P_1,0)\Big(\gamma_2 - \delta_2(P_1,0)\Big)\Big(\delta_2(P_1,0) + \overline{\gamma_2}\Big)}{\alpha_{21}\delta_2(P_1,0)}, \tag{4.21}$$

$$P_2 = \frac{g(0,P_2)\Big(\gamma_1 - \delta_1(0,P_2)\Big)\Big(\delta_1(0,P_2) + \overline{\gamma_1}\Big)}{\alpha_{12}\delta_1(0,P_2)} \tag{4.22}$$

This system, has a unique solution (P_1^*, P_2^*)

Indeed, to obtain the desired result, it suffices to show the existence of solution P_1^* to (4.21), or equivalently to

$$\delta_2(P_1,0) = D_2(P_1), \tag{4.23}$$

with

$$D_2(P_1) = \frac{-(\frac{\alpha_{21}P_1}{g(P_1,0)}+v_2)+\sqrt{(\frac{\alpha_{21}P_1}{g(P_1,0)}+v_2)^2+4\beta_2 v_2}}{2}. \quad (4.24)$$

$D_2(P_1)$ is an decreasing positive function satisfying $D_2(0)=\gamma_2$ and tending to 0 when P_1 goes to ∞. Since, $\delta_2(P_1,0)$ tending to ∞ when P_1 goes to ∞ then by the monotonicity of δ_2, into account $\delta_2(0,0)<\gamma_2$, the equation (4.23) has a unique positive solution P_1^*.
A similar argument shows that P_2^* is a unique solution to (4.22).

It is clear that, $f_*^{ss}=(P_1^*,A_1^*,P_2^*,A_2^*)$ is a non-trivial steady state of the following system

$$\begin{aligned}
\dot{P_1}(t) &= \beta_1 g(0,P_2)A_1(t)-\mu_1(0,P_2)P_1(t)\\
\dot{P_2}(t) &= \beta_2 g(P_1,0)A_2(t)-\mu_2(P_1,0)P_2(t)\\
\dot{A_1}(t) &= v_1 g(0,P_2)P_1(t)-\big(v_1 g(0,P_2)+\mu_1(0,P_2)+\alpha_{12}P_2\big)A_1(t), \quad (4.25)\\
\dot{A_2}(t) &= v_2 g(P_1,0)P_2(t)-\big(v_2 g(P_1,0)+\mu_2(P_1,0)+\alpha_{21}P_1\big)A_2(t),\\
P^k(0) &= \textstyle\int_0^1 u^k(0,x)dx,\ A^k(0)=\int_0^1 xu^k(0,x)dx\le P^k(0).
\end{aligned}$$

with, $A_1^*=\dfrac{\delta_1(0,P_2^*)}{\beta_1}P_1^*$ et $A_2^*=\dfrac{\delta_2(P_1^*,0)}{\beta_2}P_2^*$.

Moreover,

Lemma 4.15. *The critical point f_*^{ss} is unstable.*

4.5. Asymptotic Stability

Now, we study the local stability of the equilibrium f^{ss}.

The positive equilibrium f^{ss} is locally stable if all eigenvalues of the Jacobian Matrix $J(f^{ss})$ have negative real parts.

Lemma 4.16. *If $\delta_2(0,0)<\gamma_2$, then the first steady state , $(0,0,0,0)$ is unstable.*

Proof. The eigenvalues λ of the Jacobian matrix, given at $f^{ss}=0$ by : $-\mu_1(0,0)$, $-v_1-\mu_1(0,0)$, $-\mu_2(0,0)-\gamma_2$ and $-\mu_2(0,0)+\gamma_2$, under condition $\delta_2(0,0)<\gamma_2$, $(0,0,0,0)$ is unstable since $-\mu_2(0,0)+\gamma_2$, is positive. ■ Now we study the local stability of the positive equilibrium f_1^{ss} (resp. f_2^{ss})

Lemma 4.17. *If $\underline{P}_1 > P_1^*$ (resp. $\underline{P}_2 > P_2^*$) then the point f_1^{ss} (resp. f_2^{ss}) is locally asymptotically stable. If $0 < \underline{P}_1 < P_1^*$ (resp. $0 < \underline{P}_2 < P_2^*$) then f_1^{ss} (resp. f_2^{ss}) is unstable.*

Proof. The eigenvalues λ of the Jacobian matrix at $f^{ss} = f_1^{ss}$, are solutions of the following characteristic equations :

$$(\lambda+\mu_2)^2 + (\lambda+\mu_2)(v_2 g + \alpha_{21} P_1) - \beta_2 g^2 v_2 = 0 \quad (4.26)$$
$$(\lambda+\mu_1)^2 + (\lambda+\mu_1)(v_1 g + b_{11}) + b_{11} g(v_1+\delta_1) - \beta_1 g^2 v_1 = 0 \quad (4.27)$$

The solutions of the equation (4.26) are given by

$$g(\underline{P}_1,0)\big(D_2(\underline{P}_1) - \delta_2(\underline{P}_1,0)\big), \quad -g(\underline{P}_1,0)[D_2(\underline{P}_1) + \delta_2(\underline{P}_1,0) + v_2 + \alpha_{21}\frac{\underline{P}_1}{g(\underline{P}_1,0)}]$$

Where D_2 is given by (4.24).

Moreover, since $(v^k)^2 + 4\beta^k v^k = (2\delta^k + v^k)^2$, $(i = 1, 2)$, the solutions of the equation (4.27) given by

$$-g(\underline{P}_1,0)(v_1+\gamma_1) - \mu_1(\underline{P}_1,0) \text{ and } -b_{11}(\underline{P}_1,0)$$

If, $\underline{P}_1 > P_1^*$, by the monotonicity of δ_2 and D_2, (see Section 4.4), $g(\underline{P}_1,0)\big(D_2(\underline{P}_1) - \delta_2(\underline{P}_1,0)\big)$ is negative, then $(\underline{P}_1, \underline{A}_1, 0, 0)$ is stable.

If $\underline{P}_1 < P_1^*$, $g(\underline{P}_1,0)\big(D_2(\underline{P}_1) - \delta_2(\underline{P}_1,0)\big)$ is positive, then f_1^{ss} is unstable.
A similar argument shows that if $\underline{P}_2 > P_2^*$, the point f_2^{ss} is locally asymptotically stable and If $0 < \underline{P}_2 < P_2^*$, f_2^{ss} is unstable.

5. Numerical experiments

In this section, we report some numerical experiments. We use a uniform spatial grid over the interval $[0, 1]$ with $\Delta x = 0.01$. The time mesh size is $\Delta t = r\Delta x$, with a rate $r = 0.5$ destined to control stability, and our CFL stability criterion is never exceeded.

We deals with the simulation of the dynamics of a two population model of the type classified as Model (4.6),. The transition probability density

related to conservative interactions is assumed to be approximated by a Gaussian distribution function with the output defined by the mean value m^{kl}, which may depend on the activation of the interacting pairs, and with a finite variance s^{kl} :

$$\psi^{kl}(x,y,z) = \frac{1}{\sqrt{2\pi s^{kl}}} \exp\big(-\frac{(z-m^{kl}(x,y))^2}{2s^{kl}}\big).$$

In figures, the initial condition is the Gaussian distribution function with the mean value $\mu = 0.3$ and a finite variance $\sigma = 0.01$, for both densities. The graphs in the figures show the evolution in time of the densities of the system: the continuous line is the evolution of the density of the immune cells, while the dashed line is the evolution of the abnormal density.

In **Experiments 2**, and **3** , we assume that a fraction $\alpha^k \in (0,1)$ of ingested energy is channeled to growth and maintenance, and a fraction $(1-\alpha^k)$ to proliferation. We also assume that for an individual of size x in the k^{th} subpopulation, $\alpha^k g^k(\mathbf{P})x$ is the rate at which maintenance needs energy and $\alpha^k g^k(\mathbf{P})(1-x)$ is what remains for growth . Thus we have the following sub-models for the growth and reproduction rates for each subpopulation

$$v^k(\mathbf{P},x) = \bar{v}^k\alpha^k g^k(\mathbf{P})(1-x), \text{ and } \beta^k(\mathbf{P},x) = \bar{\beta}^k(1-\alpha^k)g^k(\mathbf{P})x, \quad (5.1)$$

$g = (g^1, g^2)$ will be a smooth quasi monotone decreasing, in $\mathbf{R}^+ \times \mathbf{R}^+$, g will be positive function satisfying $g(0) = (1,1)$ and tending to $(0,0)$ when $\mathbf{P}$ goes to ∞. where $\bar{v}^k$ and $\bar{\beta}^k$ are positive constants. In addition, we assume that the mortality rate for an individual in the k^{th} subpopulation is given by

$$\mu^k(\mathbf{P}) = \gamma^k - d^k + \frac{a_k\mathbf{P}^1 + b_k\mathbf{P}^2}{c_k\mathbf{P}^1 + d_k\mathbf{P}^2 + a^k}, \quad \gamma^k = \frac{-\bar{v}^k + \sqrt{(\bar{v}^k)^2 + 4\bar{\beta}^k\bar{v}^k}}{2}.$$

The function g^k here is : $g^k(\mathbf{P}) = 1 - \dfrac{a'_k\mathbf{P}^1 + b'_k\mathbf{P}^2}{c'_k\mathbf{P}^1 + d'_k\mathbf{P}^2 + c^k}$ with $(d^k, a_k, b_k, c_k, d_k, a^k)$ and $(a'_k, b'_k, c'_k, d'_k, c^k)$ are the constants positives.

The results of the simulations are reported in the following Figures, which correspond to different values of the parameters (see Table 1).

Parameter	Experiment1	Experiment 2	Experiment3
$\bar{v}^1$	10	10	10
$\bar{v}^2$	0.3	0.3	0.3
$\bar{\beta}^1$	0.2	20	0.20
$\bar{\beta}^2$	0.3	30	30
α^1	0.1	0.1	0.1
α^2	0.2	0.2	0.2
c^1	2	0.8	2
c^2	2	9	9
d^1	3.10^{-4}	3.10^{-5}	3.10^{-5}
d^2	0	10^{-5}	10^{-5}
a^1	1	10	0.1
a^2	1	20	0.2
q	0.2	$\surd$	$\surd$
e	0.9	$\surd$	$\surd$
σ_{12}	0.9	0.1	0.9
σ_{21}	0.1	0.9	0.1
(a_1, b_1, c_1, d_1)	$\surd$	(0, 1, 0, 1)	(1,0,1,0)
(a_2, b_2, c_2, d_2)	$\surd$	(1, 0, 1, 0)	(0,1,0,1)
(a_1', b_1', c_1', d_1')	$\surd$	(0,1,0,1)	(1,0,1,0)
(a_2', b_2', c_2', d_2')	$\surd$	(1,0,1,0)	(0,1,0,1)

Table 1: Different values of the model parameters

In **Experiment 1**, it is, also, interesting to notice that, for

$$\beta^1(\mathbf{P}) = \bar{\beta}^1\alpha^1\frac{\mathbf{P}^2}{c^1+\mathbf{P}^2}(1-x),\ \beta^2(\mathbf{P}) = \bar{\beta}^2\alpha^2(1-\frac{\mathbf{P}^2}{c^2})(1-x)$$

and

$$\mu^2(\mathbf{P}) = \frac{e\mathbf{P}^1}{1+q\mathbf{P}^2},\ \ \mu^1(\mathbf{P}) = \gamma^1 - d^1,$$

that is, the predator-prey system (see Experiment 1 in Table 1), as shown in Figures 2 and 3. If $\sigma_{12} < \sigma_{21}$, the ability of abnormal cells to inhibit

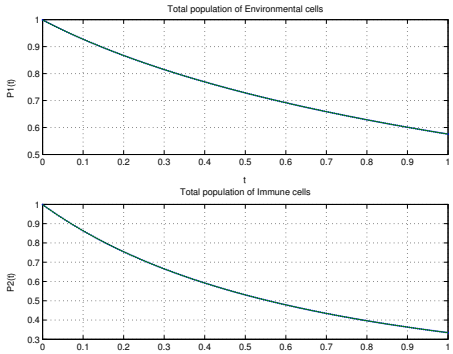

Figure 2: **"Experiment 1":** Total depletion of cells

immune cells is greater than the ability of immune cells to reduce the state of abnormal cells. The final output, if $\sigma_{12} > \sigma_{21}$, is reduction of the state of abnormal cells until their complete depletion and a final survival of immune cells, as shown in Figures 3 .

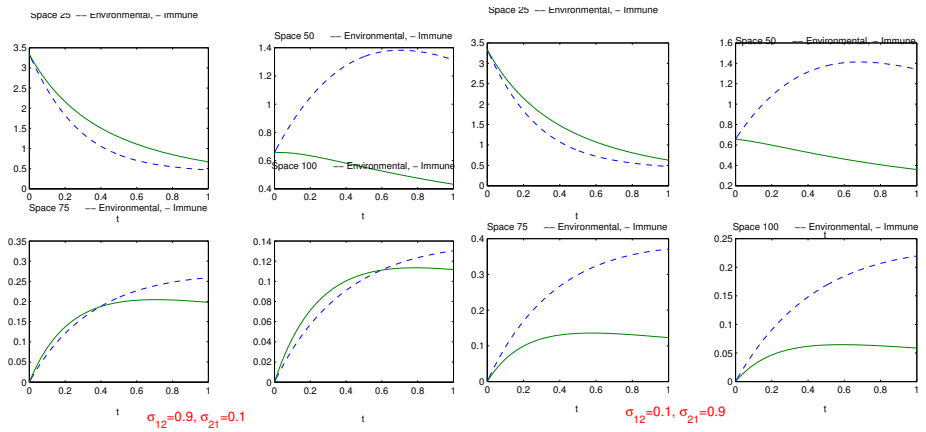

Figure 3: **"Experiment 1":** Effect of the type of parameter σ for density evolution of both population at different spaces: $x = 25$, 50, 75, 100.

In Figures 2, both abnormal and immune cells reduced during the competition. However, in Figures 4 left and 4 right, only once cell population survives and the other is completely depleted: the probability of the 2-population is an increasing function of t and the probability of the 1-population is a decreasing function of t.

6. Appendix: Proof of theorem

Proof.

Existence of a limit u

We first prove the existence of a limit u to u^{Δ} as the mesh size Δx goes to zero. Then we prove that this limit is a solution of the continuous problem (**??**).

The proof of existence of the limit $u(t, x)$ is based on the compact canonical embedding from $W^{1,1}(\Omega)$ into $L^1(\Omega)$. Let $I(u^{\Delta})$, defined on $[0, T] \times \Omega_L$,

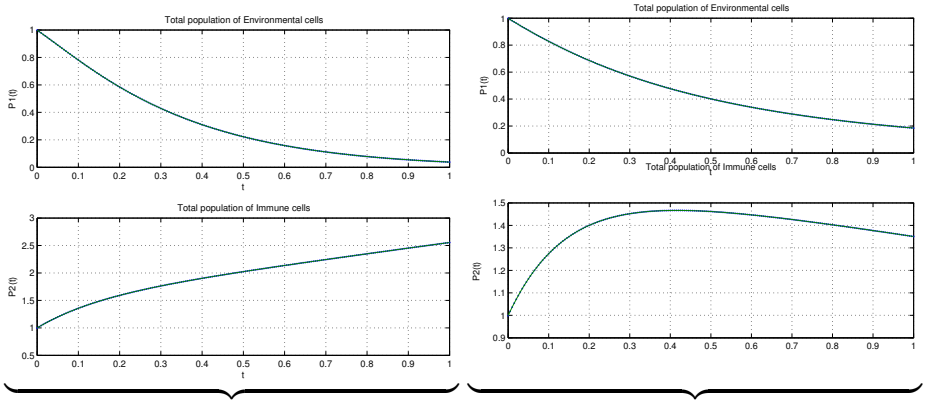

Figure 4: "Experiment 2 left and Experiment 3 right": Depletion of abnormal cells and immune activation

be the interpolate of degree one of u^{Δ} at the vertices of each rectangle $[x_i, x_{i+1}] \times [t_n, t_{n+1}]$; where it is given by

$$\begin{aligned} I(u^{\Delta})(x,t) = \quad & u_i^n + (u_{i+1}^n - u_i^n)\frac{x - i\Delta x}{\Delta x} + (u_i^{n+1} - u_i^n)\frac{t - nr\Delta x}{r\Delta x} \\ & + (u_{i+1}^{n+1} - u_i^{n+1} - u_{i+1}^n + u_i^n)\frac{(x - i\Delta x)(t - nr\Delta x)}{r(\Delta x)^2} \end{aligned} , \quad (6.1)$$

$I(u^{\Delta})$ is continuous with

$$|I(u^{\Delta})|_{L^{\infty}([0,T]\times\Omega_L)} = |u^{\Delta}|_{L^{\infty}([0,T]\times\Omega_L)} = \sup_{n,i} |u_i^n| \quad (6.2)$$

and differentiable inside each rectangle. Thus we obtain

$$\iint |\frac{\partial I(u^{\Delta})}{\partial t}| dxdt \leq \quad \sum_{n=0}^{N} \sum_{i \leq I_L} |u_i^{n+1} - u_i^n| \Delta x. \ . \quad (6.3)$$

In the same way

$$\iint |\frac{\partial I(u^{\Delta})}{\partial x}| dxdt = \quad \sum_{n=0}^{N} \sum_{i \leq I_L} |u_{i+1}^n - u_i^n| r\Delta x \ . \quad (6.4)$$

In the other hand one can check that the numerical scheme (2.2) satisfies the following a priori estimates

$$\begin{aligned}
&\sup_i |u_i^{n+1}| \leq (1 + C_1\Delta t) \sup_i |u_i^n| \\
&\sum_{i=1}^{I_L} |u_{i+1}^{n+1} - u_i^{n+1}| \leq (1 + C_2\Delta t) \sum_{i=1}^{I_L} |u_{i+1}^n - u_i^n| \\
&\sum_{i=1}^{I_L} |u_i^{n+1} - u_i^n| \leq \sum_{i=1}^{I_L} |u_{i+1}^n - u_i^n|
\end{aligned} \tag{6.5}$$

where C_1 and C_2 are two constant independent of n.

Let $u_0 \in L^\infty(\Omega_L)$, (i.e $\sup_i |u_i^0| \leq C$) and with the total variation $TV(u_0(x)) = \sum_{i=1}^{I_L} |u_0(x_{i+1}) - u_0(x_i)|$ be bounded, we have,by applying the discrete Gronvall lemma to the estimates (6.5) and using successively (6.2)and (6.3),(6.4), it follows that u^Δ is bounded and contains a subsequence u^{Δ_p} weakly star convergent to a limit $u \in L^\infty([0,T] \times \Omega_L)$ bounded by $|u_0|_L^\infty(\Omega_L)$. It follows also that

$$|I(u^\Delta)|_{L^\infty([0,T]\times\Omega_L)} + |\frac{\partial I(u^\Delta)}{\partial x}|_{L^1([0,T]\times\Omega_L)} + |\frac{\partial I(u^\Delta)}{\partial t}|_{L^1([0,T]\times\Omega_L)} \leq M. \tag{6.6}$$

Therefore from $\left\{I(u)^\Delta\right\}$ associated to $\left\{u^\Delta\right\}$, we extract a subsequence convergent to $\left\{I(u)^{\Delta_p}\right\}$ in $L^1_{loc}(]0,T[\times\Omega_L)$. Then we verify that $\left\{I(u)^{\Delta_p} - u^{\Delta_p}\right\}$ tends to zero in L^1 , for all bounded open sets $]0,T[\times\Omega_L$. Since the associate subsequence u^Δ weakly star converges to a function $u \in L^\infty(]0,T[\times\Omega_L)$, and since in the other hand $\left\{I(u^{\Delta_p})\right\}$ is convergent in $L^1_{loc}(]0,T[\times\Omega_L)$, we have

$$u^\Delta \text{ converges to } u \text{ in } L^1_{loc}(]0,T[\times\Omega_L). \tag{6.7}$$

This end the proof of the existence of a limit.

Convergence of $Q^\Delta(u^\Delta)$ to $Q(u)$

Now we prove the following lemma

Lemma 6.1. *$Q^\Delta(u^\Delta)$ converges to the continuous transfert operator $Q(u)$, u being the limit function of u^Δ as Δx goes to zero.*

Proof.

Let us write

$$\left|F^{,\Delta}(u^\Delta) - T(u)\right|_1 \leq |Q^\Delta(u^\Delta) - Q(u^\Delta)|_1 + |Q(u^\Delta) - Q(u)|_1$$

Since The transfert operator Q is Lipschitz and u^Δ converges to u the second term of the right hand side of the above inequality $\int_0^1 |Q^\Delta(u^\Delta)(x) - Q(u)(x)|dx \longrightarrow 0$ as the mesh size Δx goes to zero.

Let now calculate $Q(u^\Delta)(x)$.

$$\begin{aligned}
\widehat{T}(u^\Delta)(x) &= \sum_j \int_{x_j}^{x_{j+1}} \pi_1(x) u^\Delta(x_i + f_1(x)p) u^\Delta(x_i - (1 - f_1(x))p) dx \\
&+ \sum_j \int_{x_j}^{x_{j+1}} \pi_2(x) u^\Delta(x_i + f_2(x)p) u^\Delta(x_i - (1 - f_2(x))p) dx. \\
&= \sum_j \int_{x_j}^{x_{j+1}} \pi_1(x) dx u^n_{i+f_1(p_j)j} u^n_{i-(1-f_1(p_j))j} \\
&+ \sum_j \int_{x_j}^{x_{j+1}} \pi_2(p_j) dx \overline{u}^n_{i+f_2(p_j)j} \overline{u}^n_{i-(1-f_2(x))j}.
\end{aligned}$$

but using the mean values of π_1 and π_2

$$\pi_1(l_j) = \frac{\int_{x_j}^{x_{j+1}} \pi_1(x)dx}{\Delta x} \text{ and } \pi_2(l_j) = \frac{\int_{x_j}^{x_{j+1}} \pi_2(x)dx}{\Delta x} \tag{6.8}$$

we conclude that $T(u^\Delta) - F^\Delta(u^\Delta) = 0$. This complete the proof of the lemma. ■

Weak solution

Now we consider the consistency of the scheme, it means that this limit u of the discrete solutions u^Δ is a weak solution of the continuous problem.

For all smooth $\phi \in C^1([0,T] \times \Omega_L)$ with compact support in $[0, T[\times[0,1]$, we define

$$\forall (t,x) \in [x_{i-1}, x_i[\times[t_n, t_{n+1}[,\ \ \phi^\Delta(t,x) = \phi_i^n = \frac{1}{\Delta t \Delta x} \int_{t_n}^{t_{n+1}} \int_{x_{i-1}}^{x_i} \phi(t,x) dt\, dx.$$

Multiplying the scheme (2.2) by $\Delta x \phi_i^n$ we get,

$$\sum_{i,n} (u_i^{n+1} - u_i^n)\phi_i^n - \Delta t \sum_{i,n} F_i^n \phi_i^n \Delta x = 0, \tag{6.9}$$

then summing by part we get

$$\sum_{i,n} \left(u_i^{n+1}(\phi_i^n - \phi_i^{n+1})\right) \Delta x - \Delta t \sum_{i,n} F_i^n \phi_i^n \Delta x - \sum_i u_i^0 \phi_i^0 \Delta x = 0 \tag{6.10}$$

which is equivalent to

$$\begin{aligned}\int_0^T\int_{\Omega_L} u^\Delta(t,x)\frac{\phi^\Delta(t+\Delta t,x)-\phi^\Delta(t,x)}{\Delta t}dx\,dt \\ +\int_0^T\int_{\Omega_L} F^{,\Delta}(u^\Delta)(t,x)\phi^\Delta(t,x)dx\,dt \\ +\int_{\Omega_L} u^\Delta(0,x)\phi^\Delta(0,x)dx=0,\end{aligned} \tag{6.11}$$

we pass to the limit $\Delta x \to 0$, we obtain

$$\begin{aligned}&\int_0^T\int_{\Omega_L} u(t,x)\frac{\partial\phi}{\partial t}(t,x)dxdt+\int_0^T\int_{\Omega_L} Q(u)\phi(t,x)\,dx\,dt \\ &+\int_{\Omega_L} u(0,x)\phi(0,x)dx=0\end{aligned} \tag{6.12}$$

which means that the limit u obtained using the discrete scheme is a weak solution of the problem (3.1) with the initial data $u_0(x)$. ■

7. Conclusion

In the first part of the paper, a discret model was formulated to describe some transfer rules in population dynamics. Population was structured by a discret variable corresponding to size of transferable material. We have proved the convergence to a continuous model which is one-dimensional Boltzmann-type equation of active particles with ovoiding the spatial mechanics aspect. Mathematical analysis was performed, namely existence of solutions, the preservation of individuals number, the preservation of the number and the mass of the cells. In the second part of the paper, we have shown the global existence and the uniqueness of the state trajectories for a mathematical model of a population consisting of several species with coupled interactions and nonlocal boundary conditions. In this case the nonlinear growth, vital birth and death rates depending on the space or/and on the total population. It has also been proved that the trajectories are positive. Specifically, this paper is an analysis of the behaviour of a model of competition between progressing (tumour) cells and immune cells. The analysis refers to class of models proposed in [4]. The nonlinear operator involved in the dynamics is characterized by three phenomenological parameters related to mass conservative encounters : α_{12} and α_{21}. The asymptotic behaviors of depend on the inequality $\mu^k(0,0) < \gamma^k,\ (i=1,2)$, without into account the parameters α^{kl} of conservative interactions, where γ^k depend of known data of the vital birth and the growth rates $v^k,\ \beta^k$. The qualitative analysis provides information on the first order moments $A^k(.),\ (i=1,2)$. Note that this is relevant information towards the biological interpretation considering that the total population simply give the number of cells, while the first order moments also take into account the biological activities of the cells.

[1] S. V. Ambudkar, Z. E. Sauna, M. M. Gottesman, and G. Szakacs, *A novel way to spread drug resistance in tumor cells: Functional inter cellular transfer of P-glycoprotein (ABCB1)*, Trends Pharmacol. Sci., 26 (2005), pp. 385–387.

[2] N. Bellomo *Modeling Complex Living Systems: a kinetic theory and stochastic game approach.* Springer Science Business Media

[3] N. Bellomo, N. Li, and P. Maini, *On the foundations of cancer modelling selected topics, speculations, and perspectives,* Math. Models Methods Appl. Sci., 18 (2008), pp. 593–646.

[4] A. Bellouquid and M. Delitala, *Mathematical Modeling of Complex Biological Systems: A Kinetic Theory Approach,* Birkhäuser, Boston, Basel, Berlin, 2006.

[5] B. Dale, G. P. McNerney, D. L. Thompson, W. Hübner, T. Huser, B. K. Chen, *Visualizing Cell-to-cell Transfer of HIV using Fluorescent Clones of HIV and Live Confocal Microscopy.* JoVE. (2010) 44.

[6] Davis DM, et al. *The protean immune cell synapse: a supramolecular structure with many functions.* Semin. Immunol. 15 (2003), pp. 317–324.

[7] M. E. Dudley and S. A. Rosenberg, *Adoptive-cell-transfer therapy for the treatment of patients with cancer*, Nature Rev. Cancer 3 (2002), pp. 666–675.

[8] M. E. Dudley, et al. *Adoptive cell transfer therapy following non-myeloablative but lymphodepleting chemotherapy for the treatment of patients with refractory metastatic melanoma*, J. Clin. Oncol. 23(2005), pp. 2346–2357.

[9] C. Hansen, E. Angot, A. L. Bergstrom, J.A. Steiner, L. Pieri, G. Paul, T.F. Outeiro, R. Melki, P. Kallunki, K. Fog, J. Y. Li, P. Brundin, α-*Synuclein propagates from mouse brain to grafted dopaminergic neurons and seeds aggregation in cultured human cells*, J Clin Invest, 121 (2011), pp. 715–25.

[10] A. Levchenko, B. M. Mehta, X. Niu, G. Kang, L. Villafania, D. Way, D. Polycarpe, M. Sadelain, and S. M. Larson, *Intercellular transfer of P-glycoprotein mediates acquired multidrug resistance in tumor cells*, Proc. Natl. Acad. Sci. USA, 102 (2005), pp. 1933–1938.

[11] R.H. Martin, Jr., Nonlinear Operators and Differential Equations in Banach Spaces, Wiley, New York, (1976).

[12] A. S. Novozhilov, G. P. Karev, and E. Koonin, *Mathematical modeling of evolution of horizontally transferred genes*, Mol. Biol. Evol., 22 (2005), pp. 1721–1732.

[13] C. Villani, *A review of mathematical topics in collisional kinetic theory, in Handbook of Mathematical Fluid Dynamics*, Vol. 1, S. Friedlander and D. Serre, eds., North–Holland, Amsterdam, (2002), pp. 71–305.

Littlewood-Paley-Stein functions for Schrödinger operators

El Maati Ouhabaz

Université de Bordeaux, Institut de Mathématiques (IMB)
CNRS UMR 5251. 351, Cours de la Libération 33405 - Talence, France
Elmaati.Ouhabaz@math.u-bordeaux.fr

Abstract

We study the boundedness on $L^p(\mathbb{R}^d)$ of the vertical Littlewood-Paley-Stein functions for Schrödinger operators $-\Delta + V$ with non-negative potentials V. These functions are proved to be bounded on L^p for all $p \in (1, 2)$. The situation for $p > 2$ is different. We prove for a class of potentials that the boundedness on L^p, for some $p > d$, holds *if and only if* $V = 0$.

Mathematics Subject Classification: 42B25, 47F05
Keywords: Schrödinger operators, Littlewood-Paley-Stein functions, Functional calculus.

1 Introduction

Let $L := -\Delta + V$ be a Schrödinger operator with a non-negative potential V. It is the self-adjoint operator associated with the form

$$\mathfrak{a}(u, v) := \int_{\mathbb{R}^d} \nabla u.\nabla v dx + \int_{\mathbb{R}^d} Vuvdx$$

with domain

$$D(\mathfrak{a}) = \{u \in W^{1,2}(\mathbb{R}^d), \int_{\mathbb{R}^d} V|u|^2 dx < \infty\}.$$

*Univ. Bordeaux, Institut de Mathématiques (IMB). CNRS UMR 5251. 351, Cours de la Libération 33405 Talence, France. Elmaati.Ouhabaz@math.u-bordeaux.fr

We denote by $(e^{-tL})_{t\geq 0}$ the semigroup generated by (minus) L on $L^2(\mathbb{R}^d)$. Since V is nonnegative, it follows from the Trotter product formula that

$$0 \leq e^{-tL} f \leq e^{t\Delta} f \tag{1}$$

for all $t \geq 0$ and $0 \leq f \in L^2(\mathbb{R}^d)$ (all the inequalities are in the a.e. sense). It follows immediately from (1) that the semigroup $(e^{-tL})_{t\geq 0}$ is sub-Markovian and hence extends to a contraction C_0-semigroup on $L^p(\mathbb{R}^d)$ for all $p \in [1, \infty)$. We shall also denote by $(e^{-tL})_{t\geq 0}$ the corresponding semigroup on $L^p(\mathbb{R}^d)$.

The domination property (1) implies in particular that the corresponding heat kernel of L is pointwise bounded by the Gaussian heat kernel. As a consequence, L has a bounded holomorphic functional calculus on $L^p(\mathbb{R}^d)$ and even Hörmander type functional calculus (see [6]). This implies the boundedness on $L^p(\mathbb{R}^d)$ for all $p \in (1, \infty)$ of the horizontal Littlewood-Paley-Stein functions:

$$g_L(f)(x) := \left[\int_0^\infty t|\sqrt{L}e^{-t\sqrt{L}} f(x)|^2 dt\right]^{1/2}$$

and

$$h_L(f)(x) := \left[\int_0^\infty t|Le^{-tL} f(x)|^2 dt\right]^{1/2}.$$

Indeed, these functions are of the form (up to a constant)

$$S_L f(x) = \left[\int_0^\infty |\psi(tL) f(x)|^2 \frac{dt}{t}\right]^{1/2}$$

with $\psi(z) = \sqrt{z}e^{-\sqrt{z}}$ for g_L and $\psi(z) = ze^{-z}$ for h_L. The boundedness of the holomorphic functional calculus implies the boundedness of S_L (see [8]). Thus, g_L and h_L are bounded on $L^p(\mathbb{R}^d)$ for all $p \in (1, \infty)$ and this holds for every nonnegative potential $V \in L^1_{loc}(\mathbb{R}^d)$.

Now we define the so-called vertical Littlewood-Paley-Stein functions

$$\mathcal{G}_L(f)(x) := \left(\int_0^\infty t|\nabla e^{-t\sqrt{L}} f(x)|^2 + t|\sqrt{V}e^{-t\sqrt{L}} f(x)|^2 \, dt\right)^{1/2}$$

and

$$\mathcal{H}_L(f)(x) := \left(\int_0^\infty |\nabla e^{-tL} f(x)|^2 + |\sqrt{V}e^{-tL} f(x)|^2 \, dt\right)^{1/2}.$$

Note that usually, these two functions are defined without the additional terms $t|\sqrt{V}e^{-t\sqrt{L}} f(x)|^2$ and $|\sqrt{V}e^{-tL} f(x)|^2$.

The functions $\mathcal{G}_L$ and $\mathcal{H}_L$ are very different from g_L and h_L as we shall see in the last section of this paper. If $V = 0$ and hence $L = -\Delta$ it is a very well known fact that $\mathcal{G}_L$ and $\mathcal{H}_L$ are bounded on $L^p(\mathbb{R}^d)$ for all $p \in (1, \infty)$. The Littlewood-Paley-Stein functions are crucial in the study of non-tangential

limits of Fatou type and the boundedness of Riesz transforms. We refer to [14]-[16]. For Schrödinger operators, boundedness results on $L^p(\mathbb{R}^d)$ are proved in [10] for potentials V which satisfy $\frac{|\nabla V|}{V} + \frac{\Delta V}{V} \in L^\infty(\mathbb{R}^d)$. This is a rather restrictive condition. For elliptic operators in divergence form (without a potential) boundedness results on $L^p(\mathbb{R}^d)$ for certain values of p are proved in [2]. For the setting of Riemannian manifolds we refer to [4] and [5]. Again the last two papers do not deal with Schrödinger operators.

In this note we prove that $\mathcal{G}_L$ and $\mathcal{H}_L$ are bounded on $L^p(\mathbb{R}^d)$ for all $p \in (1, 2]$ for every nonnegative potential $V \in L^1_{loc}(\mathbb{R}^d)$. That is

$$\int_{\mathbb{R}^d} \left(\int_0^\infty t|\nabla e^{-t\sqrt{L}} f(x)|^2 + t|\sqrt{V} e^{-t\sqrt{L}} f(x)|^2 \, dt \right)^{p/2} dx \leq C \int_{\mathbb{R}^d} |f(x)|^p dx$$

and similarly,

$$\int_{\mathbb{R}^d} \left(\int_0^\infty |\nabla e^{-tL} f(x)|^2 + |\sqrt{V} e^{-tL} f(x)|^2 \, dt \right)^{p/2} dx \leq C \int_{\mathbb{R}^d} |f(x)|^p dx$$

for all $f \in L^p(\mathbb{R}^d)$.
Our arguments of the proof are borrowed from the paper [4] which we adapt to our case in order to take into account the terms with $\sqrt{V}$ in the definitions of $\mathcal{G}_L$ and $\mathcal{H}_L$. Second we consider the case $p > 2$ and $d \geq 3$. For a wide class of potentials, we prove that if $\mathcal{G}_L$ (or $\mathcal{H}_L$) is bounded on $L^p(\mathbb{R}^d)$ for some $p > d$ then $V = 0$. Here we use some ideas from [7] which deals with the Riesz transform on Riemannian manifolds. In this latter result we could replace $\mathcal{G}_L$ by $\left(\int_0^\infty t|\nabla e^{-t\sqrt{L}} f(x)|^2 dt \right)^{1/2}$ and the conclusion remains valid.

Many questions of harmonic analysis have been studied for Schrödinger operators. For example, spectral multipliers and Bochner Riesz means [6] and [12] and Riesz transforms [12], [1], [13] and [3]. However little seems to be available in the literature concerning the associated Littlewood-Paley-Stein functions $\mathcal{G}_L$ and $\mathcal{H}_L$. Another reason which motivates the present paper is to understand the Littlewood-Paley-Stein functions for the Hodge de-Rham Laplacian on differential forms. Indeed, Bochner's formula allows to write the Hodge de-Rham Laplacian on 1-differential forms as a Schrödinger operator (with a vector-valued potential). Hence, understanding the Littlewood-Paley-Stein functions for Schrödinger operators L could be a first step in order to consider the Hodge de-Rham Laplacian. Note however that unlike the present case, if the manifold has a negative Ricci curvature part, then the semigroup of the Hodge de-Rham Laplacian does not necessarily act on all L^p spaces. Hence the arguments presented in this paper have to be changed considerably. We shall address this problem in a forthcoming paper.

2 Boundedness on L^p, $1 < p \leq 2$

Recall that $L = -\Delta + V$ on $L^2(\mathbb{R}^d)$. We have

Theorem 2.1. *For every $0 \leq V \in L^1_{loc}(\mathbb{R}^d)$, $\mathcal{G}_L$ and $\mathcal{H}_L$ are bounded on $L^p(\mathbb{R}^d)$ for all $p \in (1,2]$.*

Proof. By the subordination formula

$$e^{-t\sqrt{L}} = \frac{1}{\sqrt{\pi}} \int_0^\infty e^{-\frac{t^2}{4s}L} e^{-s} s^{-1/2} ds$$

it follows easily that there exists a positive constant C such that

$$\mathcal{G}_L(f)(x) \leq C\mathcal{H}_L f(x) \tag{2}$$

for all $f \in L^1(\mathbb{R}^d) \cap L^\infty(\mathbb{R}^d)$ and a.e. $x \in \mathbb{R}^d$. See e.g. [4]. Therefore it is enough to prove boundedness of $\mathcal{H}_L$ on $L^p(\mathbb{R}^d)$.
In order to do so, we may consider only nonnegative functions $f \in L^(\mathbb{R}^d)$. Indeed, for a general f we write $f = f^+ - f^-$ and since

$$|\nabla e^{-tL}(f^+ - f^-)|^2 \leq 2(|\nabla e^{-tL} f^+|^2 + |\nabla e^{-tL} f^-|^2)$$

and

$$|\sqrt{V} e^{-tL}(f^+ - f^-)|^2 \leq 2(|\sqrt{V} e^{-tL} f^+|^2 + |\sqrt{V} e^{-tL} f^-|^2)$$

we see that it is enough to prove

$$\|\mathcal{H}_L(f^+)\|_p + \|\mathcal{H}_L(f^-)\|_p \leq C_p(\|f^+\|_p + \|f^-\|_p),$$

which in turn will imply $\|\mathcal{H}_L(f)\|_p \leq 2C_p\|f\|_p$.

Now we follow similar arguments as in [4]. Fix a non-trivial $0 \leq f \in L^1(\mathbb{R}^d) \cap L^\infty(\mathbb{R}^d)$ and set $u(t,x) = e^{-tL} f(x)$. Note that the semigroup $(e^{-tL})_{t\geq 0}$ is irreducible (see [12], Chapter 4) which means that for each $t > 0$, $u(t,x) > 0$ (a.e.). Observe that

$$(\frac{\partial}{\partial t} + L)u^p = (1-p)Vu^p - p(p-1)u^{p-2}|\nabla u|^2.$$

This implies

$$p|\nabla u|^2 + V|u|^2 = -\frac{u^{2-p}}{p-1}(\frac{\partial}{\partial t} + L)u^p. \tag{3}$$

Hence, there exists a positive constant c_p such that

$$\begin{aligned}(\mathcal{H}_L(f)(x))^2 &\leq -c_p \int_0^\infty u(t,x)^{2-p}(\frac{\partial}{\partial t} + L)u(t,x)^p dt \\ &\leq c_p \sup_{t>0} u(t,x)^{2-p} J(x)\end{aligned}$$

where

$$J(x) = -\int_0^\infty (\frac{\partial}{\partial t} + L)u(t,x)^p dt.$$

The previous estimate uses the fact that $(\frac{\partial}{\partial t}+L)u(t,x)^p \leq 0$ which follows from (3). Since the semigroup $(e^{-tL})_{t\geq 0}$ is sub-Markovian it follows that

$$\| \sup_{t>0} e^{-tL} f(x)\|_p \leq C\|f\|_p. \tag{4}$$

The latter estimate is true for all $p \in (1,\infty)$, see [15] (p. 73). Therefore, by Hölder's inequality

$$\int_{\mathbb{R}^d} |\mathcal{H}_L(f)(x)|^p dx \leq c_p \|f\|_p^{\frac{p}{2}(2-p)} \left(\int_{\mathbb{R}^d} J(x)dx\right)^{p/2}. \tag{5}$$

On the other hand,

$$\begin{aligned}
\int_{\mathbb{R}^d} J(x)dx &= -\int_{\mathbb{R}^d}\int_0^\infty (\frac{\partial}{\partial t}+L)u(t,x)^p dtdx \\
&= \|f\|_p^p - \int_0^\infty \int_{\mathbb{R}^d} Lu(t,x)^p dxdt \\
&= \|f\|_p^p - \int_0^\infty \int_{\mathbb{R}^d} Vu(t,x)^p dxdt \\
&\leq \|f\|_p^p.
\end{aligned}$$

Inserting this in (5) gives

$$\int_{\mathbb{R}^d} |\mathcal{H}_L(f)(x)|^p dx \leq c_p \|f\|_p^p$$

which proves the theorem since this estimates extends by density to all $f \in L^p(\mathbb{R}^d)$. □

3 Boundedness on L^p, $p > 2$

We assume throughout this section that $d \geq 3$. We start with the following result.

Proposition 3.1. *Let $0 \leq V \in L^1_{loc}(\mathbb{R}^d)$. If $\mathcal{G}_L$ (or $\mathcal{H}_L$) is bounded on $L^p(\mathbb{R}^d)$ then there exists a constant $C > 0$ such that*

$$\|\nabla e^{-tL} f\|_p \leq \frac{C}{\sqrt{t}} \|f\|_p \tag{6}$$

for all $t > 0$ and all $f \in L^p(\mathbb{R}^d)$.

Proof. Remember that by (2), if $\mathcal{H}_L$ is bounded on $L^p(\mathbb{R}^d)$ then the same holds for $\mathcal{G}_L$.
Suppose that $\mathcal{G}_L$ is bounded on $L^p(\mathbb{R}^d)$. We prove that

$$\|\nabla f\|_p \leq C\left[\|L^{1/2} f\|_p + \|Lf\|_p^{1/2} \|f\|_p^{1/2}\right]. \tag{7}$$

The inequality here holds for f in the domain of L, seen as an operator on $L^p(\mathbb{R}^d)$.[1] In order to do this we follow some arguments from [5]. Set $P_t := e^{-t\sqrt{L}}$ and fix $f \in L^2(\mathbb{R}^d)$. By integration by parts,

$$\|\nabla P_t f\|_2^2 = (-\Delta P_t f, P_t f) \leq (LP_t f, P_t f) = \|L^{1/2} P_t f\|_2^2.$$

In particular,

$$\|\nabla P_t f\|_2 \leq \frac{C}{t}\|f\|_2 \to 0 \text{ as } t \to +\infty.$$

The same arguments show that $t\|\nabla L^{1/2} P_t f\|_2 \to 0$ as $t \to +\infty$. Therefore,

$$\begin{aligned} |\nabla f|^2 &= -\int_0^\infty \frac{d}{dt}|\nabla P_t f|^2 dt \\ &= -\left[t\frac{d}{dt}|\nabla P_t f|^2\right]_0^\infty + \int_0^\infty \frac{d^2}{dt^2}|\nabla P_t f|^2 t\, dt \\ &\leq \int_0^\infty \frac{d^2}{dt^2}|\nabla P_t f|^2 t\, dt \\ &= 2\int_0^\infty (|\nabla L^{1/2} P_t f|^2 + \nabla L P_t f.\nabla P_t f) t\, dt \\ &=: I_1 + I_2. \end{aligned}$$

Using the fact that $\mathcal{G}_L$ is bounded on $L^p(\mathbb{R}^d)$ it follows that

$$\|I_1\|_{p/2} \leq \|\mathcal{G}_L(L^{1/2} f)\|_p^2 \leq C\|L^{1/2} f\|_p^2. \tag{8}$$

By the Cauchy-Schwartz inequality,

$$\begin{aligned} |I_2| &\leq \left(\int_0^\infty (|\nabla L P_t f|^2 t dt\right)^{1/2} \left(\int_0^\infty (|\nabla P_t f|^2 t dt\right)^{1/2} \\ &\leq \mathcal{G}_L(Lf)\mathcal{G}_L(f). \end{aligned}$$

Integrating gives

$$\|I_2\|_{p/2}^{p/2} \leq \left(\int_{\mathbb{R}^d} |\mathcal{G}_L(Lf)|^p\right)^{1/2} \left(\int_{\mathbb{R}^d} |\mathcal{G}_L(f)|^p\right)^{1/2} \leq C\|Lf\|_p^{p/2}\|f\|_p^{p/2}. \tag{9}$$

Combining (8) and (9) gives (7) for $f \in D(L) \cap L^2(\mathbb{R}^d)$. In order to obtain (7) for all $f \in D(L)$ we take a sequence $f_n \in L^2(\mathbb{R}^d) \cap L^p(\mathbb{R}^d)$ which converges in the L^p-norm to f. We apply (7) to $e^{-tL} f_n$ (for $t > 0$) and then let $n \to +\infty$ and $t \to 0$.

For $f \in L^p(\mathbb{R}^d)$ we apply (7) to $e^{-tL} f$ and we note that $\|L^{1/2} e^{-tL} f\|_p \leq \frac{C}{\sqrt{t}}\|f\|_p$ and $\|Le^{-tL} f\|_p \leq \frac{C}{t}\|f\|_p$. Both assertions here follow from the analyticity of the semigroup on $L^p(\mathbb{R}^d)$ (see [12], Chap. 7). This proves the proposition.

[1] Since the semigroup e^{-tL} is sub-Markovian, it acts on $L^p(\mathbb{R}^d)$ and hence the generator of this semigroup in $L^p(\mathbb{R}^d)$ is well defined. This is the operator L we consider on $L^p(\mathbb{R}^d)$.

Remark. In the proof we did not use the boundedness of the function $\mathcal{G}_L$ but only its gradient part, i.e. boundedness on $L^p(\mathbb{R}^d)$ of the Littlewood-Paley-Stein function:

$$\mathcal{G}(f)(x) = \left(\int_0^\infty t |\nabla e^{-t\sqrt{L}} f(x)|^2 dt \right)^{1/2}. \tag{10}$$

In the next result we shall need the assumption that there exists $\varphi \in L^\infty(\mathbb{R}^d)$, $\varphi > 0$ such that

$$L\varphi = 0. \tag{11}$$

The meaning of (11) is $e^{-tL}\varphi = \varphi$ for all $t \geq 0$.
Note that (11) is satisfied for a wide class of potentials. This is the case for example if $V \in L^{d/2-\varepsilon}(\mathbb{R}^d) \cap L^{d/2+\varepsilon}(\mathbb{R}^d)$ for some $\varepsilon > 0$, see [9]. See also [11] for more results in this direction.

Theorem 3.2. *Suppose that there exists $0 < \varphi \in L^\infty(\mathbb{R}^d)$ which satisfies (11). Then $\mathcal{G}_L$ (or $\mathcal{H}_L$) is bounded on $L^p(\mathbb{R}^d)$ for some $p > d$ if and only if $V = 0$*

Proof. If $V = 0$ then $L = -\Delta$ and it is known that the Littlewood-Paley-Stein function $\mathcal{G}_L$ (and also $\mathcal{H}_L$) is bounded on $L^p(\mathbb{R}^d)$ for all $p \in (1, \infty)$.
Suppose now that V is as in the theorem and $\mathcal{G}_L$ is bounded on $L^p(\mathbb{R}^d)$ for some $p > d$.
Let $k_t(x, y)$ be the heat kernel of L, i.e.,

$$e^{-tL} f(x) = \int_{\mathbb{R}^d} k_t(x, y) f(y) dy$$

for all $f \in L^2(\mathbb{R}^d)$. As mentioned in the introduction, due to the positivity of V,

$$k_t(x, y) \leq \frac{1}{(4\pi t)^{d/2}} e^{-\frac{|x-y|^2}{4t}}. \tag{12}$$

On the other hand, using the Sobolev inequality (for $p > d$)

$$|f(x) - f(x')| \leq C|x - x'|^{1-\frac{d}{p}} \|\nabla f\|_p$$

we have

$$|k_t(x, y) - k_t(x', y)| \leq C|x - x'|^{1-\frac{d}{p}} \|\nabla k_t(., y)\|_p.$$

Using (12), Proposition 3.1 and the fact that

$$k_t(x, y) = e^{-\frac{t}{2}L} k_{\frac{t}{2}}(., y)(x),$$

we have

$$|k_t(x, y) - k_t(x', y)| \leq C|x - x'|^{1-\frac{d}{p}} t^{-\frac{1}{2}} t^{-\frac{d}{2}(1-\frac{1}{p})}. \tag{13}$$

Thus, using again (12) we obtain

$$\begin{aligned} |k_t(x,y)-k_t(x',y)| &= |k_t(x,y)-k_t(x',y)|^{1/2}|k_t(x,y)-k_t(x',y)|^{1/2} \\ &\leq C|x-x'|^{\frac{1}{2}-\frac{d}{2p}}t^{-\frac{d}{2}+\frac{d}{4p}-\frac{1}{4}}\left(e^{-\frac{|x-y|^2}{8t}}+e^{-\frac{|x'-y|^2}{8t}}\right). \end{aligned}$$

Hence, for $x, x' \in \mathbb{R}^d$

$$\begin{aligned} |\varphi(x)-\varphi(x')| &= |e^{-tL}\varphi(x)-e^{-tL}\varphi(x')| \\ &= |\int_{\mathbb{R}^d}[k_t(x,y)-k_t(x',y)]\varphi(y)dy \\ &\leq \|\varphi\|_\infty \int_{\mathbb{R}^d}|k_t(x,y)-k_t(x',y)|dy \\ &\leq C|x-x'|^{\frac{1}{2}-\frac{d}{2p}}t^{\frac{d}{4p}-\frac{1}{4}}. \end{aligned}$$

Letting $t \to \infty$, the RHS converges to 0 since $p > d$. This implies that $\varphi = c > 0$ is constant. The equality $0 = L\varphi = Lc = Vc$ and hence $V = 0$. □

Remark. 1. The above proof is inspired from [7] in which it is proved that the boundedness of the Riesz transform $\nabla L^{-1/2}$ on $L^p(\mathbb{R}^d)$ for some $p > d$ implies that $V = 0$.
2. According to a previous remark, we could replace in the last theorem the boundedness of $\mathcal{G}_L$ by the boundedness of $\mathcal{G}$ defined by (10).

References

[1] J. Assaad and E.M. Ouhabaz, Riesz transforms of Schrödinger operators on manifolds, J. Geom. Anal. 22 (2012), no. 4, 1108-1136.

[2] P. Auscher, On necessary and sufficient conditions for L^p-estimates of Riesz transforms associated to elliptic operators on $\mathbb{R}^n$ and related estimates, Mem. Amer. Math. Soc. 186 (2007), no. 871, xviii+75 pp.

[3] P. Auscher and A. Ben Ali, Maximal inequalities and Riesz transform estimates on L^p-spaces for Schrödinger operators with nonnegative potentials, Ann. Inst. Fourier (Grenoble) 57 (2007), no. 6, 1975-2013.

[4] Th. Coulhon, X.T. Duong and X.D. Li, Littlewood-Paley-Stein functions on complete Riemannian manifolds for $1 \leq p \leq 2$, Studia Math. 154 (1) (2002) 37-57.

[5] Th. Coulhon and X.T. Duong, Riesz transform and related inequalities on noncompact Riemannina manifolds, Comm. Pure App. Math. Vol. LVI (2003) 1728-1751.

[6] X.T. Duong, E.M. Ouhabaz and A. Sikora, Plancherel-type estimates and sharp spectral multipliers, J. Funct. Anal. 196 (2002), no. 2, 443-485.

[7] P. Chen, J. Magniez and E.M. Ouhabaz, The Hodge-de Rham Laplacian and L^p-boundedness of Riesz transforms on non-compact manifolds, Nonlinear Anal. 125 (2015), 78-98.

[8] M. Cowling, I. Doust, A. McIntosh and A. Yagi, Banach space operators with a bounded H^∞ functional calculus, J. Austral. Math. Soc. Ser. A 60 (1996), no. 1, 51-89.

[9] I. McGillivray and E.M. Ouhabaz, Existence of bounded invariant solutions for absorption semigroups, in "Differential Equations, Asymptotic Analysis and Mathematical Physics", Mathematical Research, Vol 100 (1997) 226-241.

[10] T. Miyokawa and I. Shigekawa, On equivalence of L^p-norms related to Schrödinger type operators on Riemannian manifolds, Probab. Theory Relat. Fields 135 (2008) 487-519.

[11] M. Murata, Structure of positive solutions to $(-\Delta + V)u = 0$ in $\mathbb{R}^n$, Duke Math. J. 53 (1986), 869-943.

[12] E.M. Ouhabaz, Analysis of Heat Equations on Domains, London Math. Soc. Monographs, Vol. 31. Princeton Univ. Press 2005.

[13] Z. Shen, L^p-estimates for Schrödinger operators with certain potentials, Ann. Inst. Fourier (Grenoble) 45 (1995), p. 513-546.

[14] E. M. Stein, On the functions of Littlewood-Paley, Lusin and Marcinkiewicz , Trans. Amer. Math. Soc. 88 (1958), 137-174.

[15] E.M. Stein, Topics in Harmonic Analysis Related to the Littlewood-Paley Theory, Princeton Univ. Press, 1970.

[16] E.M. Stein, Singular Integrals and Differentiability Properties of Functions, Princeton Univ. Press, 1970.

On the quartic residue symbols of certain fundamental units

Abdelmalek AZIZI [1,4], Mohammed TAOUS [2] and Abdelkader ZEKHNINI [3]

1- ACSA Laboratory, Sciences Faculty, Mohammed First University, Oujda, Morocco.
2- Faculty of Sciences and Technology, Moulay Ismaïl University, Errachidia, Morocco.
3- Pluridisciplinary Faculty of Nador, Mohammed First University, Morocco.
4- Corresponding Author E-mail: abdelmalekazizi@yahoo.fr

Abstract. *Let d be a square-free integer, $\mathbf{k} = \mathbb{Q}(\sqrt{d}, i)$ and $i = \sqrt{-1}$. Let $\mathbf{k}_1^{(2)}$ be the Hilbert 2-class field of $\mathbf{k}$, $\mathbf{k}_2^{(2)}$ be the Hilbert 2-class field of $\mathbf{k}_1^{(2)}$ and $G = \mathrm{Gal}(\mathbf{k}_2^{(2)}/\mathbf{k})$ be the Galois group of $\mathbf{k}_2^{(2)}/\mathbf{k}$. We give necessary and sufficient conditions to have G metacyclic in the case where $d = pq$, with p and q are primes such that $p \equiv 1 \pmod 8$ and $q \equiv 7 \pmod 8$ and the 2-class group of $\mathbf{k}$ is of type $(2, 4)$, using the quartic residue symbols of certain fundamental units.*

Key words: 2-class groups, Hilbert class fields, 2-metacyclic groups.

1. Introduction

Let k be an algebraic number field and l be a prime; then $\mathfrak{l}_k$ will denote a prime ideal of k above l. We denote, also, by $\left(\frac{x}{\mathfrak{l}_k}\right)$ the quadratic residue symbol for the prime $\mathfrak{l}_k$ applied to x. If k contains $i = \sqrt{-1}$ and $\mathfrak{l}_k$ is prime to 2, then we can define $\left(\frac{x}{\mathfrak{l}_k}\right)_4$ by :

$$\left(\frac{x}{\mathfrak{l}_k}\right)_4 \equiv x^{\frac{N(\mathfrak{l}_k)-1}{4}} \pmod{\mathfrak{l}_k}.$$

Where $N(\mathfrak{l}_k)$ is the absolute norm of $\mathfrak{l}_k$. Let $Cl_2(k)$ denote the 2-class group of k, $k_2^{(1)}$ its Hilbert 2-class field and $k_2^{(2)}$ its second Hilbert 2-class field that is the Hilbert 2-class field of $k_2^{(1)}$. Put $G = \mathrm{Gal}(k_2^{(2)}/k)$ and G' its derived group, then it is well known that $G/G' \simeq Cl_2(k)$. An important problem in Number Theory is to characterize the structure of G using the residue symbols, since the knowledge of G, its structure and its generators solve a lot of problems in number theory such as capitulation problems, whether class field towers are finite or not and the structures of the 2-class groups of the unramified extensions of k within $k_2^{(1)}$. In this paper, we give an example of this situation.

Let $\mathbf{k}=\mathbb{Q}(\sqrt{pq},i)$, where $p\equiv 1 \pmod 4$ and $q\equiv 3 \pmod 4$ are two different primes such that $\left(\frac{q}{p}\right)=1$, then the symbols $\left(\frac{\varepsilon_q}{p}\right):=\left(\frac{\varepsilon_q}{\mathfrak{p}_{\mathbb{Q}(\sqrt{q})}}\right)$ and $\left(\frac{\varepsilon_{2q}}{p}\right):=\left(\frac{\varepsilon_{2q}}{\mathfrak{p}_{\mathbb{Q}(\sqrt{2q})}}\right)$ do not depend on the choice of $\mathfrak{p}_{\mathbb{Q}(\sqrt{q})}$ and $\mathfrak{p}_{\mathbb{Q}(\sqrt{2q})}$ (ε_m is the fundamental unit of $\mathbb{Q}(\sqrt{m})$, where $m=q$ or $2q$). According to [1], $2\varepsilon_m$ is a square in $\mathbb{Q}(\sqrt{m})$ whenever $m=q$ or $2q$, so $\left(\frac{\varepsilon_m}{p}\right)=\left(\frac{2}{p}\right)$. If $p\equiv 1 \pmod 8$, then we can define the following quartic residue symbol: $\left(\frac{\varepsilon_m}{p}\right)_4:=\left(\frac{\varepsilon_m}{\mathfrak{p}_{\mathbb{Q}(\sqrt{m},i)}}\right)_4$ (see. [8]). In the present paper, we give explicit expressions of this symbol for $m=q$ and we show that if the 2-class group of $\mathbf{k}$ is of type $(2,4)$, then it takes the value -1 and we also show that the metacyclicity of G is characterized by the value of this symbol for $m=2q\equiv 14 \pmod{16}$.

Let m be a square-free integer and k be a number field. Throughout this paper, we adopt the following notations:

- $h(m)$, (resp. $h(k)$): the 2-class number of $\mathbb{Q}(\sqrt{m})$, (resp. k).
- ε_m: the fundamental unit of $\mathbb{Q}(\sqrt{m})$, if $m>0$.
- E_k: the unit group of $\mathcal{O}_k$.
- W_k: the group of roots of unity contained in k.
- ω_k: the order of W_k.
- $i=\sqrt{-1}$.
- k^+: the maximal real subfield of k, if k is a CM-field.
- $Q_k=[E_k:W_kE_{k^+}]$ is the Hasse unit index, if k is a CM-field.
- $\mathbf{C}l_2(k)$: the 2-class group of k.

2. The quartic residue symbol of ε_m and applications

In what follows, we adopt the following notations: if $p\equiv 1 \pmod 8$ is a prime, then $\left(\frac{2}{p}\right)_4$ will denote the rational biquadratic symbol which is equal to 1 or -1, according as $2^{\frac{p-1}{4}}\equiv 1$ or $-1 \pmod p$. Moreover the symbol $\left(\frac{p}{2}\right)_4$ is equal to $(-1)^{\frac{p-1}{8}}$. A 2-group H is said to be of type $(2^{n_1},2^{n_1},...,2^{n_s})$ if it is isomorphic to $\mathbb{Z}/2^{n_1}\times\mathbb{Z}/2^{n_2}\times...\mathbb{Z}/2^{n_s}$, where $n_i\in\mathbb{N}$. Finally, r denotes the rank of the 2-class group of $\mathbb{Q}(\sqrt{q},\sqrt{p},i)$.

Theorem 1. *Let $p=u^2\mp 2\epsilon v^2\equiv 1 \pmod 8$, $q=w^2-2\epsilon z^2\equiv 3 \pmod 4$ be primes such that $\epsilon=\left(\frac{2}{q}\right)$ and $\left(\frac{q}{p}\right)=1$. If ε_q is the fundamental unit of $\mathbb{Q}(\sqrt{q})$, then*

$$\left(\frac{\varepsilon_q}{p}\right)_4=\left(\frac{2}{p}\right)_4\left(\frac{uz\pm vw}{p}\right).$$

Proof. As $p \equiv 1 \pmod 8$ and $q \equiv 3 \pmod 4$, then

$$\begin{cases} \left(\dfrac{2\epsilon}{p}\right) = \left(\dfrac{\pm 2}{p}\right) = 1; \\ \left(\dfrac{2\epsilon}{q}\right) = \left(\dfrac{\epsilon}{q}\right)\left(\dfrac{2}{q}\right) = \epsilon\epsilon = 1. \end{cases}$$

This means that p and q split in the ring of integers of $\mathbb{Q}(\sqrt{2\epsilon})$, so there exist four positive integers u, z, v and w such that

$$p = u^2 \mp 2\epsilon v^2 \quad \text{et} \quad q = w^2 - 2\epsilon z^2.$$

Let $\varepsilon_q = x + y\sqrt{q}$ be the fundamental unite of $\mathbb{Q}(\sqrt{q})$. Since $q \equiv 3 \pmod 4$, so $2\varepsilon_q$ is a square in $\mathbb{Q}(\sqrt{q})$ (see [1]). In this situation, we have that

$$\begin{cases} x + \epsilon = y_1^2, \\ x - \epsilon = q y_2^2, \end{cases} \quad \text{and} \quad \sqrt{2\varepsilon_2} = y_1 + y_2\sqrt{q}$$

where $y = y_1 y_2$, then $2\epsilon = y_1^2 - q y_2^2$ and $(y_1 - \sqrt{2\varepsilon})(y_1 + \sqrt{2\varepsilon}) = q y_2^2$. Let $q = \mu\overline{\mu}$ be the decomposition of q in $\mathbb{Q}(\sqrt{2\epsilon})$. As $y_1 - \sqrt{2\varepsilon}$ is the conjugate of $y_1 + \sqrt{2\varepsilon}$ in $\mathbb{Q}(\sqrt{2\epsilon})$, so we obtain the following decomposition:

$$\begin{cases} y_1 \pm \sqrt{2\varepsilon} = \mu\alpha^2, \\ y_1 \mp \sqrt{2\varepsilon} = \overline{\mu}\overline{\alpha}^2, \end{cases}$$

where $\overline{\alpha}$ is the conjugate of α and $y_2 = \alpha\overline{\alpha}$, which implies that $2y_1 = \mu\alpha^2 + \overline{\mu}\overline{\alpha}^2$. Using this equality we can check that

$$2\mu\sqrt{2\varepsilon_2} = (\mu\alpha + \overline{\alpha}\sqrt{q})^2.$$

Then

$$\begin{aligned} \left(\frac{\sqrt{2\varepsilon_q}}{\mathfrak{p}_{\mathbb{Q}(\sqrt{q})}}\right) = \left(\frac{\sqrt{2\varepsilon_q}}{\mathfrak{p}_{\mathbb{Q}(\sqrt{q},\sqrt{2\epsilon})}}\right) &= \left(\frac{2\mu}{\mathfrak{p}_{\mathbb{Q}(\sqrt{q},\sqrt{2\epsilon})}}\right) \\ &= \left(\frac{2}{\mathfrak{p}_{\mathbb{Q}(\sqrt{q},\sqrt{2\epsilon})}}\right)\left(\frac{w \pm \sqrt{2\epsilon}z}{\mathfrak{p}_{\mathbb{Q}(\sqrt{q},\sqrt{2\epsilon})}}\right) \\ &= \left(\frac{2}{p}\right)\left(\frac{w \pm \sqrt{2\epsilon}z}{\mathfrak{p}_{\mathbb{Q}(\sqrt{2\epsilon})}}\right) \\ &= \left(\frac{w \pm \sqrt{2\epsilon}z}{u \pm \sqrt{2\epsilon}v}\right) \\ &= \left(\frac{v}{u \pm \sqrt{2\epsilon}v}\right)\left(\frac{wv \pm \sqrt{2\epsilon}zv}{u \pm \sqrt{2\epsilon}v}\right) \\ &= \left(\frac{v}{p}\right)\left(\frac{wv \pm uv}{u \pm \sqrt{2\epsilon}v}\right) \\ &= \left(\frac{v}{p}\right)\left(\frac{wv \pm uv}{p}\right). \end{aligned}$$

According to [7, proposition 5.1, p. 154], we have $\left(\frac{v}{p}\right)=1$, then

$$\left(\frac{\varepsilon_q}{p}\right)_4=\left(\frac{2}{p}\right)_4\left(\frac{\sqrt{2\varepsilon_q}}{\mathfrak{p}_{\mathbb{Q}(\sqrt{q})}}\right)=\left(\frac{2}{p}\right)_4\left(\frac{uz\pm vw}{p}\right).$$

□

Corollary 1. *Let* $\mathbf{k}=\mathbb{Q}(\sqrt{pq},i)$*, where* $p\equiv 1 \pmod 8$ *and* $q\equiv 3 \pmod 4$*, and* ε_q *be the fundamental unit of* $\mathbb{Q}(\sqrt{q})$*. If the* 2*-class group of* $\mathbf{k}$ *is of type* $(2,4)$*, then*

$$\left(\frac{\varepsilon_q}{p}\right)_4=-\left(\frac{2}{p}\right)_4.$$

Proof. As the 2-class group of $\mathbf{k}$ is of type $(2,4)$, so $\left(\frac{p}{q}\right)=-\left(\frac{q}{p}\right)_4=1$ and $Q_{\mathbf{k}}=1$(see [2]). Recall that Kaplan has proved in [5, theorem B_2 and B_3] that if $Q_{\mathbf{k}}=1$, then $\left(\frac{uz+vw}{p}\right)=\left(\frac{q}{p}\right)_4=-1$. This completes the proof of our assertion. □

Corollary 2. *Let* $\mathbf{k}=\mathbb{Q}(\sqrt{pq},i)$*, where* $p\equiv 1 \pmod 8$ *and* $q\equiv 3 \pmod 4$*, and* r *be the rank of the* 2*-class group of* $\mathbb{Q}(\sqrt{q},\sqrt{p},i)$*. If the* 2*-class group of* $\mathbf{k}$ *is of type* $(2,4)$*, then*

$$r=\begin{cases}2, & \text{if } \left(\frac{2}{p}\right)_4=\left(\frac{p}{2}\right)_4;\\ 3, & \text{if } \left(\frac{p}{q}\right)=1 \text{ and } \left(\frac{2}{p}\right)_4=-\left(\frac{p}{2}\right)_4.\end{cases}$$

Proof. In [3], we have shown that, if $q\equiv 3 \pmod 4$, then, by putting $\eta=\left(\frac{\sqrt{2\varepsilon_q}}{\mathfrak{p}_{\mathbb{Q}(\sqrt{q})}}\right)$ if $\left(\frac{p}{q}\right)=1$,

we obtain

$$r=\begin{cases}1, & \text{if } \left(\frac{p}{q}\right)=-1;\\ 2, & \text{if } \left(\frac{p}{q}\right)=1 \text{ and } \left(\frac{2}{p}\right)_4=-\left(\frac{p}{2}\right)_4\eta;\\ 3, & \text{if } \left(\frac{p}{q}\right)=1 \text{ and } \left(\frac{2}{p}\right)_4=\left(\frac{p}{2}\right)_4\eta.\end{cases}$$

Since the 2-class group of $\mathbf{k}$ is of type $(2,4)$, then $\left(\frac{p}{q}\right) = 1$ and $\eta = -1$ (see the previous corollary). □

Lemma 1 ([6]). *Let* $\mathbf{k} = \mathbb{Q}(\sqrt{pq}, i)$, *where* $p \equiv 1 \pmod 1$ *and* $q \equiv 3 \pmod 4$. *If* $\left(\frac{q}{p}\right) = 1$, *then there exist an unramified cyclic extension of degree* 4 *containing* $\mathbf{k}^* = \mathbb{Q}(\sqrt{p}, \sqrt{q}, i)$ *the genus field of* $\mathbf{k}$.

Theorem 2. *Let* $\mathbf{k} = \mathbb{Q}(\sqrt{pq}, i)$, *where* $p \equiv 1 \pmod 8$ $q \equiv 7 \pmod 8$, *and put* $G = Gal(\mathbf{k}_2^{(2)}/\mathbf{k})$. *Assume the 2-class group of* $\mathbf{k}$ *is of type* $(2,4)$, *then the group* G *is metacyclic if and only if* $\left(\frac{\varepsilon_{2q}}{p}\right)_4 = -1$.

Proof. As the 2-class group of $\mathbf{k}$ is of type $(2,4)$, then the extension $\mathbf{k}_2^{(1)}/\mathbf{k}$ admits three abelian subextensions of degree 2 say $\mathbf{K}_{i,2}$ and three abelian subextensions of degree 4 say $\mathbf{K}_{i,4}$ where $i \in \{1,2,3\}$. The following figure illustrates the situation.

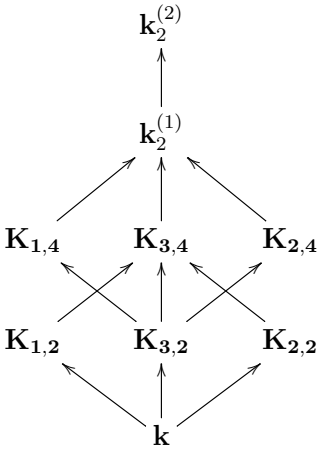

Thus [4, Theorem 14, p. 107] yields that G is metacyclic if and only if the rank of the 2-class group of $\mathbf{K_{3,2}}$ is equal to 2, this in turn is equivalent, by Corollary 2 and previous Lemma, to $\left(\frac{2}{p}\right)_4 \left(\frac{p}{2}\right)_4 = 1$. As $q \equiv 7 \pmod 8$, the [8, Theorem 1, p. 690] and the Corollary 2 imply that

$$\left(\frac{\varepsilon_{2q}}{p}\right)_4 = \left(\frac{\varepsilon_q}{p}\right)_4 \left(\frac{p}{2}\right)_4 = -\left(\frac{2}{p}\right)_4 \left(\frac{p}{2}\right)_4.$$

This completes the proof of the theorem. □

References

[1] A. Azizi, *Sur la capitulation des* 2*-classes d'idéaux de* $k = \mathbb{Q}(\sqrt{2pq}, i)$*, où* $p \equiv -q \equiv 1$ *mod* 4*,* Acta. Arith. **94** (2000), 383-399.

[2] A. Azizi et M. Taous, *Détermination des corps* $\mathbf{k} = \mathbb{Q}(\sqrt{d}, i)$ *dont les* 2*-groupes de classes sont de type* $(2, 4)$ *ou* $(2, 2, 2)$, Rend. Istit. Mat. Univ. Trieste. **40** (2008), 93-116.

[3] A. Azizi, M. Taous and A. Zekhnini, *On the rank of the* 2*-class group of* $\mathbb{Q}(\sqrt{p}, \sqrt{q}, \sqrt{-1})$, Period. Math. Hungar. Volume 69, Issue **2** , (2014), 231-238.

[4] A. Azizi, M. Taous and A. Zekhnini, *On the* 2*-groups whose abelianizations are of type* $(2, 4)$ *and applications*, Publ. Math. Debrecen. **88/1-2** (2016), 93-117.

[5] P. Kaplan, *Sur le* 2*-groupe de classes d'idéaux des corps quadratiques.* J. Reine angew. Math. **283/284** (1976), 313-363.

[6] F. Lemmermeyer, *Separants of quadratic extensions of number fields*, preprint.

[7] F. Lemmermeyer, *Reciprocity Laws*, Springer Monographs in Mathematics, Springer-Verlag. Berlin 2000.

[8] P. A. Leonard and K. S. Williams, *The quadratic and quartic character of certain quadratic units II*, Rocky Mountain J. Math. (4), 9 (1979), 683-692.

An Overview of Problems and Approaches in Machine Intelligence

Malik GHALLAB and Félix INGRAND

LAAS-CNRS, University of Toulouse

Abstract. *Robotics is an interdisciplinary research field leveraging on control theory, mechanical engineering, electronic engineering and computer science. It aims at designing machines able to perceive, move around and interact with their environment in order to perform useful tasks. Artificial Intelligence (AI) is an area of computer science, overlapping with but significantly distinct from robotics. Its purpose is to understand intelligence, through effective computational models, design and experiment with systems which implement these models .*

There is a significant convergence between Robotics and AI. Their intersection, qualified here as Machine Intelligence, is critical for both areas. Robots implement the so-called "perception - decision - action" loop; the intelligence or decision making part is central in that loop for tackling more variable and complex environments and tasks. On the other hand, AI is moving from abstract intelligence, such as in playing chess, to addressing embodied intelligence.

This paper introduces the reader to some of the research issues and approaches in Machine Intelligence. It surveys the state of the art in key issues such as planning and acting deliberately on the basis of tasks and world models, learning these models, and organizing the sensory-motor and cognitive functions of a robot into resilient and scalable architectures.

Key words: Robotics, Artificial Intelligence.

1 Introduction

Robotics and *Artificial Intelligence* are two overlapping but quite distinct research fields. *Machine Intelligence* refers to their intersection. This paper surveys the state of the art at this intersection. Its purpose is to introduce the reader to the synergies between Robotics and Artificial Intelligence and to demonstrate that Machine Intelligence is a very rich and fruitful in scientific problems.

Robotics aims at designing machines which are able to perceive, move around and interact with their environment in order to perform some specified useful tasks. It is an interdisciplinary research field, which covers several disciplines, primarily control theory, mechanical engineering, electronic engineering and computer science. Its recent links with life sciences or materials sciences have opened new and exciting perspectives. It entertains growing synergies with neuroscience for the development of cognitive models and functions (e.g., Wolpert and Flanagan [129, 128], Wolpert and Ghahramani [130]). Robotics, as an enabling technology, provides a significant technical and conceptual support for the development of several other research fields such as medicine (e.g., surgery, biomechanics), or environment and space sciences (e.g., oceanography or planetology). It addresses a wide spectrum of applications.

Artificial Intelligence (AI) is a research area of computer science, mostly independent from robotics. Its purpose is to understand intelligence through effective computational models, design systems which implement them, and experiment with these systems in order to scientifically evaluate and qualify the proposed models of intelligence. AI entertains interdisciplinary links with mathematical logics, psychology, neuroscience, linguistics, philosophy and other cognitive sciences. It already brought a wealth of mature technologies, such as machine learning techniques, that are now seamlessly integrated in many computerized devices such as smartphones, cameras, web browsers, search engines and semantic web applications.

Robotics is quite often referred to in AI research. It is a natural reference for work on embodied intelligence and for experimental validation. The early beginnings of AI are rich in pioneering projects of autonomous robots, such as Shakey at SRI of Rosen and Nilsson [101] or the Stanford Cart in the late 60s, and a few years later, Hilare at LAAS of Giralt et al. [56] or the CMU Rover of Moravec [90]. These, and many other projects since that early period, clearly lie at the intersection of Robotics and AI, seeking to understand, model and design machines that combine autonomous perception, decision and action.

AI has been less frequently referred to in robotics publications. This is due to the breadth of the robotics field. This is also due to the early challenges on which the robotics community has focused. Early robots had reduced autonomy and limited sensing, locomotion and manipulation capabilities. This naturally set the initial challenges more about sensory-motor functions than about deliberation and cognitive functions. Significant progress during the last two decades on the sensory-motor level has, fortunately, put robotics deliberation problems on the limelight.

We are now witnessing a growing convergence between Robotics and AI. Their intersection in Machine Intelligence is critical for both areas. Robots have been defined as a *"perception - decision - action"* control loop. The decision part is central in that loop. On the other hand, AI is moving from abstract intelligence, such as playing chess, to addressing *embodied intelligence*. The intersection of Robotics and AI covers in particular the following issues:

- Perception, semantic interpretation of sensory data, environment modeling;
- Acting deliberately: planning and achieving autonomously complex tasks, including navigation in open unknown environments;
- Learning to perceive, to act and behave with improved performance;
- Organizing sensory-motor and deliberation functions in a robot.

For the sake of a focused survey, the first item is not covered in this paper, to the exception of a brief mention of some aspects of perception that are specific to robotics. The survey is primarily devoted to the last three items, addressed successively in:

- Sections 3, 4 and 5, which are devoted respectively to motion planning and execution, tasks planning and acting, and interaction with humans or robots;
- Section 6 on learning; and
- and Section 7 on organization and architecture issues.

For a good understanding of the problems discussed here, the paper starts with a general introduction to robotics and its applications (Section 2). It concludes with a short perspective on future research. In each section we have chosen to illustrate with enough technical details some basic techniques, and to refer the reader to the relevant publications for further deepening. A wide coverage of robotics can be found in the handbook of Siciliano and Khatib [105]. A similar coverage for AI is given in the textbook of Russell and Norvig [102].

(a) Baxter, a robot manipulator for manufacturing (Rethink Robotics)

(b) Autonomous vehicles for logistics applications (Kiva Systems)

Figure 1: Robots (a) for a fixed environment, and (b) for a single task.

2 Overview of the Field

A robot can be defined as a machine able to perform a set of *tasks* in a class of *environments* with some degree of *autonomy* and robustness. As for any natural being, the autonomous capabilities of a robot are relative to the *diversity* of the tasks and environments it can cope with. A robot integrates several components - actuators, sensors, computers, radio transmitters - which ensure in particular the following functions:

- *motion*, with wheels, legs, wings, propellers, caterpillars, fins;
- *manipulation*, with mechanical arms, clamps, hand, cups, specialized tools;
- *perception* by *proprioceptive* sensors which estimate the internal state of the machine: odometer and angular encoders, inclinometer, magnetometer, accelerometer, inertial measurement unit, GPS, and *exteroceptive* sensors, which estimate the environment: camera, laser, radar, spectrometer, IR or ultrasound range finder;
- *communication*, and
- *decision making*.

There are several classes of generic robotics applications corresponding to different classes of environments and tasks. Each such a class emphasizes specific problems depending on the level of autonomy desired for a robot. Well known examples are the following:

- *Manufacturing robots*: robot arms with adapted sensors at fixed positions for tasks such as painting, welding, assembly, loading and unloading a press or machine tools [59];
- *Exploration robots*: mobile robots in outdoor environments [40] performing terrain mapping, soil analysis, mining [33], intervention in a contaminated site, deployment of equipments at the bottom of the ocean [6], in Antartica or on Mars [131];
- *Service robots*: mobile robots in indoor environments for cleaning, surveillance, transportation in a shop, a workshop, a clean room or an hospital [55];
- *Personal robots*: mobile robots assisting people in professional environments or at home [98];
- *Medical robots*: robots specialized in assisting surgeons, in particular in "noninvasive surgery" [119];
- *Robot carried by human*: exoskeleton allowing the extension of the sensory-motor skills of their carrier [74].

This list is not exhaustive. Other classes of robotics applications, such as agriculture, ecology, construction, demining or military operations give rise to active research. Specific environments in one of the above application classes, e.g., aerial exploration robotics, lead to particular problems. Finally, cooperation and interaction when the tasks are carried out by several robots or by human - robot teams bring additional challenges.

A key notion in robotics is the *diversity of environments and tasks* a robot must face. The technology is relatively mature when there is no diversity, that is for robots specialized in a single environment, well modeled and instrumented, and on just one well specified task. If one considers manufacturing robots, millions robot arms are operating in the industry (Figure 1(a)). In service robotics, numerous autonomous ground vehicles are used in warehouses for logistic services [58] (Figure 1(b) and in the electronic or pharmaceutical industry. In both cases, the well-modeled stable environment

(a) Mars Rover Curiosity (NASA/ JPL)

(b) Surgical robotics assistance (DaVinci Intuitive Surgical)

Figure 2: Tele-operated robots.

of the robot is the result of a significant engineering effort. The same remark applies to single-task robots, e.g., vacuum cleaner (more than 5 million sold) or lawn mower, which are a large commercial success.

When the environment or tasks are highly variable, the degree of autonomy of the robot becomes an important factor. We may distinguish three levels:

- no autonomy: the robot applies to its actuators pre-recorded or operator specified commands;
- tasks autonomy: the robot performs tasks precisely defined by the operator, e.g., goto point A then pick-up object O;
- autonomy to achieve missions specified in abstract terms, e.g., find and rescue injured persons in the area.

When there is no need for autonomy, many robotics technologies are already mature. This is due in particular to the highly simplified perception and deliberation problems. Robots tele-operated at the task level have been demonstrated in impressive experiments, e.g., in the exploration of planets (Figure 2(a)). They are also used in successful applications, e.g., robotics surgery systems have been deployed at several thousands sites, despite their high cost and complexity (Figure 2(b)). Remote manipulation has to address other technical challenges, such as how to provide good sensory feedback to a human operator to enable her to properly understand the state of the environment and the task, or how to reliably translate human commands to the robot actuators (*e.g.*, to filter the signal from the movements of the surgeon's hand to obtain a precise and safe trajectory of the scalpel and to control its motion with respect to the movement of the operated organ).

Limited autonomy simplifies perception and deliberation but it also constrains the tasks that can be performed by a tele-operated robot. Thus, Mars rovers of the previous generation, *Spirit* and *Opportunity*, were tele-operated at the motor control level. The communication delay (up to 40 minutes depending on the Mars-Earth configuration) limited their remote operation to a few meters per day. At a later stage of their mission, the introduction of autonomous motion has allowed these robots to traverse up to 140 meters per day. Today, Curiosity can perform up to 1.5 Km per day of autonomous navigation, but it is still tele-operated at the task level for its other activities. In some application, autonomy is not desired: the human operator wants to remain in full control of every command. However, it can be preferable to tele-operate a robot at the task level, *e.g.*, tell it to make a precise line of surgical sutures, or to close an underwater valve, leaving it up to the robot to translate the task

(a) NASA/JPL (b) INTRA Group

Figure 3: Robots for hazardous environments.

into controlled commands, under the supervision of the operator. Here also, the state of the art has reached some maturity, illustrated for example by robots used in hazardous environments (Figure 3). Another illustration of the autonomy at the task level can be given by telepresence robots. These are mobile platforms carrying away the image and voice of the user, giving a visual and audible feedback, capable of simple tasks, e.g., find a person, asking her to lend an object and bringing it back to the robot's user (Figure 4).

One may try to use these and similar platforms to achieve more autonomous and varied missions. But the state of the art faces many open problems, in particular for the interpretation of the environment, for planning and acting with incomplete and uncertain models and noisy sensory data.

(a) Double Robotics (b) PadBot

Figure 4: Telepresence robots

Autonomy at the mission level already achieves good experimental success when the tasks are well structured and constrained, even when the environment is highly variable. Driverless cars provide a

good illustration. The first success goes back to the 2005 "DARPA Grand Challenge": autonomous traversal of 320 km in the Mojave Desert in less than 7 hours (Figure 5(a) [123]), which was followed in 2006 by the "DARPA Urban Challenge". Since then, several companies reported millions of kilometers of autonomous driving on roads and highways (Figure 5(b)). Autonomous underwater vehicles (AUV) are another excellent example. Experimental AUVs are launched for up to 24 hours in a mission of mapping, water sampling, oceanographic and biological measurement; in case of a problem, the AUV surfaces and indicates its position to be retrieved by its operators (Figure 5(c) [84]).

(a) Stanley, DARPA challenge 2005 (Stanford U.)

(b) Autonomous Driving (Google)

(c) Dorado, AUV (MBARI)

Figure 5: Autonomous vehicles.

Robotics research relies significantly on experiments. The advance of the field has been conditioned by the availability of inexpensive reliable platforms with broad functionalities that are easily deployable and programmable. Significant progress has been witnessed in the last decade. A good illustration is provided by humanoid robots: many research groups have now access to biped robotic platforms of human size (Figure 6(a) and 6(b)). These robots demonstrate good motor skills as well as impressive mechatronics. Platforms on wheels with two arms, sometimes with an articulated trunk, also illustrate rich sensory-motor capabilities. These platforms are able for example to catch simultaneously two thrown balls (Figure 7(a)), to fold laundry or to play billiards (Figure 7(b)).

Several research competitions stimulated the progress of the field. In addition to autonomous driverless cars, there are several other competitions, e.g., in robotics assembly, aerial robotics or humanoid robotics. The robotics soccer competition "*RoboCup*" is very popular. One can be critical for the oversimplifications often introduced in these competitions (artificial or "micro-worlds" problems). However, their effects in terms of attractiveness, visibility and team commitment, especially among students, remain largely beneficial to the progress of robotics.

3 Motion Planning, Mapping and Navigation

Mobility is a critical and widely studied function for autonomous robots [78, 30, 80]. When the environment is well modeled, the movements of a robot can be planned and controlled in a robust manner. Otherwise, the robot has to explore its environment to acquire the needed geometrical and topological models. Let us discuss here these two problems of motion planning and environment modeling.

(a) HRP 4 (Kawada Industry)

(b) Atlas (Boston Dynamics)

Figure 6: Humanoid robots.

3.1 Motion planning with probabilistic road maps

We assume that the environment is described by a geometric model (such as a *Computer-Aided Design* model), which specifies the geometry of the obstacles and the free space. The robot is modeled by its kinematics, *i.e.*, the set of degrees of freedom and the constraints of its moving limbs, as well as its dynamics, *i.e.*, masses and inertia of its components, and the forces and torques of its actuators.

Motion planning consist in finding a trajectory for connecting an initial position to a goal position. This trajectory should be feasible in space and time. The problem is usually decomposed into two steps: *(i)* find a feasible path that satisfies the kinematics constraints of the robot and the geometric constraints of the environment, and *(ii)* find a control law along that path that satisfies the dynamic constraints of the robot. In simple cases these two problems *(i)* and *(ii)* can be solved independently. When there are no moving obstacles and the robot dynamic constraints are weak (e.g., slow motion), it is generally easy to map a feasible path into a feasible trajectory with simple control laws. Motion planning in robotics reduces mainly to a path planning problem, which we detail below.

A free rigid object in Euclidean space without kinematic constraint is characterized by six configuration parameters: (x, y, z) for the position of a reference point and three angles for the orientation of the solid in space. But a robot has kinematic constraints that restrict its movements. For example, a car in the plan has three configuration parameters (x, y and orientation θ), which generally are not independent (a car cannot move laterally). The PR-2 robot (Figure 7(b)) has 20 configuration parameters (3 for the base, one for the trunk, 2 for the head, and 7 per arm). The humanoid robot HRP-4 (Figure 6(a)) has 32 configuration parameters plus five for each hand.

For a robot with n configuration parameters in a given environment let us define:

- $q \in \Re^n$, the configuration of the robot, a vector of n real values that specifies the n parameters characterizing the position of the robot in a reference frame;

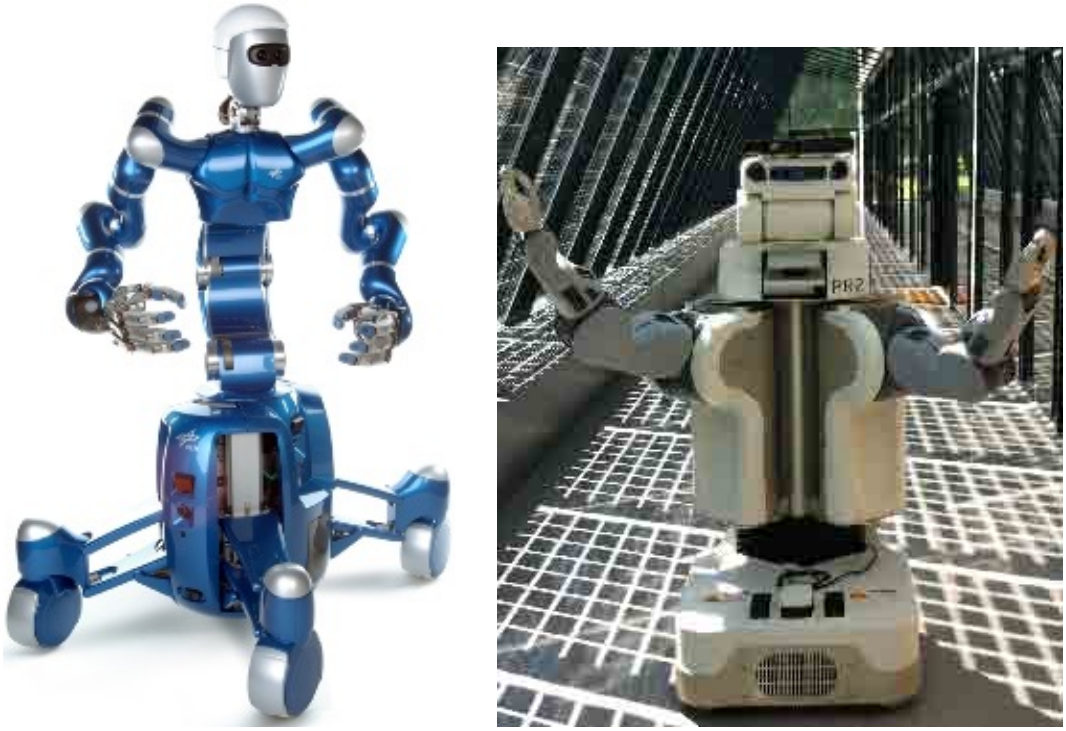

(a) Justin (DLR) (b) PR2 at LAAS (Willow Garage)

Figure 7: Mobile robots with two arms.

- $\mathcal{C}$, the configuration space of the robot, which describes all possible values of q in $\Re^n$ given the kinematic constraints, such as the max and min angular positions that each joint can have, and the dependencies between configuration parameters;
- $\mathcal{C}_f \subseteq \mathcal{C}$, the free configuration space which gives all possible values of $q \in \mathcal{C}$ given the constraints of the environment, *i.e.*, the set of configurations for which the robot does not collide with obstacles.

These concepts are illustrated in Figure 8 for a robot with two degrees of freedom.[1]

Planning a motion between an origin configuration q_o and a goal configuration q_g, both in $\mathcal{C}_f$, consists in finding a path between q_o and q_g in this n dimensional continuous space. The major difficulty here, as for any other planning problem, is that the search space $\mathcal{C}_f$ is not known explicitly. The explicit definition of $\mathcal{C}_f$ from the geometric model of the environment and the kinematic constraints of robot is an extremely complex problem, difficult to solve even for very simple robots and environments. In the trivial 2D case of the previous example, this problem corresponds to finding the analytical definition of the grey area in Figure 8(b). Significant research in computational geometry addressed this representation problem, see e.g., Schwartz et al. [104]. It opened the way to sampling-base approaches that helped to circumvent the problem, in particular with the following method.

The Probabilistic Roadmap algorithm of Kavraki et al. [73] relies on two easily computable operations:

- *kinematic guidance*: find a direct kinematic path $\mathcal{L}(q, q')$ between two configurations q and $q' \in \mathcal{C}$ without worrying about environment constraints, *i.e.*, $\mathcal{L}(q, q')$ satisfies the kinematic constraints

[1] Figure adapted from http://www.cs.cmu.edu/motionplanning/

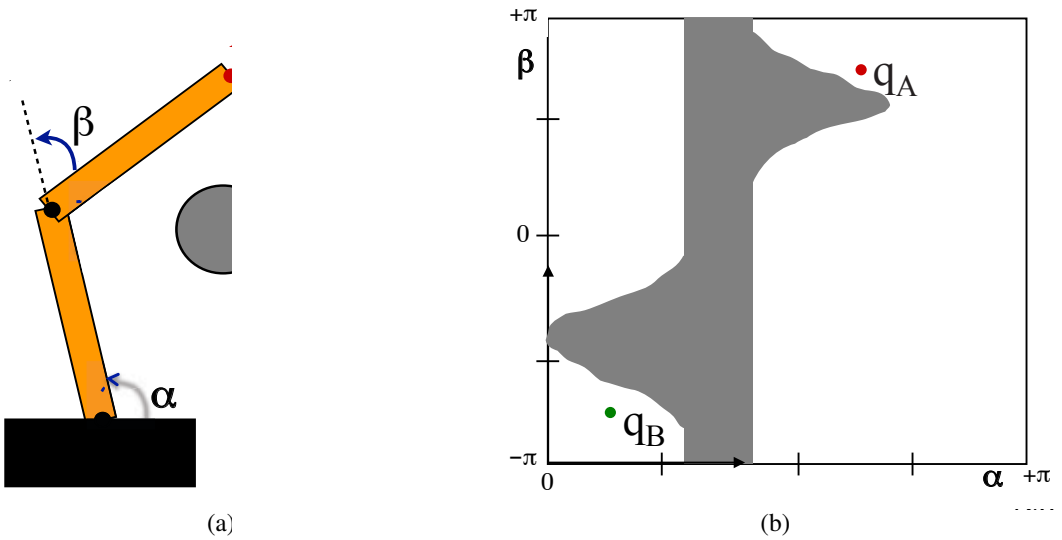

Figure 8: (a) A planar robot with two angular joints, α and β facing a circular obstacle. (b) Corresponding configuration space: the projection of the obstacle in $\mathcal{C}$ shows that the two configuration q_A and q_B are not connected : no motion of the robot can move it from points A to B.

but not necessarily the constraints of non-collision with obstacles. The techniques used for that are specific to the type of the robot kinematic constraints, *e.g.* composition of straight lines and curves;

- *collision test*: check whether a configuration q does or does not collide with obstacles, *i.e.*, if $q \in \mathcal{C}_f$; check whether a path $\mathcal{L}(q, q')$ between two configurations is collision-free, *i.e.*, if it passes entirely in $\mathcal{C}_f$. This relies on basic techniques of computational geometry.

A roadmap $\mathcal{G}$ in $\mathcal{C}_f$ is a graph whose vertices are configurations in $\mathcal{C}_f$; two vertices q and q' are adjacent in $\mathcal{G}$ iff there exists a path without collision $\mathcal{L}(q, q')$ in $\mathcal{C}_f$.

If a roadmap $\mathcal{G}$ in $\mathcal{C}_f$ is known, then planning a path between an origin configuration q_o and a goal configuration q_g can be solved with the three following steps:

- find a vertex q in $\mathcal{G}$ such that q is accessible from q_o *i.e.*, $\mathcal{L}(q_o, q) \in \mathcal{C}_f$;
- find a vertex q' in $\mathcal{G}$ such that q_g is accessible from q', *i.e.*, $\mathcal{L}(q', q_g) \in \mathcal{C}_f$;
- find a sequence of adjacent vertices in $\mathcal{G}$ between q and q'.

Path planning is then reduced to a simpler problem of finding a path in graph. If such a sequence of configurations is found, efficient algorithms allow to smooth and optimize locally this sequence of configurations in $\mathcal{G}$ into a kinematic path. It remains therefore to find a map $\mathcal{G}$ covering adequately $\mathcal{C}_f$, *i.e.*, if there is a path in $\mathcal{C}_f$ then there is also a path in the roadmap $\mathcal{G}$ using the previous three steps.

The algorithm in Figure 9 [108] provides a graph $\mathcal{G}$ which *probabilistically* satisfies this coverage property. This algorithm incrementally generates $\mathcal{G}$ starting with an empty roadmap. It adds to the map under construction a randomly drawn configuration q in the following two cases:

- if q belongs to the free space and extends the coverage of $\mathcal{G}$, allowing to reach parts of $\mathcal{C}_f$ not yet covered (step $\triangleright$*(i)*), or
- if q belongs to the free space and extends the connectivity of $\mathcal{G}$, allowing to connect two components not currently connected in the roadmap (step $\triangleright$*(ii)*).

Probabilistic Roadmap ($\mathcal{G}$)
  iterate until *Termination*
    sample a random configuration $q \in \mathcal{C}$
    if $q \in \mathcal{C}_f$ then do
      if $\forall q' \in \mathcal{G}$: $\mathcal{L}(q, q') \notin \mathcal{C}_f$ then add q in $\mathcal{G}$ ▷ *(i)*
      else if $\exists q_1, q_2$ in $\mathcal{G}$ such that q_1 and q_2 are not connected
          and $\mathcal{L}(q, q_1) \subset \mathcal{C}_f$ and $\mathcal{L}(q, q_2) \subset \mathcal{C}_f$
          then add q and the edges (q, q_1) and (q, q_2) to $\mathcal{G}$ ▷ *(ii)*
  Return($\mathcal{G}$)

Figure 9: Probabilistic roadmap algorithm for path planning

The *Termination* condition is based on the number of consecutive samples of unsuccessful random free configurations that do not add anything to the map. If k_{max} is such a number, then the probability that the resulting graph covers $\mathcal{C}_f$ is estimated by $(1-1/k_{max})$. In practice, this algorithm is very efficient. The probabilistic roadmap technique and its incremental variants (called RRT for " Rapidly exploring Random Trees" [80]) are now widely used in robotics. They are also used in other application areas such as mechanical design, video animation, or computational biology for molecular docking problems to find whether a ligand can bind to a protein. They have been extended to take into account dynamic environments.

These techniques have advanced significantly the state of the art but they do not solve all motion planning problems in robotics. Many open problems remain, in particular for handling the robot dynamics. Further, one needs to synthesize plans that are robust to the uncertainty of the models and to the sensory-motor noise in the robot localization and motion control. For example, we may want a path that relies on known landmarks to maintain the localization uncertainty below an acceptable threshold. In addition, we need to restate the problem for concrete tasks. The previous formulation refers to a completely specified motion problem, *i.e.*, from a configuration q_o to a configuration q_g. In practice, the problem arises with respect to a task, *e.g.*, grasp an object. This leads to several open problems [107]. A grasp allows to infer the configuration of the end effector (hand and fingers) from the position of the object to be grasped. But the configuration of the end effector gives only a part of q_g. It is possible to decompose the problem into: *(i)* plan the movement of the base of the robot to a configuration "close" to the object, then *(ii)* plan a movement of the arm to a grasp position. However, the manipulation of an object can require intermediate poses at different moment with respect to the object, or the manipulation of other interfering objects. It is then necessary to change the structure of the search space according to the grasps and poses of objects handled. In addition, the above decomposition is not always feasible. For example, a humanoid robot requires a coordinated movement of its body and all limbs [72] (Figure 10). Further, sensing and visibility issues bring additional constraints, e.g., planning a motion that avoids occultation between a camera carried by the robot's head and its hand, to allow for visual servoing [28].

3.2 Simultaneous Localization and Mapping

The execution of a planned motion requires the control of the actuators for achieving a trajectory, possibly with avoidance of unexpected obstacles. The synthesis of this control is done with models and methods from control theory. Robotics raises very interesting problems in automatic control, e.g., in the control of non-holonomic systems. These issues are not within the scope of this paper. We refer the reader for example to the book of LaValle [80] or the synthesis of Minguez et al. [87].

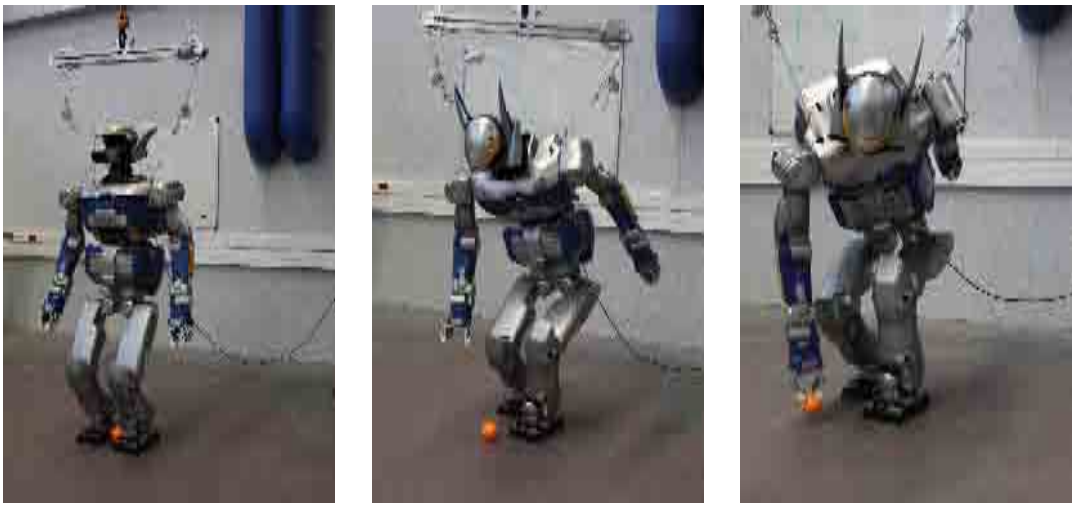

(a) (b) (c)

Figure 10: Picking up a ball requires a coordinated whole body motion planning; here the synthesized plan led the robot to step back, bend and extend opposite arm to maintain its balance (LAAS).

The execution of a planned motion requires also to maintain a good estimate of the state of the robot throughout the execution of the command. In particular, the robot must always know where it is in the environment. Sometimes, one may use absolute localisation, as given by a GPS or a radio-positioning system if the environment provides the adequate infrastructure. However, to operate autonomously in a diversity of environments, a robot must be able to locate itself directly from the perceived natural elements of its environment and a map of this environment. Further, this map is generally partially known, or even unknown. In general a robot is faced with a problem called *simultaneous localization and mapping* (SLAM). This problem has been identified quite early [27, 113], and has been since a very active research topic in robotics.[2]

To define the problem, let us discuss its two subproblems:

- *Localization*: the robot is localized in a fully known environment, modeled by k landmarks that are easily recognizable and perfectly positioned in space (2D or 3D). At time t, the robot is in a position estimated by $\tilde{x}_t$. It moves with the command u_t (giving the movement speed and orientation between t and t'). This allows to estimate the new position $\tilde{x}'$. The robot observes k landmarks where it expects to find them (from the estimated $\tilde{x}'$). It updates its position in relation to each recognized landmark. The observed positions of the landmarks are combined into a new estimated position of the robot $\tilde{x}_{t+1}$. The process is repeated at each time step as long as the robot remains within a fully known environment. The intermediate estimate $\tilde{x}'$ serves only to find landmarks. The localization error takes into account the sensing errors in the landmark observed positions, but it does not increase with time as long as the landmark locations in the map are error free. The error associated with the motor command u_t does not affect the localization.
- *Mapping*: The robot builds a map of its environment assuming it knows precisely its successive positions. The j^{th} landmark is estimated at time t as $\tilde{x}_{j_t}$. The robot moves between t and $t+1$ to a new known position, from which it observes again the position of the j^{th} landmark as $\tilde{x}'_j$

[2] See, e.g., the software repository: http://www.openslam.org/

with sensing error. $\tilde{x}'_j$ and $\tilde{x}_{j_t}$ are combined into a more reliable estimate $\tilde{x}_{j_{t+1}}$. The map quality improves with time.

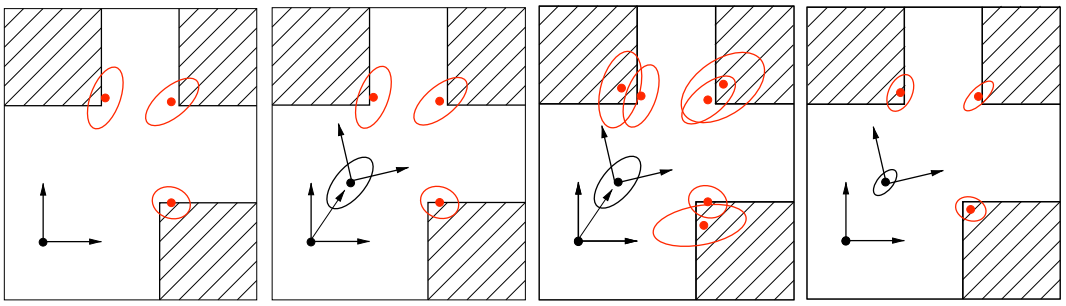

(a) (b) (c) (d)

Figure 11: SLAM procedure for a simple 2D robot: (a) Three landmarks (corners of obstacles) are detected and positioned with inaccuracy due to sensing noise. (b) The robot moves and estimates its position with a motion error. (c) The landmarks are observed and associated with the corresponding ones previously perceived. (d) Data fusion reduces the errors on the current position of the robot and the positions of the landmarks. The process is iterated for each new robot motion and sensing.

In practice, the two problems have to be addressed simultaneously. The initial map, if there is one, is never error free. Errors in the map entail localization errors. Symmetrically, the robot localization is noisy, which entails errors in its updates of the map. However, the two sources of error, from sensing and motion, are not correlated (see Figure 11). It is possible to combine the two subproblems into the simultaneous estimate of the positions of the robot and the landmarks.

One approach initially explored for solving the SLAM relies on *extended Kalman filters*. The technical details may seem complicated but a step by step presentation shows that the principle is simple. It is assumed that the environment is static and the sensors of the robot are properly calibrated and do not introduce systematic bias. Sensing errors are modeled as a Gaussian noise with zero mean and a standard deviation specific to each sensor. Let us assume two sensors, characterized respectively by σ_1 and σ_2, which both measure the distance to the same landmark. They return two values μ_1 and μ_2. We can estimate the true distance by averaging the returned values while giving more confidence to the most accurate sensor, i.e., the one with the smaller σ_i. Hence μ_i is weighted by $1/\sigma_i$. The estimated distance μ is associated with a standard deviation σ defined below (Equation 1). This estimates has good properties: it minimizes the mean squared error. The error resulting from the combination of the two measures decreases, since $\sigma <\min\{\sigma_1, \sigma_2\}$.

$$\begin{aligned} \mu &= \alpha(\mu_1/\sigma_1 + \mu_2/\sigma_2), \text{ with } \alpha = \sigma_1\sigma_2/(\sigma_1 + \sigma_2) \\ 1/\sigma &= 1/\sigma_1 + 1/\sigma_2 \end{aligned} \tag{1}$$

This process is applied incrementally. We combine the current estimate (μ', σ') to the new measure (μ_z, σ_z). The new estimate at time t (μ_t, σ_t) integrating the new measure is given by the same equation, rearranged easily into the following form (Equation 2):

$$\begin{aligned} \mu_t &= \mu' + K(\mu_z - \mu') \\ \sigma_t &= \sigma' - K\sigma' \\ K &= \sigma'/(\sigma_z + \sigma') \end{aligned} \tag{2}$$

Let us now introduce the robot's motion. At time $t-1$ the robot was in a position with respect to the landmark of interest estimated by $(\mu_{t-1}, \sigma_{t-1})$. Between $t-1$ and t the robot moves according to a command known with an uncertainty similarly modeled. Let (u_t, σ_u) be the estimate of this motion along the robot - landmark line. This estimate is given by the command sent to actuators and/or by the odometer. The relative distance to the landmark after the motion is estimated by (μ', σ'), noting that the error increases due to the motion:

$$\begin{aligned} \mu' &= \mu_{t-1} + u_t \\ \sigma' &= \sigma_{t-1} + \sigma_u \end{aligned} \tag{3}$$

We now can combine the two previous steps into a SLAM approach based on Kalman filtering. The estimate of the relative position robot - landmark is updated between $t-1$ and t in two steps:

(i) update due to motion (with Equation 3): $(\mu_{t-1}, \sigma_{t-1}) \rightarrow (\mu', \sigma')$
(ii) update due to sensing (with Equation 2): $(\mu', \sigma') \rightarrow (\mu_t, \sigma_t)$

In the general case, these updates are applied to vectors instead of simple scalar values. We run the above process to the update of the positions of the robot and the landmarks in the Euclidean space, 2D or 3D. The position of the robot does not necessarily include all its configuration parameters, but only the portion of q necessary for the localization of a reference point and for the positioning of its sensors. The map is characterized by many landmarks positioned in space. A vector μ_t, whose components are the robot configuration parameters and the positions of the landmarks, is updated at each step. The error is no longer a scalar σ_t but a covariance matrix Σ whose element σ_{ij} is the covariance components i and j of the parameters of μ. The error on the position of the robot is coupled to the errors of the map and symmetrically. Furthermore, the above approach applies only to linear relations. But the relationship between the command and the motion is not linear. We approximate a solution to this problem by linearizing around small motions. This leads finally to the extended Kalman filter formulation of SLAM:

$$\begin{aligned} \mu' &= A\mu_{t-1} + Bu_t \\ \mu_t &= \mu' + K_t(\mu_z - C\mu') \\ \Sigma' &= \sigma_{t-1} + \Sigma_u \\ \Sigma_t &= \Sigma' - K_t C\Sigma' \\ K_t &= \Sigma' C^T (C\Sigma' C^T + \Sigma_z)^{-1} \end{aligned} \tag{4}$$

Two update steps are easily identified:

(i) $(\mu_{t-1}, \sigma_{t-1}) \rightarrow (\mu', \Sigma')$: vector u_t, matrices A and B for the motion,
(ii) $(\mu', \Sigma') \rightarrow (\mu_t, \Sigma_t)$: vector μ_z, matrix C for the new measurements.

One also takes into account the covariance associated with the motion and the measurements (Σ_u and Σ_z). It should be noted that the first step uses the motion to update the position of the robot as well as those of the landmarks. Similarly, the second step integrates the new measurements for both, the localization and mapping.

This approach has been successfully implemented and frequently used [122]. It has many advantages. In particular, it maintains the robot localization and the corresponding bounds on the error. These bounds are very important in navigation: if the error grows beyond some threshold, specific action has to be taken. The method converges asymptotically to the true map, with a residual error

due to initial inaccuracies. Finally, the estimate is computed incrementally. In practice, the number of landmarks increases dynamically. The robot maintains a list of landmark candidates which are not integrated into the map (nor in the vector μ) until a sufficient number of observations of these landmarks have been made. If n is the dimension of the vector μ (*i.e.*, the number of landmarks), the complexity of the update by Equation 4 is $O(n^2)$. The computations can be done online and on board of the robot for n in the order of 10^3, which means a sparse map.

Particle filtering offers another approach to SLAM with additional advantages. Instead of estimating the Gaussian parameters (μ, Σ), the corresponding probability distributions are estimated through random sampling. Let $P(X_t|z_{1:t}, u_{1:t}) = \mathcal{N}(\mu_t\Sigma_t)$, where X_t is the state vector of the robot and landmark positions at the time t, $z_{1:t}$ and $u_{1:t}$ are the sequences of measures and commands from 1 to t. Similarly $P(z_t|X_{t-1}) = \mathcal{N}(\mu_z\Sigma_z)$.

Let us decompose the state vector X_t into two components related to the robot and the landmarks: $X_t = (r_t, \phi_1, ..., \phi_n)^T$, where r_t is the position of the robot at time t, and $\phi = (\phi_1, ..., \phi_n)^T$ the position of landmarks, which do not depend on time because the environment is assumed static.[3] The usual rules of joint probabilities entail the following:

$$\begin{aligned} P(X_t|z_{1:t}, u_{1:t}) &= P(r_t|z_{1:t}, u_{1:t})P(\phi_1, \ldots, \phi_n|z_{1:t}, u_{1:t}, r_t) \\ &= P(r_t|z_{1:t}, u_{1:t}) \prod_{i=1,n} P(\phi_i|z_{1:t}, r_t) \end{aligned} \tag{5}$$

The second line results from the fact that, given the position r_t of the robot, the positions of the landmarks do not depend on u and are conditionally independent. The robot does not known precisely r_t but it assumes that $r_t \in R_t = \{r_t^{(1)}, \ldots, r_t^{(m)}\}$, a set of m position hypotheses (or particles). Each hypothesis $r_t^{(j)}$ is associated with a weight $w_t^{(j)}$. R_t and the corresponding weights are computed in each transition from $t-1$ to t by the following three steps:

- *Propagation*: for m' positions in R_{t-1} randomly sampled according to the weights $w_{t-1}^{(j)}$, we compute $r_t^{(j)}$ the position at time t of the resulting control u_t, with $m' > m$,
- *Weighting* : the weight $w_t^{(j)}$ of particle $r_t^{(j)}$ is computed taking into account the observation z_t from the product $P(z_t|\phi, r_t^{(j)})P(\phi|z_{1:t-1}, r_{t-1}^{(j)})$.
- *Sampling*: the m most likely assumptions according to the new weights $w_t^{(j)}$ are kept in R_t.

For each of the m particles, the probability $P(\phi_i|z_{1:t}, r_t)$ is computed with a Kalman filter reduced to the 2 or 3 parameters necessary to the position ϕ_i. With good data structures for the map, this approach, called FastSLAM [88], reduces the complexity of each update to $O(n\log m)$ instead of $O(n^2)$ in the previous approach. In practice, one can keep a good accuracy for about $m \simeq 10^2$ particles, allowing to maintain online a map with $n \simeq 10^5$ landmarks.

The main limitation of these approaches is due to a well known and difficult problem of *data association*. At each step of the incremental localization process, one must be sure not to confuse the landmarks: associated measurements should be related to the same landmark. An update of the map and the robot positions with measurements related to distinct landmarks can lead to important errors, well beyond the sensory-motor errors. This argument, together with the computational complexity issue, favors sparse maps with few discriminating and easily recognizable landmarks. On a small motion between $t-1$ and t, the landmarks in the sensory field of the robot are likely to be

[3] Note that in μ_t the estimate ϕ evolves with t, but not the position of the landmarks.

recognized without association errors. But after a long journey, if the robot views some previously seen landmarks, a robust implementation of the approach requires a good algorithm for solving the data association problem.[4] In the particle filtering approach, the probability distribution of R_t is very different when the robot discovers a new place (equally likely distribution) from the case where it retraces its steps. This fact is used by active mapping approaches, which make the robot retrace back its steps as frequently as needed [114].

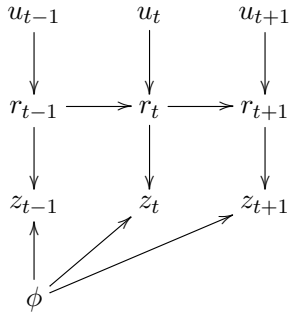

Figure 12: Formulation of SLAM with a dynamic Bayesian network; arcs stand for conditional dependencies between random variables, ϕ gives the positions of the landmarks (time-independent), u_t, r_t and z_t denote the command, the robot positions and the new measurements at time t.

In the general case, there is a need for an explicit data association step between the two stages *(i)* and *(ii)* corresponding to Equation 4. This step leads to maintain multiple association hypotheses. The SLAM approaches with Dynamic Bayesian Networks (DBN) for handling multi-hypotheses give good results. The DBN formulation of SLAM is quite natural. It results in a dependency graph (Figure 12) and the following recursive equation:

$$\begin{aligned} P(X_t|z_{1:t}, u_{1:t}) &= \alpha P(z_t|X_t) \int P(X_t|u_t, X_{t-1}) P(X_{t-1}|z_{1:t-1}, u_{1:t-1}) dX_{t-1} \\ &= \alpha P(z_t|X_t) \int P(r_t|u_t, r_{t-1}) P(X_{t-1}|z_{1:t-1}, u_{1:t-1}) dr_{t-1} \end{aligned} \tag{6}$$

Here, α is a simple normalization factor. The vector state is as above $X_t = (r_t, \phi_1, ..., \phi_n)^T$; the second line results from the fact that the environment is assumed static and that the robot motion and landmark positions are independent. The term $P(z_t|X_t)$ expresses the sensory model of the robot, and the term $P(r_t|u_t, r_{t-1})$ corresponds to its motion model. This formulation is solved by classical DBN techniques, using in particular the Expectation-Maximization algorithm (EM), as for example in Ghahramani [51], which provides a correct solution to the data association problem. However, online incremental implementation of EM are quite complex. Let us also mention another version of FastSLAM which takes this problem into account by an explicit optimization step over all possible associations [89].

Recent approaches to SLAM favor this DBN formulation with a global parameter estimation problem overs the set of landmarks and robot positions. The problem is solved by robust optimization methods. This general formulation is called the beam adjustment method, following the computational

[4] This is sometimes referred to as the *SLAM loop problem*.

vision and photogrammetry techniques [125]. Visual SLAM has also benefited from recent image processing features which are quite robust for localization and identification of landmarks [85, 93, 82].

Let us conclude this section by mentioning a few possible representations for the map of the environment. Landmarks can be any set of sensory attributes that are recognizable and localizable in space. They can be a simple collection of points. They can also be compound attributes, such as visual segments, planes, surfaces, or more complex objects. The most appropriate attributes are generally specific to the type of sensors used. The global map can be represented as a 2D occupancy grid. Simple 3D maps for indoor environments, such as the Indoor Manhattan Representation, combine vertical planes of walls between two horizontal planes for the floor and ceiling, [46]. They can be used with more elaborate representations integrating semantic and topological information (see next section).

3.3 Navigation

The previous approaches are limited to metric maps. They only take into account distances and positions in a global absolute reference. When the environment is large, it is important to explicitly represent its topology, possibly associated with semantic information. In this case, a map relies on hierarchical hybrid representations, with metric sub-maps in local reference frames, together with relationships and connectivity constraints between sub-maps. The robot re-locates itself precisely when arriving in a sub-map.

Navigation in this case is also hybrid. Within a sub-map, motion planning techniques are used. Between sub-maps other methods such as road following or beam heading are more relevant. Sensory aspects and place recognition play an important role in navigation methods for *semantic hierarchy of spatial representations* [76].

Mapping and map updates can be as flexible as in the case of SLAM through the updates of a graph of local sub-maps [77, 38]. Topological planning relies on path search techniques in graphs (using algorithms such as Dijsktra or A^*). It is associated with motion planning in sub-maps. Both types of planning can be combined incrementally. Topological planning gives a route which is updated and smoothed incrementally to optimize the motion giving the observed terrain while moving [75].

Topological planning in a graph or within a grid can be used with a partial knowledge of the environment. Extensions of the A^* algorithm (D^* [115], D^* Lite, or Focused D^*) compute shortest paths in the graph, but they use the robot sensing to update the topology and costs parameters for finding shortest paths.

Finally, a classical problem in any hybrid approach is that of the frontiers between levels and their granularity. Labels of places (doors, rooms, corridors) and topology can emerge naturally from sensing and/or from a uniform description of space into cells (grids, polygons or Delaunay triangles). Decomposition techniques by *quadtrees* (a partially occupied cell is decomposed recursively) are useful but can be computationally complex. Analysis of the levels of connectivity of a graph provides elegant solutions with low complexity when the topological graph is planar [64, 79].

4 Task Planning and Acting

Task planning is the problem of synthesizing a plan, i.e., a sequence or a structured set of actions, starting from the description of all possible actions that a robot can perform, and such that the synthesized plan achieves an intended objective. Task planning is supposed to be general enough to handle all kind of tasks, integrating mobility, manipulation, assembly, sensing, etc. A planner is a *predictive*

system: it chooses, among various projections of possible futures those likely to lead to the goal. For this, the models of possible actions are at some level of abstraction that allows easy predictions. They are mainly logical or relational models, which grasp the causal relationships between actions, their conditions, effects and the intended objectives. The plans produced are more like guidelines for acting than direct programs to execute in open loop: they seldom fully unfold as expected, along a nominal scenario. Once a plan is found, there are problems for acting according to that plan, i.e., transforming the abstract actions in the plan into commands adapted to the context, monitoring their execution, and if necessary, to taking corrective steps, including replanning.

Robotics was one of the first area that motivated the development of task planning. It led naturally to the issue of coupling of planning and acting – the STRIPS planner of Fikes and Nilsson [43], on the Shakey robot, associated with Planex [42] for the execution of plans, is a seminal work in this area.

The execution controller (controller for short) does not make prediction. It uses different types of models which allow monitoring and, possibly, diagnosis. It must know which actions, especially the sensory ones, are needed to launch a planned action and/or to observe the direct or indirect effects of the action. It must be able to update the state of the world required to monitor the plan execution. It must know the conditions which invalidate the current action, expressing the failure or absence of response time, and those which invalidate the current plan. In addition, the controller must be able to manage uncertainty and nondeterminism at various levels: the imprecision of sensory data and the uncertainty about their interpretations; the action duration; the nondeterminism inherent to the action outcomes, etc. Indeed, the controller launches the actions, but their effects and precise courses of execution depend upon conditions and contingent events partially modeled. Finally, by definition, the controller operates online: it must also be responsive to unforeseen events by the plan, and ensure some safety conditions.

The coupling of planning and acting requires a tradeoff between the constraints and models needed for the planner predictions and those needed for the acting online with action refinements, reactions, monitoring and revision. A description of a planning and acting system and how to achieve this tradeoff could be made on the basis of a hierarchical state transition system $\Sigma = (S, A, E, \gamma)$, where S, A and E are enumerable sets of *state* of *activities* and *events*, and γ is a function that describes the dynamics of the system $\gamma = S \times A \times E \rightarrow S^2$. Activities are decided and triggered by the robot, while events are not under its control; they give rise to changes in the environment which can be observed directly or indirectly. Σ is described with two levels of abstraction:

- the planner has an abstract model of Σ: its macro-states are subsets of S, its actions are subsets of activities; it rarely takes into account E;
- the controller has a finer model of Σ: it is able to refine each planned action in corresponding activities which are under its control; it knows how to launch activities and how to monitor their progress; it can trigger activities (e.g., monitoring, alarms) to observe the dynamics of S, and other activities to react to events.

A complete formalization of such a system depends on many conditions, especially the type of planning used, deterministic or non-deterministic and the system dynamics, *e.g.*, how to take into account the concurrency between activities and events within the function γ. A presentation of possible approaches is beyond the scope of this paper. We refer the reader to the textbook of Ghallab et al. [54] for a detailed coverage of tasks planning methods, and to the recent survey of Ingrand and Ghallab [66] for a broad perspective on deliberate actions in robotics . In the remainder of this section, let us review some of the main approaches for acting and execution control, focusing on relational and logic representations in deterministic and temporal approaches, and on Markov representations for nondeterministic approaches.

4.1 Deterministic Approaches

The approaches using a classical planner (as in STRIPS) often produce a plan π to which they associate a causal structure that help the controller follow the proper execution of the plan (*e.g.*, triangular tables). The purpose of these structures is to provide the conditions of use of the actions so that the controller can verify their applicability and their proper execution. If these conditions are not met the control can relaunch this action (or another) or it can call the planner to produce a new plan.

These causal structure to monitor the execution of a plan are quite limited. Richer formalisms have been proposed to permit the execution of plans. They can be classified into two broad families.

Imperative Languages such as RAP [45], PRS [65], or TDL [109]. They offer an imperative programming language that allows to specify procedures to be performed to meet some objectives (e.g. perform an action). These languages offer conventional programming control structures (test loop, recursion, parallelism, etc.), and often rely on concepts borrowed from logic programming (as in Prolog).

State Transition Systems such as SMACH, the ROS controller language of ROS [18]. The user provides a set of hierarchical finite state machines. Each state corresponds to an activity involving one or more components of the robot. According to the returned values of executions, the controller performs the appropriate transition to the next state. The overall state of the system corresponds to the composition of the hierarchical automata.

These systems, based on automatons or procedures are very useful and necessary in setting complex robot experiments where one must coordinate many software components. However, these models, used to refine actions in activities, must be directly programmed by procedures or automatons developers, and are not inferred from specifications. This is a problem with respect to their validation and verification.

Planning with Hierarchical Task Network (HTN) [118, 37] naturally incorporates a refinement process of abstract tasks in elementary actions. HTNs represent decomposition methods of task as a network (often an and/or tree) of elementary actions. The specification of knowledge in these approaches appears natural to the programmer. These approaches seldom provide ways to refine planned actions into commands, and to repair refinements when an execution failure occurs. However, several HTN systems are used in robotics and extend the formalism in various ways. For example SIPE [126] can produce plans where the duration of actions is taken into account. TCA/TDL [109] integrates execution and decomposition during the execution of tasks in plans. Xfrm [13] can produce plans following an HTN approach, but also allows the modification/repair of these plans while executing them (transformational planing).

4.2 Timed Approaches

The controller of an autonomous robot must explicitly take into account time. A state transition approach is not sufficient. Indeed, the activities of the robot are not instantaneous (motions, taking images, etc). Often, they must be executed in parallel, synchronized, and bounded with earliest and latest date. These motivations lead to explicitly include time and temporal constraints in the models: the plan produced will be more robust with respect to execution.

Several planning approaches based on temporal intervals or events formalisms [5, 52] have been developed, e.g., IxTeT [53] HSTS [92], Europa [48], APSI [49]. They led to extensions that take into account execution. They produce plans in the form of a lattice of instants (the beginnings and ends of actions) or intervals. A timeline represents the temporal evolution of a state variable (e.g., the position

of the robot); it is composed of instants or intervals in which the variable keeps a value (e.g., the robot does not move), or changes its value (the robot moves). The search for a solution plan is in the space of partial plans (where each state is a partial plan with a set of partially instantiated and ordered actions), with a least commitment strategy.

These approaches have many advantages for planning and execution in robotics. They properly manage concurrency or parallel execution. Furthermore, they generally produce plans that are temporally flexible, leaving to the execution the choices of the exact dates of occurrence (controllable or non-controllable but observable). For this, the execution controller must continually propagate the time constraints based on the date of occurrence actually observed to ensure that the plan remains consistent and repairable in case of inconsistency.

Some approaches (e.g., IDEA and T-ReX) offer a paradigm where the planner and the controller are tightly coupled in a set of reactors, each with its own horizon for planning and execution.

For events as well as intervals, these approaches rely on Simple Temporal Networks (STN) to model the temporal constraints between the events considered. An STN is a constraint network whose variables are events; constraints between two events t_i and t_j are of the form: $min_{ij} \leq t_j - t_i \leq max_{ij}$. The Allen Algebra of intervals [5] (using relations such as *before, meets, overlaps, starts, during, finishes*, their symmetrical and equality) can easily be transformed into an equivalent STN. One has just to translate the relations in precedence (or equalities) on the beginnings and ends of each interval.

The plan produced is an STN described by the corresponding constraint. Figure 13(a) shows the STN plan of a Mars rover that must go to a given location, take a picture, communicate the result to an orbiter during a window visibility, then return to its base. The network can be transformed into a distance graph (see Figure 13(b) where arcs correspond to the inequalities $t_j - t_i \leq max_{ij}$ and $t_i - t_j \leq -min_{ij}$). One finds the minimum using Floyd-Warshall algorithm 14(a). Here $dist[i, j]$ is the minimum distance from i to j, initialized with an infinite value when i and j are not constrained. One then obtains the graph in Figure 13(c).

When an STN is taken as a task to perform, the execution controller must incrementally propagate the update using algorithm 14(b) (which is of a lesser complexity, $O(n + n^2)$ instead of $O(n^3)$). In the example above, if the first Goto takes exactly 70 seconds, we get the STN in Figure 13(d) and after propagation the graph in Figure 13(e).

These approaches have been successfully implemented in many robotic experiments (e.g., MBARI [100], Willow Garage [83], NASA [44] and LAAS [81]) but their development faces the following difficulties:

- writing the planning models and debugging them is difficult, especially when one wants to take into account nonnominal execution situations (i.e., failures and error recovery),
- the search for solutions in the partial plans space must be guided by adapted heuristics,
- the temporal controllability of the STN must be taken into account. Indeed, these STNs contain *controllable* variables but also *contingent* variable. The values of the formers are selected by the robot, whereas the values of the latters are contingent and determined by the environment within their domain [5]. An STN is controllable if there a possible value assignment for controllable events depending on the values of the contingent ones. Strong controllability ensures that there exists an assignment of values of controllable events for all possible values of contingent ones. Weak

[5]For example, in the graph Figure 13(c) to move between t_0 and t_1, the starting time t_0 is controllable, but not the arrival time t_1. Travel time was reduced by propagation from 90 to 85 (Figure 13(c)), but in fact, only the observation after execution will give the exact value.

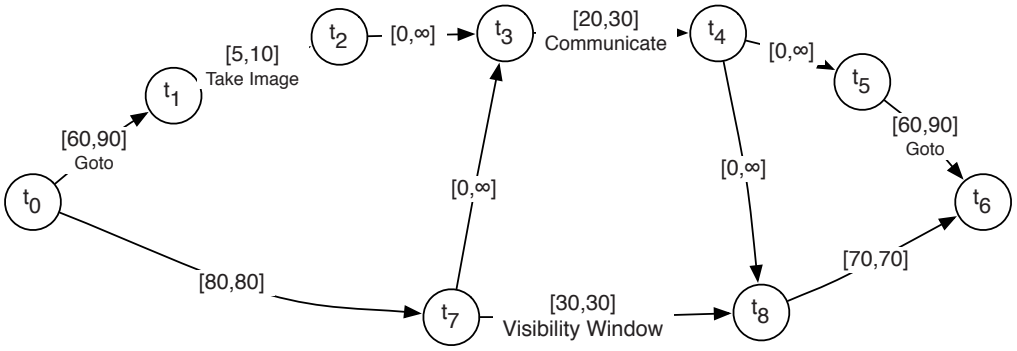

(a) Simple temporal network (STN)

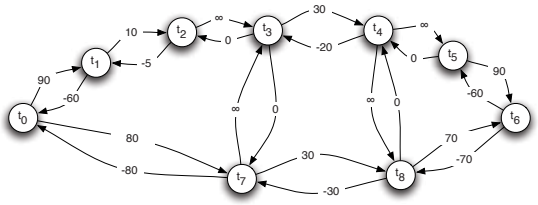

(b) Distance graph

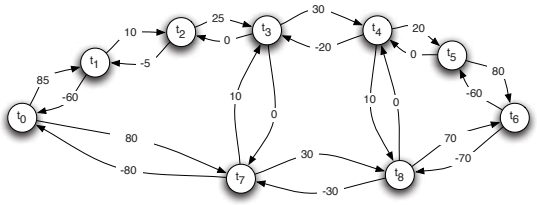

(c) After a Floyd-Warshall propagation (Algo 14(a))

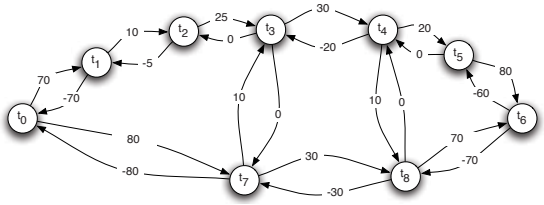

(d) After execution of the first Goto

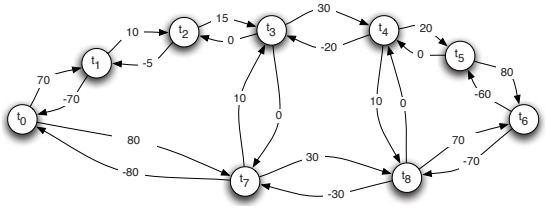

(e) After incremental propagation (Algo 14(b))

Figure 13: Successive phases of planning and execution of a temporal plan for a Mars exploration rover.

Floyd-Warshall$(dist, n)$
  for k from 1 to n
    for i from 1 to n
      for j from 1 to n
        $dist[i,j] \leftarrow min\{dist[i,j],$
          $dist[i,k] + dist[k,j]\}$

(a) Initiale propagation: Floyd-Warshall Algorithm

Incremental$(dist, n, i_0, j_0)$
  for i from 1 to n
    $dist[i,j_0] \leftarrow min\{dist[i,j_0],$
      $dist[i,i_0] + dist[i_0,j_0]\}$
  for i from 1 to n
    for j from 1 to n
      $dist[i,j] \leftarrow min\{dist[i,j_0],$
        $dist[j_0,j] + dist[i,j]\}$

(b) Incremental propagation: after changing the constrain between two events i_0 et j_0

Figure 14: Temporal contraints propagation algorithms.

controllability ensures that there is a possible value assignment for the controllable ones for all the values of the contingent ones, if they are known in advance (unrealistic). Dynamic controllability

ensures that there is an assignment for controllable ones for the values of the past contingent ones. This last property keeps the flexibility while making sure that a solution remains.

Other approaches (e.g., Aspen/Casper [29]) based on a temporal model produce complete plans without any flexibility. If a temporal (or a causal) failure occurs when executing the plan, the planner then repairs it using local search techniques.

4.3 Probabilistic Approaches

Nondeterminism is not an intrinsic property of a system but a property of its model. Interaction with the real world always involves some level of nondeterminism, that may of may not be grasped in its model. The same arguments that foster the need for autonomous deliberation in a robot, i.e., open and diverse environments and tasks, promote the use of nondeterministic models. These allow to handle various possible interactions between the robot actions and the environment own dynamics, possibly with probabilistic models. Markov Decision Processes (MDP) provide a convenient representation for planning under uncertainty. Let us introduce here the general MDP approach, which will be also useful for section 6 about learning.

Let S be a finite set of states, and A a finite set actions. If an action a is applicable in a state s, a can lead *nondeterministically* to any states in $F(s,a) \subseteq S$. Let $P(s'|s,a)$ be the probability of reaching state s' when action a is applied in s; $r(s,a) \geq 0$ is the reward associated with a in s. Let $\pi : S \rightarrow A$ be an application that associates to each state s the action to be performed in s. π is called a *policy*; it corresponds to a plan that tells the robot which action to carry in each state. π has possibly loops, i.e., following π from a state s may lead back to s after one or a few steps. The value function $V_\pi(s)$ of a state s under policy for π is the expected sum of rewards of this plan, weighted (to ensure convergence) by a decreasing coefficient:

$$\begin{aligned} V_\pi(s) &= E[\sum_{t=0}^{\infty} \xi^t r(s_t, \pi(s_t))], \text{with } \xi < 1 \\ &= r(s,\pi(s)) + \xi \sum_{s' \in F(s,\pi(s))} P(s'|s,\pi(s)) V_\pi(s') \end{aligned} \tag{7}$$

The optimal value function for a state s is $V^*(s)$ for the optimal policy π^*.

$$\begin{aligned} V^*(s) &= \max_\pi V_\pi(s) \\ &= \max_a \{Q^*(s,a)\}, \text{with} \\ Q^*(s,a) &= r(s,a) + \xi \sum_{s' \in F(s,a)} P(s'|s,a) V^*(s') \end{aligned} \tag{8}$$

Dynamic programming leads to a recursive formulation of V^* and provides easily implementable algorithms, such as Value Iteration (see Figure 15).

Value Iteration algorithm [16] terminates when a fixed point is reached, i.e., a full iteration over S without a change in any $V(s)$. It gives the optimal policy π^*. It can be initialized with an arbitrarily $V(s)$. In practice one does not need to loop until a fixed point. It is sufficient to make sure that all updates of $V(s)$ on some iteration over S remain below a threshold ϵ. The returned solution then deviates from the optimum by at most $2\epsilon \times \xi/(1-\xi)$.

The above formulation is not goal oriented: it seek an optimal policy for an infinite process. This formulation can be transformed into a goal-oriented approach by giving an initial state s_0, a set of goal states $S_g \subset S$, and by searching for an optimal policy that leads from s_0 to one of the states in

Value Iteration(S, A, P, r)
  until reaching a fixed point do
    for each $s \in S$ do
      for each a applicable in s do
        $Q(s,a) \leftarrow r(s,a) + \xi \sum_{s'} P(s'|s,a)V(s')$ ▷ *(i)*
      $V(s) \leftarrow \max_a\{Q(s,a)\}$
  for each $s \in S$ do
    $\pi(s) \leftarrow \text{argmax}_a\{Q(s,a)\}$

Figure 15: Value Iteration algorithm.

S_g. One can also integrate cost distribution on actions and variable rewards function for goal states. In such a formulation, one is not searching for policy defined everywhere, but for a partial policy, defined only in states reachable from s_0 by this policy. A *safe* policy π is guarantied to reach a goal from s_0. If a problem has a safe policy, then dynamic programming with $\xi = 1$ can find an optimal one. The algorithm Value Iteration applies to the case where there is a safe policy from every state. When this assumption does not hold, the problem is said to have *dead-ends*, i.e., states from which a goal is not reachable. Extensions to dynamic programming algorithms have been introduced, e.g., [20, 16, 9]. For example it is not necessary, nor possible iterate over all S. It is enough to search along states reachable from s_0 with a current policy. One may also estimate $Q(s,a)$ by sampling techniques [68]. The step ▷*(i)* is replaced by $Q(s,a) \leftarrow Q(s,a) + \alpha[r(s,a) + \xi \text{max}_{a'}\{Q(s',a')\} - Q(s,a)]$, where s' is taken in $F(s,a)$ by sampling according to the distribution $P(s'|s,a)$. This approach is very useful in reinforcement learning.

Value Iteration algorithm has a polynomial complexity in $|S|$ and $|A|$. Unfortunately, most of the time S has a huge size: it is exponential in the number of the state variables. There are a few more scalable approaches, using heuristics and hierarchical techniques, *e.g.*, [8, 121, 97, 96, 120]). Probabilistic planning is a very active research area with may open problems.

Given a policy π, the controller for an MDP is extremely simple. Just iterate over two steps:

- observe the state s
- execute the action $\pi(s)$

until reaching a goal state or some other stopping conditions.

The MDP approach offer several runtime advantages. It explicitly manages the nondeterminism and uncertainty. It can be extended to take into account Partially Observable domains [23]. Modeling a domain as an MDP is a difficult task, but the MDP formulation can be combined with learning techniques (see section 6). This explains the success of these approaches in many robotics applications which will be discussed later.

4.4 Integrating of Motion and Task Planning

Task planning and motion planning are two different problems that use distinct mathematical representations. The first is concerned with causal relationship regarding the effects of abstract actions, the second is concerned with computational geometry and dynamics. In simple cases a robot can decouple the two problems: task planning produces abstract actions whose refinement requires, possibly, motion planning. The two problems are however coupled for constrained environments and complex tasks. For example, moving objects in a storage room can make the motion impossible if the task is

not appropriately organized. Let us discuss here some approaches to the integration of motion and task planning.

The Asymov planner [25] combines a state-space search approach for task planning (using the FF planner [63]) with a search in the configuration space for motion planning. It defines a *place* as a state in the task planning space, as well as a range of free configurations in $\mathcal{C}_f$. A place is a bridge between the two search spaces. These two spaces are not explicitly constructed, but for every found task state, Asymov checks that there are some reachable configurations in $\mathcal{C}_f$. This approach has been extended to multi-robot problems cooperating over a joint task, e.g. two robots assembling a large furniture such as a diner table in a cluttered environment.

Another interesting technique uses hierarchical planning in a so-called *angelic* approach [127] (the term is borrowed from *"angelic nondeterminism"* which assumes that out of several issues, the best one can be chosen). An abstract action can be decomposed in different ways. An abstract plan is based on abstract actions; its set of possible decompositions is a subset of the product of all possible decompositions of its actions, some of which are not compatible. It is not necessary to ensure that all the decompositions are feasible. A plan is acceptable if it has at least one feasible decomposition. Indeed, the decomposition is not made randomly. The robot decomposes, when needed, each abstract action by choosing a feasible decomposition, if there is one. The idea is to rely on a lower bound of the set of feasible decompositions of an abstract plan such as to make sure that this set is not empty. These lower bounds are computed by running simulations of action decompositions into elementary steps, using random values of state variables. The planner relies on these estimates for searching in the abstract state space.

The approach of Kaelbling and Lozano-Perez [71] illustrates another hierarchical integration of task and motion planning. When planning at the abstract level, estimates regarding geometric information are computed with so-called *Geometric Advisers*. These advisers do not solve completely the motion planning problem submitted to them, but provide information about how feasible is a given step that enables the abstract search to continue until reaching a complete plan. When the produced plan is executed, each step that requires movements triggers a full motion planning. This approach relies on two strong assumptions: geometric preconditions of abstract actions can be calculated quickly and efficiently (by the geometric adviser); subgoals resulting from decomposition of action are executable in sequence. The approach is not complete, i.e., the geometric refinement of a planned abstract action may fail. However, for problems where actions are reversible at a reasonable cost (i.e., allowing for backtracking at the execution level) the approach is efficient and robust.

5 Interaction

Most of the approaches presented above make the assumption that there is a single agent in the environment: the robot performing the task. But complex missions may require the participation of several humans and robots. Several approaches address these issues of interaction. For example, Simmons et al. [111] proposes the Syndicate architecture, an extension to 3T [19], which allows the cooperation of several robots in collaboration with a human, for the assembly of large structures. Fong et al. [47] offers an architecture to define interaction models (tasks, teams, resources, human) needed for the cooperation of a team of astronauts and extra-planetary rovers. In the next two sections, we examine these increasingly common interactions and how they are accounted for in the planning process.

5.1 Multi-Robot Interaction

Sometimes, to achieve a complex mission, it is necessary to deploy multiple robots. Several approaches to the problems of mission planning and execution in a multi-robot framework have been developed. We may distinguish several types of problems depending on the following features:

- planning is centralized or distributed,
- plan execution by each agent is independent or coordinated,
- planning is done before acting or made as the robots proceed,
- execution failures are repaired, and if yes at which level,
- the robots can communicate between them for coordination and planning.

Many research focuses on multi-robot motion planning, with geometric and kinematic representations (see section 3), and decomposition techniques generic enough to lead to distributed implementations [36]. Recent results, e.g., [17], allow to efficiently take into account relative position constraints between the robots as well as missions featuring several sites to visit.

The Martha project illustrates an approach to manage a fleet of robots handling containers in ports and airports [4]. The allocation of tasks to robots is centralized, but on a limited horizon. Planning, execution, refinement and coordination needed for the navigation of robots and the sharing of spacial resources in the environment are distributed. Robots negotiate among themselves the navigation in the environment, which is divided into cells (e.g., intersection crossing, convoy mode, overtaking), and also negotiate their path inside these cells. The deployed system assumes a reliable local communication. Execution deadlocks between multiple robots are correctly detected by the coordination algorithm, and one of the robots automatically takes control and produces a plan that it redistributes to the other robots with which it conflicts.

Other works propose an allocation of tasks by an auction mechanism [35] to assign tasks to robots (cells crossing/surveying). Tovey et al. [124] propose a mechanism to generate appropriate auction rules adapted to the particular goal a group of exploration rover has (minimize the sum of the distances, minimize the maximum travelled distance of all robots, minimize the average time to the targets, etc.). In [132, 26], the authors apply a similar technique to tasks and subtasks of an HTN plan as it is built. Each robot can win the bids on a task, then decompose into sub-tasks following an HTN method, and auction all or part of the sub-tasks. After the initial distribution of tasks, robots maintain, during execution, the ability to auction tasks they failed to perform. Moreover, communication in these systems is not permanent and complete, thus the replanning/redistribution phases must be planned in advance.

5.2 Human - Robot Interaction

The development of service robots raises some issues with respect to human-robot interaction [57]. We focus here on approaches which are concerned with planning and the models they use.

Interactive planning (or *mixed initiative* planning), i.e., planning while keeping humans in the loop, is used in various areas. The operator takes part in the search for a plan to make choices and help the planner solve the problem.

Planning for human–robot interaction raises a completely different issue: the plan is generated automatically by the robot, but must explicitly take into account the interaction with the human while executing the plan and even in some cases, plan for a shared execution. To this end, the planner has some models (learned or programmed) of human behaviors [12]. These models specify how humans

behave with respect to the robot, what are the behaviors of the robot which are acceptable to humans. They also specify how planned actions translate into commands of the robot [116].

Various planners have been adapted to take into account the role of the human in the plans produced. Generally, these are multi-agents planners, which have been modified to consider the human as one of the agents. [24] propose an extension to GOLOG/GOLEX to plan the mission of a robot museum interacting with visitors. The approach used in [21] is based on MAPL, a PDDL based multi-agent planner to represent the beliefs of the various agents, the actions and the perception operators. A compiler then translates these PDDL models. Planning is then performed by the FF planner [63].

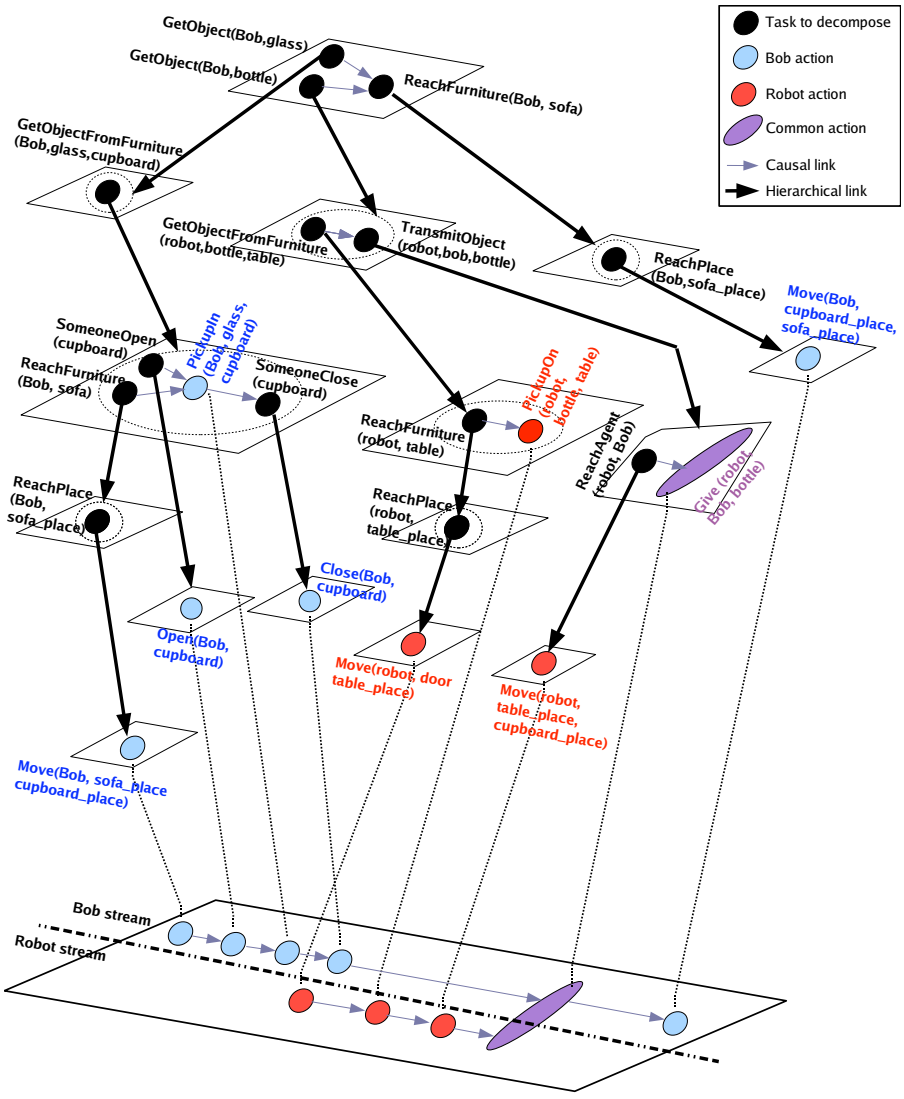

Figure 16: A plan produced by HATP with human–robot interaction: the tasks (in black) are decomposed into primitive actions for the robot (in blue), actions of the human (in red), and joint actions (in purple), which require a synchronization [3].

The HATP planner [3] plans in the context of human–robot interactions (e.g., for service robotics).

This planner extends the HTNs formalism to create plans containing two execution threads, one for the robot and one for the human who interacts with the robot. Figure 16 shows a plan produced by HATP. One can distinguish the execution of the robot thread (red) and the user thread (in blue). HATP differs from the classical HTN planning on several points. Task models and refinement methods involve human and robot. Furthermore, while the plan is produced, the system considers social rules to produce plans which are deemed acceptable and understandable to humans. For example, the robot will favor an action where it gives an object directly to the human rather than an action where it just lays the object before him. Similarly, when interacting with humans, the robot will favor a position where it faces the human, and make slower movements when it approaches him. When executing the plan, the robot must interpret and recognize human actions to properly carry out its plan. For example, if during a task the robot proposes a tool to human, and if the human loses interest, the robot should not insist, and wait for the attention of the human to return back to the robot. These good behavior recipes are not just cosmetic, they enable a more natural interaction between humans and robots.

6 Learning

Machine learning techniques have a very successful impact in many areas, and particularly in robotics. A variety of computational learning techniques are developed at various levels in robotics, from the sensory-motor level to the acquisition of tasks or environment models. A good coverage of recent learning techniques robotics can be found in [106]. We already covered environment mapping issues in section 3.2. Basic statistical learning techniques are quite useful, in particular for object recognition, but they are not specific to robotics. Let us review here two approaches that are more specific to robotics: reinforcement learning and learning from demonstration.

6.1 Reinforcement Learning

Reinforcement Learning (RL) refers to methods that improve the performance of a learner by direct interaction with the world [70, 117]. It is based on a trial and error approach. A robot learns how to act by maximizing the long term perceived benefit of its actions. Generally in RL, the learner has no teacher providing examples of good behaviors in certain situations or advices about how to choose actions. The only feedback given to the robot at each step is a scalar: the reward associated with the performed action. As long as the robot has not tried all feasible actions in all encountered situations, it will not be sure that it uses the best actions. Reinforcement learning has to solve the compromise of *exploration* vs *exploitation*: the robot must make the most of what it already knows to maximize the benefit of its behavior. To find the best one, it must explore the options that are not known enough.

To introduce the approach, consider the very simple case where a single action solves completely the task at hand and has no impact on the next task. Suppose a stationary environment and nonnegative rewards. Let $r_i(a) > 0$ be the reward received after running an action a at the i^{th} time. We can estimate the quality $Q(a)$ of an action a that has been executed k_a times by its average award:

$$Q(a) = \begin{cases} q_0 & \text{if } k_a = 0, \\ \frac{1}{k_a} \sum_{i=0}^{k_a} r_i(a) & \text{otherwise.} \end{cases} \tag{9}$$

This estimate is maintained by incremental updates:

$$Q(a) \leftarrow Q(a) + \alpha[r_{k_a+1}(a) - Q(a)], \text{with} \quad \alpha = \frac{1}{k_a + 1} \tag{10}$$

When $\forall a, k_a \rightarrow \infty$, the choice of the action which maximizes the sum of rewards is given by $\text{argmax}_a\{Q(a)\}$. However, as long as the exploration of alternatives has not been sufficient, the robot will use other options, according to various heuristics. One may define a function $\text{Select}_a\{Q(a)\}$ by one of the following methods:

- $\text{Select}_a\{Q(a)\} = \text{argmax}_a\{Q(a)\}$ with probability $(1 - \epsilon)$, and a randomly drawn action other $\text{argmax}_a\{Q(a)\}$ with probability ϵ, where ϵ is decreasing with experience,
- $\text{Select}_a\{Q(a)\}$ chooses an action according to a probabilistic sampling distribution, for example, with Boltzmann sampling, according to a probability distribution given by $e^{\frac{Q(a)}{\tau}}$, where τ is decreasing with experience.

When the environment is stationary, the update of $Q(a)$ with Equation 10 after executing an action a becomes increasingly weak with large k_a. If the environment is not stationary, we can keep $\alpha < 1$ constant. Note also that the initialization value q_0 fosters exploration if q_0 is high with respect to other rewards. For example, if $q_0 = r_{max}$, the maximum reward, new actions will be preferred to those already tested.

With these basics notions, let us now consider the interesting case where a task is performed by the combination of several actions, each interfering with the following ones, influencing the overall success of the task and the sum of rewards. The framework generally used is that of Markov decision processes introduced previously (Section 4.3). The robot seeks to learn an optimal policy that maximizes the value $V(s)$ over all s. This value is estimated from the observed rewards of the chosen actions. A major problem is how to distribute rewards over the entire task. Indeed, the rewards give an immediate return in the short term, while the quality of achievement of the task to be maximized is described by the long term sum of rewards over some horizon.

One approach is to learn the MDP model then to apply planning techniques to find the optimal policy and use it. Learning a model means collecting enough statistics through an exploratory phase to estimate the probability distributions $P(s'|s, a)$ and the rewards $r(s, a)$. An interesting application of this direct approach combines a model learning technique with a receding horizon planning algorithm [91]. It was illustrated for learning indoor navigation skills, combining different motion, localization and control modalities. The approach is applicable to any task for which the robot has several alternative methods whose performance depend on local features of the environment. The performance function is difficult to model. It is learned as an MDP whose state space is an abstract control space, which focuses on the features of the environment and current task context (including the method in use); actions correspond to available methods for performing the task. The state space is of small size (a few thousands states) which allows computing an optimal policy at each step of a receding horizon planning.

This direct approach requires a costly exploratory phase to estimate the model. It is often better to start performing the task at hand, given what is known, while continuing to learn, *i.e.*, combine the two phases of acquiring a model and finding the best action for the current model. *Q-learning* algorithm meet this objectives while avoiding to build explicitly the MDP model.

Let us use the MDP notation introduced earlier, in particular $r(s, a)$ is the observed reward after performing action a in state s, and $Q(s, a)$ is the estimated quality a in s at current time. $Q^*(s, a)$, as given by Equation 8, is unknown but it can be estimated by the expression:

$$Q(s, a) = r(s, a) + \xi \sum_{s \in F(s,a)} P(s'|s, a)\text{max}_{a'}\{Q(s', a')\} \tag{11}$$

The basic idea of the *Q-learning* algorithm (17) is to perform an incremental update of $Q(s, a)$, similar

to Equation 10. This update does not use the unknown probability parameters of the model, but the quality of successor states s', as observed in the current experience. This update is given in line *(i)* in the algorithm below.

Q-learning
  until *Termination* do
    $a \leftarrow \text{Select}_a\{Q(s,a)\}$
    execute action a
    observe $r(s,a)$ and resulting state s'
    $Q(s,a) \leftarrow Q(s,a) + \alpha[r(s,a) + \xi \max_{a'}\{Q(s',a')\} - Q(s,a)]$ ▷ *(i)*
    $s \leftarrow s'$

Figure 17: Q-learning algorithm

The values of $Q(s,a)$ are initialized arbitrarily. The function $\text{Select}_a\{Q(s,a)\}$ favors $\text{argmax}_a\{Q(s,a)\}$ while allowing for the exploration of non maximal action with a frequency decreasing with experience. The parameter $\alpha \in [0,1]$ is set empirically. When it is close to 1, Q follows the last observed values by weighting down previous experience of a in s; when it is close to zero, the previous experience is more important and Q changes marginally. α can be decreasing with the number of instances (s,a) encountered.

A variant of this algorithm (known as " SARSA" for State, Action, Reward, State, Action) takes into account a sequence of two steps (s,a,s',a') before performing the update of the estimated quality of a in s by $Q(s,a) \leftarrow Q(s,a) + \alpha[R(s,a) + \xi Q(s',a') - Q(s,a)]$. One can prove the asymptotic convergence of these two algorithms to optimal policies.

Other model-free reinforcement learning algorithms proceed by updating the value function $V(s)$ rather then the function $Q(s,a)$. Updates are performed over tuples (s,a,s') in a similar way: $V(s) \leftarrow V(s) + \alpha[r(s,a) + \xi V(s') - V(s)]$. This algorithm called $TD(0)$, is combined with a Select function permitting exploration. It is part of a family of algorithms $TD(\lambda)$ which perform updates over all states, with a weight depending on the frequency of meeting each state.

Let us also mention the DYNA algorithm and its variants that combine learning and planning: it maintains and updates an estimate of probabilities $P(s'|s,a)$ and rewards $r(s,a)$; at each step two updates are performed, a *Q-learning* type with $Q(s,a) \leftarrow r(s,a) + \xi \sum_{s'} P(s'|s,a) \max_{a'}\{Q(s',a')\}$, for the current s and a, and a Value-Iteration type for other couples (state, action) chosen randomly or according to certain priority rules, taking into account new estimates. Here, the experience allows to estimate the model and the current policy. The estimated model in turn allows to improve the policy. Each step is more computationally expensive than in *Q-Learning*, but the convergence occurs more rapidly in the number of experimental steps.

Reinforcement learning is widely used in robotics, but it is rarely implemented with explicit state space and tables of values $V(s)$ or $Q(s,a)$. The state space is generally continuous; it includes the configuration space of the robot and its environment. Even if one manages to discretize the state space appropriately (e.g., in grid type environment approaches), the astronomic size of S makes the explicit representation of S impractical. Moreover, the above algorithms are used to learn a good behavior for states encountered during learning phase, but they are not useful for states that have never been encountered: they do not allow to generalize. If one uses a continuous state space with a metric distance, one can make the reasonable assumption that *nearby* states are typically associated with close estimates of $V(s)$ or $Q(s,a)$, and thus use similar policies. Parametric approaches implement this idea.

Here S and A are described by two vectors of state and control variables. Let $\theta = (\theta_1, \ldots, \theta_n)$ be a vector of parameters. We assume that $Q(s,a)$ can be approximated parametrically by $Q_\theta(s,a)$, as a function of θ. This function is given a priori, e.g., a linear function of state and control variables. Learning involves estimating the parameters θ of this model. Q-Learning algorithm is the same as above, except that the update *(i)* does not change values in a table, but the parameters of $Q_\theta(s,a)$. The process generally involves minimizing the mean squared error of Q with respect to Q^*. The latter is estimated at each iteration from the last observed update. The gradient algorithm follows this formulation:

$$\begin{aligned} \theta &\leftarrow \theta - \frac{1}{2}\alpha\nabla_\theta[r(s,a) + \xi\max_{a'}\{Q_\theta(s',a')\} - Q_\theta(s,a)]^2 \\ &\leftarrow \theta + \alpha[r(s,a) + \xi\max_{a'}\{Q_\theta(s',a')\} - Q_\theta(s,a)]\frac{\partial Q_\theta(s,a)}{\partial\theta} \end{aligned} \tag{12}$$

This last expression replaces the *(i)* in the previous algorithm for each parameter θ_i. A similar formulation can be obtained for the estimate of V_θ.

Reinforcement learning with a parametric approach is used with success in robotics. It has been implemented in simple applications, for example to stabilize an inverse pendulum or to play darts, and in more complex demonstration, such as helicopter acrobatic flying [1, 31]. One of the main problems of these approaches is defining the action rewards.

Indeed, the previous algorithms indicates improperly "observe $r(s,a)$". But rewards are seldom directly observable by the the robot. One must provide the means to estimate the reward according to what is perceived. Sometimes the function $r(s,a)$ is easy to specify, for example as the deviation from equilibrium for a stabilization task, or the deviation from the target for tracking task. But often it is not, for example, how to specify the rewards of elementary actions for the task of driving a car?

This issue leads to the *inverse reinforcement learning* problem [2]. Here, the teacher gives the optimal behavior, the problem is to find the corresponding reward function that generates this behavior. In the case of an explicit finite MDP, the problem reduces to the following formulation (derived directly from Equation 8): we know $\pi^*(s)$ for all s; we can express $Q(s,a)$ as a function of the unknown values of $r(s,a)$ and we want $Q(s,a)$ to be maximal for $a = \pi^*(s)$. This formulation is under-specified: it has infinitely many solutions that are of no interest. It is extended with an additional criterion, for example maximize the expression: $\sum_s[Q(s,\pi^*(s)) - \max_{a\neq\pi^*(s)}Q(s,a)]$. The problem is solved by linear programming.

In parametric approaches we also define rewards r_θ as a function (usually linear) of state and control variables and seek to estimate its parameters. The previous formulation is not directly applicable because π^* is known for a small number of state samples. However the main constraint that the distribution of states generated by r_θ must be the same as the one provided by the teacher leads to a formulation that one can solve iteratively. Each iteration combines two steps, a quadratic programming optimization criterion and a dynamic programming similar to Value-Iteration.

As the reader has certainly noticed, these approaches are akin to the techniques used for inverse problems. They are also related to learning from demonstration techniques, discussed next.

6.2 Learning from Demonstration

As underlined above, the specification of the reward functions needed in reinforcement learning is far from obvious. Moreover, it is rare to have a fully observable Markov state space. We know how to transform a state space into a Markovian one, but this requires significant engineering and adds generally unobservable components. The complexity of learning and planning techniques in

partially observable MDP is prohibitive. Moreover, the experimental complexity (in the total number of needed trials) is generally much more expensive in robotics than the computational complexity. Reinforcement learning requires for converging a very large number of experiments. Finally, it is common that the task to learn cannot be treated as a simple sequence of pairs *(state, action)*. It requires a plan or a control structure, such as repeating a subsequence of actions until a termination condition. For these reasons, learning from demonstration is a good alternative when the robot can benefit of the demonstrations of a teacher.

In learning from demonstration (see the survey of Argall et al. [7]), a teacher gives to the robot the appropriate actions in well-chosen settings. This allows the teacher to control the learning process and gradually focus learning on the most difficult part of the task. The robot generalizes from the teacher demonstrations and learns the required behavior, which can be expressed as a policy in simple cases, or as a mapping from sensory states to plans in the general case. Learning from demonstration is akin to supervised learning. However in supervised learning, the teacher provides directly correct labels for training cases. Learning from demonstration involves other issues about how to map the teacher's sensing and acting spaces to those of the robot learner.

In the simplest setting, learning from demonstration reduces to acquiring the correct behavior from teleoperated training cases. The teacher acts directly in the actuator space and the proprioceptive sensor space of the robot. The latter learns actions directly as its own control environment. These approaches have resulted in many implementations, such as those presented by Sigaud and Peters [106] or Peters and Ng [95].

In the general case, the teacher acts with its own actuators rather than those of the robot to illustrate the movements and manipulations she wants to teach. The robot observes the teacher from outside. In order to learn, the robot must build up a double mapping:

- a sensory mapping to interpret the observed demonstrations, and
- a control mapping to transpose the demonstrated actions to its own actuators.

This double mapping is very complex. It often limits learning from demonstration and requires the teacher to have pedagogic skills, that is, to understand at a low level how the robot will be able to map the teacher demonstrations in its own actuation capabilities.

Moreover, learning from demonstration can be performed with or without the acquisition of a task model. The first case corresponds generally to inverse reinforcement learning. In the latter case, learning can give rise to the acquisition of a sensory-motor mapping. Here, the techniques use supervised learning, by classification or regression. Finally, learning can also lead to the acquisition of a mapping from sensory states to plans. These can be obtained by plan recognition methods. Plans can also be synthesized from the teacher specifications of operators and goals (final and intermediate) associated with observed sensory states.

Approaches relying plan recognition and synthesis allow to address a significantly more general class of behaviors that can be demonstrated by a teacher and acquired by a robot (including iterative actions and control structures). They also permit extended generalization since they lead to acquire basic principles and use the robot planning capabilities. They are finally more natural and easier for the teacher, since the teacher's actions are interpreted in terms of their effects on the environment rather than their sole order in a sequence of commands. They are illustrated for example in the work of Nicolescu and Mataric [94], Rybski et al. [103], but remain at a quite preliminary stage.

7 Integration and software architecture

Beyond the physical integration of mechanical, electrical, electronic, etc. systems, a robot is also a complex information processing system, from data acquisition to electronic commands. It integrates, various processing paradigms from real time control loops, with a hierarchy of response time, up to decisional functions conferring the autonomy and robustness required by the variability of tasks and environments. The integration of these processes should be based on architectures that defines how to articulate all these components, how they communicate and how they share data and computing resources. In any case, they must provide development methodologies to allow programming, integrating and testing of the different modules. They should provide tools and libraries to facilitate the development and deployment of the various components on the robot, especially those of interest to us: planning and execution control.

7.1 Architecture Paradigms

Most robot architectures are developed following different paradigms:

Reactive Architectures The reactive architectures, popularized by the subsumption architecture of Brooks [22], are conceptually simple. They are composed of modules which connect sensors and effectors through an internal state machine. These modules are hierarchically organized with the outputs of some which can inhibit or weight the outputs or the composition of others. These architectures were relatively popular because they are a priori easy to setup. They do not require a model of the world (the world is its own model) and are adapted to reactive simple tasks, without planning. A robot like the Roomba which has most likely been developed following this concept, achieves its task plan. But there is no quality nor efficiency objective formally pursued. Ultimately, these architectures still remain popular and are used in mono task applications. But for application associated to the variability of tasks and environments, the programming and setting of inhibitors/weights quickly becomes infeasible.

Hierarchical Architectures The hierarchical architectures and layered architectures remain the most popular in robotics. They propose to organize all robot software in two or three layers, from the functional level up to the decisional level (planning and acting). The former includes the sensory-motor functions to control sensors, effectors, and to perform the associated processing. In some instances, an intermediate level is used for execution control to verify safety conditions. Tools are typically associated with these architectures to ease the integration of the different components. Thus, the LAAS architecture [67] relies on GenoM to develop functional modules (see Figure 18), and various tools (R2C, OpenPRS, Transgen, IxTeT) for execution, supervision and tasks planning. The CLARATy architecture provides C++ basic classes which facilitate the development of the functional layer. TDL and ASPEN/Casper respectively implement the acting and the planning component.

Architectures Teleo-Reactive More recently, teleo-reactive architectures such as IDEA [44] and T-ReX [100] have emerged. They propose to decompose the problem in agents rather than in layers. Each agent [6] consists of a planner/actor tandem. It produces plans by establishing sequences of tokens on timelines representing the evolution of the state variables of the system, and ensures their execution. Planning is performed by a temporal planner (e.g. Europa [48] or APSI [49]) based on Allen [5]

[6] Agents are called reactors in the T-ReX terminology.

temporal intervals logic. These agents are organized depending on the relevant state variables. Each agent has an adapted latency, execution period and planning horizons. They communicate between them by sharing some timelines (with priority rules on which agent can change value on a shared timelines) with a dispatcher responsible for integrating the new values of token depending on the execution.

These architectures have two advantages. They have a unified agent architecture model (even functional modules are expected to be developed using this paradigm). They use the same modeling language, providing an overall consistency of models. This architecture has been deployed in a number of experiments, notably: an autonomous underwater vehicle [84], and on the PR2 robot from Willow Garage [83].

However, the deployment of these approaches is hindered by two problems. The first is performance. Agents are seldom able to properly plan fast enough (e.g. in less than a second), to be used to model functional modules. The second is the difficulty to develop the model (e.g. writing compatibilities and constraints), especially when modeling non-nominal cases.

Finally, not in these categories, there are reactive hybrid architectures that add one or more planners to reactive modules. The role of the planners is to propose plans to configure, via a coordination system, the activities of the reactive modules. The difficulty is to write this coordination module. Beaudry et al. [11] illustrate a proposal in this regard that combines a motion planner and an HTN planner which explicitly manage time; this approach seems promising for non-critical applications.

7.2 Robustness, Validation and Verification

The robustness of the software deployed on a robot poses a major problem. A first step is to robustify key components to overcome the environmental hazards, sensory noise, and the great variability of environments. One can require that a functional module, handling a sensory-motor function, knows his range of use. It should know and recognize when its data cannot be properly used, to allow corrective actions to be taken. For example, a component that makes stereo vision will recognize when its cameras are not properly calibrated; similarly, monitoring the torque on the wheel, a module that manages locomotion should detect wheel slippage or wheel blockage. Similarly, the components responsible for decision making and using formal approaches (e.g., constraints based, proposition logic,etc.) should ensure that the produced plans will not lead to undesirable states.

However, the composition of these components, as robust as they individually are, does not lead directly to an overall safety properties of the robot. For example the component taking scientific images and the locomotion component can both be correct, but all possible executions of these two components together may not be acceptable, e.g., the parameters to capture high-resolution images while moving are constrained (to avoid blurry images). The safety and robustness of embedded real-time systems [62] has been an active field for many year. With respect to robotics, one has also to consider the requirements for decisional autonomy. Modeling languages, such as UML [69] and AADL [39], can be used. They provide tools and specification methods. But we need to go further with formal approaches that provide validation and verification.

In the robotics domain, one should mention Orccad [112] and MAESTRO [34], which are based on the synchronous languages paradigm (Esterel) and have been used to implement robotic controller. Simmons et al. [110] propose a model checking approach to verify the robot controller written in the TDL language [109]. Within the LAAS architecture, the R2C [99] models all the constraints that we want to ensure and it formally checks at runtime that the commands sent by the decisional level are consistent with the model and the current state of the robot. Some research are also interested

in verifying that the code executed by the functional modules of a robot formally satisfy its logical specification [50] (at the cost of logically annotating all the code used in the module).

More recently, some work around GenoM intended to produce a formal model of the entire functional layer of a robot [15]. The modeling is based on the BIP formalism (Behavior, Interaction, Priority) [10] and exploits the fact that each GenoM module is an instance of a generic module (see Figure 18).

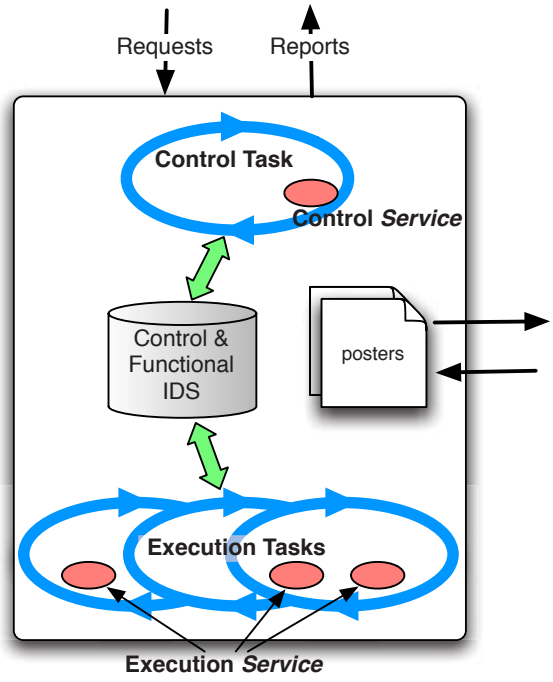

Figure 18: The internal organization of a GenoM module. The control flow is organized as follows: the control task receives requests and starts the execution of corresponding services in the execution tasks. When execution is complete, the control task returns a report to the caller. Writing or reading posters provide the data flow between the modules.

The BIP formalism [10] provides a methodology to model embedded systems from *(i)* atomic components; *(ii)* connectors that define the interactions possible between the ports of atomic components; and *(iii)* a priority relation, to select among the valid interactions. An atomic component is defined by: *(i)* a set of ports $P = \{p_1, \ldots, p_n\}$ which are used for synchronization with the other components; *(ii)* a set of states $S = \{s_1, \ldots, s_k\}$ representing states where the component awaits synchronizations; *(iii)* a set of local variables V , and *(iv)* a set of transitions. A transition is a tuple of the form (s, p, G_p, f_p, s'), representing a step from state s to s'. The transition may modify the local variables when executing the function $f_p : V \rightarrow V$. A transition is valid *iff* the guard G_p (boolean condition on V) is true and the interaction on p is possible. For example, the transition *empty* to *full* in Figure 19 is possible if $x > 0$, and if the interaction *in* is possible. The variable y then takes the value $f(x)$. The transition from *full* to *empty* has not guard, but requires an interaction on port *out*.

In this approach, all the components of a generic GenoM module are modeled in BIP. All modules of the functional layer are obtained by recomposition of these basic BIP models. It should be noted that the executable code associated to the state of the original GenoM service automata are now within

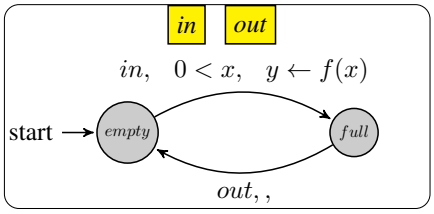

Figure 19: A simple example of an atomic BIP component comprising two states and two transitions. Transition from *empty* to *full* is associated with an interaction on port in, a boolean condition $0 < x$, and a change of the value of y. The transition in the other direction requires only an interaction with the out port.

the $f(x)$ transitions function in the BIP model. This approach is extended to the complete functional layer of a robot, and provides an extremely fine grained formal model of the system considered (e.g., the state in which each component is, the possible interactions at any time, etc.). This model is then used by the BIP Engine (an automata player which checks online guards and interactions of the entire model, and fire the valid transitions) to control the execution on the actual robot. This model can also be verified and validated with formal tools like D-Finder [14]. This formal verification method composes *component invariants* ϕ_i which define for each component a logical property it satisfies, and the *interaction invariants* Ψ that logically define the possible interactions γ between the components considered. The extraction of these invariants is automatic. The inference rule:

$$\text{if } (\bigwedge_i \phi_i) \wedge \Psi \Rightarrow \Phi \text{ then } \|_\gamma \{B_i\}_i < \Phi >$$

specifies that if the conjunction of invariants $(\bigwedge_i \phi_i) \wedge \Psi$ (overestimation of the reachable states) implies a formula Φ, then the parallel composition $\|_\gamma \{B_i\}_i$ also satisfies Φ.

This method allows, among other things, to verify that there is no deadlock in the system or to check safety properties. Note that this technique based on components and interactions invariants can potentially take into account search spaces larger than the ones model checking techniques can handle.

8 Conclusion

In this paper, we presented an overview of the state of the art at the intersection of two broad fields which are Robotics and Artificial Intelligence. We reviewed models and techniques for addressing problems of planning and execution control of movements and tasks, interaction and learning. We discussed how to integrate decision-making functions with sensory-motor functions within a robot architecture. Most of these issues have been outlined very synthetically. Some were slightly detailed to provide the reader with illustrative frequently used representations and algorithms.

As underlined in the introduction, robotics is a multidisciplinary field. Significant progress in robotics can be expected from major advances in its basic disciplines. Further, robot can be a catalyst research target to advance these disciplines. For example, a light and fast mechanical gripper with high dexterity, an inexpensive accurate 3D range sensor, or an image recognition algorithm with broad and reliable performances for ordinary objects that can be found in a house or store, will substantially enrich the functional capabilities of current platforms.

But, as we have also pointed out, robotics research is primarily integrative. One can certainly make progress in terms of basic components for the handling some particular task or environment. But the autonomy of a machine when facing a diversity of environments and tasks requires progress in the integrated *perception - decision - action* control loop.

This loop is at the core of research in robotics. It requires explicit models of objects at various levels, from their physical appearance to their functions. It also requires models of activities, events and processes that constitute the environment and its agents, including the robot. It requires knowledge representations adapted to these models. These models are mathematically heterogeneous, that is continuous/discrete, symbolic/numeric, geometric/topologic, deterministic/stochastic, etc. In robotics, the term "knowledge representations" is necessarily plural. It also requires a variety of learning techniques to acquire and improve these models. This is the research agenda, for which we have reviewed the progress over the past two or three decades, and on which more work remains to be done. This agenda is as relevant to *self-contained* robots, which integrate all their components on a single platform, as well as to *distributed* robots. Distribution is also an important item of this agenda. It concerns the distribution of cognitive functions over the components and functions of a single robot, as well as the distribution of robotics functions over a networks of sensors, actuators and processing resources on a large scale.

It can also be argued that the *perception - decision - action* control loop is at the core of AI research. Continues progress is being made in all individual subfields of AI. For example, statistical and hybrid techniques have led to dramatic advances in automatic natural language processing, illustrated for example by the victory of the WATSON system in the question/answer game "Jeopardy" [41]. Representations coupling first-order logic and uncertainty management, such as probabilistic first order logic [86], open remarkable opportunities, especially for the problems of planning and learning that we discussed here.

But the AI objective, namely *to understand, model and implement intelligence*, is seen by many researchers as being expressed in the *perception - decision - action* control loop. Consider the problem of "*anchoring*", i.e., maintaining a mapping between a symbol and the sensory data related to the same physical object [32], or the more general problem of "*symbol grounding*" [60], i.e., associating a symbol, in its context, to a signified content, object, concept or property. These problems requires the coupling of cognitive mechanisms to sensory-motor functions able to interact independently with the world to which symbols refer (the level T3 of the Turing test of Harnad [61]). For both fields, the coupling of Robotics and AI remains a very fertile research area.

References

[1] Abbeel, P., Coates, A., Quigley, M., and Ng, A. Y. (2006). An Application of Reinforcement Learning to Aerobatic Helicopter Flight. In *Neural Information Processing Systems (NIPS)*, pages 1–8.

[2] Abbeel, P. and Ng, A. Y. (2010). Inverse Reinforcement Learning. In Sammut, C. and Webb, G. I., editors, *Encyclopedia of Machine Learning*, pages 554–558. Springer.

[3] Alami, R., Clodic, A., Montreuil, V., Sisbot, E., and Chatila, R. (2006). Toward Human-Aware Robot Task Planning. In *AAAI Spring Symposium: To boldly go where no human-robot team has gone before*, pages 39–46.

[4] Alami, R., Fleury, S., Herrb, M., Ingrand, F., and Robert, F. (1998). Multi-Robot Cooperation in the MARTHA Project. *IEEE Robotics and Automation Magazine*, 5(1):36 –47.

[5] Allen, J. F. (1984). Towards a general theory of action and time. *Artificial Intelligence*, 23(2):123 – 154.

[6] Antonelli, G., Fossen, T. I., and Yoerger, D. R. (2008). Underwater Robotics. In [105], pages 987–1008.

[7] Argall, B., Chernova, S., Veloso, M. M., and Browning, B. (2009). A Survey of Robot Learning from Demonstration. *Robotics and Autonomous Systems*, 57(5):469–483.

[8] Barry, J. L., Kaelbling, L. P., and Lozano-Pérez, T. (2011). DetH*: Approximate Hierarchical Solution of Large Markov Decision Processes. In *International Joint Conference on Artificial intelligence (IJCAI)*, pages 1928–1935.

[9] Barto, A. G., Bradtke, S. J., and Singh, S. P. (1995). Learning to Act Using Real-Time Dynamic Programming. *Artificial Intelligence*, 72(1-2):81–138.

[10] Basu, A., Bozga, M., and Sifakis, J. (2006). Modeling Heterogeneous Real-Time Components in BIP. In *International Conference on Software Engineering and Formal Methods (SEFM)*, pages 3–12.

[11] Beaudry, E., Létourneau, D., Kabanza, F., and Michaud, F. (2008). Reactive planning as a motivational source in a behavior-based architecture. In *IEEE/RSJ International Conference on Intelligent Robots and Systems (IROS)*, pages 1848–1853.

[12] Beetz, M., Jain, D., Mösenlechner, L., and Tenorth, M. (2010). Towards Performing Everyday Manipulation Activities. *Robotics and Autonomous Systems*, 58(9):1085–1095.

[13] Beetz, M. and Mcdermott, D. (1997). Expressing Transformations of Structured Reactive Plans. In *European Conference on Planning (ECP)*, pages 64–76. Springer Publishers.

[14] Bensalem, S., Bozga, M., Nguyen, T.-H., and Sifakis, J. (2009). D-Finder: A Tool for Compositional Deadlock Detection and Verification. In *Computer Aided Verification (CAV)*, pages 614–619.

[15] Bensalem, S., de Silva, L., Ingrand, F., and Yan, R. (2011). A Verifiable and Correct-by-Construction Controller for Robot Functional Levels. *Journal of Software Engineering for Robotics*, 1(2):1–19.

[16] Bertsekas, D. P. (1995). *Dynamic Programming and Optimal Control*. Athena Scientific, Vol. 1 and 2.

[17] Bhattacharya, S., Likhachev, M., and Kumar, V. (2010). Multi-agent path planning with multiple tasks and distance constraints. In *IEEE International Conference on Robotics and Automation (ICRA)*, pages 953–959.

[18] Bohren, J. and Cousins, S. (2010). The SMACH High-Level Executive [ROS News]. *IEEE Robotics and Automation Magazine*, 17(4):18 –20.

[19] Bonasso, R., Firby, R., Gat, E., Kortenkamp, D., Miller, D., and Slack, M. (1997). Experiences with an Architecture for Intelligent, Reactive Agents. *Journal of Experimental and Theoretical Artificial Intelligence*, 9(2/3):237–256.

[20] Bonet, B. and Geffner, H. (2006). Learning Depth-First Search: A Unified Approach to Heuristic Search in Deterministic and Non-Deterministic Settings, and Its Application to MDPs. In *International Conference on Automated Planning and Scheduling (ICAPS)*, pages 142–151.

[21] Brenner, M., Hawes, N., Kelleher, J., and Wyatt, J. (2007). Mediating Between Qualitative and Quantitative Representations for Task-Orientated Human-Robot Interaction. In *International Joint Conference on Artificial intelligence (IJCAI)*, volume 7.

[22] Brooks, R. (1986). A Robust Layered Control System for a Mobile Robot. *IEEE Journal of Robotics and Automation*, 2:14–23.

[23] Buffet, O. and Sigaud, O., editors (2008). *Processus Décisionnels de Markov en Intelligence Artificielle*. Trait IC2, vol.1 et 2. Hermes - Lavoisier.

[24] Burgard, W., Cremers, A., Fox, D., Hähnel, D., Lakemeyer, G., Schulz, D., Steiner, W., and Thrun, S. (1998). The Interactive Museum Tour-Guide Robot. In *National Conference on Artificial Intelligence (AAAI)*, pages 11–18.

[25] Cambon, S., Alami, R., and Gravot, F. (2009). A Hybrid Approach to Intricate Motion, Manipulation and Task Planning. *International Journal of Robotics Research*, 28(1):104–126.

[26] Cao, H., Lacroix, S., Ingrand, F., and Alami, R. (2010). Complex Tasks Allocation for Multi Robot Teams under Communication Constraints. In *5th National Conference on Control Architectures of Robots*, Douai, France.

[27] Chatila, R. and Laumond, J.-P. (1985). Position referencing and consistent world modeling for mobile robots. In *IEEE International Conference on Robotics and Automation (ICRA)*, pages 138–145.

[28] Chaumette, F. and Hutchinson, S. (2008). Visual Servoing and Visual Tracking. In [105], pages 563–583.

[29] Chien, S., Knight, R., Stechert, A., Sherwood, R., and Rabideau, G. (2000). Using Iterative Repair to Improve the Responsiveness of Planning and Scheduling. In *AI Planning and Scheduling (AIPS)*.

[30] Choset, H., Lynch, K., Hutchinson, S., Kantor, G., Burgard, W., Kavraki, L., and Thrun, S. (2005). *Principles of Robot Motion: Theory, Algorithms, and Implementations*. MIT Press.

[31] Coates, A., Abbeel, P., and Ng, A. Y. (2009). Apprenticeship learning for helicopter control. *Communication ACM*, 52(7):97–105.

[32] Coradeschi, S. and Saffiotti, A. (2003). An Introduction to the Anchoring Problem. *Robotics and Autonomous Systems*, 43(2-3):85–96.

[33] Corke, P. I., Roberts, J. M., Cunningham, J., and Hainsworth, D. (2008). Mining Robotics. In [105], pages 1127–1150.

[34] Coste-Maniere, E. and Turro, N. (1997). The MAESTRO Language and its Environment: Specification, Validation and Control of Robotic Missions. In *IEEE/RSJ International Conference on Intelligent Robots and Systems (IROS)*, volume 2, pages 836 –841 vol.2.

[35] Dias, M., Zlot, R., Kalra, N., and Stentz, A. (2006). Market-Based Multirobot Coordination: A Survey and Analysis. *Proceedings of the IEEE*, 94(7):1257 –1270.

[36] Erdmann, M. and Lozano-Pérez, T. (1987). On Multiple Moving Objects. *Algorithmica*, 2:477–521.

[37] Erol, K., Hendler, J., and Nau, D. S. (1994). UMCP: a Sound and Complete Procedure for Hierarchical Task-Network Planning. In *AI Planning and Scheduling (AIPS)*, pages 249–254.

[38] Estrada, C., Neira, J., and Tardós, J. D. (2005). Hierarchical SLAM: Real-Time Accurate Mapping of Large Environments. *IEEE Transactions on Robotics and Automation*, 21(4):588–596.

[39] Feiler, P. H., Lewis, B. A., and Vestal, S. (2006). The SAE Architecture Analysis & Design Language (AADL) A Standard for Engineering Performance Critical Systems. In *IEEE International Symposium on Computer-Aided Control Systems Design*, pages 1206–1211.

[40] Feron, E. and Johnson, E. N. (2008). Aerial Robotics. In [105], pages 1009–1029.

[41] Ferrucci, D., Brown, E., Chu-Carroll, J., Fan, J., Gondek, D., Kalyanpur, A. A., Lally, A., Murdock, J. W., Nyberg, E., Prager, J., Schlaefer, N., and Welty, C. (2010). Building Watson: An Overview of the DeepQA Project. *AI Magazine*, Fall:59–79.

[42] Fikes, R. (1971). Monitored Execution of Robot Plans Produced by STRIPS. In *IFIP Congress*.

[43] Fikes, R. and Nilsson, N. (1971). STRIPS: A New Approach to the Application of Theorem Proving to Problem Solving. *Artificial intelligence*, 2(3-4):189–208.

[44] Finzi, A., Ingrand, F., and Muscettola, N. (2004). Model-Based Executive Control Through Reactive Planning for Autonomous Rovers. In *IEEE/RSJ International Conference on Intelligent Robots and Systems (IROS)*, volume 1, pages 879–884.

[45] Firby, R. J. (1987). An Investigation into Reactive Planning in Complex Domains. In *National Conference on Artificial Intelligence (AAAI)*, pages 202–206. AAAI Press.

[46] Flint, A., Murray, D., and Reid, I. (2011). Manhattan Scene Understanding Using Monocular, Stereo, and 3D Features. In *Proc. International Conference on Computer Vision*.

[47] Fong, T., Kunz, C., Hiatt, L., and Bugajska, M. (2006). The Human-Robot Interaction Operating System. In *ACM SIGCHI/SIGART Conference on Human-robot interaction*, pages 41–48.

[48] Frank, J. and Jónsson, A. (2003). Constraint-Based Attribute and Interval Planning. *Constraints*, 8(4):339–364.

[49] Fratini, S., Cesta, A., De Benedictis, R., Orlandini, A., and Rasconi, R. (2011). APSI-Based Deliberation in Goal Oriented Autonomous Controllers. In *11th Symposium on Advanced Space Technologies in Robotics and Automation (ASTRA)*.

[50] Frese, U., Hausmann, D., Luth, C., Taubig, H., and Walter, D. (2009). The importance of being formal. *Electronic Notes in Theoretical Computer Science*, 238(4):57–70.

[51] Ghahramani, Z. (1997). Learning Dynamic Bayesian Networks. *Lecture Notes In Computer Science*, 1387:168–197.

[52] Ghallab, M. and Alaoui, A. M. (1989). Managing Efficiently Temporal Relations Through Indexed Spanning Trees. In *International Joint Conference on Artificial intelligence (IJCAI)*, pages 1297–1303, San Francisco, CA, USA.

[53] Ghallab, M. and Laruelle, H. (1994). Representation and Control in IxTeT, a Temporal Planner. In *AI Planning and Scheduling (AIPS)*, pages 61–67.

[54] Ghallab, M., Nau, D. S., and Traverso, P. (2004). *Automated Planning - Theory and Practice*. Elsevier.

[55] Gini, M. L., Ohnishi, K., and Pagello, E. (2010). Advances in Autonomous Robots for Service and Entertainment. *Robotics and Autonomous Systems*, 58(7):829–832.

[56] Giralt, G., Sobek, R., and Chatila, R. (1979). A Multi-Level Planning and Navigation System for a Mobile Robot: A First Approach to HILARE. In *International Joint Conference on Artificial intelligence (IJCAI)*, pages 335–337.

[57] Goodrich, M. and Schultz, A. (2007). Human-Robot Interaction: A Survey. *Foundations and Trends in Human-Computer Interaction*, 1(3):203–275.

[58] Guizzo, E. (2008). Kiva Systems. *IEEE Spectrum*, pages 27–24.

[59] Hägele, M., Nilsson, K., and Pires, J. N. (2008). Industrial Robotics. In [105], pages 963–986.

[60] Harnad, S. (1990). The Symbol Grounding Problem. *Physica D*, pages 335–346.

[61] Harnad, S. (2001). Minds, Machines and Turing: The Indistinguishability of Indistinguishables. *Journal of Logic, Language, and Information (special issue on "Alan Turing and Artificial Intelligence"*.

[62] Henzinger, T. and Sifakis, J. (2006). The Embedded Systems Design Challenge. In *FM: Formal Methods*, Lecture Notes in Computer Science 4085, pages 1–15. Springer.

[63] Hoffmann, J. (2001). FF: The Fast-Forward Planning System. *AI magazine*, 22(3):57.

[64] Hopcroft, J. and Tarjan, R. (1973). Efficient Algorithms for Graph Manipulation. *Communications of the ACM*, 16:372–378.

[65] Ingrand, F., Chatila, R., Alami, R., and Robert, F. (1996). PRS: A High Level Supervision and Control Language for Autonomous Mobile Robots. In *IEEE International Conference on Robotics and Automation (ICRA)*, volume 1, pages 43 –49 vol.1.

[66] Ingrand, F. and Ghallab, M. (2014). Deliberation for autonomous robots: A survey. *Artificial Intelligence*.

[67] Ingrand, F., Lacroix, S., Lemai-Chenevier, S., and Py, F. (2007). Decisional Autonomy of Planetary Rovers. *Journal of Field Robotics*, 24(7):559–580.

[68] Jaakkola, T., Jordan, M. I., and Singh, S. P. (1994). On the Convergence of Stochastic Iterative Dynamic Programming Algorithms. *Neural Computation*, 6(6):1185–1201.

[69] Jacobson, I., Booch, G., and Rumbaugh, J. (1999). *The Unified Software Development Process*. Addison-Wesley Longman Publishing Co., Inc., Boston, MA, USA.

[70] Kaelbling, L. P., Littman, M. L., and Moore, A. W. (1996). Reinforcement Learning: A Survey. *Journal of Artificial Intelligence Research (JAIR)*, 4.

[71] Kaelbling, L. P. and Lozano-Perez, T. (2011). Hierarchical Task and Motion Planning in the Now. In *IEEE International Conference on Robotics and Automation (ICRA)*, pages 1470–1477.

[72] Kanoun, O., Laumond, J.-P., and Yoshida, E. (2011). Planning Foot Placements for a Humanoid Robot: A Problem of Inverse Kinematics. *International Journal of Robotics Research*, 30(4):476–485.

[73] Kavraki, L. E., Svestka, P., Latombe, J.-C., and Overmars, M. H. (1996). Probabilistic Roadmaps for Path Planning in High-Dimensional Configuration Spaces. *IEEE Transactions on Robotics and Automation*, 12(4):556–580.

[74] Kazerooni, H. (2008). Exoskeletons for Human Performance Augmentation. In [105], pages 773–793.

[75] Konolige, K., Marder-Eppstein, E., and Marthi, B. (2011). Navigation in Hybrid Metric-Topological Maps. In *IEEE International Conference on Robotics and Automation (ICRA)*.

[76] Kuipers, B. and Byun, Y.-T. (1991). A Robot Exploration and Mapping Strategy Based on a Semantic Hierarchy of Spatial Representations. *Robotics and Autonomous Systems*, 8(1-2):47–63.

[77] Kuipers, B., Modayil, J., Beeson, P., MacMahon, M., and Savelli, F. (2004). Local Metrical and Global Topological Maps in the Hybrid Spatial Semantic Hierarchy. In *IEEE International Conference on Robotics and Automation (ICRA)*, pages 4845–4851.

[78] Latombe, J.-C., editor (1991). *Robot Motion Planning*. Kluwer, Boston, MA.

[79] Laumond, J.-P. (1990). Connectivity of Plane Triangulation. *Information Processing Letters*, 34(2):87–96.

[80] LaValle, S., editor (2006). *Planning Algorithms*. Cambridge University Press.

[81] Lemai-Chenevier, S. and Ingrand, F. (2004). Interleaving Temporal Planning and Execution in Robotics Domains. In *National Conference on Artificial Intelligence (AAAI)*.

[82] Martínez-Carranza, J. and Calway, A. (2010). Unifying Planar and Point Mapping in Monocular SLAM. In *British Machine Vision Conference (BMVC)*, pages 1–11.

[83] McGann, C., Berger, E., Boren, J., Chitta, S., Gerkey, B., Glaser, S., Marder-Eppstein, E., Marthi, B., Meeussen, W., Pratkanis, T., et al. (2009). Model-based, hierarchical control of a mobile manipulation platform. In *4th Workshop on Planning and Plan Execution for Real World Systems at ICAPS*.

[84] McGann, C., Py, F., Rajan, K., Thomas, H., Henthorn, R., and McEwen, R. (2008). A deliberative architecture for AUV control. In *IEEE International Conference on Robotics and Automation (ICRA)*, pages 1049–1054.

[85] Mei, C. and Rives, P. (2007). Cartographie et Localisation Simultanée avec un Capteur de Vision. In *Journées Nationales de la Recherche en Robotique*.

[86] Milch, B. and Russell, S. J. (2007). First-Order Probabilistic Languages: Into the Unknown. In *Inductive Logic Programming*, volume 4455 of *Lecture Notes in Computer Science*, pages 10–24. Springer.

[87] Minguez, J., Lamiraux, F., and Laumond, J.-P. (2008). Motion Planning and Obstacle Avoidance. In [105], pages 827–852.

[88] Montemerlo, M., Thrun, S., Koller, D., and Wegbreit, B. (2002). FastSLAM: A Factored Solution to the Simultaneous Localization and Mapping Problem. In *National Conference on Artificial Intelligence (AAAI)*, pages 593–598.

[89] Montemerlo, M., Thrun, S., Koller, D., and Wegbreit, B. (2003). FastSLAM 2.0: An Improved Particle Filtering Algorithm for Simultaneous Localization and Mapping that Provably Converges. In *International Joint Conference on Artificial intelligence (IJCAI)*, pages 1151–1156.

[90] Moravec, H. P. (1983). The Stanford Cart and the CMU Rover. Technical report, CMU.

[91] Morisset, B. and Ghallab, M. (2008). Learning How to Combine Sensory-Motor Functions Into a Robust Behavior. *Artificial Intelligence*, 172(4-5):392–412.

[92] Muscettola, N. (1994). HSTS: Integrating Planning and Scheduling. In Zweben, M. and Fox, M., editors, *Intelligent scheduling*. Morgan Kaufmann.

[93] Newcombe, R. A. and Davison, A. J. (2010). Live dense reconstruction with a single moving camera. In *Computer Vision and Pattern Recognition (CVPR)*, pages 1498–1505.

[94] Nicolescu, M. N. and Mataric, M. J. (2003). Natural methods for robot task learning: Instructive demonstrations, generalization and practice. In *Autonomous Agents and Multi-Agent Systems (AAMAS)*, pages 241–248.

[95] Peters, J. and Ng, A. Y., editors (2009). *Autonomous Robots, Special issue on robot learning*, volume 27(1-2). Springer.

[96] Pineau, J. and Gordon, G. J. (2005). POMDP Planning for Robust Robot Control. In *International Symposium on Robotics Research (ISRR)*, pages 69–82.

[97] Pineau, J., Gordon, G. J., and Thrun, S. (2003). Policy-contingent abstraction for robust robot control. In *Uncertainty in Artificial Intelligence*, pages 477–484.

[98] Prassler, E. and Kosuge, K. (2008). Domestic Robotics. In [105], pages 1253–1281.

[99] Py, F. and Ingrand, F. (2004). Dependable Execution Control for Autonomous Robots. In *IEEE/RSJ International Conference on Intelligent Robots and Systems (IROS)*, volume 2, pages 1136–1141.

[100] Py, F., Rajan, K., and McGann, C. (2010). A Systematic Agent Framework for Situated Autonomous Systems. In *Autonomous Agents and Multi-Agent Systems (AAMAS)*, pages 583–590.

[101] Rosen, C. A. and Nilsson, N. J. (1966). Application Of Intelligent Automata to Reconnaissance. Technical report, SRI.

[102] Russell, S. and Norvig, P. (2010). *Artificial Intelligence, A modern approach*. Prencice Hall.

[103] Rybski, P. E., Yoon, K., Stolarz, J., and Veloso, M. M. (2007). Interactive robot task training through dialog and demonstration. In *Conference on Human-Robot Interaction*, pages 49–56.

[104] Schwartz, J., Sharir, M., and Hopcroft, J., editors (1987). *Planning,Geometry and Complexity of Robot Motion*. Ablex Series in Artificial Intelligence. Ablex Publishing.

[105] Siciliano, B. and Khatib, O., editors (2008). *The Handbook of Robotics*. Springer.

[106] Sigaud, O. and Peters, J., editors (2010). *From Motor Learning to Interaction Learning in Robots*, volume 264 of *Studies in Computational Intelligence*. Springer.

[107] Siméon, T., Laumond, J.-P., Cortés, J., and Sahbani, A. (2004). Manipulation Planning with Probabilistic Roadmaps. *International Journal of Robotics Research*, 23(7-8):729–746.

[108] Siméon, T., Laumond, J.-P., and Nissoux, C. (2000). Visibility Based Probabilistic Roadmaps for Motion Planning. *Advanced Robotics Journal*, 14(6).

[109] Simmons, R. and Apfelbaum, D. (1998). A Task Description Language for Robot Control. In *IEEE/RSJ International Conference on Intelligent Robots and Systems (IROS)*, volume 3, pages 1931 –1937 vol.3.

[110] Simmons, R., Pecheur, C., and Srinivasan, G. (2000). Towards Automatic Verification of Autonomous Systems. In *IEEE/RSJ International Conference on Intelligent Robots and Systems (IROS)*, volume 2, pages 1410 –1415 vol.2.

[111] Simmons, R., Singh, S., Heger, F., Hiatt, L., Koterba, S., Melchior, N., and Sellner, B. (2007). Human-Robot Teams for Large-Scale Assembly. In *Proceedings of the NASA Science Technology Conference*. Citeseer.

[112] Simon, D., Espiau, B., Kapellos, K., and Pissard-Gibollet, R. (1997). ORCCAD: Software Engineering for Real-Time Robotics. A Technical Insight. *Robotica*, 15:111–115.

[113] Smith, R., Self, M., and Cheeseman, P. (1986). Estimating uncertain spatial relationships in robotics. In *Proc. Uncertainty in Artificial Intelligence*, pages 435–461.

[114] Stachniss, C. and Burgard, W. (2004). Exploration with active loop-closing for FastSLAM. In *IEEE/RSJ International Conference on Intelligent Robots and Systems (IROS)*.

[115] Stentz, A. (1994). Optimal and efficient path planning for partially-known environments. In *IEEE International Conference on Robotics and Automation (ICRA)*, pages 3310 –3317 vol.4.

[116] Stulp, F. and Beetz, M. (2008). Combining Declarative, Procedural and Predictive Knowledge to Generate and Execute Robot Plans Efficiently and Robustly. *Robotics and Autonomous Systems (Special Issue on Semantic Knowledge)*.

[117] Sutton, R. S. and Barto, A. G. (1998). *Reinforcement Learning: An Introduction*. MIT Press.

[118] Tate, A., Drabble, B., and Kirby, R. (1994). *O-Plan2: An Architecture for Command, Planning and Control*. Morgan-Kaufmann.

[119] Taylor, R. H., Menciassi, A., Fichtinger, G., and Dario, P. (2008). Medical Robotics and Computer-Integrated Surgery. In [105], pages 1199–1222.

[120] Teichteil-Königsbuch, F. and Fabiani, P. (2005). Symbolic Heuristic Policy Iteration Algorithms for Structured Decision-Theoretic Exploration Problems. In *Workshop on Planning Under Uncertainty for Autonomous Systems at ICAPS*, pages 66–74.

[121] Teichteil-Königsbuch, F., Kuter, U., and Infantes, G. (2010). Incremental plan aggregation for generating policies in MDPs. In *Autonomous Agents and Multi-Agent Systems (AAMAS)*, pages 1231–1238.

[122] Thrun, S. (2002). Robotic Mapping: A Survey. In Lakemeyer, G. and Nebel, B., editors, *Exploring Artificial Intelligence in the New Millenium*. Morgan Kaufmann.

[123] Thrun, S. (2006). Stanley: The robot that won the DARPA Grand Challenge. *Journal of Field Robotics*, 23(9):661–692.

[124] Tovey, C., Lagoudakis, M., Jain, S., and Koenig, S. (2005). The Generation of Bidding Rules for Auction-Based Robot Coordination. In Parker, L., Schneider, F., and Schultz, A., editors, *Multi-Robot Systems. From Swarms to Intelligent Automata Volume III*, pages 3–14. Springer Netherlands.

[125] Triggs, B., McLauchlan, P., Hartley, R., and Fitzgibbon, A. (2000). Bundle Adjustment – A Modern Synthesis. In Triggs, B., Zisserman, A., and Szeliski, R., editors, *Vision Algorithms: Theory and Practice*, volume 1883 of *Lecture Notes in Computer Science*, pages 298–372. Springer-Verlag.

[126] Wilkins, D. (1988). *Practical Planning: Extending the classical AI planning paradigm*. Morgan Kaufmann.

[127] Wolfe, J., Marthi, B., and Russell, S. (2010). Combined Task and Motion Planning for Mobile Manipulation. In *International Conference on Automated Planning and Scheduling (ICAPS)*, volume 5, page 2010, Toronto, Canada.

[128] Wolpert, D. M. and Flanagan, J. R. (2010). Q&A: Robotics as a Tool to Understand the Brain. *Bmc Biology*, 8.

[129] Wolpert, D. M. and Flanagan, J. R. (2016). Computations Underlying Sensorimotor Learning. *Current Opinion in Neurobiology*, 37:7–11.

[130] Wolpert, D. M. and Ghahramani, Z. (2000). Computational Principles of Movement Neuroscience. *Nature Neuroscience*, 3:1212–1217.

[131] Yoshida, K. and Wilcox, B. (2008). Space Robots and Systems. In [105], pages 1031–1063.

[132] Zlot, R. and Stentz, A. (2006). Market-Based Multirobot Coordination Using Task Abstraction. In Yuta, S., Asama, H., Prassler, E., Tsubouchi, T., and Thrun, S., editors, *Field and Service Robotics*, volume 24 of *Springer Tracts in Advanced Robotics*, pages 167–177. Springer Berlin / Heidelberg.

Efficient Algorithms for Reliability Evaluation of General Networks

Mohamed-Larbi Rebaiaia[1,2] and Daoud Ait-kadi[1,2]

(1) Interuniversity Research Center on Enterprise Networks, Logistics and Transportation
Laval University, Quebec (QC), Canada
Mohamed-larbi.rebaiaia@cirrelt.ca

(2) Mechanical Engineering Department, Laval University
Laval University, Quebec (QC), Canada
Daoud.ait-kadi¤gmc.ulaval.ca

ABSTRACT

Several production systems either for goods or services can be modeled by a network where nodes are production centers, warehouses, distributions and others, and arcs represent the relationship between nodes. Nodes and arcs are often subjected to random failures that may result from several causes. These networks include one or more sources and one or more destinations. Given the stochastic nature of the failure, the reliability and the robustness of the network become an important criteria for safety, economical and environment reasons.

Several methods based on graph theory and stochastic processes are proposed in the literature. The concepts of minimal paths set (MPS) and minimal cuts set (MCS) as well as decomposition techniques based on Bayes' theorem have been widely used. The performance of these methods is greatly affected by network size (number of nodes and arcs) and its density.

Generally, except for special structure of some networks (e.g series, parallel, standby, etc.) there is no mathematical expression based on the reliability of its nodes and its arcs that has been proved compact for representing the expression of the reliability function of any network. This paper attempts to provide solutions to this problem by proposing and testing a unified approach based on MPS/MCS and Binary Decision Diagrams (BDD). This approach is illustrated by several simple examples. A tool has been developed to handle complex networks such as telecommunication networks and other network's tests published in the literature.

Keywords

Reliability, Networks, Algorithms, MPS, MCS, BDD.

1. INTRODUCTION

The assessment of network's reliability has been addressed in many papers [1, 9, 10, 11, 12, 13, 14, 18, 20, 24, 25, 26, 35, 39]. Efficient computation techniques have been proposed for the network reliability over a given mission duration. The complexity of network's reliability algorithms increases with the size of the networks (number of arcs and nodes).

This paper proposes an integrated approach using MPS/MCS and BDD for generating the network structure function which can be used for evaluating the reliability of networks so that the considered system meets its end-to-end service availability objective. A concrete telecommunication is used to testify the applicability of all the algorithms that will be proposed in the following sections and a series of network's benchmark are also used to show the strength of the algorithms and to compare their performance within those published in the literature.

Most of the methods and algorithms proposed up to now for determining the reliability of networks consider three categories of techniques which are different in the form but are very close in substance. These techniques have been discussed in many publication researches and concern a large number of physical systems such as electric power systems, telecommunication networks [24, 25, 26, 27], traffic and transportation systems, just to name a few. Generally, reliability engineers model the functioning and the physical connectivity of system components by a network. Mathematically, a network is a graph $G(V, E)$ in which V represents the components (e.g. devices, computers, routers, etc.) and E the interconnections (e.g. HF-VHF and microwave transporters [24]. In the sequel, we suppose that graphs and networks and systems are of the same object and can be used to design the same system.

Network reliability analysis consists of evaluating the 2-terminal reliability of networks (K and all-terminal) [10, 11, 31, 33]. General theory, has discussed extensively two techniques; exact [1, 8, 12, 13, 14, 20, 21, 24, 34] and approximate methods [23]. The exact method uses the concept of MPS/MCS [11, 25, 26, 29, 32, 34, 35]. Determining MCS is essential not only to evaluate the reliability but also to investigate different scenarios in order to find for instance the redundant components that could be replaced to improve the load point reliability and for predicting the risk that a part of a system could fail or not with a certain probability value [26, 38]. Enumerating all MCS may be a preferable way if the number of paths is too huge to be practically enumerated than the number of cuts. Examples of this kind of preferences is the 2x100 lattice which has 2^{99} paths and just 10000 cuts [20], and complete network with 10 nodes contains 109601 minimal paths and just 256 cuts [26]. In existing algorithms [11, 24, 35], minimal paths are deduced from the graph using simple and systematic recursive algorithms that guarantee the generated paths set to be minimal. The enumeration of MCS is more problematic because they need advanced mathematics, set theory and matrices manipulation. Many algorithms have been published in the literature and some of them are implemented in commercial tools. Enumeration appears to be the most computationally efficient. An initiative of solution has been proposed in [21, 22] where author presented a method for generating MPS directly from MCS, or vice-versa. It starts with the inversion of the reliability expression accomplished by a recursive method combining a 2-step application of De Morgan's theorem. Yan et al. [34] presented a recursive labelling algorithm for determining all MCS in a directed network, using an approach adapted from dynamic programming algorithms. The algorithm produces all MCS, and uses comparison logic to eliminate redundant cuts. This algorithm is an enumeration technique derived from the approach of Jensen & Bellmore [14] and follows an extension of Tsukiyama et al. [32] to improve the computational efficiency and space requirements of the algorithm. Jasmon and Kai [13] use an algorithm which proceeds by deducting first the link cuts set from node cuts set and, second the basic minimal paths using network decomposition. In addition to the enumeration of cuts set directly, it is possible to obtain them from the inversion of minimal paths [22], Shier and Whited [29]. In such topic, one of the best algorithms is proposed by Al-Ghanim [3] which is based on a heuristic programming algorithm for generating all MPS and Cuts set. Recently, Rebaiaia and Ait-Kadi [24] propose an elegant and fast algorithm for enumerating MPS using a modified DFS technique [30]. The

procedure uses each discovered path to generate new MPS from subpaths. The above procedure is repeated until all minimal paths (MP) are found. The algorithm didn't produce any redundant MPS. Furthermore, they extended their work with theoretical proofs and the usage of sophisticated techniques for dynamic data structures manipulation of complex networks.

The paper is structured as follows. Section 2 presents some related preliminaries. Section 3 details some algorithms for determining the MPS, MCS and BDD. Section 4 and section 5 present some experienced applications using a series of benchmarks and a real telecommunication system. The paper concludes the paper in section 6.

2. Backgrounds

2.1. Stochastic Graph

A probabilistic graph $G = (V, E)$ is a finite set V of nodes and a finite set E of incidence relations on the nodes called edges. The edges are considered as transferring a commodity between nodes with a probability p called reliability. They may be directed or undirected and are weighted by their existence probabilities. The graph in such case, models a physical network, which represents a linked set of components giving services. The reliability of networks is defined as the probability that systems (networks) will perform their intended function without failure over a given period of time. Figure 1 shows an example of an undirected graph where node 1 and node 6 are respectively initial node and terminal node.

For a specified set of nodes $K \subseteq V$ of G, we denote the K-terminal reliability of G by $R(G_K)$. When $|K| = 2$, $R(G_K)$ is called a 2-terminal (or terminal-pair) reliability which defines the probability of connecting (s, t) a source node with a target node [25, 31, 33]. A success set, is a minimal set of the edges of G such that the vertices in K are connected; the set is minimal so that deletion of any edges causes the vertices in K to be disconnected and this will invalidate the evaluation of the reliability. Topologically, a success set is a minimal tree of G covering all vertices in K. The computation of the K-terminal reliability of a graph may require efficient algorithms. One such solution can be derived directly from the topology of the network by constructing a new parallel-series network using MPS of the original network such that each minimal path constitutes a branch of the parallel-series graph. Then, a characteristic expression $\Phi(x)$ called structure function is derived from the disjoint expressions of paths terms, and from which the reliability is evaluated after applying Boolean simplification processing [25].

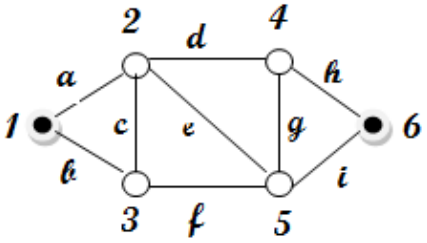

Figure 1. A probabilistic weighted graph with six nodes $(\mathbf{1}, \mathbf{2}, \mathbf{3}, \mathbf{4}, \mathbf{5}, \mathbf{6})$ and nine undirected edges $(\mathbf{a}, \mathbf{b}, \ldots, \mathbf{i})$.

2.2. Multicomponent Reliability

Let $f(x)$ be the failure probability density function of any component and t the time period beginning from time zero. The reliability of a component may be expressed as

$$R(t) = \int_t^{\infty} f(x)dx \tag{1}$$

When a system is composed by m identical components disposed in series or n identical components disposed in parallel, the mathematical expressions of their reliability function are respectively

$$R_s(t) = \prod_{i=1}^{m} \int_t^{\infty} f_i(x)\, dx \tag{2}$$

$$R_p(t) = 1 - \prod_{i=1}^{n} \left(1 - \int_t^{\infty} f_i(x) dx\right) \tag{3}$$

It is simple to combine series with parallel and parallel with series configurations. Their expressions are respectively

$$R_{s,p}(t) = 1 - \prod_{i=1}^{m} \left(1 - \prod_{j=1}^{n} \int_t^{\infty} f_{i,j}(x)\right) dx \tag{4}$$

$$R_{p,s}(t) = \prod_{i=1}^{n} \left(1 - \prod_{j=1}^{m} \left(1 - \int_t^{\infty} f_{i,j}(x) dx\right)\right) \tag{5}$$

When systems are complex and does not possess a well-defined structure, it would be necessary to determine their reliability using methods which proceed by successive transformations. An interesting introduction to such methods has been published in [25] and [26].

2.3 Structure Function

Consider a system composed of *m* components numbered from 1 to *m*. Each of these components may be in functioning state or in failed state with a probability p_i respectively a probability q_i. Let x_i be the state component and x the state vector, they can be defined as follows:

$$x_i(t) = \begin{cases} 1 & \text{if the component } i \text{ (node/edge)is UP at time } t \\ 0 & \text{if the component i (node/edge) is down} \end{cases}$$

$x = (x_1, x_2, \dots, x_m)$ is the state vector of a system *S* of order *m* such that $x \in \Omega_i = \{0,1\}^m$ the state space of the system.

Mathematically, any system can be represented by its structure function which is an application function taking its value in the Boolean domain, such that,

$$\Phi(x) = \begin{cases} 1 & \text{if the system is functioning when the state vector is } x \\ 0 & \text{if the system has failed when the state vector is } x \end{cases}$$

In this paper, we consider only systems that are coherent represented by structure functions that are non-decreasing [4].

2.4 Minimal Paths set and Minimal Cuts set

Let (s, t) be a fixed initial and terminal nodes in a graph representing the system. A minimal path is any path composed by a series of successive edges linking *s* to *t* and such that if any one of such edges is removed from the path, the link between *s* to *t* is broken. Respectively, a minimal cut is composed by a set of edges such that if one edge is removed from the cut, the link from *s* to *t* still functioning. Note that if we remove any minimal cut edge, the link from *s* to *t* is broken.

Thus, a minimal paths set (MPS) respectively a minimal cuts set (MCS) are composed by all minimal paths respectively all minimal cuts in the graph.

If we suppose that a system is composed by a set MPS $= \{P_1, P_2, \dots, P_p\}$ and a set MCS $= \{C_1, C_2, \dots, C_c\}$ its structure function can be expressed by:

$$\Phi(x) = \max_{1\le j\le P} \min_{i\in P_j} x_i = \min_{1\le j\le C} \max_{i\in C_j} x_i \tag{6}$$

and if $E\{\Phi(X)\}$ is expected mathematical expression, the reliability of a system is computed according to the following formula:

$$R(G) = E\{\Phi(X)\} = Pr\{\Phi(X) = 1\} = \sum_{X\in\Omega_i} \Phi(X) Pr\{X = x\} \tag{7}$$

and such that the probability $Pr\{X = x\}$ is determined by $p_i = Pr\{X = 1\}$ and $q_i = Pr\{X = 0\} = 1 - p_i$.

Note that the formula in Equation (6) means that the structural function of any complex system is equivalent to the structural function after transforming such system to a parallel-series or series-parallel one. Figure 2 shows clearly such transformation.

2.5 Reliability Evaluation

After enumerating MPS and MCS, the reliability evaluation needs the development of the symbolic expression in terms of the probability of the various components being operational/non-operational, for that calculation, Equation (6) and Equation (7) can be used. But, it is not always easy to do so, especially for complex systems. Fortunately, we can find in the literature many other techniques and algorithms to calculating the reliability [12, 16, 17, 33, 34].

2.5.1 Illustrative example

Consider a directed *bridge* network as represented in Figure 2 (a). The MPS (Figure 2 (c)), MCS (Figure 2 (d)), the structure function and the reliability expression are respectively:

MPS : $p_1 = \{x_1, x_4\}$; $p_2 = \{x_2, x_5\}$ and $p_3 = \{x_1, x_3, x_5\}$.

MCS: $c_1 = \{x_1, x_2\}$; $c_2 = \{x_1, x_5\}$; $c_3 = \{x_4, x_5\}$ and $c_4 = \{x_2, x_3, x_4\}$.

Structure function:

$\Phi\big(X(t)\big) = 1 - (1 - x_1x_4)(1 - x_2x_5)(1 - x_1x_3x_5)$ (Determined from MPS), and the reliability is,

$R(t) = \Pr\big(\Phi\big(X(t)\big) = 1\big) \quad = r_1r_4 + r_2r_5 + r_1r_3r_5 - r_1r_2r_4r_5 - r_1r_3r_4r_5 - r_1r_2r_3r_5 + r_1r_2r_3r_4r_5$

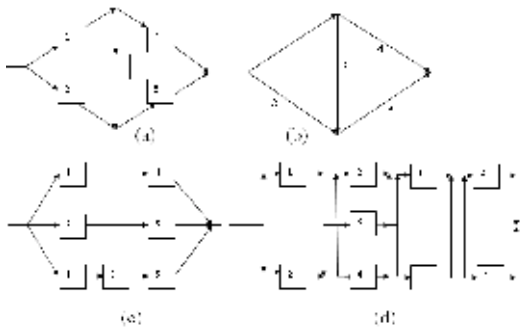

Figure 2. a) System structure, b) Reliability bloc diagram, c) Reliability structure based on MPS. d) Reliability structure based on MCS.

3. Algorithm for determining Network Structure Function

We have just say above that the structure function plays a very important role for calculating the reliability of any system provided that it can be modelled as a graph, and their determination is not as easy as we thought, especially for large networks. Also, to make the structure function expression possible, we have to enumerating all the minimal paths/minimal cuts. For doing that, we can apply any one of the many algorithms published in the literature [25]. But, the problem with MPS and MCS determination is related to their size that can grows exponentially and reaches millions of paths/cuts for graphs that are supposed to be simple such as complete, grid and lattice graphs that represent the most adequate structures to represent systems similar to those of telecommunication and transportation networks [26, 20, 35] .

There is another interesting mathematical tool called BDD for binary decision diagram that can be used for determining the system structure function and possibly from which it can be possible to generating both MPS and MCS [6, 7, 8, 26, 27, 35].

3.1 Binary Decision Diagram

Binary Decision Diagrams are the state-of-art data structure for manipulating and simplifying large Boolean expressions such that of analogic and digital function, and specifically those that cannot be handled with traditional techniques such as Table truth and Karnaugh mape. Bryant [6, 7] was the first to binary decision diagrams for symbolic verification of integrated circuits. The problem with BDD representation despite their effectiveness is their exponential growing size due to wrong ordering declaration of variables. Bollig *et al.* [5] demonstrate that improving the Variable Ordering of OBDD is NP-Complete. Ruddell [28] first used an algorithm based on dynamic programming techniques to reduce the size of the BDD.

In engineering, Coudert and Madre [8] and Rauzy [27] applied first, BDDs for evaluating networks reliability. Figure 3 shows the BDD relative to the network presented in Figure 2, and its representation in the computer memory.

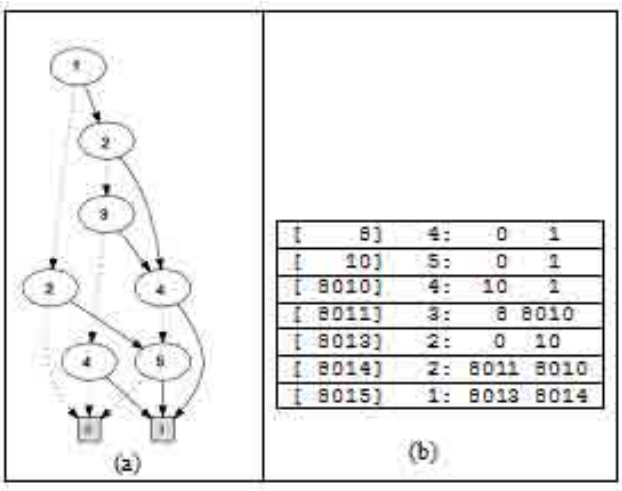

Figure 3. (a) : ROBDD corresponding to the network of figure 2.(a) and

(b) : its representation code in memory similar to table in figure 5 (right).

The implementation and manipulation of BDD algorithms is composed by three procedures, *restrict*, *apply* and *ite*. The are used for simplifying and reducing Boolean functions. For example, the *ite* for (If _ Then _ Else) function for a Boolean expression is expressed by

$f = ite(x, F_1, F_2) = x.F_1 + \bar{x}.F_2$; with $F_1 = f_{x=1}$ and $F_2 = f_{x=0}$.
The following pseudo-code gives the *ite* function.

```
Function ite(f, g, h)
  if f = 0 then
     Return h;
  else if f = 1 then
        Return g;
     else if (g = 1) ∧ (h = 0) then
        Return f;
      else if g = h then
        Return g;
          else if ∃ computed-table entry (f, g, h,H)
then
             Return H;
               end if
            x_k ←top variable of f, g, h;
            H ← new non-terminal node with label
x_k;
           then H ← ite (f |x_k=1, g |x_k=1, h |x_k=1);
            else H ← ite (f |x_k=0, g |x_k=0, h |x_k=0);
     Reduce  H;
 Add entry (f, g, h,H) to computed-table;
     Return  H;
 end.
```

Another important algorithm incorporated in BDD is the *apply* procedure which can manipulating Boolean operator like conjunction, disjunction and complementation Boolean operators and the objective is to mix individual formulas composing a Boolean expression. An example of composition using *apply* procedure is shown in Figure 4.

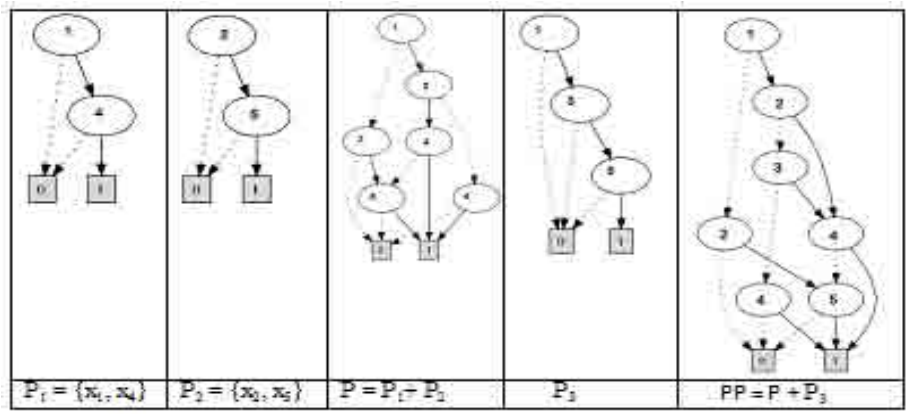

Figure 4. APPLY procedure mixing the minimal paths formulas of the Network in Figure 2.

3.1.1 Algorithm for BDD procedure

The representation and the simplification of a Boolean expression proceeds in 4-steps:

- Construct the binary decision tree (BDT) associated with the graph formula.
- Transform the BDT to a BDD by applying the following rules :

a- Merging equivalent leaves of a binary decision tree.
b- Merging isomorphic nodes.
c- Elimination of redundant tests

- Transform the BDD to OBDD by just a wise choice on variables and then to obtain a Reduced OBDD
- OBDD can be reduced to a ROBDD by repeatedly eliminating in a bottom-up fashion, any instances of duplicate and redundant nodes. If two nodes are duplicates, one of them is removed and all of its incoming pointers are redirected to its duplicate. If a node is redundant, it is removed and all incoming pointers are redirected to its just one child.

In the following, we propose three categories of algorithms for determining the structure function of any graph network. The first algorithm try to determine the MPS, the second the MCS and the third is more general and can be applied on the fly for determining the function structure and at the same time the reliability.

3.2 Algorithm for MPS determination

Let $G = (V, E)$ be the graph network modelling a system and suppose that the couple (s, t) represents the initial and the terminal nodes of the graph.

It is recognized that the best technique for enumerating the MPS is to use a procedure based on the well-known recursive algorithm called depth first search (DFS) which search successive nodes and edges composing a path from s to t. When reaching the last node (target node), the algorithm turned back to try to concatenate another part of a path to create a new path. As the procedure is recursive, it continues to explore new paths using other directions until it is not possible to generate other paths.

The algorithm proceeds as follows

```
Function stack S = pathDFS(G, v, z)
   setLabel(v, VISITED)
   S.push(v)
   if  v = z
    return S.elements()
   for all e in G.incidentEdges(v)
    if getLabel(e) = unvisited
         w ← opposite(v,e)
    if getLabel(w) = unvisited
        S.push(e)
        pathDFS(G, w, z)
        S.pop(e)
    else
     S.pop(v)
end
Program Main()
    Input: A connected graph with node set, edge set, a
source node, and a sink node .
Declaring dynamics vectors and stacks (put in them
zeros)
Declaring initial and terminal nodes (v, z)
Do While .true.
  pathDFS(G, v, z)
  if "the last minimal path have been encountered"
  return .false.
enddo
Output: All MPS in the graph.
```

3.2.1 Example

Using the graph in figure 1 and applying the MPS algorithm, we determine all the minimal paths for directed and undirected graphs.

a. Directed graph

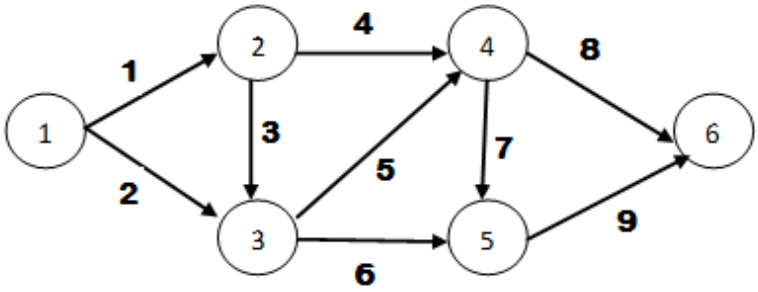

Figure 5. A 6-node, 9-link example network (directed)

Table 1. The MPS corresponding to the network in Figure 5.

#	Minimal Pathset
1	1, 3, 5, 7, 9
2	1, 3, 5, 8
3	1, 3, 6, 9
4	1, 4, 7, 9
5	1, 4, 8
6	2, 5, 7, 9
7	2, 5, 8
8	2, 6, 9

b. Undirected graph (Figure 1)

Because the graph is undirected we must duplicating the edges as two arcs in both opposite directions and then to rename them differently. Table 2 gives such renaming.

Table 2. Adjacent matrix of the network in Figure 1.

G =

Nodes	1	2	3	4	5	6
1		1	2			
2	3		4	5		
3	6	7		8	9	
4		10	11		12	13
5			14	15		16
6				17	18	

Table 3. The MPS corresponding to the network in Figure 1.

#	Minimal Pathset
1	1, 4, 8, 12, 16
2	1, 4, 8, 13
3	1, 4, 9, 15, 13
4	1, 4, 9, 16
5	1, 5, 11, 9, 16
6	1, 5, 12, 16
7	1, 5, 13
8	2, 7, 5, 12, 16
9	2, 7, 5, 13
10	2, 8, 12, 16
11	2, 8, 13
12	2, 9, 15,13
13	2, 9, 16

3.3 Algorithm for MCS determination

We propose three algorithms for enumeration all minimal cuts set in a graph. They are as follows:

3.3.1 Algorithm for directed graphs

This algorithm is similar of the one published by Yan et al [34], but instead using set theory as a support to data structure, it uses lists objects. It is as follows:

Algorithm DirectedMCS

Let A_j, OA_j, p, k, S_k are successively set of input and output arcs to and from a node j, p is a label, k is node name and S_k.

Step 1. Set $X_1 = \{1\}, Y_1 = \{2,3,\cdots,n\}$ // n : is the number of nodes

- Node 1 is marked
- Select the successor and predecessor of node j (say $\{j\}$) or (OA_j, IA_j) and define
- $X_i = X_{i-1} + \{j\}$, $Y_i = Y_{i-1} - \{j\}$ and determine the C_j^p using the formula:

$C_j^p = C_j^p \cup OA_j - C_j^p \cap IA_j$, $p = \{1,2,3,\cdots,S_k\}$ for all k.

Step 2.

- *if* $Y_i = \{n\}$ and all nodes of $X_i = \{1,2,3,\cdots,n-1\}$ have been marked then return and STOP.
  else GOTO Step 1

end.

3.3.2 Algorithm for undirected graphs

There are many algorithms published in the literature used for determining MCS, but few of them are simple to be used especially the following one:

Algorithm UndirectedMCS
Let X be the set of nodes including the initial node and such that these nodes are connected between themselves, and let $G * i$ be the graph the transformation of the graph G in which the node i has been merged into X by deleting any edge connecting i and X.
Let (s, t) be the initial and the terminal nodes of the graph, and suppose that
$i = s$ (initialization); hash table = nil; MCS = nil; (hash table and MCS are empty);
Begin
If $G(E, V)$ is empty (there isn't at least two nodes linked by an edge)
Return and STOP
else if $(i = t)$ return
else $G = G * i, X = X + \{i\}$;
If (X is present in the hash table) return;
else Add X *to hash table*; end
Add X to MCS;
For all i adjacent to X do
Call Undirected MCS
end
end
end.

3.3.3 Algorithm for determining MCS from MPS

Locks [22] and Shier and Whited [29] propose a technique for obtaining MCS by complementing MPS using DeMorgen's laws [19].

If we transpose the idea of generating MCS by inversion but instead on Boolean formulas, we applied such idea directly on the structure of the BDD (e.g. Figure 3.(a)).
The procedure to deduce the MCS is a depth first search algorithm; it works on the graph using data information's taken from matrix of the Figure 3 (b). It can be presented as follows:

Procedure *Generation_of MCS*
- Place the squared node on top of a stack 1 //* records DFS visits to ROBDD nodes *//.
- Place the squared node on top of a stack 2 //* records cut's nodes.
- Place on the top of the stack 1 all the ascending nodes of the top variable in the stack.
- Place the node top of the stack 1 on top of the stack 2, if the edge (link) is dotted.
- Continue until the variable reach the root node.
- If so, a cut has been found. Write the content of the stack 2 as a line of a matrix. Remove top variable from stack 1 and from stack 2.
- Continue the procedure until stack 1 is empty.
- Apply the filtering process by removing all the redundant paths (cuts) using the matrix of paths (cuts)
- Display MSC Matrix.

end

3.4 Algorithm for determining the reliability from BDD data structure

Network reliability is calculated the following algorithm:

```
Procedure Reliability_Evaluation(F, G)
 if ( F == 0) return 1     //*  Boolean value 1 (one)  *//
 else  if  (F == 1) return 0     //*  Boolean value 0 (zero)  *//
       else  if (computed-table has entry {F, P_F})
                return  P_F
             else  P_F = Prob(F1) + P(x) * (Prob(F2)-  Prob(F1))
            end
      end
 Insert_computed_table ({F, P_F})
 return  P_F
 end
end
```

The following BDD structure shows how the values corresponding to each level are communicated to the upper level until the root.

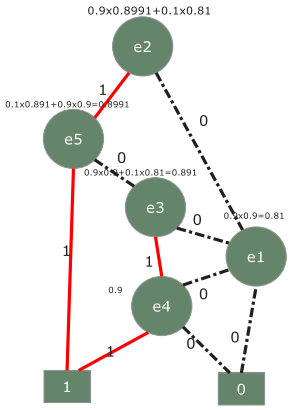

Figure 6. Solution given by the earlier algorithm

4. Experimental results

The proposed algorithms and procedures have been implemented in MatLab 8 and Java Jdk 1.6. A communicating interface has been written to render easy data and results transfer between MatLab system and Java packages running under jGrasp a graphical tool written in Java JDK. The operating system is 32 bits and 2038 MO of Windows Vista of Microsoft. The machine is an HP notebook PC with an Intel(R) core (TM) 2 Duo processor of 1.67. The benchmark networks in figure 9 were used and the results are shown in Table 4 and Table 5. All the networks are 2-terminal and they have been used in different publication papers. We can remark from table 5, that the value of execution time is interesting despite the fact that the performance of the machine characteristics is not high. The importance of this work shows the efficiency of the algorithms. Note that no comparison was made with another implementation but they can be compared for example with the results of Lin *et al.* [20].

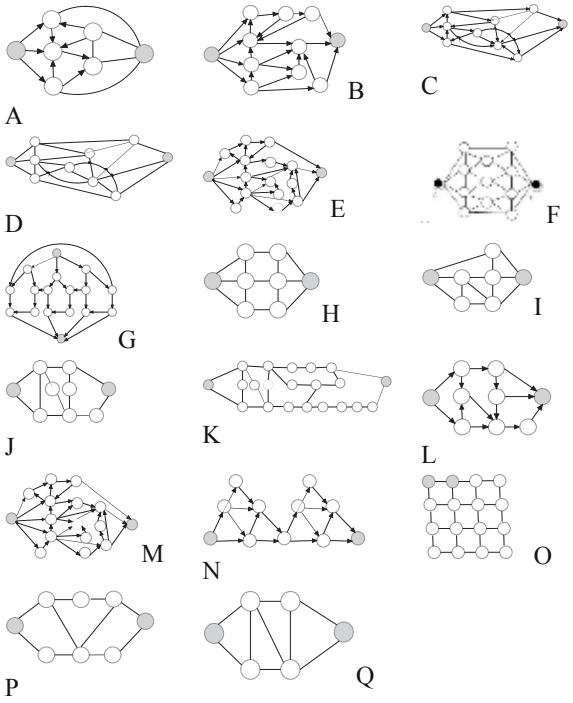

Figure 7. Benchmark networks

Table 4. Benchmark results for 2-terminal networks

Networks	MPS	MCS	Time(sec.)
A	8	12	0.075591
B	18	110	0.282727
C	115	85	313.17
D	33	72	11.29
E	35	30	0.046
F	114	562	21236.06
G	10	959	818.80
H	29	29	0.708676
I	25	20	0.332611
J	13	21	4.059842
K	44	528	2572.03
L	6	23	0.226500
M	36	96	11.166
N	100	16	8.3297
O	98	105	283.38
P	5	16	0.768533
Q	13	9	0.945836

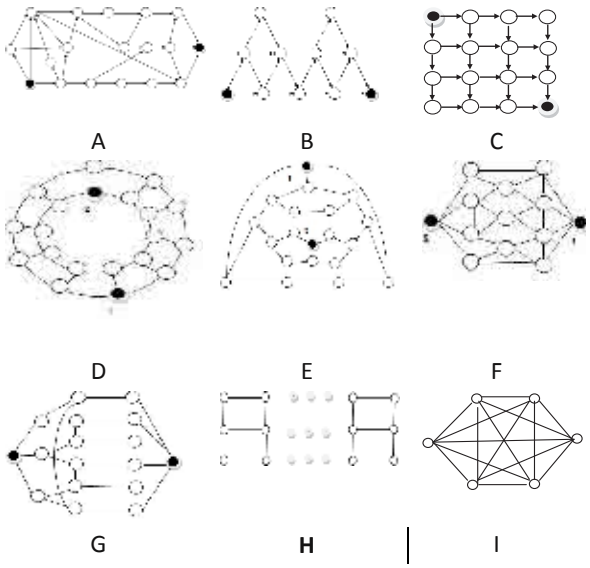

Figure 8. S set of directed and undirected networks

Table 5. Computational results of experimental networks.

Networks	Nodes	Links	MPS	Runtime Seconds	Reliability value
A	18	29	44	0.060	0.99185255
B	11	18	36	0.031	0.87046009
C	36	60	252	0.368	0.88653767
D	20	60	432	38.062	0.96302007
E	20	60	780	>60	0.99712
F	13	56	1808	1.029	0.98989967
G	17	50	136	>60	0.99806
H	16	48	98	0.063	0.98781674
I	6	20	65	0.117	0.99998996

5. CASE STUDY- A Radio communication network

To illustrate the performance of the algorithms presented in sections 3 and 4, we propose a practical application to a case study problem of undirected regional radio communication network showed in Figure 90 and 10. The system composed of equipment s is scattered across a wide geographic area. It consists of a set of mobile and portable transmitter-receivers deserved by a network of fixed equipment s located in Canada. There are two master site in operation 24 hours a day and a third one in standby, which is used in case of urgency, and more than 150 base stations used to transmit the signal generated through the microphone to portable and mobile equipment. A master site consists of core and exit routers, WAN and LAN switches, controllers and some operative computers plus others monitoring and dispatching hardware/software systems such as gateway routers, AEB, PBX, dispatching consoles Elite, and so. The radio sites is equipped with one or two antennas for broadband coverage on which is terminated 4 to 8 transmitter-receiver transponders (Tx / Rx). The transponders are connected to each antenna via filtration equipment of type Multicoupler. The multicouplers form a chain of multicoupling able to accept other transponders in expansion. The range of the base station depends on its power, antenna system, terrain, carrier transporter (e.g. T1 or E1) and environmental conditions (see. [24, 25, 26] for more details).

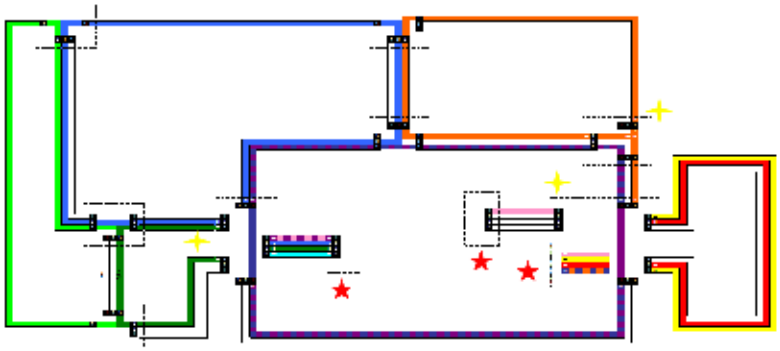

Figure 9. The reduced architecture of the radio communication network presented in Figure 10 (The case study)

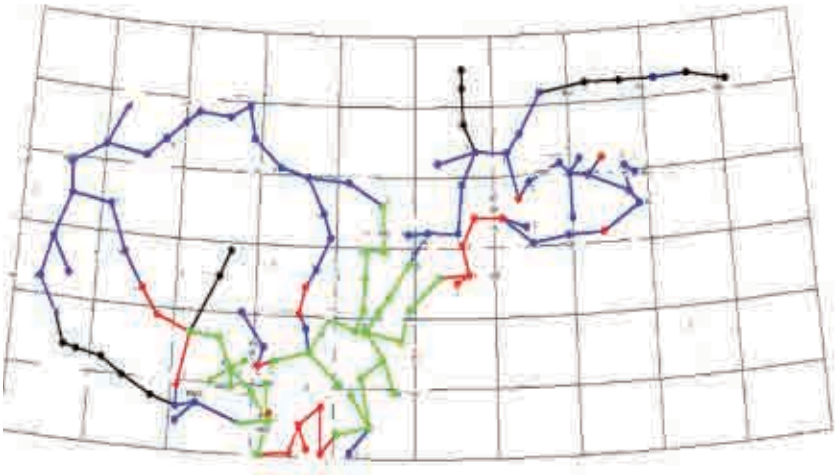

Figure 10. A regional radio communication network

Table 6. The reliability values on each node of the network

	I	II	III	IV	V	VI
A	0,99992	0,99992	0,99992	0,99990	0,99990	0,99996
B	0,99993	0,99987	0,99996	0,99918	0,99989	0,99980
C	0,99987	0,99993	0,99996	0,99991	0,99992	0,99993
D	0,99999	0,99997	0,99995	0,99987	0,99970	0,99993
E	0,99998	0,99992	0,99990	0,99996	0,99996	0,99992
F	0,99992	0,99993	0,99987	0,99996	0,99988	0,99996
G	0,99992	0,99992	0,99995	0,99986	0,99987	0,99987
H	0,99992	0,99987	0,99996	0,99987	0,99992	0,99996
I	0,99993	0,99992	0,99984	0,99996	0,99993	0,99987
J	0,99993	0,99990	0,99996	0,99986	0,99992	0,99996
K	0,99997	0,99992	0,99987	0,99998	0,99993	0,99996
L	0,99992	0,99995	0,99992	0,99993	0,99975	0,99996
M	0,99992	0,99987	0,99992	0,99988	0,99986	0,99990
N	0,99991	0,99987	0,99992	0,99984	0,99993	0,99992
O	0,99992	0,99992	0,99992	0,99997	0,99992	0,99999
P	0,99997	0,99996	0,99937	0,99996	0,99987	0,99999
Q	0,99945	0,99980	0,99990	0,99980	0,99992	0,99999
R	0,99987	0,99992	0,99980	0,99960	0,99993	0,99987
S	0,99993	0,99987	0,99987	0,99987	0,99992	0,99993
T	0,99992	0,9999	0,99990	0,99986	0,99988	0,99998

Table 7. The reliability of each microwave link between two nodes.

	I	II	III	IV	V	VI
A	0,99998	0,99999	0,99999	0,99999	0,99999	0,99999
B	0,99992	0,99999	0,99999	0,99999	0,99999	0,99999
C	0,99998	0,99999	0,99998	0,99999	0,99999	0,99999
D	0,99999	0,99998	0,99998	0,99998	0,99999	0,99999
E	0,99999	0,99998	0,99998	0,99999	0,99998	0,99998
F	0,99997	0,99997	0,99999	0,99998	0,99999	0,99997
G	0,99999	0,99999	0,99999	0,99999	0,99999	0,99998
H	0,99999	0,99999	0,99999	0,99999	0,99999	0,99999
I	0,99999	0,99998	0,99998	0,99999	0,99999	0,99999
J	0,99998	0,99999	0,99999	0,99998	0,99999	0,99998
K	0,99998	0,99999	0,99998	0,99999	0,99999	1
L	0,99999	0,99999	0,99998	0,99999	0,99999	0,99999
M	0,99998	0,99999	0,99998	0,99999	0,99997	0,99999
N	0,99999	0,99999	0,99998	0,99998	0,99997	0,99999
O	0,99999	0,99998	0,99999	0,99999	0,99999	0,99999
P	0,99996	0,99999	0,99999	0,99998	0,99997	0,99997
Q	0,99999	0,99998	0,99999	0,99999	0,99999	0,99998
R	0,99999	0,99999	0,99998	0,99999	0,99999	0,99998
S	0,99999	0,99999	0,99999	0,99997	0,99999	0,99999
T	0,99999	0,99999	0,99999	0,99998	0,99999	0,99999
V	0,99999	0,99999	0,99999	0,99999	0,99998	0,99999

Table 8. (s, t)- Reliability joining any two nodes (dimension = 156 x 156 links).

	I	II	III	IV	V	VI
A	0,999853	0,9997959	0,999923	0,999843	0,99984	0,99985
B		0,9998054	0,999788	0,999853	0,99985	0,99986
C			0,999931	0,999717	0,99971	0,99973
D				0,999914	0,99991	0,99992
E				0,999697	0,99969	0,99971
F				0,999841	0,99984	0,99985
G					0,99984	0,99985
H						0,99985

6. CONCLUSION

The network reliability evaluation is an NP-complete problem. The complexity increases with the density of the networks. For small size networks, minimal paths set and minimal cuts can be easily used efficiently for reliability calculation.

This paper introduced a series of algorithms for evaluating the reliability of general networks regardless of their orientation. The proposed algorithms were validated on several test networks. They perform efficiently in terms of computation time and robustness.

Some computer tools were developed and used for computing the reliability of an extensive telecommunication network. They have also been used to identify key components of the network to improve network performance indicators in terms of security, availability and serviceability, both in design and in operations. These tools are currently used to determine the spare parts inventory t maximize network availability while respecting budgetary constraints and the service levels required by the different network's users.

REFERENCES

[1] Abraham J. A., 1979, An Improved Algorithm for Network Reliability, IEEE Transactions on Reliability, pp. 58–61.

[2] Akers. S. B., 1978, Binary Decision Diagrams, IEEE Transactions on Computers, C-27(6), pp. 509–516.

[3] Al-Ghanim A. M., 1999, A heuristic technique for generating minimal path and cutsets of a general network, Computers & Industrial Engineering, Vol. 36, pp. 45–55.

[4] Barlow R. E. and F. Proschan, 1965, Mathematical Theory of Reliability, J. Wiley & Sons, (Reprinted 1996).

[5] Bollig B., Ingo W., 1996, Improving the Variable Ordering of OBDDs Is NP-Complete, IEEE Transactions on Computers, Vol. 45, NO. 9, pp. 993–1002.

[6] Bryant. R. E., 1986, Graph-Based Algorithms for Boolean Function Manipulation, IEEE Transactions on Computers, C-35(8), pp. 677–691.

[7] Bryant. R. E., 1992, Symbolic Boolean Manipulation with Ordered Binary Decision Diagrams, ACM Computing Surveys, Vol. 24, No. 3, pp. 293–318.

[8] Coudert O. and J. C. Madre, 1992, Implicit and incremental computation of primes and essential primes of Boolean functions, in Proc. of the 29th ACM/IEEE Design Automation Conference, IEEE Computer Society Press, pp. 36-39.

[9] Dotson W. P., J. 0. Gobien., 1979, A new analysis technique for probabilistic graphs, IEEE Trans. Circuits and Systems, Vol-Cas 26, No. 10, pp. 855-865.

[10] Hardy. G., C. Lucet, and N. Limnios., 2007, K-Terminal Network Reliability Measures With Binary Decision Diagrams, IEEE Transactions on Reliability, Vol. 56, NO.3, pp. 506-515.

[11] Hariri, S., and Raghavendra, Syrel: A symbolic reliability algorithm based on path and cutest methods, IEEE Transactions on Reliability, C-36(10), pp. 1224-1232.

[12] Heidtmann K.D., 1991, Smaller Sums of Disjoint Products by Subproduct Inversion, IEEE Transactions on Reliability, Vol. 38, pp. 305-311.

[13] Jasmon, G. B. and Kai O. S.., 1985, A New Technique in Minimal Path and Cutset Evaluation, IEEE Transactions on Reliability, Vol. R-34, NO. 2, pp. 136-143.

[14] Jensen P., M. Bellmore, 1969, An algorithm to determine the reliability of a complex system, IEEE Transactions on Reliability, Vol R-18, NO. 1, pp. 169-174.

[15] jGRASP, Auburn University. http://www.jgrasp.org.

[16] Kroese Dirk P., Hui Kin-Ping, and Sho Nariai, (2007), Network Reliability Optimization via the Cross-Entropy Method, IEEE Transactions on Reliability, VolL. 56, NO. 2., pp 275-287.

[17] Kvassay M., Zaitseva E., Kostolny J., Levashenko V, 2015, New algorithm for calculation of Fussel-Vesely importance with application of direct partial derivatives, Safety and reliability Engineering, (Eds) Podofillini et al., Taylor & Francis Group, pp. 1423-1430.

[18] Kuo S. Y, Yeh., F.M, and Lin.,Y.H., 2007, Efficient and Exact Reliability Evaluation for Networks With Imperfect Vertices, IEEE Transactions on Reliability, Vol. 56, No 2, pp. 288-300.

[19] Lee. C. Y., 1959, Representation of Switching Circuits by Binary-Decision Programs, Bell Systems Technical Journal, Vol. 38, pp. 985-999.

[20] Lin, H. Y., Kuo, S. Y. and Yeh, F. M, 2003, Minimal cutset enumeration and network reliability evaluation by recursive merge and BDD, in Proc. of the Eighth IEEE International Symposium on Computers and Communication, Vol. 2, pp. 1341-1346.

[21] Locks, M. O. and Wilson, J. M, 1992, Note on disjoint products algorithms, IEEE Transactions on Reliability, Vol. 41, No 1, pp. 81-84.

[22] Locks, M., 1978, Inverting and minimalizing path sets and cutsets, IEEE Transactions on Reliability, Vol R-27, Jun, pp. 107-109.

[23] Lomonosov M., 1994, On Monte Carlo estimates in network reliability, Probability in the Engineering and Informational Sciences, Vol. 8, pp. 245-264.

[24] Rebaiaia M-L and Ait-Kadi D., 2010, A Program for Computing the Reliability of Communication Networks, ACCA IFAC, IEEE Conference LACC Latin Americain Control Conference Chili, August, pp. 24-27.

[25] Rebaiaia M-L and Ait-Kadi D. 2011, Contribution to the evaluation and optimization of the reliability of networks, Ph.D thesis, Laval University, Canada.

[26] Rebaiaia M-L and Ait-Kadi, 2013, A New Technique for Generating Minimal Cut Sets in Nontrivial Network, AASRI'13 Conference on Parallel and Distributed Computing and Systems, pp. 67-76.

[27] Rebaiaia M-L and Ait-Kadi D., 2013, Network Reliability Evaluation and Optimization: Methods, Algorithms and Software tools, Report Paper, CIRRELT-2013-79, Laval University, Canada.

[28] Rauzy, A., 1993, New Algorithms for fault tree analysis, Reliability Eng. and Systems Safety, vol. 40, pp. 203-210.

[29] Rudell, R, 1993, Dynamic variable ordering for ordered binary decision diagrams, in Proc. of the 1993 IEEE/ACM international conference on Computer-aided design, pp. 42-47.

[30] Shier D. R., D.E. Whited, 1985, Algorithms for generating minimal cutsets by inversion, IEEE Transactions on Reliability, vol R-34, pp 314- 319.

[31] Tarjan, R, 1972, Depth-first search and linear graph algorithms, SIAM Journal of Computing, Vol. 1, No 2, pp. 146-160.

[32] Theolougou R., J.G. Carlier, 1991, Factoring & Reduction for networks with imperfect vertices, IEEE Transactions on Reliability, Vol. 40, No 2, pp. 210-217.ress

[33] Tsukiyama, S.I., Shirakawa, H. Ozaki, H. Ariyoshi, 1980, An algorithm to enumerate all cutsets of a graph in linear time per cutset", Journal of the Association for Computing Machmery, Vol 27, No 4, pp 619-632.

[34] Wood R. K., 1986, Factoring algorithms for computing K-terminal network reliability, IEEE Transactions on Reliability, R-35, 269-278.

[35] Yan, L., Taha, H., and Landers, L. L., 1994, A recursive Approach for Enumerating Minimal Cutsets in a Network, IEEE Transactions on Reliability, Vol 43, No 3, 383-388.

[36] Yeh W-C, 2007, A Simple Heuristic Algorithm for Generating All Minimal Paths, IEEE Transactions on Reliability, Vol. 56, NO 3, pp. 488-494.

[37] Dharmaraja S., Vinayak R., Trivedi K.S., 2016, Reliability and survivability of vehicular ad hoc networks: An analytical approach, Reliability Engineering & System Safety, Volume 153, July 2016, pp.28-38.

[38] Yeh W-C, Bae C., Huang C-L, A new cut-based algorithm for the multi-state flow network reliability problem**,** Reliability Engineering & System Safety, Volume 136, April 2015, pp. 1-7.

[39] Bistounia F. and Jahanshahi M., 2014, Analyzing the reliability of shuffle-exchange networks using reliability block diagrams, Reliability Engineering & System Safety, Volume 132, December 2014, Pages 97–106.

Instructions for authors

Frontiers in Science and Engineering an International Journal edited by Hassan II Academy of Science and Technology uses author-supplied PDFs for all online and print publication.

1. Type of Manuscripts

The FSE Journal publishes the following article types :

Reviews/State of the art, usually through Academy invitation and organized into themed issues, report on recent advances in science and technology. 20 pages maximum according to the format given.

Original Research Papers contain innovative and hypothesis-driven research; supported by sound experimental design, methodology, proofs, and data interpretation. 16 pages maximum according to the format given.

Letters to the Editor: May be submitted by readers commenting articles already published by the Journal. 1 to 2 pages maximum according to the format given.

2. Organization of the Manuscript

The entire manuscript, including mathematical equations, flow-sheets, chemical structures, tables, and figures must be prepared in electronic form and submitted as pdf files. Use Times New Roman size 12. For all special characters (e.g., Greek characters) use the font Symbol. Use carriage returns only to end headings and paragraphs, not to break lines of text. Automatic hyphenation should be turned off. Do not insert spaces before punctuation. Verify the correct spelling for the final version with the Spelling and Grammar function of Word.

3. Language

Manuscripts should be written in English.

4. Submission of the Manuscript

The manuscript and supplementary material must be send by the corresponding author to the Editor in an electronic form as pdf files.

You may be required to register as a new user within the Publication System Manager upon your first visit. Straightforward login and registration procedures can be found on the website. Editorial Manager allows authors to track the progress of manuscript review in real time. Detailed, step-by-step instructions for submitting manuscripts can be found on the website. All correspondence regarding your manuscript must go through Publication System Manager.

Authors are asked to prepare their papers, and PDF files, according to the templates and guidelines provided below.

The author(s) need to supply the following items :

- the PDF file of the paper
- a signed Assignment of Copyright Form (once the paper accepted)

We highly recommend that authors prepare their papers/PDFs using the following Microsoft Word or LaTeX templates, which can be downloaded from the following links :

- Microsoft guidelines and templates
- Latex guidelines and class file

A copyright license form will be provided to the corresponding author only when a paper is accepted for publication.

5. Peer Review

All submissions will be reviewed anonymously by at least two independent referees, and a referee should never communicate directly with an author. A referee must treat as confidential material the manuscript and any supplementary material. Authors may suggest names and email addresses of expert reviewers, but selection remains a prerogative of the Editors. Authors may include supplementary notes to facilitate the review process. If an accepted paper is cited

that has not yet appeared in print and is required for evaluation of the submitted manuscript, authors should provide an electronic version for use by the Reviewers. Authors are responsible for all statements in their work, including changes made by the copy editor after a manuscript is accepted.

6. Revision of the Manuscript
All comments made by referees must be addressed. A letter describing all changes that were made should be attached with the revised version of the manuscript. A copyright license form must accompany the final version of the manuscript.

7. Special Features, Appendices and Supplementary Material
Special features containing highly interactive features or large databases can be included. All authors are encouraged to take advantage WEB online publishing capabilities (i.e. 3-D, video, and interactive graphics). All special features must be created by the Author›s).
Authors who wish to publish electronic supplementary material to their article (Excel files, images, audio/video files) must submit the supplementary files/materials with their manuscript submission via our online peer review tracking Publication System Manager. Note that supplementary files are not automatically included in the reviewer PDF. Please therefore note in the cover letter if these materials should be evaluated by reviewers.

8. Preprint Option
Before making a PDF file of your article, please check the following tips in the next section.

Article checklist
There are a number of essential basic requirements which must be followed during preparation of your article. If article PDFs are prepared without following these essential requirements, publication may be delayed until a usable and compatible PDF is received.
Articles must not contain page numbers, headers or footers
This is extremely important. Page numbers, copyright details etc are added by the Publication System Manager Publishing during the production and publication process. If you put page numbers on your paper we will have to contact you for a replacement PDF, which could delay publication.

Article margins must be adequate
We recommend a minimum 15mm all round. The Microsoft Word template or Latex templates automatically provide the correct margins so their use is highly recommended.
All articles must have an abstract
When readers are searching for information online, an abstract of an article is the first thing they see. Your abstract needs to be concise but convey as much information as possible about the content of your article. In addition, our Publication System Manager Publishing will supply your abstract to many other database systems used by researchers to find papers.

Addresses should be complete and include the country and a contact name
The title of the article, author names with full first name (no degrees), each author's affiliation, and a suggested running head (of less than 50 characters, including spaces). The affiliation should comprise the department, institution (usually university or company), city, and country and should be typed as a footnote to the author's name. For the corresponding author designated to correspond with the Editorial Office and review proofs, indicate his/her complete mailing address, office/cellular telephone number, fax number, and e-mail address. During production of the electronic paper we may need to contact you if there is something to check or for a request a replacement PDF file.

References should be complete and carefully formatted
Online versions of all reference lists will, wherever possible, be electronically linked to the articles that you cite. Reference lists containing many links direct to the cited paper are a valuable research tool. The time and effort spent in preparing your references, so that they can be linked, will be very appreciated by readers of your paper. Please, notice also that all the citations should be justified according to the contents of the proposed article. Abusive citations of the same author may induce a certain delay in the overall review process

PrePrint
Any manuscript received for publication in FSE can be published on the Web as preprint. All authors submitting a manuscript must clearly indicate that they wish to publish it as a preprint. The referees appreciate if the manuscript meets the basic requirements for publication and recommend its publication as preprint. A preprint not accepted for publication by the referees will be immediately removed from the preprint collection. A published paper which was previously available as a preprint will have clearly indicated the date when it was first published on the Web. A work published as preprint can benefit from comments from the readers which can eventually improve the manuscript. Revised versions that incorporate corrections from reviewers and suggestions from readers can be also published as preprints.

9. Publication of the Manuscript
Accepted papers are published as PDF files available at the Web site of the Academy.

Transfer of Copyright Form
A signed copy of the Transfer of Copyright must be submitted online as part of the manuscript submission process (FSECopyright.pdf).

Astract
Reviews/State of the Art, Original Research Articles, require an abstract. The abstract is limited to 300 words or less. For Research Articles, the abstract should include a brief statement for each of the sections related to Introduction, Methods/Approaches/Materials and Discussion, and Conclusion written in paragraph form. All abstracts must be written in one paragraph, with no subheadings, equations, tables, reference citations or graphics.

Keywords
Provide a list of no more than 5 key words.
Introduction
Required for Reviews/State of the art and Original Research Articles.

Main Text Body
For Original Research Articles, organize the main text as follows: Introduction, Approach/Materials and Methods, Results, Discussion, and Conclusion. The use of subheadings to divide the text is encouraged. Primary, Secondary, and Third level headings should be clearly defined, but do not use numbers or letters.
Recommended word counts are as follows: Reviews/State of the art: 8000, Original Research Articles : 6000.
Use abbreviations sparingly, and define them at the first insertion in the text. Use the metric system for all measurements. Express metric abbreviations in lowercase letters without periods (cm, ml, sec). Define all symbols used in equations and formulas. When symbols are used extensively, the authors may include a list of all symbols in a table.

Conclusion
The conclusion should be a brief paragraph, containing 3 to 4 sentences, that summarizes the findings presented.

Acknowledgments
Include funding source(s) and other contributions. If the work has been funded by any organisation please provide name(s) of funding institute(s) and grant number(s).

References
References should conform to Vancouver style and be numbered consecutively in the order in which they are cited in the text. Cite in the text by the appropriate Arabic numeral enclosed in parentheses, e.g., (1), (2-5), etc.
It is advisable to limit the maximum number of references as really needed only.
References to unpublished peer-reviewed, personal communications, including conference abstracts, and papers in preparation or in review, cannot be listed, but can be notated parenthetically in the text.
Abbreviations for journal names should conform to those of Vancouver style (as depicted in http://www.library.uq.edu.au/training/citation/vancouv.pdf). The style and punctuation of the references should conform to conventional referencing.
Whenever, the paper is not yet published officially but accepted, please write down the corresponding DOI within the reference.
Authors may identify uniform resource locators (URLs) for websites that provide the reader with additional information on the topic addressed in the manuscript. Although URLs are an important feature of electronic publishing, authors are encouraged to be very selective in their choice of sites to include. Do not include links to sites that are not accessible without a password.
All on-line documents should contain author(s), title, On-line document/ Web /FTP /organisation /On-line database/ Supplementary material/ Private homepage , and Accessed Day Month Year, so that readers can refer to.

Tables
Tables must be created in Microsoft Word /Latex table format. Tables should be numbered (with Roman numerals) and referred to by number in the text. Center the title above the table, and type explanatory footnotes (indicated by superscript lowercase letters) below the table. Data must be placed in separate cells of the table to prevent text and numbers from shifting when the table is converted for publication on the Internet. Empty cells may be inserted to create spacing. Tables should not duplicate information provided in the text. Instead, tables should be used to provide additional information that illustrates or expands on a specific point the author wishes to make. Each table should be self-explanatory.

Figures
The FSE offers authors the use of color figures in online published manuscripts. Figures (as well as photographs, drawings, diagrams, and charts) are to be numbered in one consecutive series of Arabic numerals in the order in which they are cited in the text. All Electronic artwork must be submitted online via our online peer review tracking system, Publication System Manager.
The maximum combined count for tables and figures for papers should not exceed 15 to 20.

Footnotes
Footnotes should be avoided. When their use is absolutely necessary, footnotes should be numbered consecutively using Arabic numerals and should be typed at the bottom of the page to which they refer. Place a line above the footnote, so that it is set off from the text. Use the appropriate superscript numeral for citation in the text.

Guidelines

We highly recommend that authors prepare their papers/PDFs using the following Microsoft Word or LaTeX templates, which can be downloaded from the following links:

• Latex guidelines and class file http://www.academie.hassan2.sciences.ma/fse/FSE%20Sample%20cls.tex.txt

• PDF guidelines and templates http://www.academie.hassan2.sciences.ma/fse/FSE%20Sample%20cls.pdf

• Microsoft word guidelines and templates

Contractual issues

1. Full Disclosure
During the manuscript submission process, all authors will be required to confirm that the manuscript has not been previously published in any language anywhere and that it is not under simultaneous consideration by another journal.

2. Conflicts of Interest
Authors must declare all conflicts of interest (or their absence) in their cover letter upon submission of a manuscript. This conflict declaration includes conflicts or potential conflicts of all listed authors. If any conflicts are declared, FSE publish them with the paper. In cases of doubt, the circumstance should be disclosed so that the editors may assess its significance.
Conflicts may be financial, academic, commercial, political or personal. Financial interests may include employment, research funding (received or pending), stock or share ownership, patents, payment for lectures or travel, consultancies, nonfinancial support, or any fiduciary interest in a company.

3. Copyright Transfer
The Copyright Revision Act requires that Authors transfer their copyrights to the Publisher, HIIAST, in order to provide for the widest possible dissemination of professional and scientific literature. A signed Transfer of Copyright form must be submitted online with the manuscript. The Transfer of Copyright form for an accepted manuscript must be on file with the HIIAST Editorial Office prior to production for publication. Corresponding Authors may print and sign the form on behalf of all authors The Transfer of Copyright form can be found at fsecopyright.pdf.

4. Use of Copyrighted Tables and Figures
A copy of the granted permission to use copyrighted figures and tables must be included with the submitted manuscript.

Dépôt légal : 2012 PE 0007
ISSN : 2028 - 7615

ACADEMY Press MA

Email : fse@academiesciences.ma
www.academiesciences.ma/fse/